TU/e EINDHOVEN UNIVERSITY OF TECHNOLOGY

Translational cell based therapies to repair the heart

Citation for published version (APA):
Emmert, M. Y. (2013). *Translational cell based therapies to repair the heart*. [Phd Thesis 1 (Research TU/e / Graduation TU/e), Biomedical Engineering]. Technische Universiteit Eindhoven.
https://doi.org/10.6100/IR751862

DOI:
10.6100/IR751862

Document status and date:
Published: 01/01/2013

Document Version:
Publisher's PDF, also known as Version of Record (includes final page, issue and volume numbers)

Please check the document version of this publication:

• A submitted manuscript is the version of the article upon submission and before peer-review. There can be important differences between the submitted version and the official published version of record. People interested in the research are advised to contact the author for the final version of the publication, or visit the DOI to the publisher's website.
• The final author version and the galley proof are versions of the publication after peer review.
• The final published version features the final layout of the paper including the volume, issue and page numbers.

Link to publication

General rights
Copyright and moral rights for the publications made accessible in the public portal are retained by the authors and/or other copyright owners and it is a condition of accessing publications that users recognise and abide by the legal requirements associated with these rights.

• Users may download and print one copy of any publication from the public portal for the purpose of private study or research.
• You may not further distribute the material or use it for any profit-making activity or commercial gain
• You may freely distribute the URL identifying the publication in the public portal.

If the publication is distributed under the terms of Article 25fa of the Dutch Copyright Act, indicated by the "Taverne" license above, please follow below link for the End User Agreement:

www.tue.nl/taverne

Take down policy
If you believe that this document breaches copyright please contact us at:

openaccess@tue.nl

providing details and we will investigate your claim.

Download date: 17. Nov. 2023

Translational cell based strategies to repair the heart

Maximilian Emmert

Translational cell based strategies to repair the heart

A catalogue record is available from the Eindhoven University of Technology Library.

ISBN: 978-90-386-3358-9

Copyright © 2013 by M.Y. Emmert

All rights reserved. No part of this book may be reproduced, stored in a database or retrieval system, or published, in any form or in any way, electronically, mechanically, by print, photo print, microfilm or any other means without prior written permission by the author.

Translational cell based therapies to repair the heart

PROEFSCHRIFT

ter verkrijging van de graad van doctor aan de
Technische Universiteit Eindhoven, op gezag van de
rector magnificus, prof.dr.ir. C.J. van Duijn, voor een
commissie aangewezen door het College voor
Promoties in het openbaar te verdedigen
op donderdag 11 april 2013 om 14.00 uur

door

Maximilian Emmert

geboren te Hannover, Duitsland

Dit proefschrift is goedgekeurd door de promotoren:

prof.dr. S.P. Hoerstrup

en

prof.dr.ir. F.P.T. Baaijens

Copromotor:

dr. A. Driessen-Mol

Contents

Chapter 1

1 General Introduction 1

1.1 Part A Cardiac Cell Therapy 2

1.1.1 Cardiovascular Disease and limitations of conventional Therapies 2

1.1.2 Stem Cells for myocardial repair and regeneration 2

1.1.3 Stem Cell Sources 4

1.1.4 Routes and Strategies for Stem Cell Applications 6

1.1.5 Advanced Stem Cell Formats for enhanced Cell Retention and Survival 8

1.1.6 Cell tracking and assessment of in-vivo Cell fate 8

1.1.7 Surrogate animal models for cardiovascular Stem Cell Research 9

1.1.8 Ten years of Clinical Cell Therapy – where do we stand? 9

1.1.9 Limitations of current Stem Cell Concepts 10

1.2 Part B Heart Valve Tissue Engineering 11

1.2.1 Valvular Heart Disease and current therapy options 11

1.2.2 The Evolution of Transcatheter Valves 11

1.2.3 The Concept of Tissue Engineering 13

1.2.4 Strategies in tissue engineering: in vitro, in vivo or in situ? 13

1.2.5 Starter Matrices for heart valve tissue engineering 14

1.2.6 Cell Sources 14

1.3 Rationale and outline of the thesis 16

Chapter 2

2 BCRP+ cardiac resident cells in ischemic human myocardium 17

2.1 Abstract 18

2.2 Introduction 19

2.3 Methods 19

2.4 Results 23

2.5 Discussion 28

2.6 Acknowledgements 32

Chapter 3

3 Transplantation of human MSCs into the pre-immune fetal sheep 33

3.1 Abstract 34

3.2 Introduction 35

3.3 Methods 35

3.4 Results 42

3.5 Discussion 54

3.6 Acknowledgements 56

Chapter 4

4 Transplantation of 3D microtissues in the porcine heart 57

4.1 Abstract 58

4.2 Introduction 59

4.3 Methods 60

4.4 Results 67

4.5 Discussion 77

4.6 Acknowledgements 79

Chapter 5

5 Marrow Stromal Cell-based Tissue Engineered Heart Valves 81

5.1 Abstract 82

5.2 Introduction 83

5.3 Methods 83

5.4 Results 87

5.5 Discussion 94

5.6 Acknowledgements 96

Chapter 6

6 Stem Cell Based Transcatheter Aortic Valve Implantation 97

6.1 Acute technical feasibility pre-study 98

6.2 Abstract 100

6.3 Introduction 101

6.4 Methods 101

6.5 Results 107

6.6 Discussion 112

Chapter 7

7 General Discussion 115

7.1 Summary and main findings 116

7.2 Discussion and study considerations 118

7.3 Next steps, challenges and future outlook 124

7.4 Conclusion and clinical relevance 130

References 131

Acknowledgements 142

Curriculum Vitae 143

Summary

Translational cell based therapies to repair the heart

Cardiovascular disease comprising of Coronary Artery Disease (CAD) and Valvular Heart Disease (VHD) represents the leading disease in western societies accounting for the death of numerous patients. CAD may lead to heart failure (HF) and despite the therapeutic options for HF which evolved over the past years the incidence of HF is continuously increasing with a higher percentage of aged people. Similarly, an increase of VHD can be observed and although valve replacement represents the most common therapy strategy for VHD, approximately 30% of the treated patients are affected from prosthesis-related problems within 10 years. While mechanical valves require lifelong anticoagulation treatment, bioprosthetic valves present with continuous degeneration without the ability to grow, repair or remodel. The concept of regenerative medicine comprising of cell-based therapies, bio-engineering technologies and hybrid solutions has been proposed as a promising next generation approach to address CAD and VHD. While myocardial cell therapy has been suggested to have a beneficial effect on the failing myocardium, heart valve tissue engineering has been demonstrated to be a promising concept to generate living, autologous heart valves with the capability to grow and to remodel which may be particularly beneficial for children. Although these regenerative strategies have shown great potential in experimental studies, the translation into a clinical setting has either been limited or has been too rapid and premature leaving many key questions unanswered. The aim of this thesis was the systematic development of translational, cell-based bio-engineering concepts addressing CAD (part A) and VHD (part B) with a particular focus on minimally invasive, transcatheter-based implantation techniques.

In the setting of myocardial regeneration, in the second chapter the intrinsic regenerative potential of the heart is investigated. Myocardial samples were harvested from all four chambers of the human heart and were assessed for resident stem/progenitor cell populations. The results demonstrated that $BRCP^{+}$ cells can be detected within the human heart and that they were more abundant than their $c\text{-}kit^{+}$ counterparts. In the non-ischemic heart they were preferentially located in the atria while following ischemia, their numbers were increased significantly in the left ventricle. There were no $c\text{-}kit^{+}/BCRP^{+}$ co-expressing stem/progenitor cell populations suggesting that these two markers are expressed by two distinct cell populations in the human heart. Although these results provided a valuable snapshot at cardiac progenitor cells after acute ischemia, the data also indicated that the absolute numbers of cells acquiring a myocardial phenotype are rather low and further effort is needed to upscale such cells into clinically relevant numbers.

In chapter three, it is demonstrated that human bone marrow and adipose tissue derived mesenchymal stem cells can be efficiently isolated via minimally invasive procedures and expanded to clinically relevant numbers for myocardial cell therapy. Thereafter, these cells were tested in a uniquely developed intra-uterine, fetal, preimmune ovine myocardial infarction model for the evaluation of human cell fate in vivo. After the successful intrauterine induction of acute myocardial infarction, the cells were intramyocardially transplanted and tracked using a multimodal imaging approach comprising MRI, Micro CT as well as in vitro analysis tools. The principal feasibility of intra-

myocardial stem-cell transplantation following intra-uterine induction of myocardial infarction in the preimmune fetal sheep could be demonstrated suggesting this as a unique platform to evaluate human cell-fate in a relevant large animal model without the necessity of immunosuppressive therapy.
In chapter four, adipose tissue derived mesenchymal stem cells (ATMSCs) were processed to generate three dimensional microtissues (3D-MTs) prior to transplantation to address the important issue of cell retention and survival. Thereafter, the ATMSCs based 3D-MTs were transplanted into the healthy and infarcted porcine myocardium using a catheter-based, 3D electromechanical mapping guided approach. The previously used MRI based tracking concept was successfully translated into this preclinical model allowing for the in vivo monitoring of 3D-MTs.

To address Valvular Heart Disease (part B), in chapter five, marrow stromal derived cells were used to develop a unique autologous, cell-based engineered heart valve *in situ* tissue engineering concept comprising of minimally-invasive techniques for both, cell harvest and valve implantation. Autologous marrow stromal derived cells were harvested, seeded onto biodegradable scaffolds and integrated into self-expanding nitinol stents, before they were transapically delivered into the pulmonary position of non-human primates within the same intervention while avoiding any in vitro bio-reactor period. The results of these experiments demonstrated the principal feasibility of generating marrow stromal cell-based, autologous, living tissue engineered heart valves (TEHV) and the transapical implantation in a one-step intervention.

In chapter six, this concept was then successfully applied to the high-pressure system of the systemic circulation. After detailed adaption of the TEHV and stent design to the anatomic conditions of an orthotopic aortic valve, marrow stromal cell-based TEHV were implanted into the orthotopic aortic position. The implantation was successful and valve functionality was confirmed using fluoroscopy and trans-esophageal echocardiography. While displaying an ideal opening and closing behaviour with a sufficient co-aptation and a low pressure gradient, there were no signs of coronary occlusion or mal-perfusion.

In conclusion, the results of this thesis represent a promising portfolio of translational concepts for cardiovascular regenerative medicine addressing CAD and VHD. In particular, it was demonstrated that mesenchymal stem cells / multipotent stromal derived cells represent a clinically relevant cell source for both myocardial regeneration and heart valve tissue engineering. It was shown that the preimmune fetal sheep myocardial infarction model represents a unique platform for the in vivo evaluation of human stem cells without the necessity of immunosuppressive therapy. Moreover, the concept of transcatheter based intramyocardial transplantation of mesenchymal stem cell-based 3D-MTs was introduced to enhance cellular retention and survival. Finally, in the setting of VHD it could be shown that marrow stromal cell based issue engineered heart valves can successfully generated and transapically implanted into the pulmonary and aortic position within a one-step intervention.

Chapter 1

General introduction

The concept of regenerative medicine including cell-based therapies, bio-engineering approaches and hybrid techniques has been suggested as a next generation technology to treat cardiovascular diseases including Coronary Artery Disease (CAD) and Valvular Heart Disease (VHD). While cardiac cell therapy has been proposed to be beneficial for the failing heart, the concept of heart valve tissue engineering has been shown to be a promising approach to fabricate living, autologous heart valves with the ability to remodel and to grow which may be particularly beneficial for children. Although these regenerative strategies have demonstrated great potential in experimental studies, the translation into the clinical arena has either been limited or has been too quick and premature leaving many key issues unresolved. This chapter provides an overview of the current status and future challenges of cardiac cell therapy (part A) and a summary of current *state-of-the-art* treatment strategies for VHD and its current limitation along with the principle concept of clinically relevant heart valve tissue engineering (part B).

1.1 Part A Cardiac Cell Therapy

1.1.1 Cardiovascular Disease and Limitations of Conventional Therapies

Cardiovascular disease still is the "Killer number one" in western societies. Due to aging societies (in 2030 all "baby boomers" will be 65 or older), the expected increase of heart failure patients will further challenge our already stressed socio-economic systems. The American Heart Association foresees more than 100 million heart disease patients in 2030 for the US only and projects related health care costs of more than USD 800 billion (American Heart Association 2010). Ischemic heart disease leads to myocardial infarction (heart attack) followed by death of the cardiomyocytes. The adult heart cannot regenerate after ischemic injury as cardiomyocytes do not possess an ability to divide while the heart lacks of sufficient reserve of precursor or stem cells. Thus, the loss of myocytes leads to progressive dilation of the myocardial wall what may finally end up in heart failure. The therapeutic options for end-stage CAD are medical therapy, assist device implantation (as a bridge to transplant or destination therapy) and heart transplantation which is the ultima ratio therapy that has evolved over the past years. However, conventional medication can only treat the symptoms. The disproportion between the number of donor organs and the number of potential transplantation candidates limits heart transplantation to a minority of patients, which is why many patients die while being on the "waiting list". The mean survival time of severe heart failure is approximately 1.75 years, while only 25% of these patients survive more than five years [1]. This points the substantial and urgent therapeutic need out to develop alternative therapy options.

1.1.2 Stem Cells for myocardial repair and regeneration

Stem cells have been repeatedly suggested as a next generation therapeutic approach for the treatment of heart failure due to myocardial infarction or cardiomyopathy. Based on numerous pre-clinical animal trials, there are increasing numbers of early phase patient studies aiming to demonstrate the feasibility and potential efficacy of stem cell-based therapies in the clinical setting [2-7]. In particular, mesenchymal stem cells (MSCs) either derived from the bone marrow or more

recently from the adipose tissue are considered as a clinical benchmark cell and have been repeatedly used for cardiac repair. They are considered safe and easily available in clinically relevant numbers. However, while numerous experimental and preclinical studies using various types of stem and progenitor cells have shown promising results, the outcomes of first clinical pilot trials have only shown marginal effects with regards to the improvement of cardiac performance. Current meta-analyses demonstrate a mean of only 3% improvement of cardiac function. Clearly, the optimal utilization and exploitation of stem cells for myocardial regeneration is by far not understood. One major reason is certainly the too rapid and ineffective translation from small animal studies or non-comparable large animal studies into clinical human studies. Key questions with regards to the so called ``stem cell fate`` which is crucial to explain a beneficial effect, have not been elucidated yet. The optimal cell type, the number of cells, the optimal delivery format, the most suitable route for cell delivery, and importantly the specific mechanism by which therapeutic cells contribute to functional improvement remain to be investigated. However, advanced, non-invasive imaging techniques as well as the development of appropriate animal models are mandatory for the assessment of cell based-therapies and represent the key requisite for a safe translation into the clinical setting (figure 1).

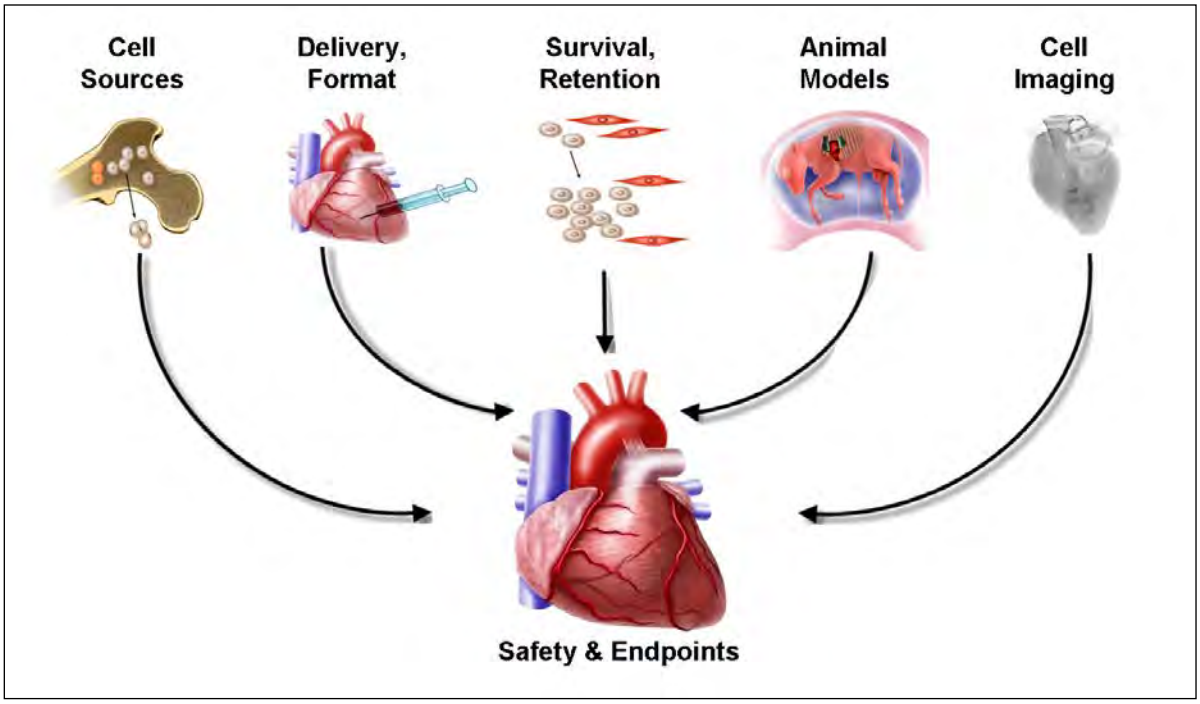

Figure 1: Challenges in Translational Cardiac Stem Cell Research

Current challenges in translational cardiac stem cell research comprise of: 1) the definition of the ideal cell type 2) the optimal application format and delivery mode 3) the sufficient survival and intramyocardial retention 4) the development of appropriate animal models to study human cell fate 5) advanced imaging tools for in cell tracking and vivo monitoring 6) the definition of appropriate safety and efficacy endpoints

1.1.3 Stem Cell Sources

Several stem cell sources are currently under evaluation for their potential to promote myocardial repair and regeneration [8] (figure 2). These include crude bone marrow-derived/circulating progenitor cells (BMPCs) and their subpopulations, such as mesenchymal stem cells (MSCs) and endothelial progenitor cells (EPCs); skeletal myoblasts (SM), adipose tissue derived MSCs, cardiac resident stem cells (CSCs), umbilical cord derived stem cells (UPCs), embryonic stem cells (ESCs) and induced pluripotent cells (iPS) [8].

Most researchers have been focusing on BMPCs after a large number of clinical trials have demonstrated their clinical benefit. It was recently demonstrated that for acute myocardial infarction and chronic ischemia the long-term mortality after 1 and 5 years was significantly reduced [3]. The paracrine effects after transplantation appear to be the major mechanism of BMPCs, while the evidence of BMPCs trans-differentiation into cardiomyocytes remains controversial. Several studies have shown that cardiac differentiation capacity of BMPCs *in vivo* is very low and cannot explain the short term therapeutic effect provided to the infracted heart [8, 9]. Autologous skeletal myoblasts were also one of the first cell types tested for cardiac repair [10]. It has been demonstrated that transplanted skeletal myoblasts integrate and differentiate into myotubules after transplantation and improve cardiac function in animal models. The major limitation is the lack of the gap junction protein connexin-43 expression after *in vitro* differentiation, resulting in the failure of electrical integration with the host myocardium and a consequent high risk of arrhythmia [11] [12]. Ongoing human trials have been terminated because of marginal therapeutic benefits [13].

In this context, the presence of a stem cell population in the heart has been described. These newly isolated cardiac stem cells (CSCs) are detectable in all four heart chambers, particularly in the atrium [14]. Previous studies isolated a novel population of cells able to proliferate as well as to differentiate into cardiac cells from rat, mouse and human post-natal hearts. These cells expressed the cardiac progenitor marker islet-1 but not the stem cell markers Sca-1 or c-kit [15]. Whereas $isl1^{+}$ cells also express early cardiac differentiation markers like Nkx2.5 and GATA-4, they lack transcripts of mature myocytes. However, when co-cultured *in vitro* with differentiated myocytes, they spontaneously acquired myocyte characteristics including electromechanical coupling. CSCs might be isolated from human heart using a minimally invasive biopsy procedure [16, 17]. Therefore, the autologous implantation of these cells would have the minimal risk of immune rejection or teratoma formation. To address the safety and feasibility of intracoronary delivered CSC the “cardiac stem cell infusion in patients with ischemic cardiomyopathy” (SCIPIO) trial is ongoing [18]. However, the expansion to sufficient numbers is a major limitation and their long-term effect on the myocardial function is still unclear.

Human ESCs display the highest plasticity and are therefore the most versatile of stem cells. Several studies investigated the effect of ESCs to treat myocardial infarcts in the animals [19] and reported a significant survival rate along with the improved ventricular function [20]. These results open up exciting prospects for the treatment of cardiac diseases; however, ESCs are still primarily in preclinical evaluation. Until the problems of tumorigenicity, immunogenicity and the ethical discussion are not resolved, the clinical application of ESCs will be rather limited. Potential ways to avoid the teratoma formations might be the complete differentiation of ESC into cardiomyocytes [19] and efficient cell sorting prior to implantation. Characteristics comparable to ESC are shown by

the so-called ESC-like cells, also defined as induced pluripotent stem cells (iPSCs). Previous studies demonstrated the possibility to generate this cell type by reprogramming using a combination of specific stem cell transcription factors such as Oct 3/4, Klf4, Sox2 and c-Myc [21] [22] [23] [24]. These iPSCs were able to differentiate into beating cardiac myocytes and cardiac specific marker. Following the transplantation in the infarcted myocardium, they differentiated into cardiac myocytes and formed gap junction proteins [25]. While autologous-derived iPSCs show the advantage over ESCs by avoiding ethical and immunological issues for autologous transplantation, safety issues remain.

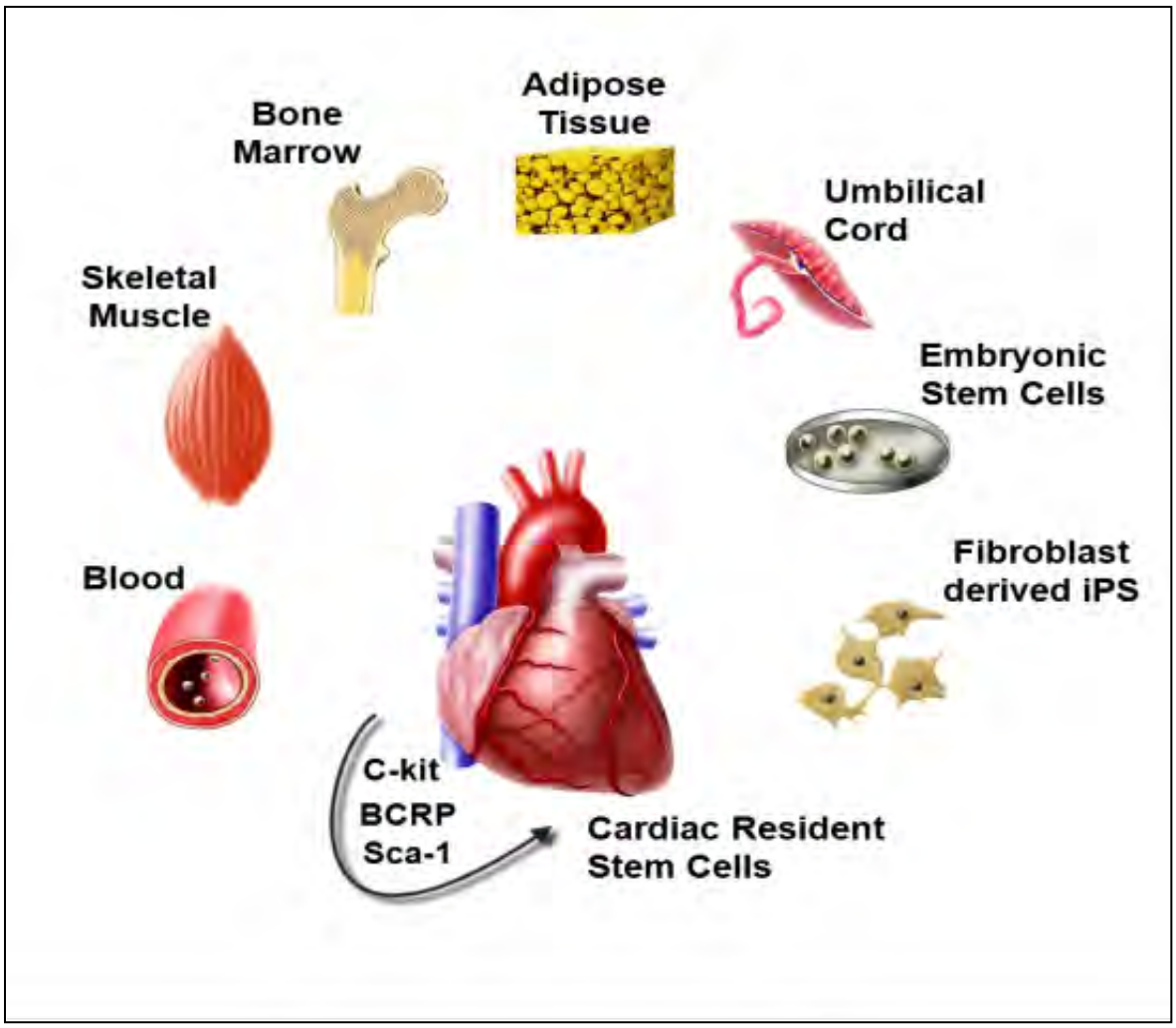

Figure 2: Stem Cell Sources for Myocardial Repair and Regeneration

Numerous cell sources are currently under evaluation for their capability to promote cardiac repair and regeneration. These include: blood derived progenitor cells, skeletal myoblasts, bone marrow derived progenitor cells and their subpopulations, adipose tissue derived stem cells, umbilical cord derived stem cells, embryonic stem cells, induced pluripotent cells as well as cardiac resident stem and/or progenitor cells.

Mesenchymal stem cells (MSCs) either derived from the bone marrow or the adipose tissue are considered a clinical benchmark cell for cardiac repair [26-28]. They have been repeatedly investigated in animal and human trials as they are considered safe and easily available in clinically relevant numbers [3, 29]. In particular, bone-marrow derived MSCs have been repeatedly used in preclinical animal models as well as in clinical pilot trials [7]. Importantly, recent reports indicate that bone-marrow MSCs can be programmed into a cardiac committed stage increasing their clinical relevance and potential [30]. This is besides their suggested function through multiple paracrine effects [29] comprising the secretion of cytokines and growth factors that suppress the immune response, inhibit fibrosis and apoptosis, enhance angiogenesis or stimulate the endogenous precursor cells for cardiac differentiation [29]. Similarly, the adipose tissue also represents a rich source of MSCs and is comparable to those derived from the bone marrow with regards to the surface marker profile and the differentiation capacity. Due to their abundant availability and the even lesser invasive access, adipose tissue derived MSCs should be considered as an attractive and clinically highly relevant stem cell source for future therapy concepts [31].

1.1.4 Routes and Strategies for Stem Cell Applications

In the last years different application strategies have been described (figure 3): 1. intravenous injection [32], 2. intra-coronary injection [33], 3. transcatheter endocardial injection based on electromechanical mapping [34, 35], 4. direct epicardial injection [36] and 5. retrograde application via the coronary sinus [37]. The advantage of each strategy depends on the clinical scenario (i.e intracoronary injection following myocardial infarction vs. intramyocardial injection due to ischemic cardiomyopathy) and the applied cell type.

Systemic intravenous Infusion

The systemic venous application is a less invasive strategy and is based on the principle of guided stem cell homing to the area of infarction [38]. Despite the advantage of low invasiveness, the major drawback of this strategy is that the cells have to pass the pulmonary circulation which is a major barrier before entering the arterial circulation leading to an overall low number of cells finally reaching the myocardium [32].

Percutaneous intracoronary injection

The percutaneous intracoronary injection represents the most frequently used approach in the clinical setting. The cells are injected via a balloon catheter into the coronary vessels corresponding with the ischemic area the therapy is aimed for. The main criticism for this method is the high wash-out phenomena associated with this method. To enhance the migration of the cells the balloon is kept inflated for a certain period of time. The efficacy of this approach may also be related to the type of stem cells used. A recent study showed an up to seven-fold higher retention of bone-marrow derived stem cells in the myocardium after intra-myocardial injection when compared to the intra-coronary approach [39]. In this context, the proposed wash-out phenomena were confirmed by an up to ten-fold higher detection of the cells in the lungs.

Percutaneous trans-endocardial intra-myocardial injection

This approach is based on a two-step procedure: After an initial electromechanical mapping to identify the ischemic areas as well as the border zones of the infarction area, the cells are endocardially injected via a small needle [35]. Based on the initial mapping, a very high accuracy can be achieved to inject the cells exactly to the aimed area. However, adverse cardiac events such as ventricular arrhythmia and non-cardiac complications reported an overall higher inflammatory response when compared to an intra-coronary approach. Furthermore, the risk of ventricular rupture has to be kept in mind, particularly when apical areas of the myocardium are addressed.

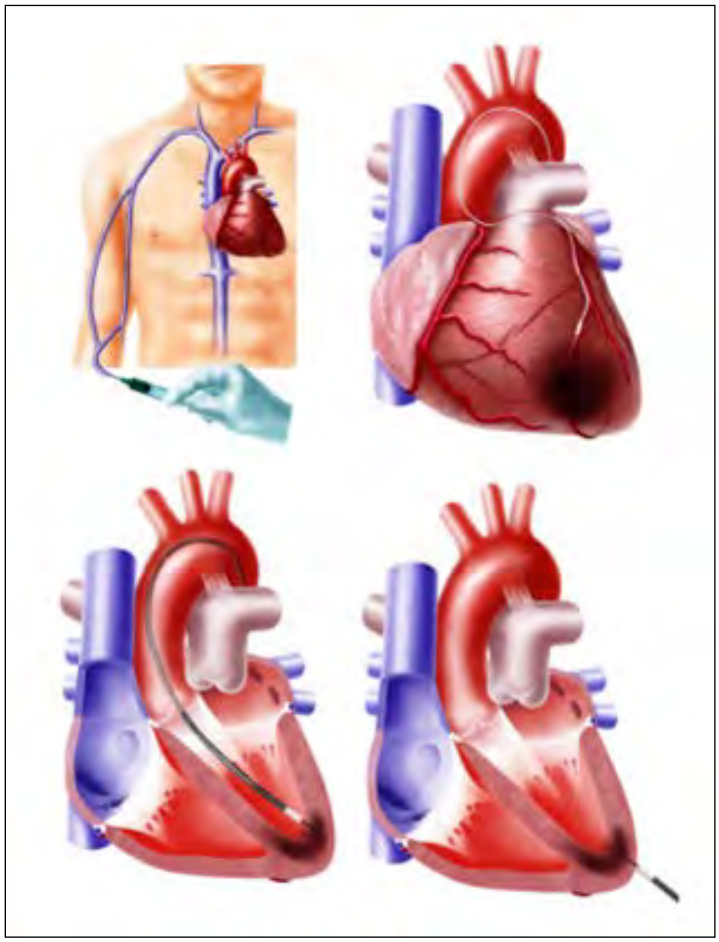

<u>Figure 3:</u> Routes for Stem Cell Delivery

Several routes for stem cell delivery have been established in the last years. While the systemic intravenous application is rarely used due to the low degree of cardiac homing, the most commonly utilized approaches comprise of an intracoronary application or an intramyocardial approach that can be either carried out endocardially via a transcatheter based route or epicardially during a surgical approach.

Direct epicardial intramyocardial injection

In this approach the cells are directly applied during cardiac surgery by using an epicardial technique [36]. Despite the visual identification of the target area, the exact discrimination between the infarction zone (scar) and the border zone may be challenging. Also the accurate injection of the cells may proof difficult, particularly if it is done in a beating heart fashion. The migration of the cells into the tissue has been reported as limited with this technique.

Injection via Sinus Coronarius

This technique represents an alternative method to apply stem cells to the heart via a pressure-controlled retrograde into the coronary veins [37]. However, this approach may be limited as not all ischemic regions may be treated and it could be technically challenging to address a specific coronary vein for infusion.

1.1.5 Advanced Stem Cell Formats for enhanced Cell Retention and Survival

Sufficient cell therapy depends on efficient application along with engraftment and survival of the applied cells. To achieve functional repair of the diseased myocardium, retention and integration of the transplanted cells is mandatory. The mode of cell transplantation, the cell quality, and the host environment play a pivotal role for effective cell engraftment after the transplantation. The faster the implanted cells are integrated within the hosting myocardium and supplied with blood the more efficient will the treatment benefit be. The application of 2D single cell suspensions provides the benefit that these can be delivered either by the intracoronary or by the intra-myocardial route. However, the intra-myocardial retention and integration rate of 2D single cell suspensions has been repeatedly criticized to be limited. Thus, preconditioning of the cells appears to be an effective strategy to protect the cells and to improve their viability after transplantation. Cellular self-assembly into three dimensional microtissues prior to transplantation has also demonstrated characteristics that may overcome 2D single cell suspensions with regards to improved cell survival. Based on the hanging drop technique, a novel microtissue technology was recently developed [40-44] allowing for a 3D culture of various cell types that can generate endogenous extracellular matrix environments with enhanced adhesion properties [40-44]. Myocardial microtissues derived from neonatal rat cardiomyocytes have demonstrated to integrate into the myocardial wall after intra-pericardial injection. Moreover, the 3D environment appears to stimulate the production of pro-angiogenic factors such as VEGF which supports the reconstruction of a cardiac vascular network [44]. This presence of vascular structures led to maintenance of long-term survival and contractile capacity of cardiac microtissues [45].

1.1.6 Cell tracking and assessment of in-vivo cell fate

Imaging modalities for stem-cell tracking and the in vivo monitoring with regard to survival, engraftment and differentiation are crucial to justify potential functional effects of cell-based therapy concepts [46, 47]. Different imaging strategies are currently being assessed comprising of MRI imaging with direct cell-labelling of cells using super-paramagnetic agents, PET- or SPECT-imaging utilizing radio-nuclides, as well as reporter-genes [46, 47]. The major part of recent preclinical studies have utilized MRI based imaging to track super-paramagnetic agents as MRI has also become an important endpoint to evaluate efficacy in clinical pilot trials [46-49]. As it provides detailed morphologic and functional data on the heart, it seems to be an efficient imaging technique to address both, functional assessment and cell-tracking. Importantly, in preclinical animal trials using micron- or nano-sized iron-oxide particles it the feasibility of non-toxic labelling of mesenchymal stem cells (MSCs) without compromising their trans-differentiation ability could be shown. In the setting of cardiac cell therapy, this labelling approach was combined with transcatheter, intramyocardial delivery strategies, demonstrating that the transplanted cells could be detected instantly after delivery with a significant degree of resolution when using MRI. The major disadvantage of using super-paramagnetic agents is the fact that the imaging signal is not directly linked to cell viability which makes it difficult to discriminate between vital, labelled cells and particle-loaded cell-debris or hosting macrophages. These may have actively phagocytised the particles after cell-death significantly biasing an effective tracking evaluation [48, 49]. However,

when using advanced super-paramagnetic agents that are co-labeled with fluorochromes [50], this risk may be reduced and allows for histological in-vitro tracking after harvest.

1.1.7 Surrogate animal models for cardiovascular stem cell research

To approach the key issues in cardiac stem cell research, a surrogate animal model is crucial allowing for sufficient in vivo human cell tracking without the necessity for immunosuppressive therapy. However, except gene-modified murine models, the availability of suitable animal models to evaluate human stem cell fate and bio-distribution is limited. Most available animal models require immunosuppressive therapy when applying human cells [51], and thus the clinical relevance of results obtained from these animal models is sub-optimal. The fetal sheep has been proposed as an ideal animal model for the evaluation of human cell-fate [52, 53]. Although it has a normal functioning immune-system, it is still able to accept and support human cell engraftment and differentiation if the cells are applied before day 75 of gestation [52, 53]. Following ultrasound-guided, intra-peritoneal stem cell transplantation, reports have indicated that the fetal sheep is immunologically tolerant to human skin grafts and to allogenic or xenogenic stem cells during this "pre-immune" period of development. This allows for significant engraftment of human cells in the absence of any significant immune-reaction. Considering this significant advantage as well as the large size and the long life-span, this animal model represents a highly valuable model to evaluate human cell-fate and provides experimental opportunities that are not available in other animal models [52, 53].

1.1.8 Ten years of Clinical Cell Therapy – where do we stand?

In 2001, Professor Bodo Strauer was the first to treat patients with bone marrow derived progenitor cells. Six days after myocardial infarction the patients received an intracoronary infusion of the cells following percutaneous balloon intervention [2]. Ten weeks after the treatment the patients displayed a reduction of infarction size, an improvement of ejection fraction and a reduction of wall motion irregularities [2]. Following these findings, numerous small- and medium sized studies were performed using progenitor cells derived from the bone marrow and the peripheral blood [54]. The first randomized trial was the BOOST Study (NCT00224536) which was performed at the Hanover Medical School [55]. While in the early follow up a significant improvement of ejection fraction was noted in the treated group, this benefit was found not to remain statistically significant at 18 months follow up. [56]. However, a recently performed meta-analysis of 29 randomized studies comprising of 1830 patients with acute myocardial infarction displayed a significant short term and long term improvement of ejection fraction (2,7% and 3,31%) [57]. The STAR-heart-study, one of the biggest randomized trials for patients with ischemic cardiomyopathy (ejection fraction <35%), detected a significantly reduced mortality in the treated study arm [58]. It could also be identified that patients with large, transmural myocardial infarction and severely decreased ejection fraction do benefit the most from cell therapy [6, 59]. In addition, the number of cells appeared to play a crucial role for the success of cell therapy [57, 60]. Besides bone marrow derived progenitor cells, skeletal myoblasts have also been used in clinical settings such as the multicenter, randomized, placebo controlled MAGIC trial (NCT00102128) for patients with ischemic cardiomyopathy [10]. Due

to the repetitive occurence of significant arrhythmia after the treatment, some of the patients had to undergo implantation of an internal defibrillator [61]. This was due to the fact that skeletal myoblasts not differentiating into functional cardiomyocytes and even more importantly not forming gap junctions to ensure electromechanical coupling with the host myocardium [62]. The initial assumption of the trans-differentiation of bone marrow derived progenitor cells into functional cardiomycytes could not be confirmed in subsequent studies [63-65]. In contrast, it could be demonstrated that the therapeutic effect of these cells is primarily linked to paracrine effects [29]. Furthermore, mesenchymal stem cells derived from the bone marrow [7, 66] (NCT00587990, NCT00768066, NCT00810238)and newer cell sources such as adipose tissue derived mesenchymal stem cells (NCT01502514, NCT00442806), as well as cardiac progenitor cells [5, 67] (NCT00474461, NCT00893360) have advanced into phase 1 and 2 clinical trials for the treatment of patients with ischemic cardiomyopathy.

1.1.9 Limitations of current stem cell concepts

While stem cells have shown great potential, their precise role and mechanism in cardiovascular regeneration remains unclear. One major reason is certainly the too rapid translation from non-comparable small animal studies or large animal studies (mainly pigs and sheep) into human studies. Key questions to the so called ``stem cell fate`` which are crucial for explaining the beneficial effects, have not been elucidated yet. Despite clinicians claiming a certain beneficial effect after stem cell applications in humans, it to date remains almost completely unclear what exactly happens after the delivery of stem cells to the myocardium with regards to immunologic response, cell retention, engraftment and importantly survival. It is also unclear, if stem cells – depending on which type is applied – trans-differentiate or act through paracrine mechanisms while attracting endogenous cells to support myocardial repair. The bio-distribution of these cells after delivery and the specific mechanism by which stem cells contribute to functional improvement remain to be investigated. While researchers tried to answer these questions with the help of small animal studies, critiques argue that these results cannot be extrapolated into the human clinical setting. Moreover, the optimal cell type and format (2D single cells versus 3D micro structures), the most suitable route for cell delivery, the optimal time point for cell delivery after myocardial infarction and most importantly the number of cells to be delivered are still unknown. In the clinical setting, different amounts of cells have been used in different studies; however, the ideal dose for the specific patient still has to be elucidated. In the ASTAMI trial [68] only low numbers of mononuclear cells (~60-70Mio) and CD34 positive cells (~0.7Mio) have been used when compared to the BOOST study (Bo-ne Marrow Transfer to Enhance ST-Elevation Infarct Regeneration) in which the number of applied mononuclear and CD34 positive cells were much higher (~240Mio mononuclear cells and ~10Mio CD34 positive cells) [55]. This discrepancy of cell numbers in the ASTAMI trial may be a reason why no significant benefit with regards to ventricular function, end-diastolic volume and infarct size could be detected, while the BOOST trial demonstrated at least a significant temporary increase of ventricular function in the treated patients when compared to the control group. In the TOPCARE-AMI-Study (Transplantation of Progenitor Cells and Regeneration Enhancement in Acute Myocardial Infarction) a significant increase of ventricular function was reported for patients who had received a mean of $24{,}5\times10^{7}$ mononuclear cells and 7×10^{6} CD34 positive cells [54]. So far, when using the current available delivery modes, the retention of the cells in the myocardium after injection has been reported to be limited. In parallel, when an improved retention has been reported, the

engraftment and more importantly survival of these cells were also demonstrated to be very low [69].

1.2 Part B Heart Valve Tissue Engineering

1.2.1 Valvular Heart Disease and current therapy options

Valvular heart disease represents a major global disease load with an increasing number of patients in the developed world suffering from degenerative valve disease as well as an increasing patient cohort in the developing countries due to rheumatic diseases [70-72]. For this reason VHD is a significant cause of morbidity and mortality worldwide [73] with more than 20 000 deaths in the United States every year (Rosengart et al. 2008). More than 250,000 heart valve replacements are performed worldwide per annum [74] with a continuously increasing tendency that is expected to have tripled by the year 2050 [75]. Surgical heart valve replacement using mechanical or bioprosthetic prosthesis represents the most common therapy for end-stage valvular disease and is a safe and efficient approach. Although current available prostheses demonstrate excellent structural durability [70, 76-78], several limitations remain unsolved including the lack of growth capacity as well as in-vivo repair and remodeling properties. Mechanical valves are known to have an increased risk of thromboembolic events due to a non-physiological flow pattern and the associated high shear stress permanently causing erythrocyte damage. A lifelong anticoagulation therapy is required for these patients carrying a risk of spontaneous bleeding and embolism [79]. Bioprotheses, either originating from animals (xenografts) or from human donors (homografts), do not require lifelong anticoagulation but are more prone to dysfunctional, degenerative processes requiring high-risk redo operations. Therefore, these prostheses are less suitable for middle-aged and younger patients [76, 77, 80].

The native heart valve consists of living tissue with the capacity to continuously adapt to the hemodynamic environment [81]. None of the above mentioned prostheses is capable to fully replace the native valvular function due to the lack of these adaptive properties. In theory, the use of cryopreserved donor heart valves would represent an ideal concept with a low risk for thromboembolic events and infection. However, the real clinical world appears to be quite different due to the shortness of these prostheses, bearing in mind the number of indigent patients is permanently increasing [82]. Current therapy options of heart valve replacements are still suboptimal and the ideal concept needs to be developed [75].

1.2.2 The Evolution of Transcatheter Valves

The therapy for valvular heart disease is currently undergoing rapid changes. In addition to conventional surgical valve replacement, representing the gold standard for several decades now, transcatheter techniques have been introduced into the clinical arena for the treatment of elderly high-risk patients. Current data demonstrate satisfactory hospital outcomes and mid-term results [83-87]. While the conventional approach provides very precise and safe suturing of standard valves with low failure rates and excellent proven long-term outcomes [70, 76-78], transcatheter

techniques can be performed in off-pump beating-heart fashion that can also be performed without general anesthesia in selected patients. As it is long-term safety proven via clinical, randomized trials, it can be assumed that the indications for this minimally invasive procedure will be continuously extended towards younger and less riskful candidates. Driven by the idea of implanting stented valves into the aortic annulus in the 1990s, the *first-in-man* transcatheter aortic stent-valve implantation was performed by Dr. Cribier in Rouen, France [88] in the beginning of 2002. Two specific routes for implantation have been established since then: the antegrade way via a surgical, direct transapical access, and the retrograde way using a transfemoral catheter-based concept [85, 89]. The transapical approach requires a left anterolateral mini-thoracotomy followed by a pledged purse-string suture to enter the apex, whereas the transfemoral method requires an adequate peripheral vascular access and can be performed fully percutaneously (figure 4).

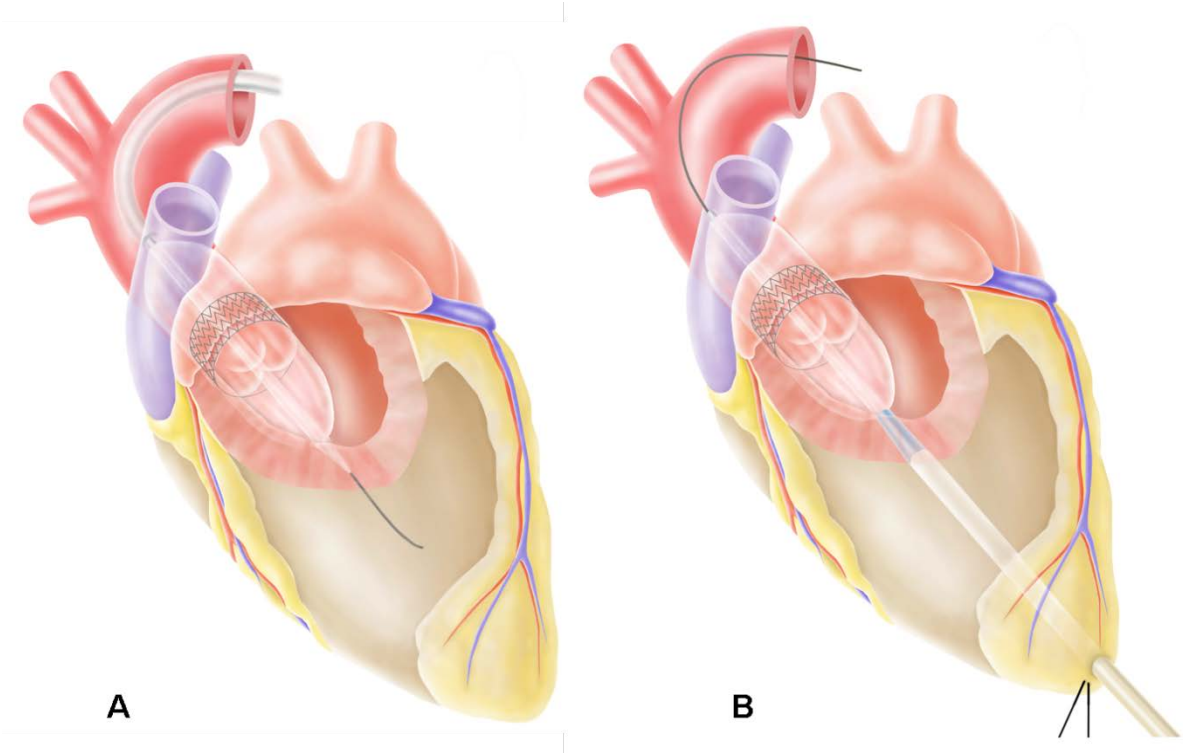

Figure 4: The concept of transcatheter heart valve implantation: *Transcatheter valves can either be implanted via a retrograde, transfemoral approach (A) or via an antegrade transapical approach (B).*

The main advantages of the transapical technique are the independence from concomitant peripheral vascular disease and previous aortic surgery. Furthermore, the delivery system appears to be more “steady” and the procedure itself more “straightforward”. This access potentially reduces the risk of calcium embolism which may occur when a stiff trans-femoral device passes from a peripheral vessel into a diseased aortic arch. The major benefit of the transfemoral approach is the feasibility of a fully percutaneous implantation in conscious patients. However, this only applies to patients with absence of peripheral artery disease and an adequate caliber (>6 mm diameter) of their not very tortuous peripheral vessels.

Since the breakthrough of transcatheter techniques in 2002, two different suture-less transcatheter aortic stent valves have been developed and were successfully introduced into the current clinical routine: the Edwards Sapien™ THV stent-valve system by Edwards Lifesciences INC, Irvine, CA, and

the CoreValve® system by Medtronic, Minneapolis, MN. Numerous other devicescurrently under clinical investigation are arising on the clinical horizon comprising of the Medtronic Engager® Valve, JenaValve® System, the Symetis® Valve as well the St. Jude Portico® system.

1.2.3 The Concept of Tissue Engineering

Tissue engineering technologies may potentially overcome the limitations of current available heart valve prostheses by creating living autologous valve replacement substitutes that may prevent from an immune reaction, valvular degeneration and thromboembolic events, while offering the significant advantages of growth capacity, remodelling, and regeneration throughout the patient's lifetime. The principle idea of tissue engineering is the generation of autologous living tissues being equal in architecture and function to their native counterparts. Therefore, a meticulous understanding of the fundamental characteristics of native tissue represents the key factor for the successful generation of native analogous tissue-engineered constructs. While none of the currently available valvular replacement prostheses are capable to fully restore the native function due to the limited long-term adaptive capacity [90], the compose of living, dynamic tissue is capable of continuous remodelling. Therefore, native heart valves are permanently adapting to the constantly alternating hemodynamic situation in the circulation [91]. The central dogma of most tissue engineering concepts is the use of temporary, biodegradable supporter matrices in order to support tissue functionality and stability during the engineering process until a sufficient amount of neo-tissue is produced to achieve an adequate physiological function [90]. In the early nineties, Langer and Vacanti summarized the early milestones in the field and defined the original tissue engineering concept. This paradigm comprises of three main steps: (1) a temporary, biodegradable supporter matrices (scaffold) that is seeded with autologous cells that are isolated from the recipient in advance, (2) in-vitro culturing, pre-conditioning and tissue formation and (3) in-vivo remodeling and tissue growth post implantation [92] which may involve the endogenous attraction and recruitment of the recipient’s inflammatory cells resulting in a compilation of in vitro seeded and in vivo recruited cells within the TEHV [93]. The entire in vitro and in vivo process of neo-tissue formation, cell proliferation and migration comprises on the one hand of efficient extracellular matrix production and organization, and simultaneously on the other hand of controlled scaffold degradation to ensure the long-term success of the living valve replacement representing a key factor for a safe translation into future clinical therapy strategies [91, 94].

1.2.4 Strategies in tissue engineering: in vitro, in vivo or in situ?

While various approaches of heart valve tissue-engineering have been evaluated in the past, three major tissue engineering strategies have been established to generate living autologous constructs: The in vitro, the in vivo and the in situ concept. According to the original approach described by Langer and Vacanti [92], the in-vitro concept aims at the complete in vitro generation of the tissue engineered heart valve. In contrast, the in vivo approach completely circumvents the in vitro tissue culturing period by implantation of a scaffold into the body (e.g. intraperitoneal) which will then, after sufficient neo-tissue formation in vivo, serve as a valve substitute [95].

The third concept, the in-situ tissue-engineering approach is based on the intrinsic regenerative capacity of the body. Either decellularized heart valves (xenogenic or allogenic) or synthetic scaffold materials are implanted directly, without in-vitro pre-seeding, aiming at the in vivo recruitment of circulating endogenous cells [90, 96]. In addition, based on the idea of endogenous cell recruitment, the direct seeding of the substitute prior to implantation with autologous stem cells including progenitor and/or mononuclear cells may further enhance the attraction of endogenous cells supporting the remodeling process and the neo-tissue formation process via recently described chemo-attractive paracrine pathways [97].

1.2.5 Starter Matrices for heart valve tissue engineering

Currently different types of scaffold / starter matrices comprising biodegradable polymers, natural materials such as fibrin and collagen, and xenogenic or allogenic decellularized heart valves are under evaluation for tissue engineering concepts [90, 98]. In principal, the design of a scaffold should be adapted to the native counterpart as exactly as possible and the scaffold should be capable of sufficient cellular growth including cell-to-cell interaction and neo-tissue formation displaying an organ specific extracellular matrix. The surfaces of these starter matrices must provide sufficient biocompatibility including a significant potential of cellular in-growth, as well as an optimized degradation rate for cellular expansion [99]. Decellularized xeno- or homografts are advantageous as they closely resemble native human valve geometry and structure, and have optimal mechanical and hemodynamic properties. When using xenografts in the clinical setting the important risks of zoonoses, such as Creutzfeldt-Jakob disease and infections with porcine endogenous retroviruses remain. However, the availability of homografts is limited. Besides the unlimited availability, synthetic scaffold matrices have the significant advantage to avoid the risk for xenogenic diseases. Various biodegradable polymers, such as PGA, P4HB and PCL [100-103], and natural materials, such as fibrin and collagen [104-107], were demonstrated to be useful for tissue-engineering of heart valves [108-116]. One of the most frequently used scaffolds is the combination of PGA coated with P4HB as it can easily be molded into the desired shape, presents with excellent thermoplastic properties and optimal porosity [108-110, 112, 117-122].

1.2.6 Cell Sources

The selection of the ideal cell type is an important aspect for the long-term success of heart valve tissue engineering [91, 121] and currently different cell sources are under evaluation [90, 112, 116, 121-125].

Vascular cells

The use of vascular cells derived from various saphenous and arterial vessels is an established approach for heart valve tissue engineering [121].In brief, two cell types can be isolated: Endothelial cells (ECs) with antithrombogenic properties and myofibroblasts which are capable to develop extracellular matrix (ECM) [114, 115, 126]. Following preliminary data in sheep [79, 109, 114, 115,

117, 118, 126, 127], human vascular-derived cells revealed sufficient tissue formation after seeding on biodegradable scaffolds [118, 122, 128, 129].

Marrow stromal derived stem cells

Marrow stromal cells (MSCs) traditionally derived from the bone marrow represent an ideal, clinically relevant cell source with regards to availability, safety and regenerative potential [79, 108, 130]. MSCs were successfully used for the in vitro production of heart valves [108, 130], and also demonstrated sufficient in vivo functionality [111]. When compared to vascular cells, these cells can be harvested without the necessity of surgical interventions and can be considered as an easy-to-access cell source. In brief, the utilization of MSCs offers several advantages in a) easy harvest by a simple bone marrow puncture (hip puncture or sternal puncture); b) high regenerative potential due to the capacity to differentiate into multiple cell lineages, and c) advantageous immunological characteristics allowing for clinically relevant allogenic scenarios. MSCs display a significant similarity to valvular interstitial cells [131], show antithrombogenic properties and can be used in the allogenic setting. Importantly, their capability to promote in-vivo endothelialization may circumvent the necessity of preseeding with endothelial cells. Moreover, MSC are able to differentiate into endothelial cells, fibroblasts or myofibroblasts, and smooth muscle cells [132]. In a recent report, MSCs were harvested via bone marrow puncture, were seeded onto scaffolds and successfully implanted in sheep and baboons using a trans-apical approach [26-28]. The aim of these proof-of-concept studies was to stimulate the homing and differentiation of endogenous cells via paracrine pathways inducing the secretion of growth and chemotactic factors enabling tissue remodeling and regeneration [133].

Endothelial progenitor cells (EPCs)

Endothelial progenitor cells can easily be isolated from peripheral blood [134] which has been established as a source of ECs [134, 135]. While representing an easily accessible cell source, the current focus of research aims at their potential to trans-differentiate into myofibroblast-like cells. Its potential proven, the blood may represent an interesting cell source for heart valve tissue engineering [90].

Umbilical cord derived Cells

The umbilical cord represents a valuable source of different cell types that can be used for heart valve tissue engineering: (1) umbilical cord vein-derived and artery-derived cells, (2) Wharton's Jelly-derived MSCs, and (3) umbilical cord blood-derived EPCs. These cells have been repeatedly demonstrated a high regenerative potential, excellent tissue formation and growth capacities [123, 124, 136, 137]. The feasibility using umbilical cord derived stem cells to generate different cardiovascular constructs was recently demonstrated [113, 123, 124] suggesting this cell source to be clinically relevant.

Adipose Tissue derived mesenchymal stem cells

Similar to the bone marrow, the adipose tissue also contains mesenchymal stem cells with the potential to differentiate into multiple lineages in vitro [138, 139] and in vivo [140, 141]. Due to the easy access and the high availability, adipose-derived stem cells are likely to represent an alternative stem cell source when compared to the bone marrow derived MSCs [142].

Prenatal Progenitor Cells

When focussing on paediatric tissue engineering, an ideal concept would comprise of a prenatal fetal cell harvest giving the opportunity for tissue engineering processes during pregnancy followed by the implantation instantly after birth [90]. Based on this concept, Schmidt et al. successfully generated autologous heart valve leaflets using human prenatal progenitor cells derived from chorionic villi and umbilical cord blood [123]. The fabrication of living autologous heart valves prior to birth using human amniotic fluid-derived cells could be demonstrated [112, 143].

1.3 Rationale and outline of the thesis

The concept of regenerative medicine comprising cell-based therapies, bio engineering technologies and hybrid solutions has been suggested as a promising next generation approach to address cardiovascular diseases including myocardial infarction and Valvular Heart Disease. Although these regenerative strategies have shown great potential in experimental studies, the translation into a clinical setting has either been limited or has been too rapid and premature leaving many key questions unanswered. The major aim of this thesis is the systematic development of translational, marrow stromal cell-based bio-engineering concepts addressing myocardial regeneration in the setting of myocardial infarction (part A) as well as VHD (part B) with a particular focus on minimally invasive, catheter-based implantation techniques.

In part A, the human heart was assessed for its intrinsic regeneration capacity and human marrow stromal cells were characterized and defined as a benchmark cell type for cardiovascular applications (Chapter 2).

Thereafter, a unique ovine fetal transplantation model was developed to address key questions in human stem cell research comprising in-vivo cell fate, bio-distribution and cell tracking (Chapter 3).

In order to improve the integration and survival of transplanted stem cells in the myocardium, a three dimensional marrow stromal cell-based delivery format (“preorganized” microtissues) was developed in-vitro and applied in vivo using a minimally invasive, catheter-based, intra-myocardial approach in a porcine model (Chapter 4).

In part B, marrow stromal cells were then used to develop a unique autologous, cell-based engineered heart valve concept comprising minimally-invasive techniques for both, cell harvest and valve implantation. The results of these experiments demonstrated the principal feasibility of transcatheter stem cell-based TEHV-implantation into the pulmonary and aortic position within a novel one-step intervention of approximately 2hours. This may significantly simplify classical heart valve tissue engineering concepts requiring cell culturing and bio-reactor based preconditioning. In a systematic manner using preclinical animal models the low pressure system (pulmonary valve) (Chapter 5) and the high pressure system (aortic valve) was challenged (Chapter 6).

Finally, the main findings of the thesis are discussed in chapter 7. Current challenges and implications for future research are presented to further develop these promising concepts towards the translation into the clinical setting.

Chapter 2

Higher frequencies of BCRP^{+} cardiac resident cells in ischemic human myocardium

The contents of this chapter are part of **Emmert MY,** Emmert LS, Martens A, Ismail I, Schmidt-Richter I, Gawol A, Seifert B, Haverich A, Martin U, Gruh I. *Higher frequencies of BCRP+ cardiac resident cells in ischemic human myocardium.* Eur Heart J. 2012 Jun 26. [Epub ahead of print]

Abstract

Aims: Several cardiac resident progenitor cell types have been reported for the adult mammalian heart. Here we characterize their frequencies and distribution pattern in non-ischemic human myocardial tissue and after ischemic events.

Methods and Results: We obtained 55 human biopsies from atria and ventricles and used immunohistological analysis to investigate two cardiac cell types, characterized by the expression of BCRP/ABCG2 (for side population cells) or c-kit. Highest frequencies of $BCRP^+$ cells were detected in right atria with a median of 5.40% (range: 2.48%-11.1%) vs. 4.40% (1.79%-7.75%) (p=0.47). Significantly higher amounts were identified in ischemic compared to non-ischemic ventricles 5.44% (3.24%-9.30%) vs. 0.74% (0%-5.23%) (p=0.016). Few numbers of $BCRP^+$ cells co-expressed the cardiac markers titin, sarcomeric α-actinin or Nkx2.5; no co-expression of BCRP and progenitor cell marker Sca1 or pluripotency markers Oct-3/4, SSEA-3 and SSEA-4 was detected. $C\text{-}kit^+$ cells displayed higher frequencies in ischemic (ratio: 1:25,000±2,500 of cell counts) vs. non-ischemic myocardium (1:105,000±43,000). $BCRP^+/c\text{-}kit^+$ cells were not identified. Following *in vitro* differentiation, $BCRP^+$ cells isolated from human heart biopsies (n=6) showed expression of cardiac troponin T and α-myosin heavy-chain, but no full differentiation into functional beating cardiomyocytes was observed.

Conclusion: We were able to demonstrate that $BCRP^+/CD31^-$ cells are more abundant in the heart than their $c\text{-}kit^+$ counterparts. In the non-ischemic heart they are preferentially located in the atria. Following ischemia, their numbers are elevated significantly. Our data might provide a valuable snapshot at potential progenitor cells after acute ischemia *in vivo*, and mapping of these easily accessible cells may influence future cell therapeutic strategies.

Introduction

Stem cell-based therapies might provide alternative therapeutic options to restore myocardial function after damage or disease, which are highly desirable as the heart lacks significant endogenous regenerative potential [144, 145]. With increasing knowledge on stem cell-based therapies new hope has arisen for the treatment of heart failure. Various stem cell types are undergoing evaluation including hematopoietic stem cells [63], endothelial progenitors [146], mesenchymal stem cells (MSC) [147] and the so-called side population cells (SP cells) [148, 149]. Furthermore, skeletal myoblasts [150] as well as embryonic stem cells (ESC) [151] or induced pluripotent stem cells (iPS) [152, 153] are being considered. However, the lack of efficacy, non-specific differentiation, clinical safety issues as well as the ethical debate concerning ESC still limit the clinical application and underline the demand for cardiac-specific stem cell types.

Recent data indicate that the heart is hosting its own stem/progenitor cell populations [154-156] with the capacity to differentiate along all cardiac cell lineages [155, 157, 158]. These cardiac resident progenitor cells (CRPC) include primitive cells expressing c-kit, the stem-cell-factor receptor (CD117) [158] and sca-1^+ cells detected in mice [154] and in human [159]. Despite their frequent denomination as stem cells, not all these cell types were demonstrated to fulfill the criteria of *bona fide* stem cells as being self-renewing, clonogenic, and multipotent [160]. Martin et al. detected cardiac side population (cSP) cells in the heart [161]. SP cells can be isolated by dual-wavelength flow cytometry because of their capacity to efflux Hoechst dye, a process mediated by the ATP-binding cassette transporter breast cancer resistance protein (BCRP) [148, 149]. BCRP (also known as ABCG2) has been recently reported to play a functional role in modulating the proliferation, differentiation, and survival of cSP cells [162], but is also present within endothelial cells of the human heart [163]. Another CRPC population was isolated by Messina et al. from the murine and human heart, they were the first to demonstrate extensive *in vitro* proliferation of the isolated cells in so-called cardiosphere cultures [14]. *In vitro* cultivation of CRPC might be a decisive step forward for future myocardial restoration requiring large cell numbers.

The expression pattern and frequency of CRPC in healthy or diseased human heart has not been explored so far. Herein we identify and quantify human $BCRP^+$ and c-kit^+ cells in the different compartments of the heart and ischemic vs. non-ischemic myocardium, and assess whether human $BCRP^+$ cells can be considered as cardiac progenitor cells. The detailed clarification of distribution and frequencies of CRPC in ischemic and non-ischemic heart samples might have an important impact on effective stem cell treatment strategies in the future.

Materials and Methods

Patient demographics

After informed consent, fifty-five tissue-samples were obtained from 50 patients (male=32 / female=18). Patients were Caucasians (17-83 years) and suffered either from ischemic heart disease (n=33) or non-ischemic heart-diseases, including valve-disease (n=13), non-ischemic, dilative cardiomyopathy (n=2) and congenital heart disease (n=2). Except three emergency cases including two Left ventricular Assist Device (LVAD) implantations due to ischemic cardiomyopathy (n=2) and one CABG for instable angina (n=1) within the ischemic group, and two heart transplantations due

to dilated cardiomyopathy (n=2) in the non-ischemic group, all others were elective cases. Treatment included, aspirine, angiotensin converting enzyme inhibitors, beta-blockers and others. Demographics are summarized in table 1.

Tissue samples

Tissue samples sized 5x5 millimeters were harvested from all areas of the heart. They were obtained from the right atrium (n=36) after cannulation during coronary artery bypass grafting (CABG). Endomyocardial biopsies of the left atrium (n=4), left ventricle (n=10) and right ventricle (n=5) were taken during CABG and all other open heart procedures. For ischemic patients, after careful intra-operative macroscopic evaluation biopsies were harvested from the border zone of the ischemic/infarcted area of the left ventricle, however not directly from the infarcted area. Samples were fixed in 4% paraformaldehyde for 2 hours following 24 hours in 30% sucrose, embedded in TissueTek (Sakura-Finetek), frozen in liquid nitrogen and cut into 6µm sections.

Immunostaining and cell counts

For a quantitative analysis of progenitor cell frequencies, immunostaining was performed in at least four sections of each tissue sample. Positive controls were as follows: $BCRP^+$ trophoblast cells in human placenta (supplemental figure 1A), c-kit^+ melanocytes in human skin (supplemental figure 1B), c-kit^+/$tryptase^+$ mast cells in inflammatory skin lesions (suppleental figure 1C-F); $titin^+$ cells and $CD31^+$ endothelial cells in human cardiac tissue. For pluripotent stem cell markers Oct-3/4, SSEA-3 and SSEA-4, human induced pluripotent stem cell colonies served as positive controls (supplemental figure 2).

In brief, tissue sections were fixed by incubation with 2% paraformaldehyde for 10 min, blocked and permeabilized with TBS buffer containing 0.25% Triton-X 100 (Sigma-Aldrich, Munich, Germany) and the serum of the respective secondary antibody host species. Primary and secondary antibodies (see Supplemental Tables 1 &2) were diluted in PBS with 5% BSA, as were matching isotype control antibodies (from DakoCytomation, Glostrup, Denmark) used for negative control staining. Nuclei were stained by 4',6-diamidino-2-phenylindole (DAPI, Life Technologies Darmstadt, Germany).

Analysis of 4 slides per tissue sample was performed. At least twelve randomized images per slide were collected with an Olympus-IX81 fluorescence-microscope using a F-View-II camera and Olympus-analysisD® software (Olympus; *Tokyo, Japan*). Images were analyzed with ImageJ® software and cell numbers for $BCRP^+$ and c-kit^+ cells were counted in at least twelve randomized microscopic fields per slide. It was discriminated between $BCRP^+$/$CD31^+$ endothelial cells and $BCRP^+$/$CD31^-$ cells. Similarly we discriminated between c-kit^+/mast-cell-$tryptase^+$ mast cells and c-kit^+/$tryptase^-$ resident progenitor cells.

Table 1: Patient demographics

n = 50	**Ischemic (n=33)**	**Non-ischemic (n=17)**
Male	26	6
Female	7	11
Height (cm)	171 ± 7	172 ± 7
Weight (kg)	77 ± 12	80 ± 7
BMI	26 ± 4	27 ± 3
EuroScore	4 ± 3	7 ± 4
Ejection fraction	56 ± 13	53 ± 18
Blood pressure systolic (mmHg)	134 ± 24	136 ± 20
Blood pressure diastolic (mmHg)	71 ± 17	75 ± 11
Smoker	17 (52%)	14 (82%)
Positive family history of any cardiac disease	15 (45%)	11 (64%)
Diabetes Mellitus	9 (27%)	5 (29%)
Hypertension	14 (42%)	12 (70%)
Dyslipidemia	20 (61%)	13 (76%)
Ischemic heart disease	33 (100%)	0 (0%)
Heart Valve disease	0 (0%)	13 (76%)
Dilative Cardiomyopathy	0 (0%)	2 (12%)
Congenital heart disease	0 (0%)	2 (12%)
CABG	23 (70%)	0 (0%)
Heart Valve surgery	0 (0%)	13 (76%)
Combined heart surgery (CABG + Valve)	8 (24%)	0 (0%)
Transplantation due to DCM	0 (0%)	2 (12%)
LVAD Implantation due to ICM	2 (6%)	0 (0%)
Congenital heart surgery	0 (0%)	2 (12%)
Aspirine	27 (82%)	16 (94%)
Beta Blockers	11 (33%)	8 (47%)
ACE Inhibitors	4 (12%)	3 (18%)

CABG = Coronary Artery Bypass Grafting, DCM = Dilative Cardiomyopathy, ICM = Ischemic Cardiomyopathy, LVAD = Left Ventricular Assist Device; *All values are mean (± SD)

Isolation of BCRP$^+$ cells from adult human heart samples

BCRP$^+$ cells were isolated from human cardiac tissue samples using collagenase B and dispase II as described by Pfister et al. [164]. In brief, human cardiac tissue samples were minced in PBS and dissociated into single cells using digestion buffer containing 0.1% collagenase B and 2.4 U/ml dispase II (both from Roche Applied Science, Mannheim, Germany) as described by Pfister et al. 2010. After filtration with a 100µm and a 40µm cell strainer, BCRP$^+$ cells were enriched by immunomagnetic bead separation using a primary rat-anti BCRP antibody (clone BXP-53, Enzo Life Sciences, Loerrach, Germany) together with Anti-Rat IgG MicroBeads, LS separation columns and a MidiMACS Separator according to the manufacturer's instructions (all from Miltenyi Biotec, Bergisch-Gladbach, Germany).

***In vitro* differentiation of BCRP$^+$ cells**

Cells were seeded into 24well plates (Nunc/Thermo Fisher Scientific) after coating with Matrigel (1:30, BD Biosciences, Heidelberg, Germany), cell culture medium consisted of 80% IMDM (with Glutamax), 20% fetal calf serum (HyClone/Thermo Fisher Scientific, Bonn, Germany), 1 mM L-glutamine, 0.1 mM β-mercaptoethanol, 1% non-essential amino acids, 100 µg/ml penicillin and 100 µg/ml streptomycin (from PAA Laboratories, Coelbe, Germany). 24 hours after seeding, cells were treated with 100 nM oxytocin (Sigma-Aldrich, Munich, Germany) for 72 hours as described by Oyama et al. [165].

Gene expression analysis

Quantitative real time PCR was used to determine gene expression of BCRP$^+$ cells after *in vitro* differentiation. In brief, total RNA was prepared from cultured cells using TriZol Reagent (Invitrogen). Contaminating DNA was digested by DNAse I (Fermentas, St. Leon-Rot, Germany) for 30 min at 37°C followed by phenol/chloroform-extraction. After ethanol precipitation, 50-100 ng RNA was used for random-primed cDNA synthesis with the RevertAid™ H Minus First Strand cDNA Synthesis Kit (Fermentas). For quantitative real-time PCR analysis, 1 µl of cDNA was amplified with the ABsolute^{TM} QPCR SYBR® Green Mix (ABgene Ltd, Epsom, UK) and 1 µM of each primer in a 25 µl reaction using a Mastercycler® ep realplex2 (Eppendorf, Hamburg, Germany). Sequences of primers were as follows: human β-actin forward 5'-attgccgacaggatgcagaa-3', human β-actin reverse 5'-gggccggactcgtcatactc-3' (product size 176 bp); human α-myosin heavy chain (α-MHC) forward 5'-gatgcccagatggctgactt-3' and human α-MHC reverse 5'-ggtcagcatggccatgtcct-3' (product size 276 bp). PCR conditions included an initial denaturation step at 95°C for 15 min, followed by 40 cycles of denaturation at 95°C for 1 min, annealing at T_A for 1 min, and polymerization at 72°C for 1 min. Uniform size of amplicons and absence of nonspecific products were controlled by melting curves. Relative expression levels compared to the reference gene β-Actin were calculated using the ΔΔCt-method using the Pfaffl equation correcting ΔCt values for differences in PCR efficiencies. Data are presented as mean ± SEM for two independent experiments, each with two PCR runs performed in triplicate.

Results

Morphological assessment of putative progenitor cells detected in the heart

$BCRP^+/CD31^-$ cells were identified in all areas of the heart, appearing mostly small and oval-shaped. They were distributed evenly over the whole microscopic field (figure 1A-C). The major part of these cells did not stain positive for the cardiac marker titin, but were either located between or in close relation to the surrounding cardiomyocytes as well as in the interstitial space. However, also titin-positive $BCRP^+/CD31^-$ cardiac progenitors could be found, albeit in low numbers (figure 1D-F). Some $BCRP^+/CD31^-$ cells stained positive for sarcomeric α-actinin, or the earlier cardiac marker Nkx2.5 for the identification of cardiac progenitor cells (supplemental figures 3 and 4). In $BCRP^+/CD31^-$ cells we did not detect staining for the progenitor cell marker Sca1 (supplemental figure 5) or pluripotent stem cell markers Oct-3/4, SSEA-3 and SSEA-4 (supplemental figures 6 and 7). Single cells expressing Sca1 and Oct-3/4 were observed within the myocardium (supplemental figure 5 and 6). Cells expressing SSEA-3 or SSEA-4 were detected in vessels and single cells staining positive for CD31 (supplemental figure 7), however we did not further analyze these cells.

$BCRP^+/CD31^+$ cells were also detected in all areas, representing endothelial cells with the typical elongated morphology. They were characteristically located in small capillaries and in the inner wall of arterioles (figure 1G-I).

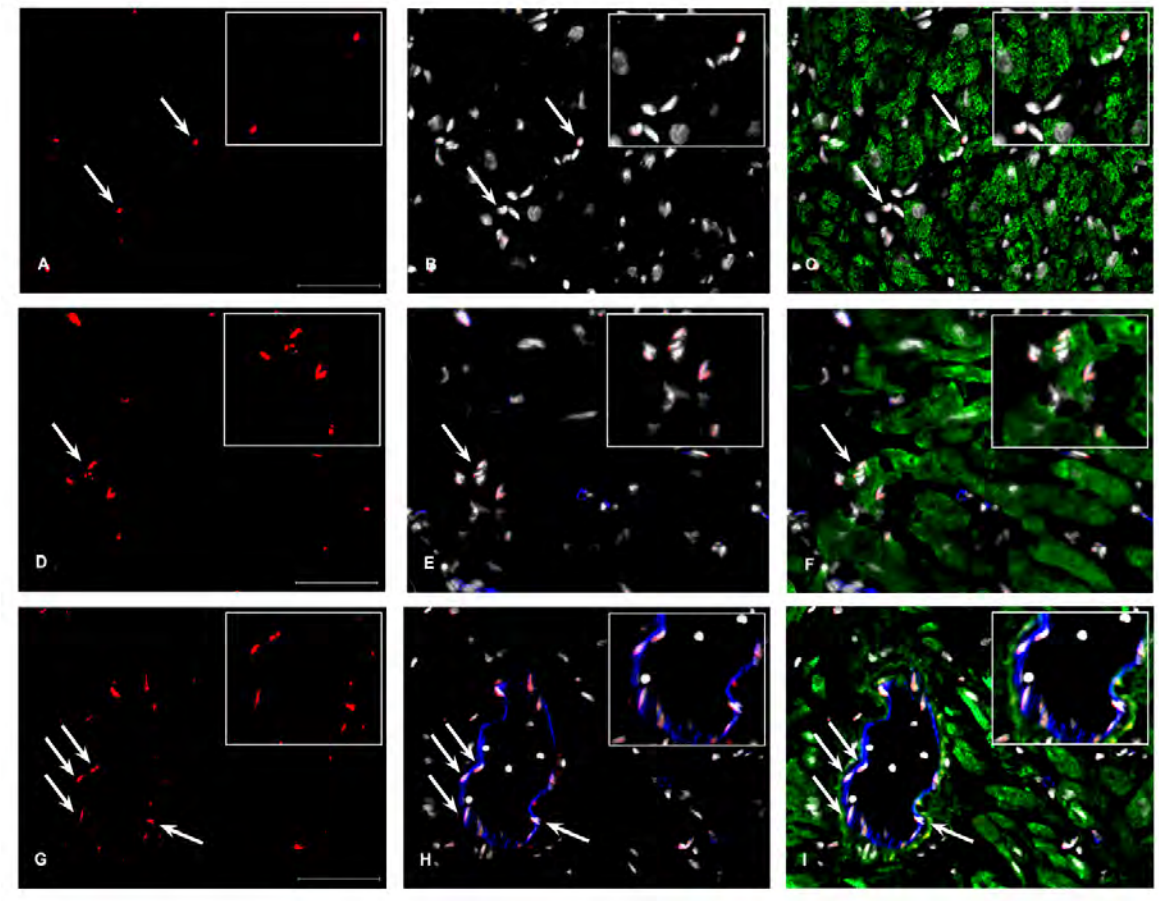

Fig. 1: $BCRP^+$ cells in the adult human heart. Cryosections of heart tissue were stained with antibodies to BCRP (red), titin (green), and CD31 (blue). Nuclei were stained with DAPI (white) (x40). Inset shows cells pointed out by arrows. **A-C** (right atrium/♀/61yrs): $BCRP^+/CD31^-$ cells (arrows) presumably representing resident cardiac progenitors were identified in all areas of the heart. **D-F**

(right atrium/♂/70yrs): A subset of BCRP$^+$/CD31$^-$ cells (arrows) stain also positive for the cardiac marker titin (here: 0.50% of total cell numbers). **G-I** (right atrium/♂/83yrs): BCRP$^+$/CD31$^+$ cells (arrows) representing endothelial cells could be detected in all areas of the heart, mostly located in small capillaries and arterioles. Scale bar: 50 µm.

Resident c-kit$^+$ cells were detected in both ventricles and in the right atrium. These cells were small and round-shaped, without the typical cardiomyocyte morphology, and did not stain positive for cardiac markers (figure 2A-C).

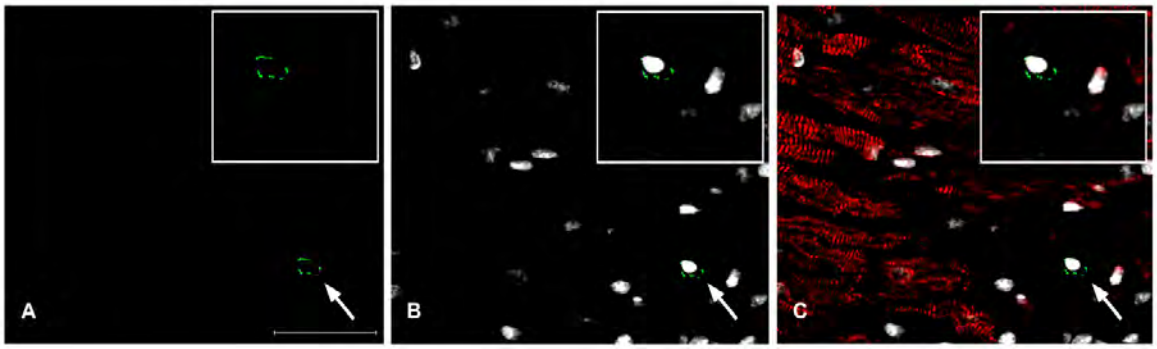

Fig. 2: C-kit$^+$ cells in ischemic human myocardium. Cryosections of adult human heart tissue were stained with antibodies to c-kit (green, indicated by arrows), titin (red), and mast cell tryptase (blue). Nuclei were stained with DAPI (white). Inset shows cells pointed out by arrows. **A-C** Tissue sample (left ventricle/♂/75yrs) after myocardial infarction; very low frequencies of c-kit$^+$/ mast cell tryptase$^-$ cells were detected (arrow), while no mast cells were observed. Scale bar: 50 µm.

Distribution and frequencies

BCRP$^+$/CD31$^-$ cells were found more frequently in ischemic heart (n=33) vs. non-ischemic (n=22) heart with a median of 5.38% (range: 2.48% to 11.1%) vs. 3.57% (0% to 7.75%) (p = 0.026) (figure 3A). In the atria, the highest frequency of BCRP$^+$/CD31$^-$ cells was detected in the right atria of the ischemic group (n=26) with a median of 5.40% (2.48% to 11.10%) vs. 4.40% (1.79% to 7.75%) (p = 0.47) in the non-ischemic group (n=10) (figure 3B). Also in ventricles, a significantly increased number of BCRP$^+$/CD31$^-$ cells was detected in ischemic ventricle (n=6) compared to non-ischemic ventricle (n=9) with median of 5.44% (3.24% to 9.30%) vs. 0.74% (0% to 5.23%) respectively (p=0.016) (figure 3C).

The frequency of BCRP$^+$/CD31$^-$ cells was analyzed with respect to age and gender. In both groups (>65y and ≤65y), BCRP$^+$/CD31$^-$ cells were found more frequently in ischemic heart vs. non-ischemic heart (data not shown). Interestingly, the number of BCRP$^+$/CD31$^-$ cells tended to be higher in the age group >65y than for patients ≤65y years. This was found for the ischemic group with 5.79% (2.48% to 11.10%) BCRP$^+$/CD31$^-$ cells (n=21) vs. 4.74% (2.51% to 7.35%) (n=12), respectively (p=0.24). Similarly, in the non-ischemic samples the number of BCRP$^+$/CD31$^-$ cells was 4.17% (3.57% to 6.23%) (n=7) in patients >65y vs. 1.63% (0% to 7.75%) (n=15) in patients ≤65y (p=0.20).

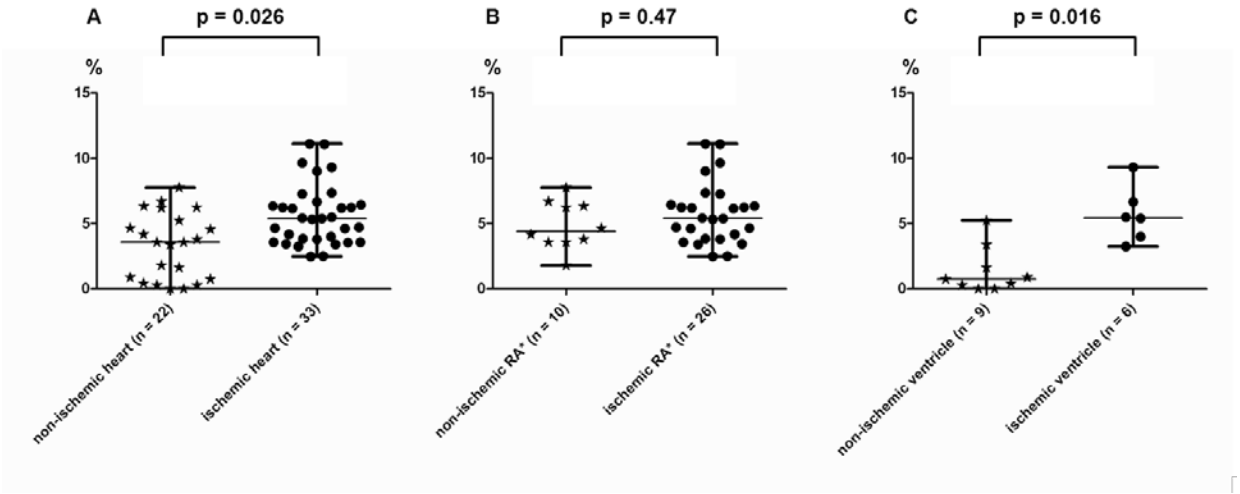

Fig. 3: Higher frequency of cardiac resident BCRP$^+$/CD31$^-$ cells in the ischemic human heart. Distribution and frequencies (percentage of all cardiac cells) of all BCRP$^+$/CD31$^-$ cells in non-ischemic vs. ischemic heart **(A)**, non-ischemic vs. ischemic atria (**B**) as well as non-ischemic vs. ischemic ventricles (**C**). Graphs are shown with median and range. In order to avoid biased estimates for patients that provided more than one cardiac sample, the Mann-Whitney test was performed patient specific. **RA = right atrium*

Analyzing ischemic samples from all parts of the heart, we found a slight tendency towards higher numbers of BCRP$^+$/CD31$^-$ cells in female patients of 5.42% (3.54 to 11.10%) (n=7) vs. 5.01% (2.48% to 9.64%) in male patients (n=26), however, this effect did not reach statistical significance (p=0.35).

BCRP$^+$/CD31$^-$ cells were analyzed for cardiac differentiation in the heart to investigate whether they can be considered as progenitor cells. In 50% of all tissue-samples some BCRP$^+$/CD31$^-$ cells stained positive for the cardiac marker titin, albeit in low numbers (median of 0.36% (0% to 1.27%) vs. 0.18% (0% to 0.39%) (p = 0.013) (figure 4A). The distribution of BCRP$^+$/CD31$^-$/titin$^+$ cells was identified as follows: 0.33% (0% to 0.92%) of cells were detected in the ischemic right atria (n=26) vs. 0.27% (0.08% to 0.39%) in non-ischemic right atria (n=10) (p=0.60) (figure 4B). Higher BCRP$^+$/CD31$^-$/titin$^+$ cell numbers were detected in ischemic ventricles (n=9) compared to non-ischemic ventricles (n=6) (median of 0.50% (0.35% to 1.27%) vs. 0% (0% to 0.39%; p=0.005) (figure 4C).

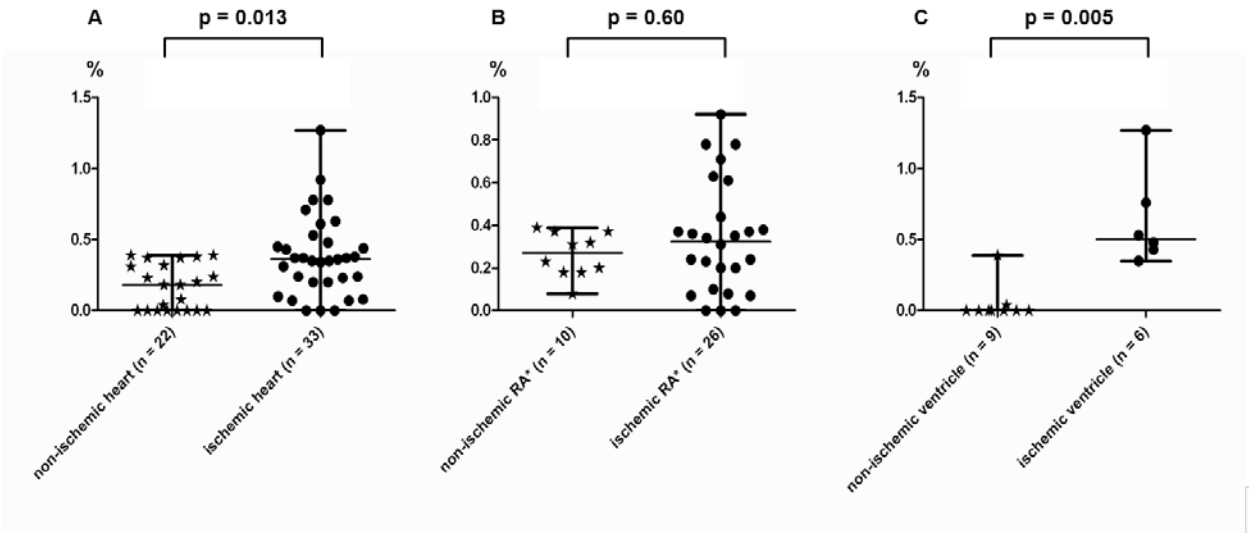

Fig. 4: Higher frequency of Titin$^+$ subsets of BCRP$^+$/CD31$^-$ cardiac resident progenitor cells in the ischemic human heart. Distribution and frequencies (percentage of all cardiac cells) of BCRP$^+$/CD31$^-$/Titin$^+$ cells in non-ischemic vs. ischemic heart **(A)**, non-ischemic vs. ischemic atria (**B**) as well as non-ischemic vs. ischemic ventricles (**C**). Graphs are shown with median and range. In order to avoid biased estimates for patients that provided more than one cardiac sample, the Mann-Whitney test was performed patient specific. **RA = right atrium*

BCRP$^+$/CD31$^+$ cells, representing endothelial cells, were also found more frequently in ischemic heart compared to non-ischemic heart (median of 5.50% (0.91% to 11.98%) vs. 3.14% (0% to 8.33%); p=0.04) (supplemental figure 8). In detail, the distribution pattern of BCRP$^+$/CD31$^+$ cells was identified as follows: 7.37% (5.51% to 11.09%) BCRP$^+$/CD31$^+$ cells were detected in ischemic ventricle vs. 2.18% (0% to 6.89%) in non-ischemic ventricle (p=0.01). In contrast to this, the right atria showed almost the same amount of BCRP$^+$/CD31$^+$ cells in the ischemic (n=26) and non-ischemic group (n=10) (5.27% (0.91% to 11.98%) vs. 4.53% (2.17% to 8.33%); p=0.60).

C-kit$^+$ cells were detected in 30% of the samples and were found in higher numbers within ischemic (ratio: 1:25,000 ± 2,500 of cell counts) vs. non-ischemic myocardium (1:105,000 ± 43,000) including ventricles and the right atrium. The detailed comparison between ischemic and non-ischemic ventricles showed an increased frequency of c-kit$^+$ cells within ischemic ventricle (1:25,000 ± 2,500) vs. either no or only very low numbers of c-kit$^+$ cells (1:120,000 ± 50,000) within non-ischemic ventricle. The cell ratio in ischemic ventricles increased up to fivefold (p=0.022). Although BCRP$^+$ and c-kit$^+$ cells were found in close proximity (figure 5), no BCRP$^+$/c-kit$^+$ double positive cells were detected

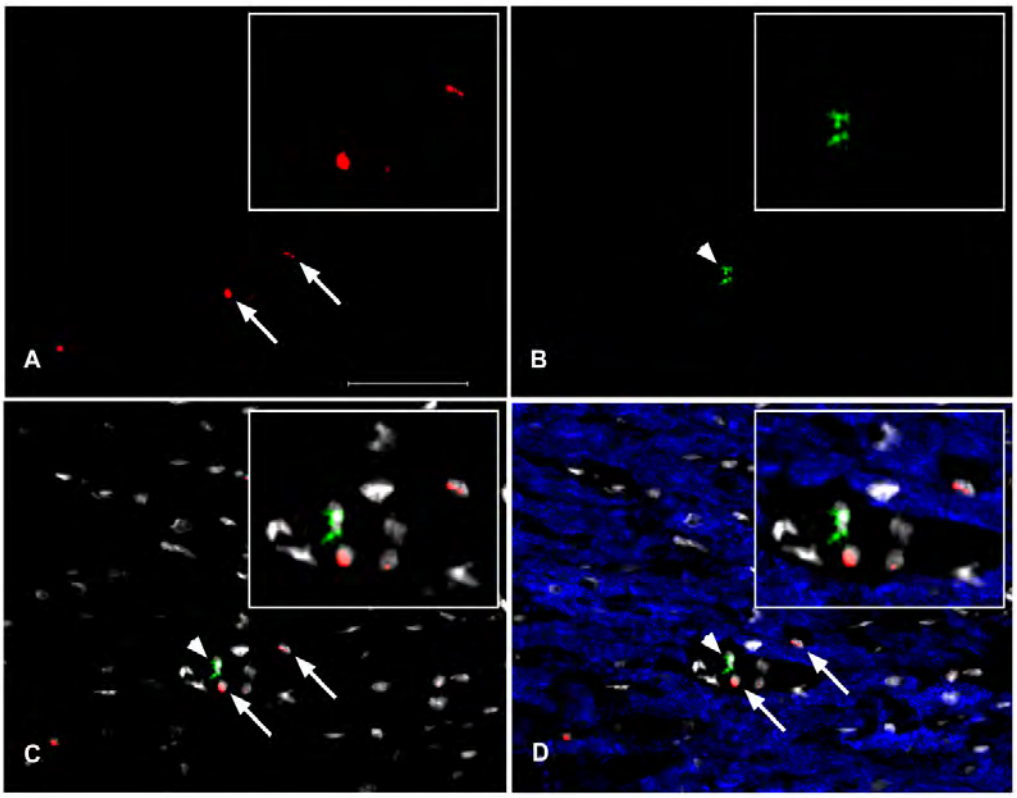

Fig. 5: No c-kit / BCRP double-positive cells detected in the adult human heart.

Tissue sample (left ventricle/♂/53yrs) after myocardial infarction, cryosections were stained with antibodies to BCRP (red, indicated by arrows; **A,C,D**), c-kit (green, indicated by arrowheads; **B,C,D**) and titin (blue; **D**). Nuclei were stained with DAPI (white). Although $BCRP^+$ and $c\text{-}kit^+$ cells were found in close proximity (**D**), no $BCRP^+/c\text{-}kit^+$ double-positive cells were detected. Inset shows cells pointed out by arrows/arrowheads. Scale bar: 50µm

Isolation and *in vitro* differentiation of $BCRP^+$ cells

Using immunomagnetic bead separation, cells were enriched from dissociated human heart samples (n=6) based on their expression of the surface marker BCRP. Co-purified adult human cardiomyocytes did not adhere to the cell culture dishes (supplemental figure 9A) and were removed upon medium exchange. $BCRP^+$ and $BCRP^-$ cells were cultivated on matrigel-coated plates in differentiation medium. $BCRP^-$ cell fractions showed higher proliferation rates than $BCRP^+$ cells and were frequently overgrown with fibroblast-like cells during cultivation (supplemental figure 9B-D). To test for differentiation potential as described by Oyama et al. in the rat model [165] cells were treated with 100nM oxytocin for 72 hours. However, no spontaneous beating of isolated cells was observed during cultivation for 21 days.

After 21 days, no cTnT expression was detected in $BCRP^-$ cells by immunostaining (figure 6D). In contrast, the majority of $BCRP^+$ cells stained positive for cTnT (figure 6E&F), with a diffuse and/or a punctuate dotted linear staining pattern (figure 6F). Interestingly, $BCRP^+$ cells not treated with

oxytocin seemed to display a similar differentiation capacity, a direct comparison of oxytocin-treated vs. untreated cells is given in supplemental figure 10. On day 21, quantitative real time PCR detected an 8.3-fold (± 2.4) increase of α-myosin heavy chain expression in oxytocin-treated $BCRP^+$ cells vs. untreated $BCRP^+$ cells (supplemental figure 10E). However, it has to be noted that the small sample number and size did not allow for statistical analysis or the evaluation of other markers of cardiac differentiation.

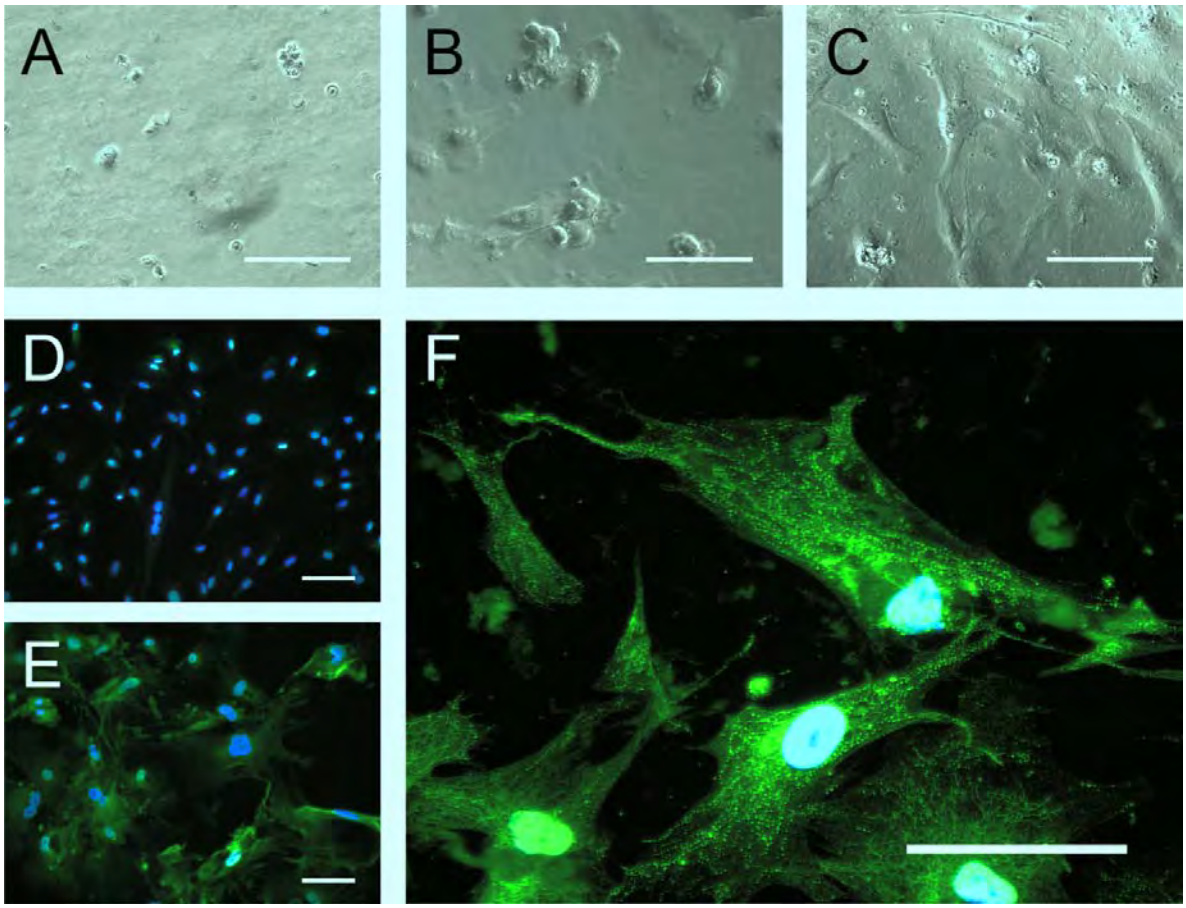

Fig. 6: $BCRP^+$ cells isolated from the adult human heart differentiate *in vitro*.

Morphology of oxytocin-treated $BCRP^+$ cells on d3 (**A**), d14 (**B**) and d21 (**C**) of cultivation. After 21 days of cultivation, cells were fixed and stained for cardiac troponin T (cTnT, green). Nuclei were stained with DAPI (blue). While $BCRP^-$ cells did not express cTnT (**D**), $BCRP^+$ cells stained positive for cTnT (**E, F**) with punctuate dotted linear staining pattern, resembling premyofibrils, in oxytocin-treated cells (**F**). Scale bar: 100 μm.

Discussion

It was proposed that the cardiac SP cell population functions as a progenitor cell population for the development, maintenance, and repair of the heart [161]. Oyama et al. were the first to demonstrate that cSP cells from postnatal rat hearts can differentiate into spontaneously beating cardiomyocytes after induction with non-toxic/-carcinogenic reagents such as oxytocin, as well as into other cell lineages, including endothelial cells and smooth muscle cells [165]. These results

support the concept that BCRP$^+$/CD31$^-$ side population cells might be a possible source for regeneration.

BCRP$^+$ cells in the adult human heart

In this study, BCRP$^+$/CD31$^-$ cells were detected in atrial tissue of ischemic but also in non-ischemic patients in very similar levels. From the clinical point-of-view the occurrence of CRPC even in non-ischemic atria as described by Urbanek et al. [166, 167] poses an excellent opportunity for a safe isolation during heart surgery or even by catheterization. Interestingly, there was a significant increase of BCRP$^+$/CD31$^-$ cells in ischemic compared to non-ischemic ventricle. These results might reflect repair mechanisms which are activated after ischemic events. In the murine setting, Pfister et al. found that *in vitro* cardiomyogenic differentiation was exclusively observed in cardiac SP cells lacking CD31 [168]. For the human heart, a potential activation and mobilization of these CRPC *in vivo* by a local cytokine application as proposed by Urbanek et al. [166, 167] might be optimized by help of a detailed CRPC mapping. The localization of BCRP$^+$ cells in non-ischemic atria is in line with previous reports on the special role of the atria for c-kit$^+$ cells, described as protected niches located in anatomical areas exposed to low levels of wall stress [169], with higher numbers of cardiac progenitor cells produced from right atrial tissue than obtained from other parts of the heart [170].

Meissner et al. reported that ABCG2 is variably expressed in endothelial cells of the human heart [163]. In our study, BCRP$^+$/CD31$^+$ endothelial cells [165, 168] were detected in all areas of the heart within capillaries and small arterioles. Higher numbers were detected in ischemic as well as in non-ischemic atria and after myocardial infarction increased numbers were identified in the ischemic area of the ventricle, probably supporting angiogenesis. Only a few BCRP$^+$/CD31$^-$ cells expressed the cardiac marker titin. Likewise, individual BCRP$^+$/CD31$^-$ cells were found to express other cardiac markers such as sarcomeric α-actinin and Nkx2.5; however their frequency was not quantified in this study. At the same time, the absence of expression of Oct-3/4, SSEA-3 and SSEA-4 in BCRP$^+$ cells clearly indicates the lack of pluripotency. Based on these data, we assume that the BCRP$^+$ cell population described in this study might represent an already committed mesodermal progenitor state, as described by Ott et al. [171]. As we did not detect human BCRP$^+$/Sca1$^+$ cells, we conclude that the progenitor cell population described in our study is not identical to the Sca1$^+$ progenitor population found earlier in the human heart [159]. However, we cannot rule out heterogeneous Sca1 expression in a subset of human BCRP$^+$ cells, as was described for the mouse heart [168, 172].

C-kit$^+$ cells in the adult human heart

Additionally, we were able to confirm the presence of c-kit$^+$ CRPC in the adult myocardium [158, 173], with higher frequencies (up to fivefold) in ischemic ventricles and much lower numbers in the non-ischemic myocardium. A comparison of progenitor cell frequencies observed in the human heart is difficult. Earlier reports used a variety of units, e.g. c-kit$^+$ cells per 100 mm^2 [157, 158], c-kit+ cells per cm^3 (x 10^3) [166, 167] (reviewed in [174, 175], there: cells per mm^3) or c-kit$^+$ cells as percentage of the entire cell population [16]. The latter publication described a frequency of c-kit$^+$ cells of 1.1 % ± 1.0 % after enzymatic dissociation of about 60 mg myocardial tissue (n=6). Highest numbers of c-kit$^+$ cells with 8.9% ± 0.4 % were reported for the right atrium of neonatal children <

30d of age [176]. Numbers of c-kit$^+$ cells found in our study in adult patients are significantly lower, with about 0.004% in the non-ischemic samples and 0.001% in the ischemic samples. However, our data are in line with independent reports on frequencies of c-kit$^+$ cells of about 0.002% in the adult human heart [177]. C-kit$^+$ resident cells did not stain positive for the cardiac marker titin. In compliance with the CRPC classification by Anversa et al. [174, 175], these cell types are considered rather primitive. Furthermore, we could show that there were no c-kit$^+$/BCRP$^+$ co-expressing stem/progenitor cell populations. This suggests that these two markers are expressed by two distinct cell populations in the human heart as was already proposed by Anversa et al. for various species [174, 175, 178].

In vitro differentiation of BCRP$^+$ cells isolated from the adult human heart

Although elevated numbers in ischemic human heart might indicate a regenerative role for BCRP$^+$ cells, currently there is no proof of a direct link between progenitor cell numbers and myocardial restoration *in vivo*. As described for other stem/progenitor cell types, a variety of mechanisms is possible: The cells could: i) differentiate into tissue specific cells, ii) induce growth and differentiation through secreted factors, iii) attract immune cells and affect their cytokine production, or iv) secrete anti-apoptotic factors [179]. To investigate potential differentiation into cardiomyocytes, we performed first *in vitro* experiments using BCRP$^+$ cells isolated from human heart tissue samples. In contrast to reports from Oyama et al. describing spontaneous beating of cardiomyocytes derived from rat side population cells [165], we did not observe beating of BCRP$^+$ cells isolated from human heart tissue at any time. This might be in line with reports by Yamahara et al., who did not find the generation of spontaneously beating cells from murine cardiac SP cells [172]. It is currently unknown whether further optimized culture conditions for individual species, and/or prolonged cultivation periods of more than 3 weeks could lead to full cardiac differentiation of human BCRP$^+$ cells. After cultivation for 21 days, we observed that a majority of BCRP$^+$ cells displayed diffuse staining of troponin T, moreover, some cells showed periodically localized foci of intense labeling. While we did not detect a mature sarcomeric organization, this staining pattern might represent premyofibrils before lateral alignment [180], as sometimes observed for early stages of cardiac differentiation in primate embryonic stem cells [181]. The interesting observation that both oxytocin-treated and untreated BCRP$^+$ cells displayed troponin T expression in our study, might be explained by the fact that both were cultivated in differentiation medium containing a distinct lot of FCS selected for efficient cardiac differentiation of human iPS cells. According to our quantitative PCR data, higher levels of α-MHC seem to be expressed in oxytocin-treated BCRP$^+$ cells, however, the small sample number and size did not allow for statistical analysis. Although we cannot fully exclude the possibility that BCRP$^+$ cell cultures were contaminated with adult human cardiomyocytes, potentially contributing to α-MHC expression levels, such a contamination can be considered unlikely because of the absence of beating cells at any time. In our setting, troponin T staining in the majority of cells showed that human BCRP$^+$ cells can adopt some markers of immature cardiomyocytes *in vitro*. In contrast to rat cells, however, we were did not observe full differentiation into functional beating cardiomyocytes or other cardiac cell types, therefore it remains unclear whether they could represent cardiac progenitor cells in the human heart. This might argue for fundamental species differences with respect to differentiation potential and the physiological role of cardiac BCRP$^+$ progenitor cells, similar to differences in differentiation capacity

observed for mesenchymal stem cells or cardiospheres [14, 182]. Although the significantly increased number of those cells in the ischemic myocardium strongly suggests an important role in regeneration processes, the formation of functional *de novo* myocardium from human cardiac $BCRP^+$ progenitor cells appears rather unlikely. Clearly, further studies will be needed to fully characterize the regenerative potential of this interesting cell population from the adult human heart.

Conclusion

In conclusion, we were able to demonstrate that $BRCP^+/CD31^-$ cells are more abundant in the human heart than their c-kit^+ counterparts. In the non-ischemic heart they are preferentially located in the atria. Following ischemia, their numbers are increased significantly and, most interestingly, the highest change can be found in the left ventricle. At the same time, also the number of these $BCRP^+$ cells expressing the cardiac marker titin is highest in the left ventricle. $BCRP^+$ cells could be isolated from the human heart and adopted certain markers of immature cardiomyocytes *in vitro*, however without differentiation into beating cells. Therefore, our data might provide a valuable snapshot at cardiac progenitor cells after acute ischemia, even though absolute numbers of cells acquiring a myocardial phenotype are low and the overall impact on cardiac regeneration *in vivo* has to be investigated in the future.

Study Limitations

In this proof of concept study, the patient cohort displayed certain heterogeneity, and only a minimal data set was collected for each patient with regards to demographic profiling. Therefore, in subsequent studies when including higher numbers of patients, it may be of value to correlate more specific patient characteristics (including complete medication) with the expression and frequencies of BCRP cells. Additionally, we restricted our study to c-kit^+ and $BCRP^+$ cells and did not evaluate the frequency and distribution of further cardiac stem and progenitor cell populations such as sca-1^+ cells.

Clearly, expression of titin in a subpopulation of human $BCRP^+$ cells *in vivo*, as well as cardiac troponin T and α-MHC expression *in vitro* indicate that BCRP+ cells acquire certain myocardial characteristics *in vivo* and might have progenitor potential; however, it is uncertain whether human $BCRP^+$ cells can form functional beating cardiomyocytes similar to rat cells. In case of c-kit^+ cells, the low numbers detected in our study might argue against a pivotal role in regenerative processes in the human heart. Furthermore it has to be noted that the small number and size of myocardial tissue samples did not allow for statistical analysis or the evaluation of other markers. Further investigation will be needed to thoroughly assess the role of human $BCRP^+$ and c-kit^+ cells in endogenous cardiac regeneration and their impact for regenerative therapies.

Acknowledgements:

The authors would like to thank Prof Dr Theo Kofidis for organizing the sample collection and for helpful discussions. We thank PD Dr Otmar Pfister for helpful suggestions, David Skvorc for excellent technical assistance and PD Dr. Sacha P. Salzberg for revising the language of the manuscript.

Statistical analysis

Descriptive data are presented as mean ± standard deviation or median with range where appropriate. For statistical analysis using SPSS 18 (SPSS Inc., Chicago, IL) the Mann-Whitney Test was performed. In order to avoid biased estimates for patients that provided more than one cardiac sample (n=3), medians of samples within patients were computed and the Mann-Whitney test was performed patient specific (n=50). Significance was evaluated by two-tailed testing, and assumed at $p<0.05$.

Chapter 3

Intramyocardial transplantation and tracking of human mesenchymal stem cells in a novel intra-uterine pre-immune fetal sheep myocardial infarction model: A proof of concept study

The contents of this chapter are part of **Emmert MY,** Weber B, Wolint P, Frauenfelder T, Zeisberger SM, Behr L, Sammut S, Scherman J, Behnke S, Brokopp CE, Schwartländer R, Vogel V, Vogt P, Grünenfelder J, Alkadhi H, Falk V, Boss A, Hoerstrup SP. *Intramyocardial transplantation and tracking of human mesenchymal stem cells in a novel intra-uterine pre-immune fetal sheep myocardial infarction model: A proof of concept study.* PLOS ONE 2013; *in press*

Abstract

Although stem-cell therapies have been suggested for cardiac-regeneration after myocardial-infarction (MI), key-questions regarding the in-vivo cell-fate remain unknown. While most available animal-models require immunosuppressive-therapy when applying human cells, the fetal-sheep being pre-immune until day75 of gestation has been proposed for the in-vivo tracking of human cells after intra-peritoneal transplantation. We introduce a novel intra-uterine myocardial-infarction model to track human mesenchymal stem cells after direct intra-myocardial transplantation into the pre-immune fetal-sheep. Thirteen fetal-sheep (gestation age: 70-75 days) were included. Ten animals either received an intra-uterine induction of MI only (n=4) or MI+intra-myocardial injection (IMI;n=6) using micron-sized, iron-oxide (MPIO) labeled human mesenchymal stem cells either derived from the adipose-tissue (ATMSCs;n=3) or the bone-marrow (BMMSCs;n=3). Three animals received an intra-peritoneal injection (IPI;n=3; ATMSCs;n=2/BMMSCs;n=1). All procedures were performed successfully and follow-up was 7-9days. To assess human cell-fate, multimodal cell-tracking was performed via MRI and/or Micro-CT, Flow-Cytometry, PCR and immunohistochemistry. After IMI, MRI displayed an estimated amount of $1x10^5$-$5x10^5$ human cells within ventricular-wall corresponding to the injection-sites which was further confirmed on Micro-CT. PCR and IHC verified intra-myocardial presence via detection of human-specific β-2-microglobulin, MHC-1, ALU-Sequence and anti-FITC targeting the fluorochrome-labeled part of the MPIOs. The cells appeared viable, integrated and were found in clusters or in the interstitial-spaces. Flow-Cytometry confirmed intra-myocardial presence, and showed further distribution within the spleen, lungs, kidneys and brain. Following IPI, MRI indicated the cells within the intra-peritoneal-cavity involving the liver and kidneys. Flow-Cytometry detected the cells within spleen, lungs, kidneys, thymus, bone-marrow and intra-peritoneal lavage, but not within the heart. For the first time we demonstrate the feasibility of intra-uterine, intra-myocardial stem-cell transplantation into the pre-immune fetal-sheep after MI. Utilizing cell-tracking strategies comprising advanced imaging-technologies and in-vitro tracking-tools, this novel model may serve as a unique platform to assess human cell-fate after intra-myocardial transplantation without the necessity of immunosuppressive-therapy.

Introduction

Stem cells have been repeatedly suggested as a next generation therapeutic approach for the treatment of heart failure due to myocardial infarction or cardiomyopathy [8]. Based on various animal trials, there are increasing numbers of early phase patient trials that aim to demonstrate the feasibility and potential efficacy of stem cell-based therapies in the clinical setting [4-7, 183]. However, despite the plethora of generated data in the field [51], the in-vivo cell fate with specific regards to cell retention and engraftment, survival, and importantly contribution to cardiac regeneration after stem-cell transplantation into the heart remains to be elucidated. One major reason is certainly the too rapid translation from small animal studies or non-comparable large animal studies (mainly pigs and sheep) to clinical human studies, while only a systematic evaluation of the early and late stem cell fate will allow defining the optimal stem cell therapy concept for sustained cardiac regeneration.

To assess the cell fate including cellular in-vivo bio-distribution, engraftment and survival after transplantation, a surrogate animal model is mandatory allowing for sufficient cell tracking in absence of any immunologic rejection [52, 53, 184, 185]. However, with the exception of gene-modified murine models, the availability of suitable animal models to assess human stem cell fate and bio-distribution is very limited. As most available animal models are associated with the necessity for immunosuppressive therapy when applying human cells, the clinical relevance of findings obtained from such animal models is compromised.

The fetal sheep has been suggested to be an optimal animal model for the assessment of human cell-fate [52, 53, 184-189]. Although the fetal sheep has a normal functioning immune-system, it is still able to support human cell engraftment and differentiation if the cells are transplanted before day 75 of gestation [52, 53, 184, 185, 190]. Following ultrasound-guided, intra-peritoneal stem cell transplantation, previous reports have shown that the fetal sheep is immunologically tolerant to human skin grafts and to allogenic or xenogenic stem cells during this “pre-immune” period of development allowing for a significant engraftment of human cells without the necessity of immunosuppressive therapy [52, 53, 190-197]. Taking this unique advantage of this pre-immune status as well as the large size and the long life-span into account, the fetal sheep represents an highly interesting animal model to study human cell-fate offering experimental opportunities that are not available in murine models [184, 185, 190].

In this study and for the first time, we investigated the feasibility to use the pre-immune fetal sheep model for the assessment of human stem cell fate after direct intra-myocardial mesenchymal stem cell transplantation following acute myocardial infarction with specific attention to cell retention and early bio-distribution using advanced, imaging-guided cell tracking protocols.

Materials and Methods

Study Animals & Experimental Design

We studied 8 pregnant Pre-Alp ewes between 70 to 75 days’ gestation (term 145 days) with a total of 13 fetal-sheep. Ten animals either received an intra-uterine induction of MI only (n=4) or MI + intra-myocardial injection (IMI; n=6) using micron-sized, iron-oxide (MPIO) labeled human mesenchymal stem cells either derived from the adipose tissue (ATMSCs; n=3) or the bone-marrow (BMMSCs; n=3). Three animals received an intra-peritoneal injection (IPI; n=3; ATMSCs; n=2 /

BMMSCs; n=1) (figure 1). All animals received humane care in compliance with the "Principles of Laboratory Animal Care" as well as the US National Institutes of Health guidelines for the care and use of animals. All procedures were approved by the Institutional Ethics Committee of the IMM RECHERCHE, Institut Mutualiste Montsouris, Paris, France [Approval-No 10-18/2010].

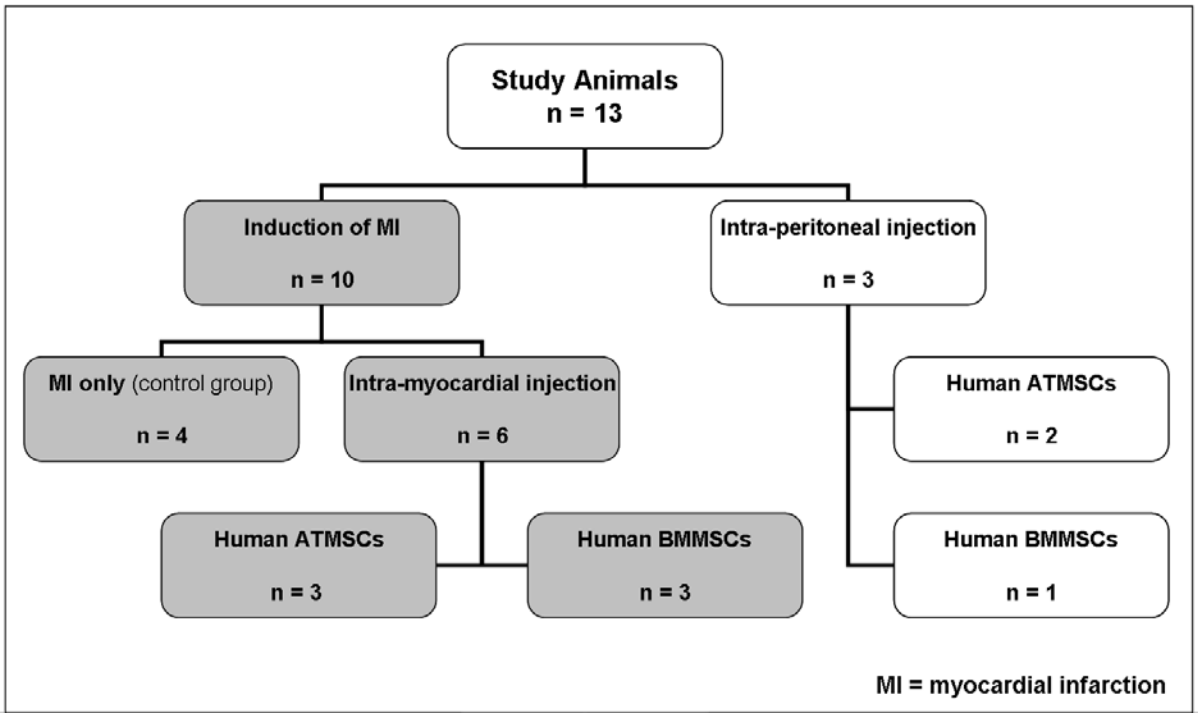

Figure 1: Study Design and Animal Distribution

Cell Isolation, Characterization and Labeling

Isolation of human bone marrow derived mesenchymal stem cells (BMMSCs)

After written informed consent and approval of the institutional review board of the University Hospital of Zurich, 80mL of bone marrow was aspirated from the sternum of a 52 years old male patient using a bone marrow aspiration syringe with a needle prior to cardiac surgery at the University Hospital Zurich. BMMSCs were isolated as previously described [198]. Briefly, BM was diluted with Hank's balanced salt solution (HBSS; Kantonsapotheke Zürich) and layered on a Histopaque 1077-gradient (Sigma Aldrich, Buchs, Switzerland). Mononuclear cells were isolated, washed twice in HBSS and re-suspended in Minimum Essential Medium (MEM) alpha supplemented with 2 mM L-glutamine, 100 U/ml penicillin, 100 ug/ml streptomycin (all Invitrogen, Carlsbad, CA, USA) and 10% (v/v) fetal bovine serum (Biowest, France). The MSCs were cultured in control medium at 37°C in a humidified atmosphere containing 5% CO_2. Non-adherent cells were removed after 24 hours and the medium was replaced. At near confluency, the cells were detached with 0.05% trypsin-EDTA (Invitrogen, Carlsbad, CA, USA) and then passaged for further expansion and analysis.

Isolation of human adipose tissue derived mesenchymal stem cells (ATMSCs)

ATMSCs (isolated from a 45 years old female patient after written informed consent and approval of the institutional review board of the University Hospital of Zurich) were generously provided by Dr.

Maurizio Calcagni from the Clinic for Plastic and Reconstructive Surgery, University Hospital Zurich. The cells were isolated from tissue according to a standard protocol as described elsewhere [199].

Characterization of human BMMSCs and ATMSCs using Flow Cytometry

The surface markers of hBMMSCs and hATMSCs were analyzed using the following mouse anti-human monoclonal antibodies: CD31, CD34, CD44 (ImmunoTools, Germany), CD45, CD90, CD105, CD146 (R&D Systems, Switzerland), CD73 and CD166 (BioLegend, Switzerland). Specific expression was determined by comparison with the appropriate isotype control. Cells were incubated with direct labelled primary antibodies for 20 min at 4°C. Finally, the cells were washed with FACS buffer consisting of 2% FCS (Biowest, France), 0.5 M EDTA and 0.05% sodium azide (Sigma Aldrich, Switzerland) in phosphate buffered saline (Invitrogen, Switzerland) and fixed in PBS containing 1% paraformaldehyde (Sigma Aldrich, Switzerland). The samples were acquired by BD FACS Calibur Cytometer (Becton Dickinson, USA) and analyzed using FlowJo software (Tree Star, USA).

Differentiation Potential of human BMMSCs and ATMSCs

Expanded hBMMSCs and hATMSCs were characterized for differentiation toward osteogenic, adipogenic and chondrogenic lineages as previously described [198]. Briefly, to induce mineralization, the hBMMSCs were incubated with DMEM low glucose (Invitrogen, Switzerland), 10% FCS (Biowest, France), 10 mM β-Glycerophosphate, 50 µM L-Ascorbic acid 2-phosphate, 10 nM Dexamethasone (Sigma Aldrich, Switzerland) and 1% Penicillin and Streptomycin (Invitrogen, Switzerland). For the differentiation of hATMSCs 100 nM Dexamethasone was used. After three weeks cells were fixed with 4% formalin (Kantonsapotheke Zürich, Switzerland) and calcium deposits were detected using 2% Alizarin red (Sigma Aldrich, Switzerland). For adipogenic differentiation cells were stimulated with induction medium containing DMEM low glucose, 10% FCS, 1 µM Dexamethasone, 10 µg/ml Insulin, 120 µM Indomethacin, 0.5 mM 3-Isobutyl-1-methylxantine (IBMX, Sigma Aldrich, Switzerland) and 1% Penicillin and Streptomycin for 3 days. Afterwards the medium was changed to maintenance medium consisting of induction medium without IBMX supplementation. Three weeks later, the cultures were fixed with 4% formalin and accumulation of lipid vacuoles was stained with 3% Oil Red-O (Sigma Aldrich, Switzerland). Cultures were observed under an inverted microscope (Axiovert 40 CFL, Zeiss, Germany). To evaluate the chondrogenic potential cell aggregates were incubated in induction medium consisting of DMEM high glucose (Invitrogen, Switzerland), 1% FCS, 0.5 µg/ml Insulin, 50 µM L-Ascorbic acid 2-phosphate, 10 ng/ml Transforming growth factor-beta1 (PeproTech, UK) and 1% Penicillin and Streptomycin. After three weeks the pellet was fixed in 4% formalin, paraffin embedded and the staining of the proteoglycan synthesis was performed using 0.1% Toluidine blue (Sigma Aldrich, Switzerland). The slides were analyzed by microscopy (Leica CTR6000, Leica Microsystems AG, Switzerland).

Labeling of human BMMSCs and ATMSCs with CM-DiI and MPIOs

The cells were first labeled with a fluorescent dye (CellTracker CM-DiI, Invitrogen, Switzerland) according to the manufacturer's instructions. CM-DiI is a lipophilic carbocyanine tracer and incorporates into membranes. Afterwards the cells were incubated with culture medium supplemented with 1.63 um-large encapsulated super-paramagnetic microspheres (MPIOs; Bang Laboratories, USA) at a final concentration of 2.75 ug/ml iron for 24 to 36 hours as described previously [48]. The particles were co-labeled with Dragon-green fluorochromes for additional

analysis using fluorescence-based techniques. To remove excessive MPIOs after labeling, the cells were washed three times with phosphate-buffered saline (PBS; Invitrogen, Switzerland). The viability and labeling efficiency was determined by trypan blue exclusion and FACS analysis, respectively. Prussian blue staining was used to detect ferric iron of labelled cells with MPIOs [50, 200, 201]. Cells were fixed with 4% formalin for 1 h and afterwards incubated with Prussian blue staining solution (Accustain, Sigma Aldrich, Switzerland) according to the manufacturer's instructions. The slides were analyzed with a light microscope (Leica CTR6000, Leica Microsystems AG, Switzerland). Hemosiderin, some oxides and salts of iron are shown in blue up to brown and nuclei and cytoplasm in pink to red.

The Fetal Sheep Cell Transplantation Model

The fetal sheep model has proven to be an appropriate model for the assessment of in-vivo cell fate and bio-distribution of human cells with specific regards to survival and engraftment [184-186, 188, 190]. In contrast to other animal models either being genetically modified (i.e. nude mice) or requiring immunosuppressive therapy (xenogenic models such as adult porcine or ovine models) for the assessment of human stem cells, the fetal sheep has a normal functioning immune system, but is still able to support cell engraftment and survival if the cells are transplanted before day 75 of gestation (term 145 days). Taking advantage of this "window of opportunity" and this "pre-immune" period of development, this model allows for a significant engraftment of human cells without the necessity of immunosuppressive therapy [52, 53, 184-186, 188, 190].

Operative Procedures

Following overnight fasting, the animals were sedated by intravenous injection of pentothal (10mg/kg body weight). The animals were placed in supine position, intubated, ventilated with 100% oxygen and 1-2% isoflurane and monitored continuously throughout the entire procedure. No anti-arrhythmic agents were used during or after the procedure. After the ewes were placed in dorsal recumbency on the operating table, the uterus was exteriorized through a maternal midline laparotomy. Following digital palpation of the fetus, the uterus was opened through a 10cm incision. The amniotic fluid was collected, stored in a sterile reservoir and out back into the ewe's belly to maintain the temperature until the end of the procedure. While the upper part of the fetal body remained within the maternal uterine cavity, the fetal chest was opened via a left-sided mini-thoracotomy (4^{th} intercostals space). After sharp dissection of the pericardium, the heart was positioned for an optimal access of the anterior wall and the apex.

Induction of Myocardial Infarction

After evaluation of the myocardial vasculature, the left anterior descending coronary artery (LAD) and the diagonal branches (DB) were identified. To achieve a sufficient myocardial infarction involving the anterior wall and the apex, the LAD (± appropriate diagonal branches) were suture ligated using a 7/0 suture. Sufficient ligation was confirmed by instant changes of the regional wall movement and the colour in the anterior-apical area.

In utero Stem Cell Transplantation

Intra-myocardial Injection

After ligation of the coronary vessels and an ischemic period of 15-20min to achieve sufficient anterior-apical myocardial damage, 6 target zones for cell transplantation were defined in the left-ventricular anterior area above the apex. Following careful exposure of the fetal heart, a mean of 1.25±0.30 x10^6 cells was slowly injected (60 sec) into the fetal myocardium using a 29 gauge needle (table 1). The exact injection sites were carefully documented. After stem cell delivery, the absence of myocardial bleeding from the injection sites and cardiac arrhythmia was confirmed before layered closing of the fetal chest using Vycril sutures. Thereafter, the fetus was carefully re-positioned with particular regards to the umbilical cord and the amniotic fluid was re-injected before closing the uterus.

Study Animals	**Myocardial Infarction (MI)**	**MI + intramyocardial Stem Cells**	**Intraperitoneal Stem Cells**
Animal Weight (gr) / Size (cm)	331 ± 81 / 20 ± 2		
Cell Type (ATMSCs / BMMSCs) (n)	n/a	3 / 3	2 / 1
Number of Cells (Mio/10^6)	n/a	1.25 ± 0.30	11.75 ± 2.81
Injection Volume (ul)	n/a	100 ± 30	960 ± 60
Number of Injections (n)	n/a	6	1
Injection Needle (gauge)	n/a	29	23
Duration of Procedure (min)	32 ± 4	51 ± 9	33 ± 11
Time between MI Induction and Cell Injection (min)	n/a	19 ± 1	n/a
Procedural Mortality (%)	0 (0%)	0 (0%)	0 (0%)
Major complications	none	none	None
Mortality during Follow Up	1 (25%)	2 (33%)*	0 (0%)
Overall Survival (%)	10 (77%)		

Table 1

Intra-peritoneal Injection

The procedure was performed as previously described [194, 195, 197]. In brief, using trans-uterine ultrasound, the number, positioning, viability and the gestational age of the fetuses (measuring

crown-rump length) was determined. Under ultrasound guidance, a 23 gauge 15cm disposable needle (Cook Medical, USA) was trans-abdominally inserted into the ewe's uterus and carefully advanced into the peritoneal cavity of the fetus [194, 195, 197]. To avoid fetal injury, the needle was inserted superior-lateral to the fetal bladder to avoid the umbilical arteries and abdominal organs. After confirming optimal needle placement, a mean amount of 11.75±2.81 $x10^6$ cells was slowly injected (60 sec) and appropriate distribution in the peritoneal cavity was observed (table 1). In case of multiple fetuses, each fetus was injected using separate needles.

Post-interventional Care, Follow Up and Animal Harvest

After cell transplantation, the fetal heartbeat was monitored to confirm post-procedural wellbeing. After confirming stable hemodynamic conditions the anaesthetics were stopped. The ewes were left to recover and checked daily for their health status and signs of spontaneous abortion. The ewes were sacrificed and the ovine fetuses were harvested abdominally 7-9 days post transplantation and were processed for further analysis in compliance with the "Principles of Laboratory Animal Care" as well as the US National Institutes of Health guidelines for the care and use of animals. All sacrifice and harvest procedures were approved by the Institutional Ethics Committee of the IMM RECHERCHE, Institut Mutualiste Montsouris, Paris, France [Approval-No 10-18/2010].

Histology & Immunohistochemistry of myocardial infarction

To assess myocardial infarction, necrosis and cell death, standardized H&E staining, Masson's Trichrome and van Giesson staining was performed. In addition, cleaved Caspase-3 staining (1:300; Cell Signaling Technology) and TUNEL staining was performed to further access the presence of apoptosis. For TUNEL staining pre-treatment was performed with Enzyme 2 (Leica) for 15 min at 37°C. Detection of Digoxin was done with a biotinylated mouse anti-Digoxigenin antibody (1:500; Sigma Chemical Company). Incubation of TUNEL-Staining was performed on Leica BondMax with Intense-R HRP-Detection-Kit.

Detection and tracking of CM-DiI$^+$/MPIO$^+$ human mesenchymal stem cells in the fetal sheep myocardium

To assess the presence and survival of CM-DiI$^+$/MPIO$^+$ human mesenchymal stem cells a multimodal evaluation strategy was applied comprising Flow Cytometry, PCR and immunohistochemistry. In brief, the heart was processed as follows: After cutting away the apical and basal region, the left ventricular, anterior region (area of injection) was divided into three parts (each approximately 5mm x 5mm) which were then either processed freshly for Flow-Cytometry (part 1), snap frozen for PCR (part 2) or in formaldehyde for immunohistochemistry (part 3).

Flow Cytometry

A defined cardiac sample of approximately 5mm x 5mm from the area of injection as well as control samples from non-injected sheep heart was processed for Flow Cytometry analysis. In addition, defined samples of the following organs were immediately analyzed after animal sacrifice: bone marrow, brain, kidneys, liver, lung, spleen and thymus. In addition, a lavage of the intra-peritoneal cavity was performed. As previously described [194, 195], the samples of each organ were mashed through a 70 µm nylon cell strainer (BD Biosciences, Switzerland) and rinsed with PBS. Afterwards,

the cell suspension was incubated with red blood cell lysis buffer (Sigma Aldrich, Switzerland) for 5 min at 37°C, washed with PBS and fixed in 1% paraformaldehyde. Single cells were analyzed by Flow Cytometry as described. The cells were gated on the forward (FSC-H) and side scatter (SSC-H) dot plot to select mononuclear cells preferentially [194].

PCR Analysis

RNA was isolated from snap-frozen tissues using RNeasy mini kit (Qiagen AG, Switzerland). The quantity and quality was measured with a nanodrop machine (Witec AG, Switzerland). The first-strand cDNA synthesis was generated with 1 µg of total RNA and random-hexamer primer using ThermoScript RT-PCR system (Invitrogen, Switzerland). PCR was performed as described previously [53]. The human specific β -2-microglobulin sequence (upstream primer: 5'-GTGTCTGGGTTTCATCCATC-3', downstream primer: 5'–GGCAGGCATACTCATCTTTT–3') and the housekeeping gene β -actin (upstream primer: 5'–CGGGACCTGACTGACTAC–3', downstream primer: 5'–GAAGGAAGGCTGGAAGAG–3') were amplified with the following conditions: initialization at 95°C for 9 min followed by 45 cycles of denaturation at 95°C for 30 s, annealing at 55°C for 30 s, elongation at 72°C for 15 s and final elongation at 72°C for 5 min. The PCR product was analyzed on a 2% agarose gel stained with GelRed nucleic acid stain (Chemie Brunschwig, Switzerland). Afterwards, DNA fragments of 163 bp for β -2-microglobulin or 252 bp for β -actin were detected.

Immunohistochemistry

To assess the presence and the survival of human mesenchymal stem cells in the fetal myocardium the following immunohistochemical analysis was performed after dewaxing process of the paraffin slides: human cell-specific MHC-1 (1:500; Epitomics), rabbit anti-FITC (1:1000; Invitrogen BV + Research Genetics), human ALU Sequence (ALU Probe; Leica Microsystems AG, Switzerland) and double staining for rabbit anti-FITC + human ALU Sequence. Immunohistochemistry and in situ hybridization was performed on Leica BondMax instruments using Refine AP and Refine HRP-Kits (including all buffer solutions from Leica Microsystems Newcastle, Ltd.) according to the manufacturer's guidelines.

Assessment of intrinsic immune response versus CM-DiI$^+$/MPIO$^+$ human mesenchymal stem cells in the fetal sheep myocardium

To assess a potential intrinsic immune response against the injected CM-DiI$^+$/MPIO$^+$ human mesenchymal stem cells a detailed immunohistochemical analysis for ovine inflammatory cells was performed using anti-human antibodies reactive to CD3 (Thermo Scientific), CD20 (Cell marque Lifescreen Ltd.) and CD68 (Biosystems Switzerland AG) to detect CD3$^+$ T-cells, CD20$^+$ B-lymphocytes and CD68$^+$ macrophages in the fetal myocardial tissue respectively. The detection of ovine inflammatory cells using cross-reactive anti-human antibodies was histologically confirmed on ovine spleen tissue sections.

Magnetic Resonance Imaging (MRI)

All measurements were performed in a Bruker 4.7T Biospec 47/40 with a gradient strength of 60mT/m and a slew rate of 1100 T/m/s equipped with a circular polarized 1H mouse whole body RF coil. The imaging protocol consisted after gradient-echo (GRE) localizers in 3 spatial directions of 2D

T2w fast spin-echo (FSE) sequences (TR/TE 2500ms/11 ms; effective TE 33 ms; echo train length 8; matrix 256 x 256; FoV 40 x 40 mm; slice thickness 1 mm; averages 3) in transversal, sagittal and coronal orientation. To estimate the amount of MPIO-labelled cells in the myocardium an in vitro dilution series was performed. Therefore labelled human MSCs of various counts (1x 10^6, 5x 10^5, 1x 10^5, 5x 10^4, 2x 10^4) were mixed in each case with 1x10^6 ovine cardiomyocytes. The cell pellets were embedded in a 2% (w/v) agarose gel in PBS. The measurement was performed as described above.

Micro Computed Tomography (Micro CT)

The Micro-CT analysis was performed using a Mirco50 tomographer (Scanco Medical; 90kVp) with a voxelsize of 1.2 um.

Disclosures and Freedom of Investigation

The equipment and technology used in the study were purchased using academic funds. The authors had full control of the design of the study, methods used, analysis of data, and production of the written report.

Results

Characterization and MPIO Labeling of human BMMSCs and ATMSCs

Cell surface proteins of human BMMSCs and human ATMSCs were evaluated by Flow cytometry. Positive expression of CD44 (mean ± SD, 93.0%±4.3%), CD73 (97.8%±0.3%), CD90 (97.5%±0.7%), CD105 (84.2%±12.5%), and CD166 (94.7%±3.3%) was observed for both MSC cell types, while there was none or only weak expression of CD146 (29.4%±14.7%). Negative levels were detected for CD31 (2.5%±3.5%), CD34 (2.8%±3.9%) and CD45 (2.5%±1.9%) (figure 2A and B). Using the assays described, Human ATMSCs and human BMMSCs demonstrated their differentiation potential to the adipogenic, osteogenic and chondrogenic lineages (figure 2C-H).

Successful labeling of human BMMSCs and human ATMSCs was demonstrated on Prussian Blue staining as well as on immunofluorescence clearly showing the presence of MPIOs (figure 3A-G). This was further confirmed on FACS analysis which also demonstrated an excellent cell labeling efficiency in excess of 95% (figure 3H).

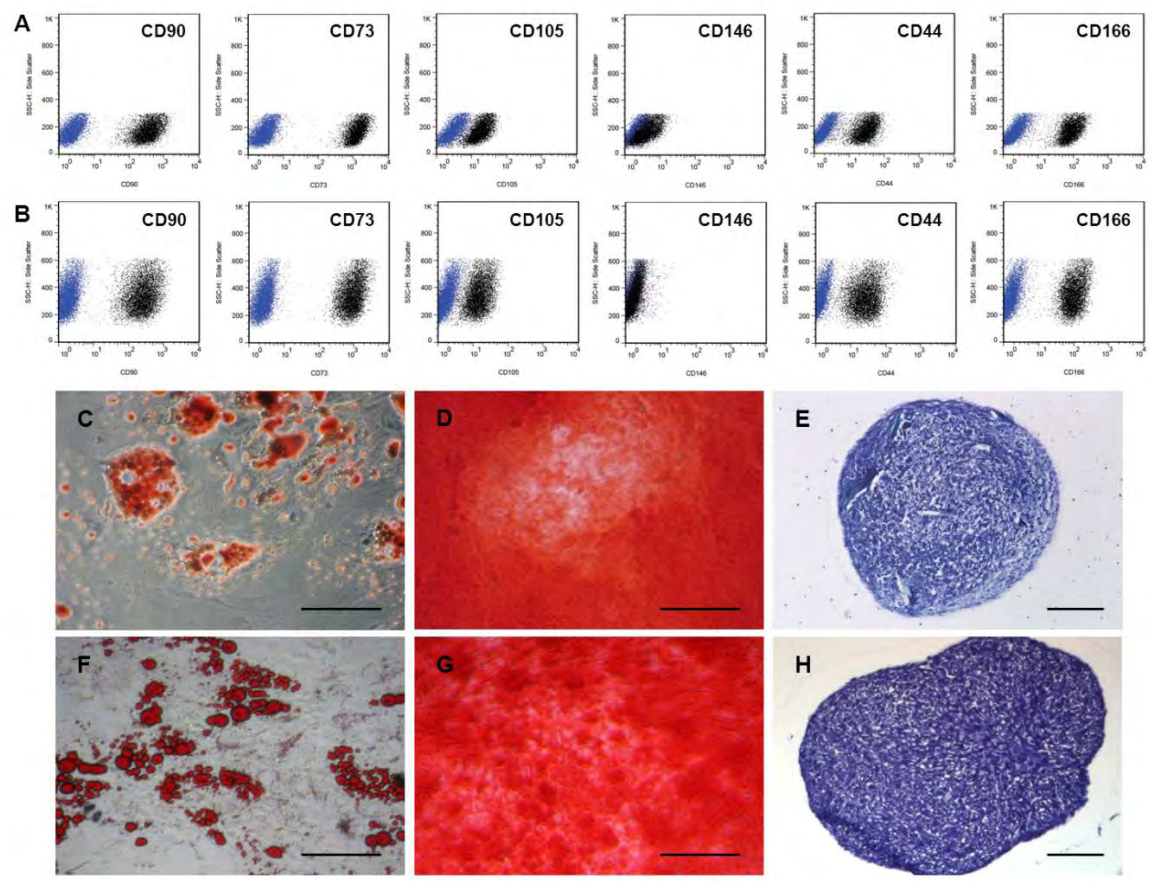

Figure 2: Characterization of human BMMSCs and ATMSCs

Cell surface proteins of human BMMSCs and ATMSCs were evaluated by flow cytometric analysis **(panel A and B;** *blue population represents isotype control*). Positive expression of CD44, CD73, CD90, CD105, CD166 and none / weak expression of CD146 was observed for both MSC cell types. Human BMMSCs **(C-E)** and ATMSCs **(F-H)** demonstrated their differentiation potential to the adipogenic *(Oil Red O Staining, magnification x20 (C, F))*, osteogenic *(Alizarin Red S Staining, magnification x20 (D, G))* and chondrogenic lineages *(Toluidine Blue Staining, magnification x10 (E, H)). Scale Bar: 100um.*

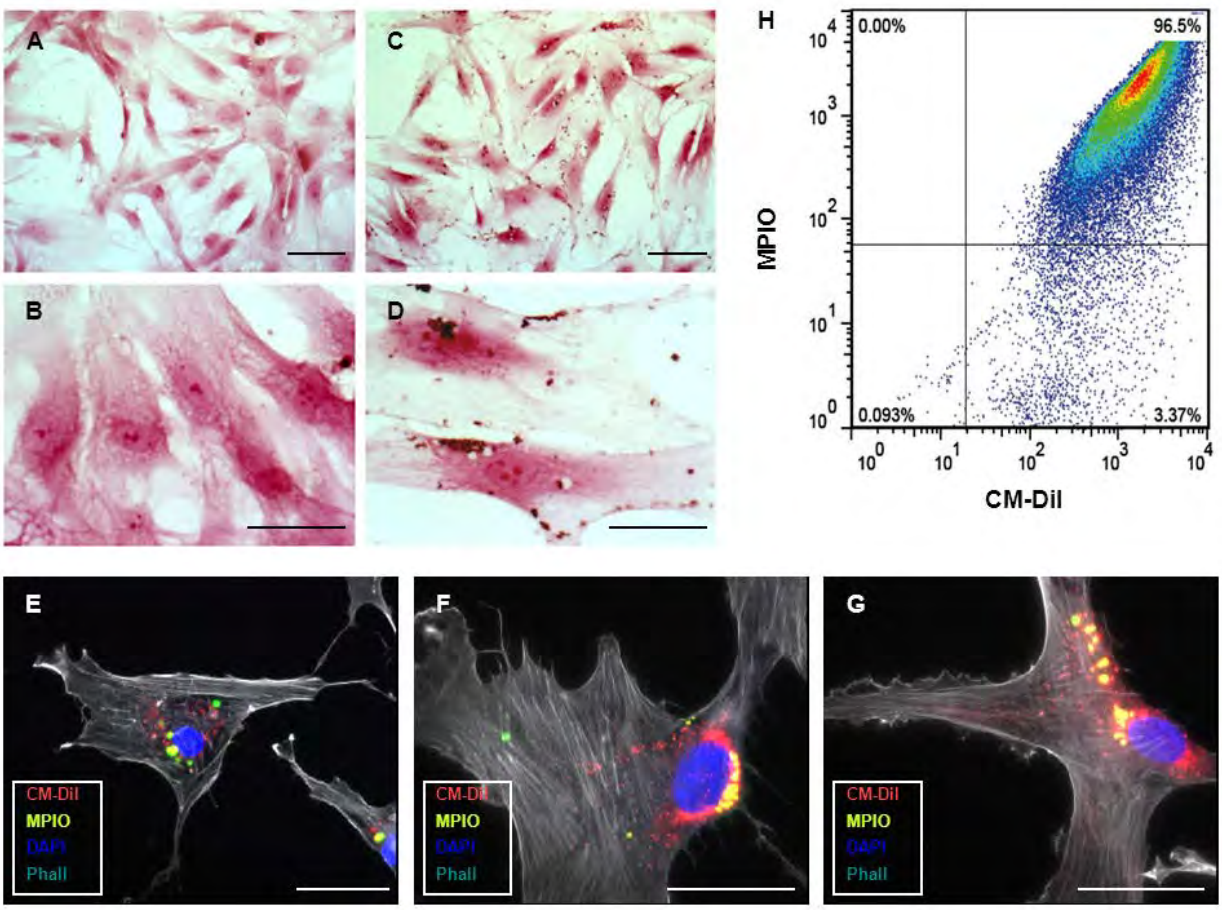

Figure 3: Labeling of human BMMSCs and ATMSCs with superparamagnetic microspheres (MPIOs; co-labeled with Dragon-green fluorochromes) and CM-DiI

Successful labeling of human BMMSCs and ATMSCs was demonstrated on Prussian Blue staining before **(A and B;** *magnification x10 and x40*) and after MPIO labeling **(C and D;** *magnification x10 and x40*) as well as on immunofluorescence clearly showing the presence of MPIOs **(E-G;** *magnification x20 and x63*). After labeling, CM-DiI$^+$ / MPIO$^+$ cells displayed excellent cell labeling efficiency in excess of 95% on FACS analysis **(H)***. Scale Bar: 100um (A and C), 50um (B, D-G).*

Surgical Procedures and Induction of myocardial infarction

The surgical procedure and the induction of myocardial infarction (MI) could be successfully performed in all animals (figure 4A-G) scheduled for intra-myocardial stem-cell transplantation or MI only (n=10, table 1) and was intra-operatively confirmed by instant changes of the regional wall movement and the colour in the anterior-apical area (figure 5A). The respective animals remained hemodynamically stable during the entire procedure and did not display any major complications (table 1). In three animals, a short bradycardic episode was present immediately after ligation of the coronary vessel, but normalized quickly after a few minutes. In addition, two animals encountered mild bleeding from the stitching channels of the ligation suture which self-terminated after a few minutes or was managed with a hemostatic sealant.

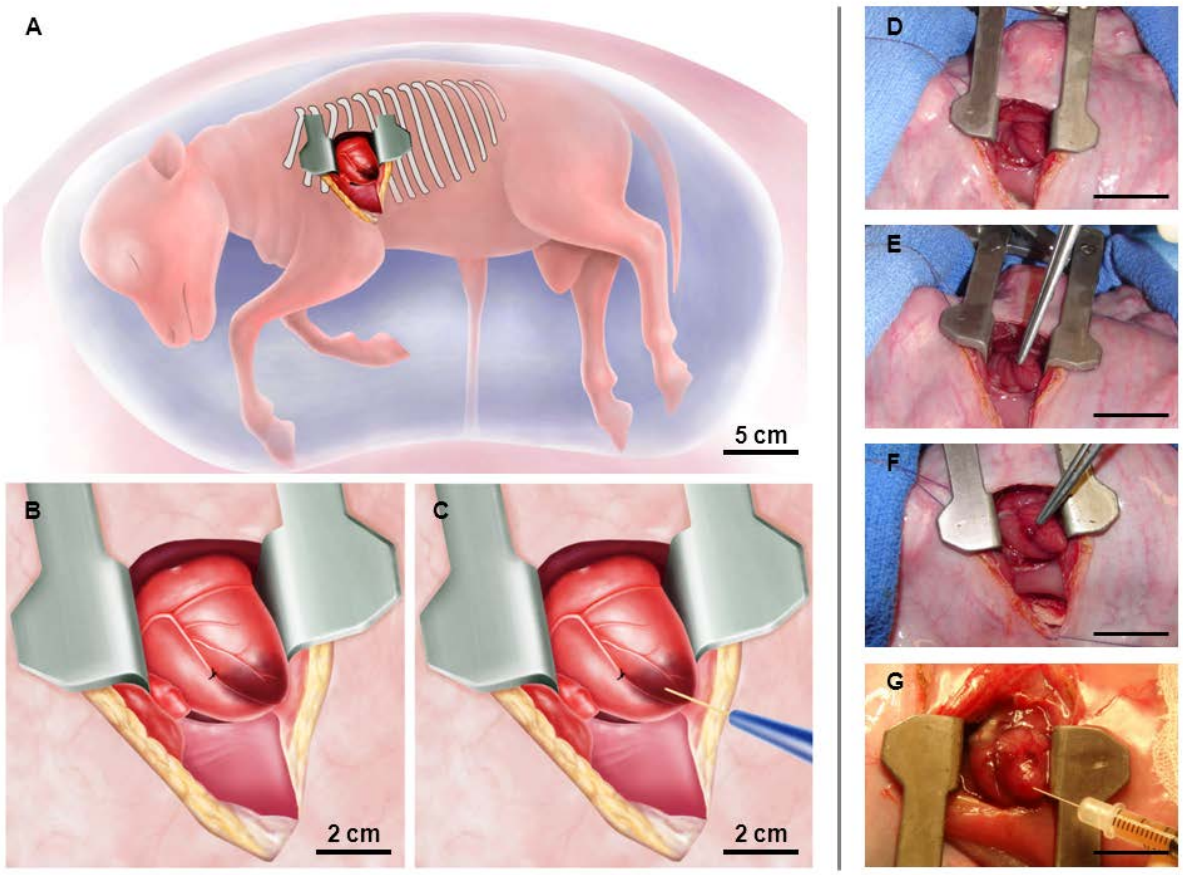

Figure 4: Concept of intra-uterine induction of myocardial infarction and intra-myocardial stem cell delivery into the pre-immune fetal sheep

The uterus was exteriorized through a maternal midline laparotomy. Following digital palpation of the fetus, the uterus was opened through a 10cm incision. The fetal chest was opened via a left-sided mini-thoracotomy *(4th intercostal space)* **(A)**. After sharp dissection of the pericardium, the heart was positioned for an optimal access of the anterior wall and the apex **(A and D)**. After evaluation of the myocardial vasculature, the left anterior descending coronary artery (LAD) and the diagonal branches (DB) were identified **(E)**. To achieve a sufficient myocardial infarction involving the anterior wall and the apex, the LAD (± appropriate diagonal branches) were suture ligated using a 7/0 suture **(B and F)**. Sufficient ligation was confirmed by instant changes of the regional wall movement and the colour in the anterior-apical area **(B and F)**. After ligation of the coronary vessels, the 5-6 target zones for stem cell delivery were defined. Following careful exposure of the fetal heart, the cells were slowly injected into the fetal myocardium (**C and G)**. *Scale Bar: 5cm (D-G).*

The successful induction of myocardial infarction was also confirmed on histology and immunohistochemistry. On H&E staining, the area of myocardial infarction (MI) could be easily identified showing the typical areas of necrosis when compared to the surrounding border zone and the healthy myocardium (figure 5B). In detail, loss of the classical myocardial morphology, necrotic cell death with the loss of the nuclei and cardiac proteins as well as the complete loss of entire muscle fibres could be observed (figure 5B). These findings were further confirmed on Masson's Trichrome and van Giesson staining (data not shown). In addition, also an apoptotic component

could be confirmed by positive staining for activated caspase-3 and TUNEL suggesting a programmed cell-death in the area of infarction (figure 5C-E).

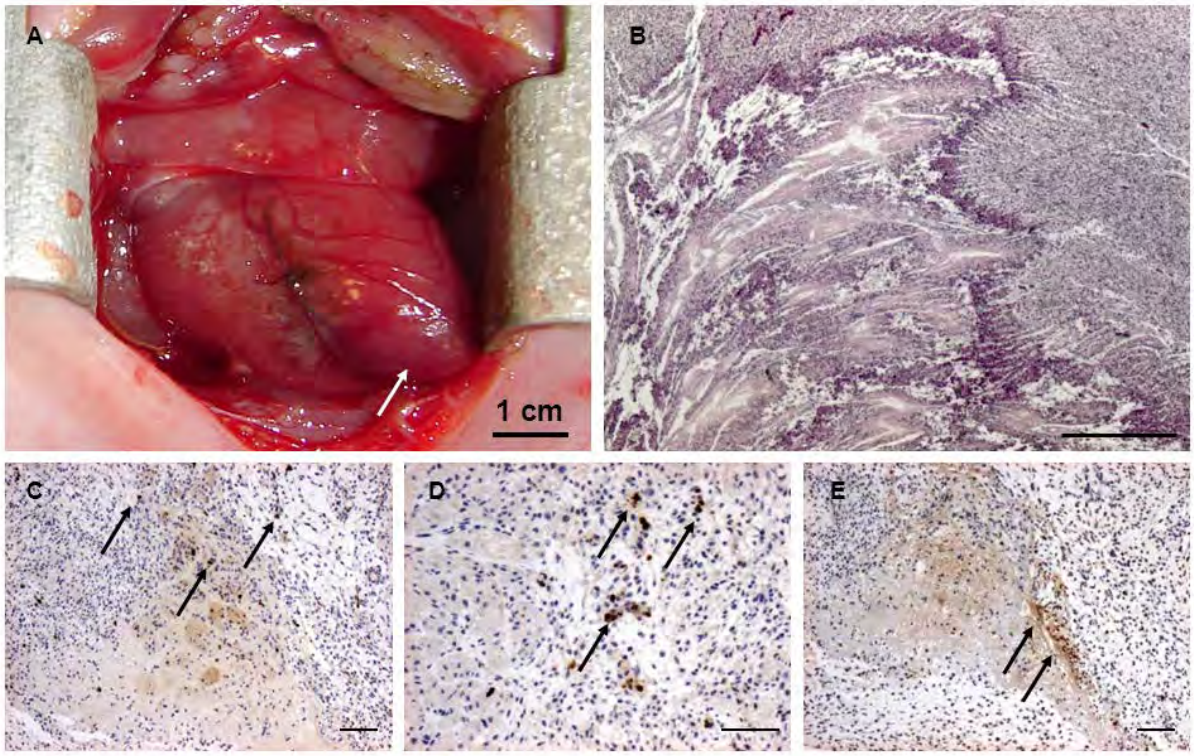

Figure 5: Assessment of of intra-uterine induction of MI in the pre-immune fetal sheep

Induction of acute myocardial infarction (MI) was confirmed by instant changes of the regional wall movement and the colour in the anterior-apical area **(A;** *purple discolouration; white arrow*). The area of myocardial infarction (MI) could be easily identified showing the typical areas of necrosis when compared to the surrounding border zone and the healthy myocardium. In detail, loss of the classical myocardial morphology, necrotic cell death with the loss of the nuclei and cardiac proteins as well as the complete loss of entire muscle fibres could be observed **(B***; magnification x2.5*). MI was further confirmed on histology via positive staining for activated caspase-3 **(C and D;** *black arrows; magnification x2.5 and x10*) and TUNEL **(E;** *black arrows; magnification x2.5*) in fetal infarcts at 7 days suggesting programmed cardiomyocyte death within the infracted region. *Scale Bar: 500um (B), 100um (C-E).*

Intra-myocardial and intra-peritoneal stem cell transplantation

After induction of MI and the definition of 5-6 target zones in the antero-apical area, intra-myocardial transplantation either using human BMMSCs (n=3) or ATMSCs (n=3) was successfully performed. All animals tolerated the procedure very well without any major complications. Two animals displayed transient arrhythmia during intra-myocardial stem cell delivery and one animal had minor bleeding from the injection sites. The intra-peritoneal transplantation was also carried out successfully in all animals (n=3; ATMSCs; n=2 / BMMSCs; n=1) and no complications such as bleeding or organ damage occurred (table 1).

Postoperative Complications and Follow Up

Postoperatively, no major complications occurred in the ewes and in the fetuses. However, as known from previous reports [194, 195] and despite postoperative monitoring, during follow up, three (23%) of the fetuses of which one animal underwent induction of MI only and two animals had received intramyocardial transplantation of BMMSCs died due to spontaneous abortion and were expelled overnight which was primarily related to the fragile in-utero approach itself (table 1).

MRI and Micro CT for Stem Cell Tracking

CM-DiI$^+$/MPIO$^+$ human BMMSCs and ATMSCs could be successfully detected after stem cell transplantation on high resolution MRI. In selected animals that had received an intra-myocardial transplantation after MI, the labeled cell clusters were clearly visible as areas of strong focal signal loss in the septal and anterior-lateral ventricular wall corresponding to the injection sites (figure 6A and B). In addition, cells were also detectable in the costal area, para-vertebral and in the *Sinus Phrenico Costalis* indicative that the cells had been distributed in the thorax over time. Animals that underwent an intra-peritoneal transplantation displayed a distribution within the entire intra-peritoneal cavity involving the liver, the kidneys, the *Gerota's Fascia*, intestines as well as diffuse cell clusters in the surrounding areas (figure 6C-E).

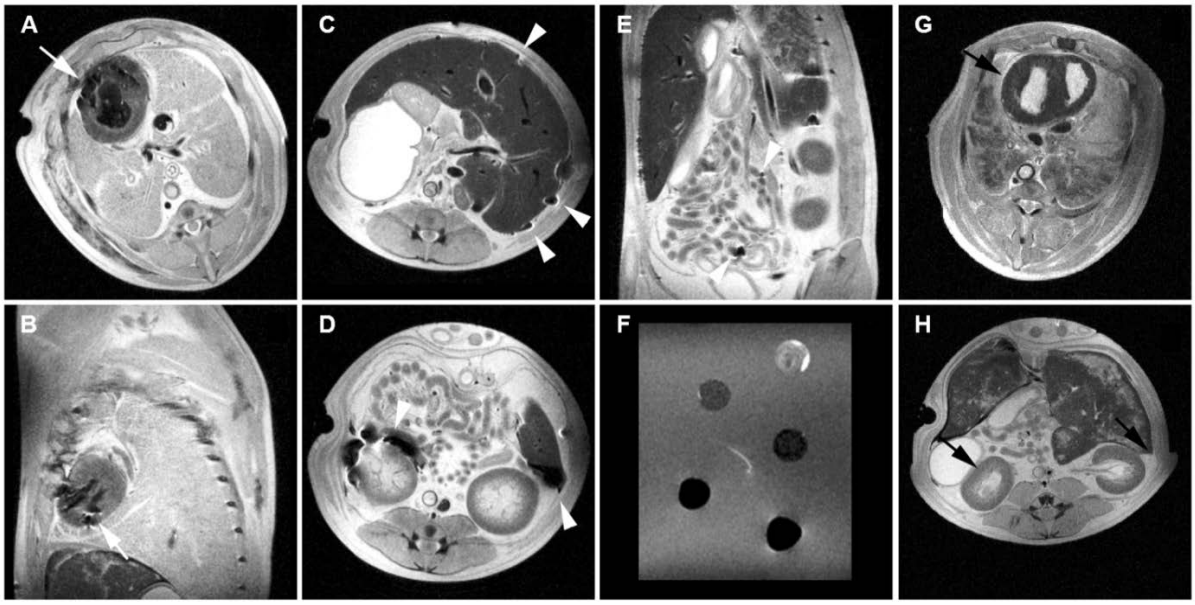

Figure 6: Tracking of CM-DiI$^+$/MPIO$^+$ human ATMSCs and BMMSCs on two-dimensional magnetic resonance imaging (MRI)

CM-DiI$^+$/MPIO$^+$ human ATMSCs and BMMSCs could be detected after stem cell transplantation on high resolution 4.7 Tesla MRI. Exemplary image series of an animal that had received an intra-myocardial injection of CM-DiI$^+$/MPIO$^+$ human ATMSCs the labeled cell clusters were clearly visible as areas of strong focal signal loss in the anterior-lateral and septal ventricular wall corresponding to the injection sites **(A and B;** *white arrows; axial and sagittal view;* **and G;** *black arrow; showing a non-injected myocardium as respective negative control)*. Next, an exemplary image series of an animal that underwent intra-peritoneal injection of CM-DiI$^+$/MPIO$^+$ human BMMSCs displayed the distribution within the entire intra-peritoneal cavity **(C-E;** *white arrow heads;* **and H;** *black arrows; showing a non-injected intra-peritoneal cavity as respective negative control)* involving the liver **(C;** *white arrow heads; axial and view*), the kidneys, the Gerota's fascia **(D;** *white arrow heads; axial view*), diffuse cell clusters in the surrounding intra-peritoneal areas **(D;** *white arrow heads; axial*

view) as well as between the intestines **(E;** *white arrow heads; sagittal view*). Comparing the dilution series **(F)** of MPIO labeled mesenchymal stem cells to the morphological images, the amount of cells in the myocardium could be estimated to approximately 1 x10^5 - 5 x10^5 cells and the cells found in the liver to 5 x10^5 cells and around the kidneys to 5 x10^5 - 1 x10^6 cells **(A-D and F)**. *(Cell Dilution: 1x 10^6 [1], 5x 10^5 [2], 1x 10^5 [3], 5x 10^4 [4], 2x 10^4 [5]. Scale Bar: 2.5 cm.*

Comparing the dilution series (figure 6F) of MPIO-labeled cells to the morphological images, the amount of cells in the myocardium could be estimated to approximately 1x10^5-5x10^5 cells and the cells found in the liver to 5x10^5 cells and around the kidneys to 5x10^5 -1x10^6 cells. Three dimensional MRI reconstruction confirmed the previous results on 2D MRI (figure 7A-D) and in selected tissue samples, the intra-myocardial presence of the iron-oxide labeled cells was confirmed high-resolution Micro CT showing several labeled cell clusters in the myocardium (figure 7E).

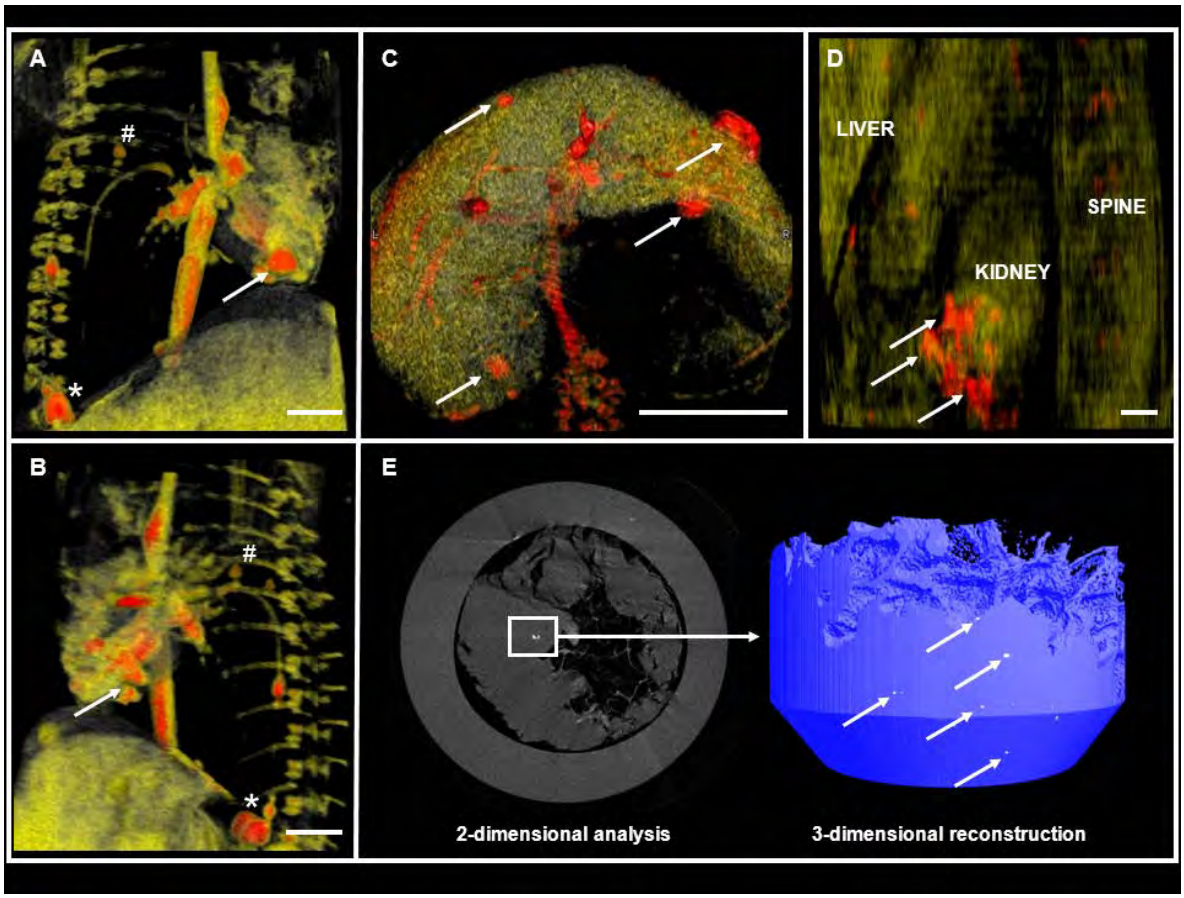

Figure 7: Tracking of CM-DiI⁺/MPIO⁺ human ATMSCs and BMMSCs on three-dimensional reconstruction MRI and Micro CT Scanning

Exemplary three-dimensional reconstruction analysis confirmed labeled cell clusters of human CM-DiI⁺/MPIO⁺ ATMSCs after intramyocardial transplantation in the anterior-lateral and septal ventricular wall **(A and B;** *white arrows; anterior-lateral and septal view*). In addition, labeled cells were also detectable in the costal / para-vertebral area **(A and B;** *white **) and in the Sinus phrenico-costalis **(A and B;** *white #*) indicative that the cells had been distributed in the fetal thorax. Abdominal 3D reconstruction analysis showed labeled cell clusters of CM-DiI⁺/MPIO⁺ human BMMSCs following intra-peritoneal injection within and around the liver **(C;** *white arrows; anterior-inferior view*) as well as in the anterior the Gerota's fascia **(D;** *white arrows; lateral view*). The intra-myocardial presence of CM-DiI⁺/MPIO⁺ human ATMSCs could be further confirmed showing several

labeled cell clusters in the fetal myocardium on 2-dimensional as well as 3-dimensional high-resolution Micro CT analysis **(E)**. *Scale Bar: 2 cm.*

Explant Macroscopy

Ten fetuses completed follow-up and could be uneventfully harvested 7-9 days post transplantation prior to ewes euthanization. The fetal heart was carefully excised and the ligation site as well as the area of myocardial infarction could be easily identified. In selected animals, the heart appeared to be slightly adhered to the pericardium and required careful dissection. The other fetal organs including lungs, liver, kidneys, spleen and others also appeared to be in good shape and were harvested for further analysis. Interestingly, most of the animals that had received left-sided thoracotomy displayed almost complete healing of the incision already after 7-9 days indicating an accelerated healing and regeneration potential in the fetal stage.

Assessment of cell fate and early bio-distribution of injected human BMMSCs and ATMSCs

Detection of CM-DiI$^+$/MPIO$^+$ human ATMSCs and BMMSCs in fetal tissue by Flow Cytometry

After intra-myocardial injection, presence of CM-DiI$^+$/MPIO$^+$ human ATMSCs and BMMSCs could be primarily confirmed within the heart and within the spleen (table 2, figure 8 A and B). Positive cells were also found within the bone marrow, the kidneys, lungs and in the brain (table 2). In animals that had received intra-peritoneal injection, CM-DiI$^+$/MPIO$^+$ human ATMSCs and BMMSCs were primarily identified within the lymphatic organs, including spleen, thymus and the bone-marrow, while in none of the animals CM-DiI$^+$/MPIO$^+$ cells were found within the heart (table 2, figure 8C and D). Positive cells were also detected in the intra-peritoneal lavage supporting the results on MRI. Additionally, low levels of positive cells were distributed in different organs such as liver, lungs and kidneys (table 2).

Table 2	Intra-myocardial Stem Cell Transplantation		Intra-peritoneal Stem Cell Transplantation	
	Analyzed	Detected	Analyzed	Detected
Tissue	**n**	**n (%)**	**n**	**n (%)**
Heart	**4**	**4 (100%)**	**3**	**0 (0%)**
Brain	**4**	**3 (75%)**	**3**	**0 (0%)**
Spleen	**4**	**4 (100%)**	**3**	**2 (66%)**
Kidneys	**4**	**4 (100%)**	**3**	**2 (66%)**
Lavage	**4**	**0 (0%)**	**3**	**3 (100%)**
Bone Marrow	**2**	**2 (100%)**	**3**	**2 (66%)**
Liver	**4**	**1 (25%)**	**3**	**1 (33%)**
Lung	**4**	**3 (75%)**	**3**	**2 (66%)**
Thymus	**4**	**1 (25%)**	**2**	**2 (100%)**

Detection and tracking of CM-DiI$^+$/MPIO$^+$ human ATMSCs and BMMSCs in the pre-immune fetal sheep myocardium via PCR Analysis and IHC

Following detection of CM-DiI$^+$/MPIO$^+$ human ATMSCs and BMMSCs in the fetal myocardium in the imaging analysis (MRI and Micro CT scanning) and the FACS assessment, intra-myocardial presence was further confirmed via PCR analysis using human β-2 microglobulin, a component of the class I antigen complex (figure 8E). Negative controls from non-injected sheep hearts as well as human mesenchymal stem cells used as a positive control clearly confirmed the human specificity of the staining for human β-2 microglobulin within the fetal myocardium (figure 8E).

Morphologically the cells could be easily identified within the fetal myocardium, appeared to in physiological shape and viable (figure 9A-I). The cells had integrated within the fetal heart and could be found in clusters as well as in the interstitial and intravascular spaces (figure 9A-I). CM-DiI$^+$/MPIO$^+$ human ATMSCs and BMMSCs were positive for both human-cell specific MHC-1 staining (figure 9A and B) as well as anti-FITC staining detecting the MPIOs within the cytoplasma of the injected human cells (figure 9C and D). In addition, double positive staining for the human-specific ALU Sequence in combination with the anti-FITC staining clearly confirmed the presence of the injected CM-DiI$^+$/MPIO$^+$ human ATMSCs and BMMSCs within the fetal myocardium (figure 9E-I).

Figure 8: Assessment of cell fate and early bio-distribution of injected of human ATMSCs and BMMSCs via Flow Cytometry and PCR analysis

Flow cytometric analysis in an exemplary recipient after direct intra-myocardial injection (IMI) of human ATMSCs. CM-DiI$^+$/MPIO$^+$ human ATMSCs were primarily detected within the heart and within the spleen **(A and B)**. In an animal that had received intra-peritoneal injection (IPI) of human BMMSCs, CM-DiI$^+$/MPIO$^+$ BMMSCs were primarily identified within the lymphatic organs, in particular within spleen, while no CM-DiI$^+$/MPIO$^+$ cells were found within the heart **(C and D)**. Intra-myocardial presence of CM-DiI$^+$/MPIO$^+$ human ATMSCs was further confirmed via PCR analysis using human β-2 microglobulin **(E)**, a component of the class I antigen complex. Negative controls from non-injected sheep hearts as well as human mesenchymal stem cells used as a positive control clearly confirmed the human specificity of the staining for human β-2 microglobulin within the fetal heart: Agarose gel analysis of human β-2 microglobulin *(left panel, A)* and β -actin *(right panel, B)* PCR products. Lane 1: molecular size marker (100 bp DNA ladder, Genecraft). Lane 2: human mesenchymal stem cells as a positive control. Lane 3: ovine fetal heart after human ATMSCs injection. Lane 4: tissue from sheep heart as a negative control for the human β-2 microglobulin sequence.

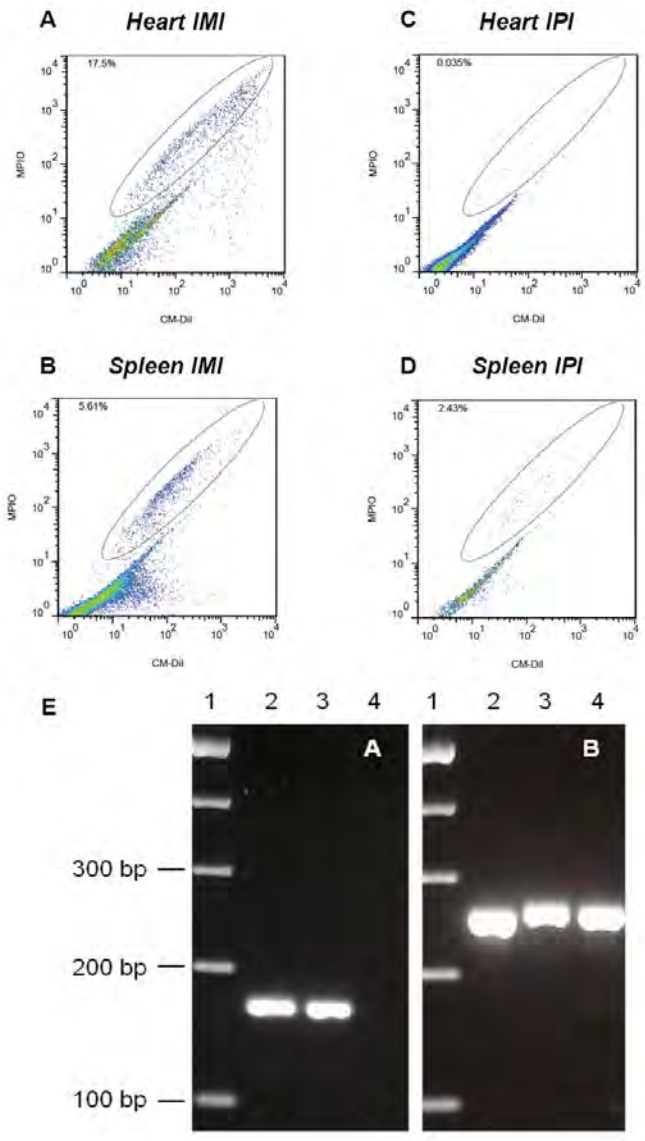

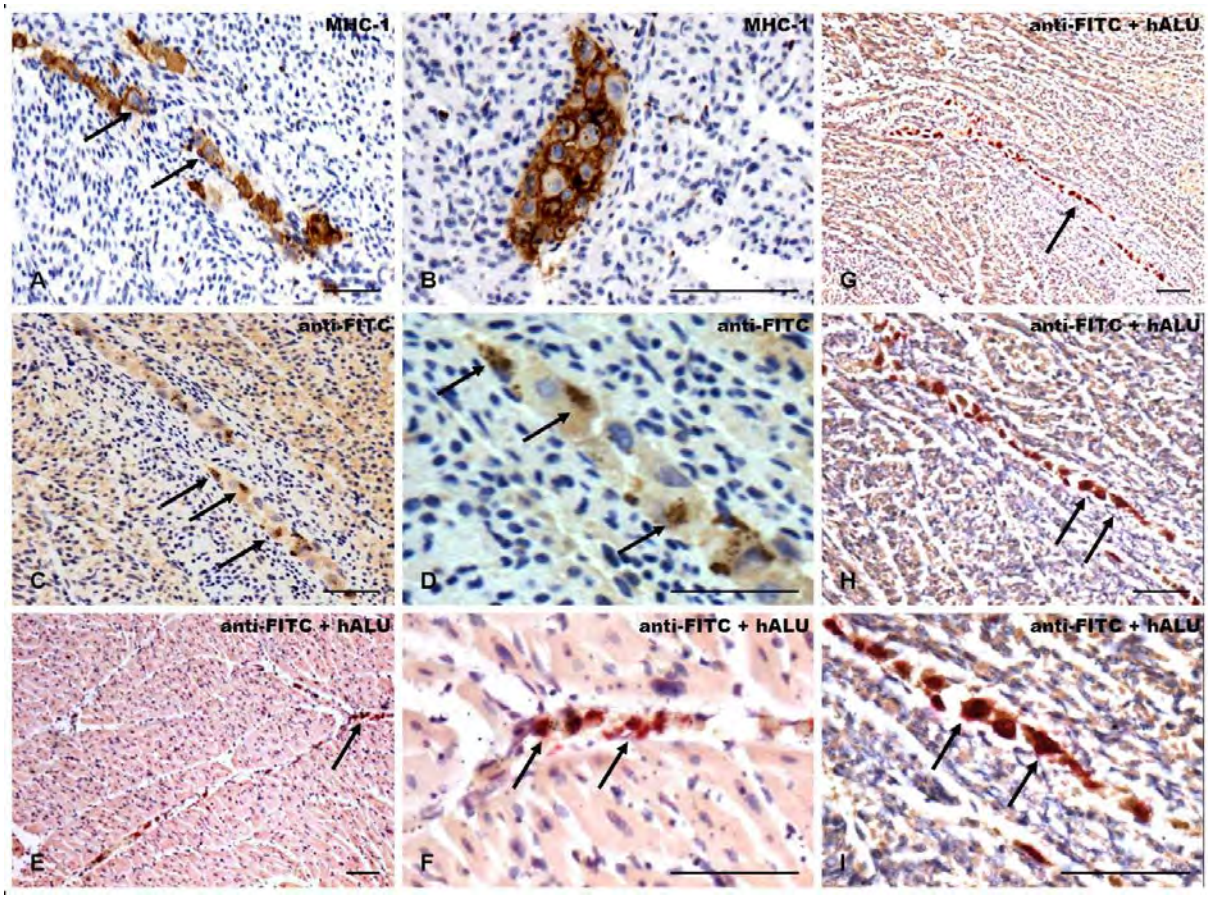

Figure 9: Detection of CM-DiI⁺/MPIO⁺ human ATMSCs in the pre-immune fetal sheep myocardium via immunohistochemistry

Exemplary image series post intramyocardial transplantation of human ATMSCs into the fetal myocardium. Morphologically CM-DiI⁺/MPIO⁺ human ATMSCs could be easily identified within the fetal heart tissue suggesting to be in good shape and viable. The cells appeared to be integrated within the fetal myocardium and could be found as clusters as well as in the interstitial and intravascular spaces **(A-I;** *black arrows*). The cells stained positive for human specific Major Histo Compatibility Complex 1 (MHC-1) clearly confirming the human origin **(A and B;** *black arrows; magnification x10 and x20*) and also stained positive for anti-FITC detecting the Dragon Green fluorochrome labelled MPIOs within the human cells **(C and D;** *black arrows; magnification x10 and x40*). In addition, double staining for ALU Sequence and anti-FITC further confirmed the presence of the injected CM-DiI⁺/MPIO⁺ human ATMSCs within healthy heart tissue **(E and F;** *black arrows; magnification x2.5 and x40*) as well as in infarcted myocardium **(G-I;** *black arrows; magnification x2.5, x10 and x40*). *Scale Bar: 100 um (A-C, E, G, H), 50 um (D, F, I).*

Assessment of intrinsic immune response versus CM-DiI⁺/MPIO⁺ human ATMSCs and BMMSCs in the fetal sheep myocardium

Detailed assessment for ovine CD3⁺ T-cells, CD20⁺ B-lymphocytes as well as CD68⁺ macrophages in the fetal myocardial tissue did not show a potential intrinsic immune response against the injected CM-DiI⁺/MPIO⁺ human ATMSCs and BMMSCs (figure 10A-I). The ovine immune cells could be detected in normal, tissue-specific frequencies and appeared to be disseminated within the entire fetal myocardium without any sign of activation due to an immune response against the human cell graft (figure 10D-F). In particular, neither a T- or B-cell infiltration into the area of the human cell graft, nor increased numbers of macrophages in this area could be observed (figure 10D-F). In

contrast, CM-DiI$^+$/MPIO$^+$ human ATMSCs and BMMSCs could be easily identified morphologically, and by positive staining for human-specific ALU-sequence as well as the specific intracellular, brown colour dots given by the iron-oxide particles clearly indicating that the human cells were in physiological shape, have kept the MPIOs intra-cellular and have not been phagocytized by ovine macrophages (figure 10G-I).

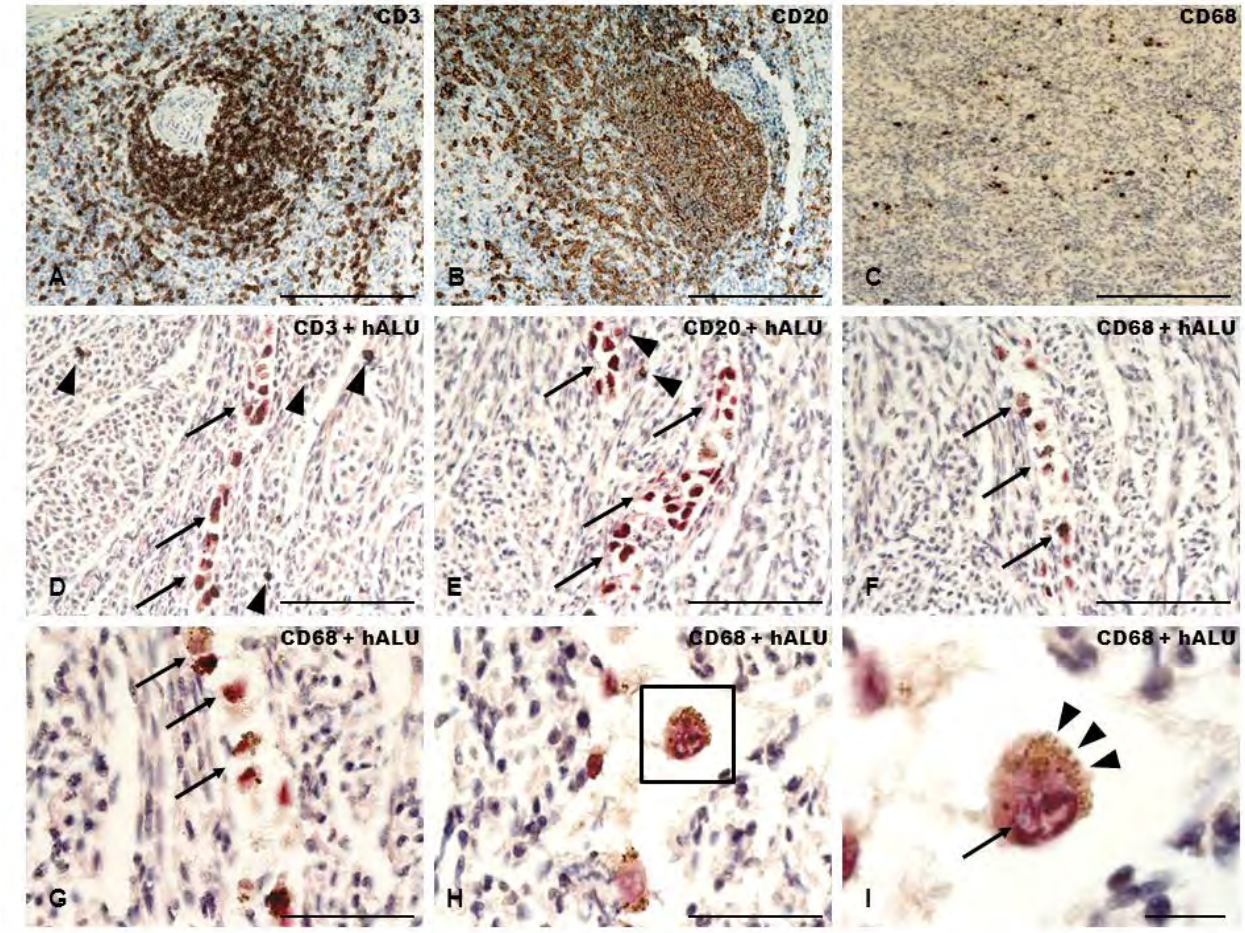

Figure 10: Assessment of intrinsic immune response versus CM-DiI$^+$/MPIO$^+$ human ATMSCs in the pre-immune fetal sheep myocardium

Control staining of CD3$^+$ T-cells, CD20$^+$ B-lymphocytes and CD68$^+$ macrophages in ovine spleen tissue **(A-C;** *magnification x10*). After direct intra-myocardial injection of CM-DiI$^+$/MPIO$^+$ human ATMSCs **(D-I;** black arrows; *magnification x20, x40, x63*), CD3$^+$ T-cells **(D;** black arrow heads; *magnification x20*) CD20$^+$ B-lymphocytes **(E;** black arrow heads; *magnification x20*) could be detected in normal, tissue-specific frequencies and appeared to be disseminated within the entire fetal myocardium without any sign of activation due to an immune response against the human cell graft. In particular, neither a T- or B-cell infiltration into the area of the human cell graft, nor increased numbers of CD68$^+$ macrophages **(F;** *magnification x20*) in this area could be observed. In contrast, CM-DiI$^+$/MPIO$^+$ ATMSCs could be easily identified morphologically and by positive staining for human-specific ALU-sequence **(D-I;** black arrows; *magnification x20, x40, x63*). The human cells were in physiological shape **(G and H;** black arrows and black frame; *magnification x40*), have kept the MPIOs intra-cellular **(I;** black arrow heads; *magnification x63*) and have not been phagocytized by ovine macrophages. *Scale Bar: 100 um (A-F), 50 um (G and H) and 20um (I).*

Discussion

Stem cells have shown great promise as a therapeutic strategy for the failing heart after myocardial infarction and based on encouraging preclinical studies [51], there are growing numbers of clinical pilot trials showing the principal feasibility of stem cell-based therapies [4-7, 183]. However, the rapid and often too premature translation into the clinical arena has left many key questions unanswered with special regards to the in-vivo cell fate which is fundamental to fully understand the possible beneficial effect on the diseased heart. In addition, the availability of suitable animal-models to assess human stem-cell fate and bio-distribution in-vivo is limited. As most available large animal models require immunosuppressive therapy when applying human cells to the myocardium [51] the clinical relevance is compromised and a surrogate animal model is mandatory to evaluate human stem-cell fate including bio-distribution, engraftment and survival in the absence of any xenogenic immune response.

To overcome these limitations, for the first time we demonstrate the principal feasibility to use a pre-immune fetal sheep intra-uterine myocardial infarction model for the assessment of human stem-cell fate after direct intra-myocardial stem-cell transplantation. Using advanced, imaging-guided cell-tracking protocols comprising magnetic-resonance imaging (MRI) and micro computed-tomography (Micro CT) as well as in-vitro cell-tracking tools, this novel model offers an excellent platform to evaluate human cell-fate in the absence of immunosuppressive therapy.

The pre-immune fetal sheep model has been previously suggested to represent an appropriate animal model for the assessment of human cell-fate. Before day 75 of gestation the immune-system of the fetal sheep is normal functioning, but is still largely immuno-naïve supporting the engraftment and differentiation of human stem cells without the necessity of immunosuppressive therapy that would also compromise the transplanted cells [52, 53, 184-186, 190, 191]. In line with that, in our study we did not detect a potential intrinsic xenogenic immune response after direct intra-myocardial injection of human mesenchymal stem cells.

While the pre-immune fetal sheep has been primarily used in the field of experimental haematology to assess in-vivo cell-fate and bio-distribution after ultrasound-guided, intra-peritoneal stem cell delivery [53, 194-197, 202], this is the first report demonstrating the feasibility of direct intra-myocardial stem-cell transplantation after myocardial infarction. While previous studies reported a limited homing to the myocardium after intra-peritoneal stem-cell transplantation [53, 194-197, 202] indicating the clear limitations of this model with regards to myocardial regeneration, our novel concept of intra-uterine, direct intra-myocardial stem-cell transplantation appears to be more appropriate in the setting of cardiovascular stem cell therapy concepts and offers a significant improvement with regards to myocardial cell retention.

In this study, we used an advanced concept of imaging-guided tracking methodology including MRI / Micro-CT Scanning as well as multiple analysis tools comprising Flow Cytometry, PCR and IHC to track human cells in the fetal sheep myocardium. Using novel micron-sized, Dragon-green fluorochrome labelled iron-oxide particles (MPIO) that had so far been used in the field of liver research [50, 200, 201], we were able to evaluate human cell-fate after intra-myocardial stem cell transplantation on MRI which was then followed by detailed Flow Cytometry, PCR and IHC assessment highlighting the advantage of the fluorochrome co-labelled MPIOs. On MRI, the MPIO labeled cell-clusters were clearly visible within the septal and anterior-lateral ventricular-wall corresponding to the injection sites. Thereafter, the intra-myocardial presence was verified on Flow-

Cytometry and PCR, before it was further confirmed on IHC via positive staining for human-specific MHC-1, ALU-Sequence as well as anti-FITC detecting the fluorochrome labeled part of the iron-oxide particles. Considering the initially performed dilution series, the amount of cells within the myocardium could be estimated to approximately 1 $x10^5$ - 5 $x10^5$ providing a brief quantitative estimation of cell-retention after intra-myocardial stem-cell transplantation as a precondition to explain potential beneficial effects of stem-cell therapy concepts.

Advanced imaging technologies for stem-cell tracking with regard to survival, engraftment and differentiation represent a key-requisite to validate functional effects of cell-based therapy concepts [47, 203]. Various imaging-concepts are currently under evaluation including MRI imaging with direct cell-labelling of cells using super-paramagnetic agents, PET- or SPECT-imaging using radio-nuclides, as well as reporter-genes [47, 203]. While each of these approaches has advantages and disadvantages, most of the recent large animal-studies applied MRI technology to detect super-paramagnetic agents as this technique has become an important endpoint to demonstrate efficacy in clinical pilot studies [47]. It offers detailed morphologic as well as functional cardiac information and therefore appears to be an appropriate imaging tool to comprise both, efficacy evaluation and the capability for cell-tracking. Current studies aim on refining contrast-agents to achieve a maximum signal for minimum labelling [47]. While the lowest cell amount detectable with a conventional MRI scanner was 10^5, a recent study highlighted that this threshold of detection can be further reduced whit the use of high resolution scanners (11.7-T) that may even allow for single cell tracking [49]. In addition, preclinical animal studies applying micron- or nano-sized iron-oxide particles showed the feasibility of non-toxic labelling of mesenchymal stem cells (MSCs) without compromising their trans-differentiation capacity [49, 204-206].
On the other hand, it has been described that the main disadvantage of using super-paramagnetic agents is the fact that the imaging signal is not directly linked to cell-viability and the inability to discriminate between vital, labelled cells and particle-loaded cell-debris or hosting macrophages that may have actively phagocytised the particles after cell-death significantly confounding a sufficient call tracking analysis [203]. However, utilizing a detailed in-vitro tissue evaluation and importantly, advanced super-paramagnetic agents such as micron-sized, Dragon-green fluorochrome co-labeled iron-oxide particles [50, 200, 201], we were able to proof the MRI findings and to confirm the presence of the transplanted cells within the fetal myocardium. Using specific antibodies to either detect human cells, the fluorochrome co-labelel MPIOs or both, we were able to clearly detect the transplanted cells highlighting the efficacy of this cell-tracking approach.
Finally, while various stem cell sources are currently under evaluation for their ability to promote cardiac repair [14, 63, 146, 152, 153, 165, 207, 208], in this study we used human mesenchymal stem cells (MSCs) either derived from the bone-marrow or from the adipose tissue as they are considered clinically safe, easily available and immuno-privileged [29]. In particular, bone-marrow derived MSCs representing a benchmark cell for cardiovascular stem cell therapies have been repeatedly used in preclinical animal models [209-213] as well as in clinical pilot trials [7, 29, 183]. Importantly, beside their suggested function through multiple paracrine effects [7] recent reports indicate that bone-marrow MSCs can be programmed into a cardiac committed stage increasing their clinical relevance and potential [30]. Similarly, the adipose tissue also represents a rich source of MSCs being well comparable to those derived from the bone marrow [214] with regards to the surface marker profile and the differentiation capacity. Furthermore, due to their abundant

availability and the even lesser invasive access, adipose tissue derived MSCs should be considered as an attractive and clinically highly relevant stem cell source for future therapy concepts [31].

There are several limitations in our report that need to be addressed in further studies: First, since it was the overall aim of this proof-of-concept study to establish a novel model of intra-uterine induction of MI and direct intra-myocardial stem cell transplantation in a technically challenging and very delicate fetal environment, the number of animals was low and the follow-up time was relatively short. Therefore, further studies with an increased number of animals and a longer follow-up are mandatory in order to address the important aspect of long-term engraftment and bio-distribution. Secondly, in the context of the presented multimodal approach for an advanced cell tracking comprising Flow-Cytometry, PCR and IHC, it is to mention that the Flow Cytometry results may have been influenced by the location and size of the harvested cardiac sample as well as the gating strategy. To address the key aspect of cellular retention more accurately including absolute number of cells, the analysis of the entire heart with only a single assessment strategy either using Flow-Cytometry or qPCR would be necessary. Third, in this study two different types of human mesenchymal stem cells were used potentially influencing the study results to some extent. In addition, and although the cardiovascular differentiation potential of human mesenchymal stem cells is of particular interest, this was beyond of this proof-of-concept study. Moreover, besides the infarction histology, a functional assessment (i.e. with echo) of the fetal heart after myocardial infarction was not performed in this first feasibility study. Finally, the MRI analysis was based on T2w sequences. To further enhance cell number estimation accuracy, T2w and T2*w relaxation curves of the tissue will be performed.

Conclusions

For the first time we demonstrate the principal feasibility of direct intra-myocardial stem-cell transplantation following intra-uterine induction of myocardial infarction in the pre-immune fetal sheep. Using an advanced cell-tracking strategy comprising *state-of-the-art* imaging techniques including magnetic-resonance imaging (MRI) and micro computed-tomography (Micro CT) as well as multimodal in-vitro tracking tools, this model offers a unique platform to evaluate human cell-fate and to track human stem cells in a relevant large animal-model without the necessity of immunosuppressive therapy.

Acknowledgements:

We thank Scanco Medical for performing the Micro-CT analyses.

Statictical Analysis

Quantitative data are presented as mean ± standard deviation (SPSS 17.0, IBM, Somers, NY, USA).

Chapter 4

Transcatheter based electromechanical mapping guided intramyocardial transplantation and *in vivo* tracking of human stem cell based three dimensional microtissues in the porcine heart

The contents of this chapter are part of **Emmert MY,** Wolint P, Winklhofer S, Stolzmann P, Cesarovic N, Fleischmann T, Nguyen T, Frauenfelder T, Böni R, Scherman J, Bettex D, Grünenfelder J, Schwartlander R, Vogel V, Gyöngyösi M, Alkadhi H, Falk V, Hoerstrup SP. *Transcatheter based electromechanical mapping guided intramyocardial transplantation and in vivo tracking of human stem cell based three dimensional microtissues in the porcine heart.* Biomaterials 2013 Mar;34(10):2428-41.

Abstract

Stem cells have been repeatedly suggested for cardiac regeneration after myocardial infarction (MI). However, the low retention rate of single cell suspensions limits the efficacy of current therapy concepts so far. Taking advantage of three dimensional (3D) cellular self-assembly prior to transplantation may be beneficial to overcome these limitations. In this pilot study we investigate the principal feasibility of intramyocardial delivery of *in-vitro* generated stem cell-based 3D microtissues (3D-MTs) in a porcine model. 3D-MTs were generated from iron-oxide (MPIO) labeled human adipose-tissue derived mesenchymal stem cells (ATMSCs) using a modified hanging-drop method. Nine pigs (33±2kg) comprising seven healthy ones and two with chronic MI in the left ventricle (LV) anterior wall were included. The pigs underwent intramyocardial transplantation of $16x10^3$ 3D-MTs (1250cells/MT; accounting for $2x10^7$ single ATMSCs) into the anterior wall of the healthy pigs (n=7) / the MI border zone of the infarcted (n=2) of the LV using a 3D NOGA electromechanical mapping guided, transcatheter based approach. Clinical follow-up (FU) was performed for up to five weeks and *in-vivo* cell-tracking was performed using serial magnet resonance imaging (MRI). Thereafter, the hearts were harvested and assessed by PCR and immunohistochemistry. Intramyocardial transplantation of human ATMSC based 3D-MTs was successful in eight animals (88.8%) while one pig (without MI) died during the electromechanical mapping due to sudden cardiac-arrest. During FU, no arrhythmogenic, embolic or neurological events occurred in the treated pigs. Serial MRI confirmed the intramyocardial presence of the 3D-MTs by detection of the intracellular iron-oxide MPIOs during FU. Intramyocardial retention of 3D-MTs was confirmed by PCR analysis and was further verified on histology and immunohistochemical analysis. The 3D-MTs appeared to be viable, integrated and showed an intact micro architecture. We demonstrate the principal feasibility and safety of intramyocardial transplantation of *in-vitro* generated stem cell-based 3D-MTs. Multimodal cell-tracking strategies comprising advanced imaging and *in-vitro* tools allow for *in-vivo* monitoring and post-mortem analysis of transplanted 3D-MTs. The concept of 3D cellular self-assembly represents a promising application format as a next generation technology for cell-based myocardial regeneration.

Introduction

The therapeutic options for end-stage myocardial disease comprising medical therapy, assist device implantation (as a bridge to transplant or destination therapy) and heart transplantation as the ultima ratio therapy have evolved over the past years. However, while conventional medication or assist devices can treat only the symptoms, the disproportion between the number of donor organs and the number of potential transplantation candidates limits heart transplantation to a minority of patients and many patients die while being on the "waiting list". Therefore, there is a substantial and urgent therapeutic need to develop alternative therapy options.

As a next generation therapeutic concept, stem cells have shown significant promise in regenerative medicine and in particular with regard to the treatment of the failing heart [8]. On the basis of encouraging preclinical studies [51], patient trials focusing on safety, feasibility and potential efficacy of cell-based therapies have been initiated [4-7, 67, 183]. Several categories of stem cells are being evaluated for their ability to promote cardiac repair and regeneration [10, 17, 29, 31, 63, 146, 152, 165, 168]. Mesenchymal stem cells (MSCs) either derived from the bone marrow [29] the adipose tissue [31] or other sources are considered as a clinical benchmark cell for cardiac repair as they are considered safe and easily available in clinically relevant numbers [29, 31, 213]. However, although stem cells have shown clinical potential the anticipated beneficial effects (that is relevant improvement of cardiac function) have been marginal so far. Clearly, the optimal utilization and exploitation of stem cells for myocardial regeneration comprising the the optimal cell type, the number of cells, the most suitable route for cell delivery (intracoronary vs. intramyocardial) and importantly the optimal application format remain to be investigated and represent the prerequisite for the safe translation into an efficient routine clinical therapy.

After successful delivery, effective cell therapy depends on the intramyocardial retention, survival and engraftment of the transplanted cells [215]. The faster the implant is integrated within the host tissue and supplied with nutrients and oxygen the more efficient the effect of cell therapy can be. Single cell suspensions offer the advantage of a simple and flexible administration via an intracoronary route or by an intramyocardial delivery that can be either carried out by a direct surgical approach or by a minimally invasive, transcatheter based, endocardial approach using the three dimensional NOGA electromechanical mapping system allowing tor the online assessment of myocardial viability via simultaneous evaluation of the electrical and mechanical activity of the left ventricle (LV). The advantages of the NOGA system are multifaceted as it efficiently can distinguish between viable, nonviable, stunned, and hibernating myocardium, can simultaneously analyze LV wall motion and thus precisely can localize the ischemic and peri-ischemic myocardial region (border zone) to determine the optimal transplantation site [35].

However, despite these technical advances, the overall low retention and integration rate within the myocardium when using single cell suspensions limits the efficacy of current therapy concepts [216-218].

In this context, the concept of three dimensional cellular self-assembly prior to transplantation has shown characteristics which might be superior to single cell injections [40-43, 219, 220]. Based on a modified hanging drop culture, we have recently established a microtissue technology allowing for the 3D culture of different cell types which produce endogenous extracellular matrix environments with improved adhesion and integration properties [40-42]. In addition, we were able to demonstrate that 3D cardiac microtissues derived from neonatal rat cardiomyocytes show the capacity to connect to a host vascular system and to integrate into the myocardial wall after intra-pericardial injection [41, 42]. Moreover, this 3D micro environment stimulates the production of

pro-angiogenic factors such as VEGF [40-44] which promotes the reconstruction of a myocardial vascular network [41, 221]. Importantly, Garzoni and colleagues highlighted that the presence of these vascular structures are crucial to maintain contractile capacity and long-term survival of cardiac microtissues [45]. Next, Bartosh et al. recently demonstrated mesenchymal stem cell based 3D microtissues can increase the therapeutic potential by enhancement of their anti-inflammatory properties [222].

Taking into account these potential advantages of 3D cellular self-assembly prior to transplantation, in this pilot study we investigate the safety and the principal feasibility of a catheter-based, 3D NOGA mapping guided intramyocardial transplantation of in-vitro generated stem cell based 3D microtissues (3D-MTs) in a porcine model. Utilizing multimodal cell-tracking strategies comprising advanced imaging and in vitro tools, in vivo monitoring and post mortem analysis of transplanted 3D-MTs is performed to evaluate intramyocardial 3D-MT retention, survival and integration.

Material & Methods

Study Design

The aim of this study was to investigate the principal feasibility and safety of a catheter-based, 3D NOGA mapping guided, intramyocardial transplantation of in-vitro generated, stem cell based 3D microtissues (3D-MTs) into the porcine heart (figure 1). The study animals (adult pigs; 33±2kg; n=9) were divided into four groups: group A (non-infarcted; follow up: 4 hours; n=2), group B (non-infarcted; follow-up: 5 weeks; n=3) and group C (left anterior chronic myocardial infarction (CMI); follow-up: 5 weeks; n=2). In addition, and as first set of experiments two pigs (non-infarcted; follow-up: 4 hours; n=2) received a direct, intramyocardial transplantation of 3D-MTs via an anterior, left sided thoracotomy to assess the technical feasibility and the safety of the intramyocardial transplantation of 3D-MTs with a specific focus on potential arrhythmogenic, embolic or neurological events. In the non-infarcted animals (n=7), two transplantation sites were defined. The LV anterior wall was selected for the intramyocardial transplantation of the 3D-MTs, while the lateral wall was chosen to receive the same amount of ATMSCs single cells as a control. In the animals with CMI (n=2), the 3D-MTs were administered into the border zone of the infarcted myocardium.

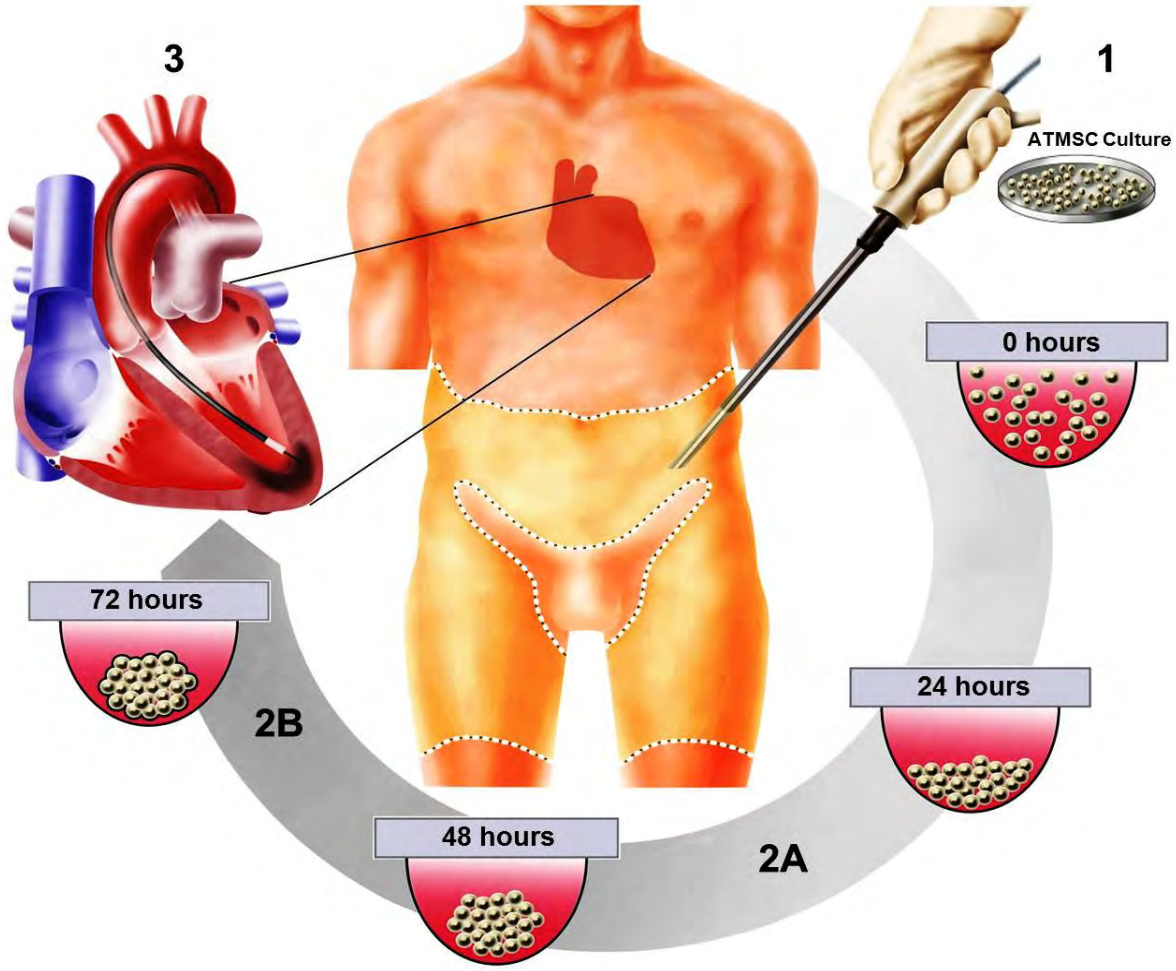

Figure 1: Concept of in vitro generation and NOGA mapping guided, intramyocardial transplantation of human ATMSCs based three dimensional microtissues (3D-MTs)

After liposuction, human ATMSCs are isolated from the adipose tissue and labelled with superparamagnetic microparticles (MPIOs) ***(step 1)***. Using a modified hanging drop culture and based on gravity-enforced three dimensional cellular self-assembly, human ATMSCs based 3D-MTs are generated in vitro over the period of three days ***(step 2A and B)***. A loose formation into 3D-MTs can be instantly observed within the first 24-48 hours ***(step 2A)*** which appears to be stable after 72 hours ***(step 2B)***. Thereafter, transcatheter based, 3D NOGA mapping guided intramyocardial transplantation of 3D-MTs is performed ***(step 3)***.

All procedures were approved by the Institutional Ethics Committee and all animals received humane care in compliance with the "Principles of Laboratory Animal Care" and according to the *Guide to the Care and Use of Experimental Animals* published by the U.S. National Institutes of Health (NIH Publication 85-23, revied 1996). A detailed description of the study design is shown in Figure 2.

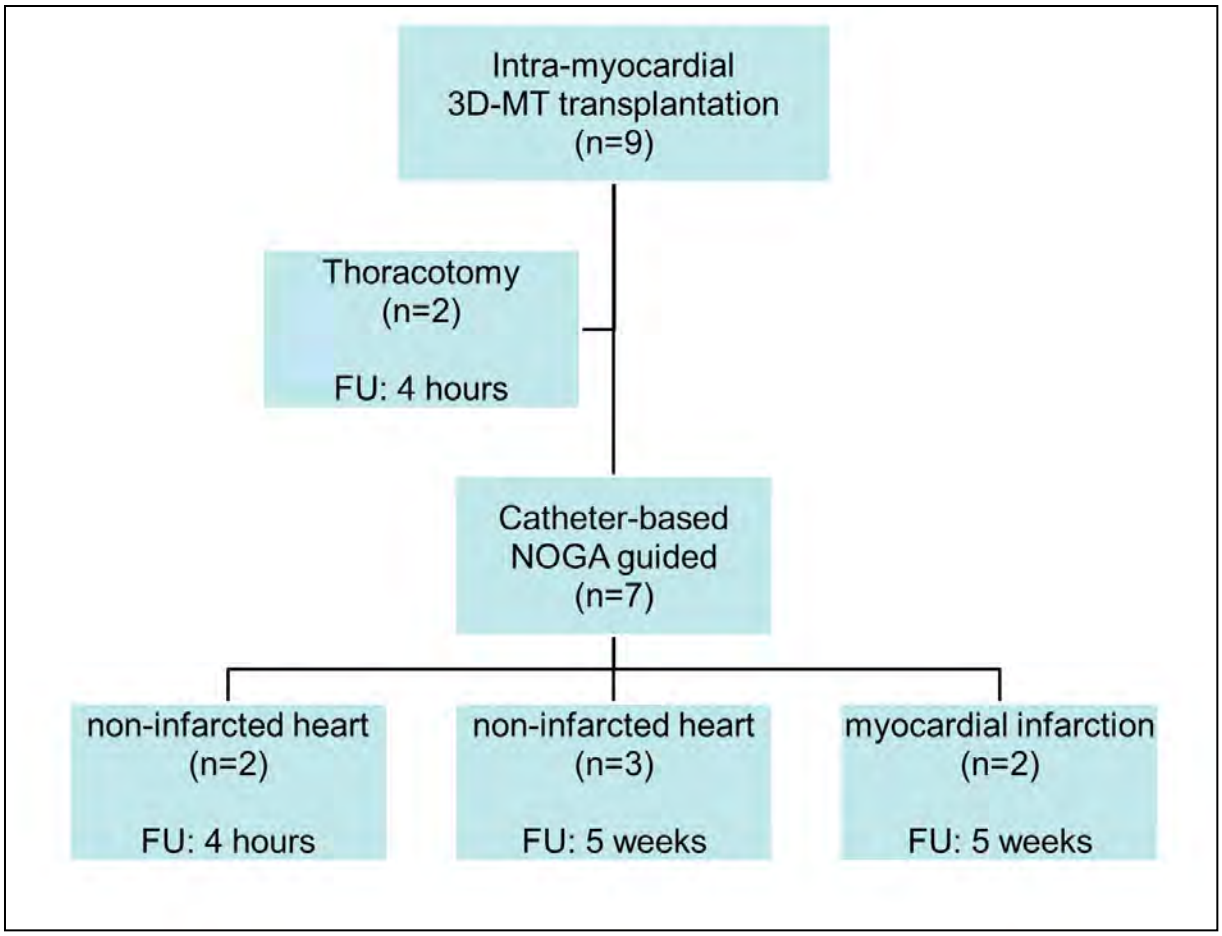

Figure 2: Study design and distribution of animals

Cell Isolation, Characterization and Labeling

Isolation of human adipose tissue derived mesenchymal stem cells (ATMSCs)

After informed consent and approval of an institutional review board and ethics committee, human ATMSCs of three patients (29±8 years) were isolated and processed as described elsewhere [223]. The isolated ATMSCs were cultured in medium (Dulbecco's modified Eagle's medium (DMEM) containing 4.5 g/l glucose (Invitrogen, Switzerland), 2 mM L-glutamine, 100 U/ml penicillin, 100 ug/ml streptomycin and 10% (v/v) hPL) until reaching 80% confluency.

Flow-cytometric characterization of human ATMSCs

In brief, the following mouse anti-human monoclonal antibodies were used: CD31, CD34, HLA-ABC (ImmunoTools, Germany), CD45, CD90 (R&D Systems, Switzerland), CD14, CD29, CD73 and CD166 (BioLegend, Switzerland). Specific expression was determined by comparison with the appropriate isotype control. Cells were incubated with direct labeled primary antibodies for 20 min at 4°C. Next, the cells were washed with FACS buffer consisting of 2% FCS (Biowest, France), 0.5 M EDTA and 0.05% sodium azide (Sigma Aldrich, Switzerland) in phosphate buffered saline (Invitrogen, Switzerland) and fixed in PBS containing 1% paraformaldehyde (Sigma Aldrich, Switzerland). The samples were acquired by BD FACS Canto II Cytometer (Becton Dickinson, USA) and analyzed using FlowJo software (Tree Star, USA).

Differentiation Potential of human ATMSCs

In brief, to induce mineralization, the hATMSCs were incubated with DMEM low glucose (Invitrogen, Switzerland), 10% hPL (Blood donor centre Zürich, Switzerland), 10 mM b-Glycerophosphate, 50 uM L-Ascorbic acid 2-phosphate, 100 nM Dexamethasone (Sigma Aldrich, Switzerland) and 1% Penicillin and Streptomycin (Invitrogen, Switzerland). After three weeks cells were fixed with 4% formalin (Kantonsapotheke Zürich, Switzerland) and calcium deposits were detected using 2% Alizarin red (Sigma Aldrich, Switzerland). For adipogenic differentiation cells were stimulated with induction medium containing DMEM low glucose, 10% hPL, 1 uM Dexamethasone, 10 ug/ml Insulin, 120 uM Indomethacin, 0.5 mM 3-Isobutyl-1-methylxantine (IBMX, Sigma Aldrich, Switzerland) and 1% Penicillin and Streptomycin for 3 days. Afterwards the medium was changed to maintenance medium consisting of induction medium without IBMX supplementation. Three weeks later, the cultures were fixed with 4% formalin and accumulation of lipid vacuoles was stained with 3% Oil Red-O (Sigma Aldrich, Switzerland). Cultures were observed under an inverted microscope (Axiovert 40 CFL, Zeiss, Germany). To evaluate the chondrogenic potential cell aggregates were incubated in induction medium consisting of DMEM high glucose (Invitrogen, Switzerland), 1% hPL, 0.5 ug/ml Insulin, 50 uM L-Ascorbic acid 2-phosphate, 10 ng/ml Transforming growth factor-beta1 (PeproTech, UK) and 1% Penicillin and Streptomycin. After three weeks the pellet was fixed in 4% formalin, paraffin embedded and the staining of the proteoglycan synthesis was performed using 0.1% Toluidine blue (Sigma Aldrich, Switzerland). The slides were analyzed by microscopy (Leica CTR6000, Leica Microsystems AG, Switzerland).

Labeling of human ATMSCs with micron-sized iron oxide particles (MPIOs)

Human ATMSCs were incubated with culture medium supplemented with 1.63um large encapsulated super-paramagnetic microspheres (MPIOs; Bangs Laboratories, USA) at a final concentration of 2.75 ug/ml iron for 24-36 hours as described previously. The particles were co-labeled with Dragon-green fluorochromes for additional analysis using fluorescence-based techniques such as Flow Cytometry and immunohistochemistry. To remove excessive MPIOs after labeling, the cells were washed three times with phosphate-buffered saline (PBS; Invitrogen, Switzerland). The viability and labeling efficiency was determined by trypan blue exclusion and FACS analysis, respectively. To assess the potential impact of MPIO labeling on cell doubling, the time between two cell doublings (generation time) was calculated using the formula: $[\log_{10}2 \times \triangle t]/[\log_{10}(N_H)-\log_{10}(N_1)]$, where $\triangle t$ is the time between passages, N_H is the harvested cell number and N_1 is the initial seeded cell number [224]. Next, the metabolic activity was evaluated using MTT assay directly after MPIO labeling of the cells. The absorbance was measured at a wavelength of 550 nm with 630 nm as a reference.

Generation and characterization of three dimensional microtissues (3D-MTs) derived from human ATMSCs

Generation of human ATMSC based 3D-MTs using a modified hanging drop procedure

Labelled human ATMSCs were seeded with a concentration of $5x10^4$ cells per milliliter into Terasaki microtest plates (Greiner bio-one, Germany). Using a modified hanging drop concept and based on gravity-enforced three dimensional cellular self-assembly human ATMSCs were cultured in hanging drops containing 25 ul of cell suspension per drop. The cells were incubated using the appropriate cell culture medium under standard conditions. After 72 hours 3D-MTs were analyzed by

microscopy (Axiovert 40 CFL, Zeiss, Germany) and the size distribution was determined by using a colony counter (Oxford optronix, United Kingdom) [225].

Histology and Immunohistochemistry

3D-MTs were fixed with 4% formalin (Kantonsapotheke Zürich, Switzerland) for 1 h at RT and afterwards transferred in an agarose plug (Lonza, Switzerland). Stepwise dehydration was performed, followed by paraffin embedding and preparing of 5 um sections. To evaluate the formation potential of the 3D-MTs over time, light microscopy analysis and Hematoxylin and eosin staining (Kantonsapotheke Zürich, Switzerland) was done after 72 hours following 3D-MT generation. To characterize the ATMSC based 3D-MTs, staining for CD90 (BioLegend, Switzerland) was performed. To further assess the proliferation potential of ATMSCs based 3D-MTs staining for the differentiation marker Ki67 (Cell Marque Lifescreen Ltd., Switzerland), Laminin (Serotec Ltd., UK), Collagen IV (Novocastra Ltd., Switzerland).

Size and shape assessment and in vitro evaluation of optimal 3D-MT size for NOGA catheter based applications

After 3D formation, the generated 3D-MTs were assessed via light microscopy and with the colony counter (Oxford optronix, United Kingdom) to evaluate their size. To further determine the ideal 3D-MT size for a NOGA catheter based application, human ATMSC based 3D-MTs were generated in different sizes (10.000, 5.000, 2.500, 1.250 625 cells / per 3D-MT). Thereafter, the 3D-MTs were injected through a NOGA catheter needle (OD: 410um) in vitro and were assessed for their stability with regards to size, shape and uniformity. After the ideal size was defined, the respective 3D-MTs were further characterized and assessed via histology and immunohistochemistry before the respective total number for the in-vivo experiments were produced.

Large animal model and induction of myocardial Infarction

Nine female landrace pigs (33±2kg) were used in the present study. Animals were immunosuppressed with cyclosporine A (Novartis Pharmaceuticals, East Hanover, New Jersey) starting 3 days before cell transplantation with a loading dose of 10 mg/kg daily which was then continued with a dose of 5 mg/kg daily until sacrifice.

Induction of Myocardial Infarction in the LV anterior wall

Myocardial infarction was induced using a standardized *"closed chest occlusion-reperfusion protocol"* according to the protocols described elsewhere [35]. In brief by after selective coronary angiography, a balloon was inflated in the mid part (after the origin of the first major diagonal branch) of the left anterior descending coronary artery (LAD) for 90 minutes followed by reperfusion (Supplementary Figure 1)**.**

Direct intra-myocardial transplantation of 3D MTs via an anterior left sided thoracotomy

The surgical procedure was performed as previously described [183, 213]. In brief, the porcine heart was assessed via an anterior, left sided thoracotomy through the 5th intercostal space. The pericardium was opened and the heart was carefully exposed using surgical swabs to gain access to

the anterior wall / the lateral wall respectively. The injection sites (anterior wall: 3D-MTs / lateral wall: ATMSCs single cells) were visually defined and marked with a pledged stay suture. A total of $16x10^3$ 3D-MTs (1250cells/MT accounting for $2x10^7$ single ATMSCs) and $2x10^7$ single ATMSCs (control) were injected in a total volume of 2 ml of 0.9% NaCl (B.Braun, Melsungen, Germany) (250ul/per injection) using a 1 mL syringe equipped with a 21-gauge butterfly infusion set (Hospira, Lake Forest, Illinois, USA). The injections were administered epicardially into the anterior wall / the lateral wall with a total of up to 8 injections at each transplantation site. After injections, the heart rhythm was monitored and careful haemostasis was achieved hemostatic sealants where necessary. Thereafter, the pericardium was closed and a chest tube was placed. Next, intra-pleural analgesia was given, before the thoracotomy was closed.

3D NOGA mapping guided, catheter-based intra-myocardial transplantation of 3D-MTs

The three dimensional NOGA electromechanical mapping system (Biologics Delivery Systems, Biosense Webster, Johnson & Johnson, Irvindale CA) simultaneously analyzes the electrical and mechanical activities of the left ventricle (LV), enabling online assessment of myocardial viability. The system distinguishes between viable, nonviable, stunned, and hibernating myocardium, can assess wall motion and thus precisely localizes the ischemic and peri-ischemic myocardial regions (border zone) [35].

Electromechanical mapping

Three dimensional NOGA mapping was performed as previously described [35, 226]. In brief, the mapping catheter was inserted across the aortic valve into the apical region of the left ventricle. To generate a detailed 3D electromechanical map of the left ventricle (LV), the catheter was stepwise navigated along the entire LV endocardium and approximately 150-200 measuring points for the complete 3D reconstruction were defined. The unipolar voltage values (in mV) and the ventricular function (shown as lineal local shortening (LLS)) were color coded according to the myocardial viability and superimposed on the 3D geometry of the map.

NOGA mapping guided intra-myocardial transplantation

Intra-myocardial transplantation of 3D-MTs was performed using the 8F MyoStar injection catheter (Bioscience-Webster) using a 27-G needle (outer diameter: 0.41mm). Based on the generated 3D map of the heart, the non-infarcted animals (n=5), were planned to receive transplantation of $16x10^3$ 3D-MTs (1250cells/MT accounting for $2x10^7$ single ATMSCs) into the anterior wall and administration of the same amount of $2x10^7$ ATMSCs single cells (control) into the lateral wall. In animals with CMI (n=2), the 3D-MTs were administered into the border zone of the infarcted myocardium. Before each injection, a ventricular extrasystole verified the intra-myocardial position of the NOGA catheter and a total of up to eight injections (250ul/per injection) was applied slowly (45-60 seconds per injection) at each transplantation site.

Magnetic Resonance Imaging

In vivo cell tracking was performed using serial MRI postoperatively and after 1, 2, 4 and 5 weeks under veterinary anaesthesia and under physiologic monitoring. Data acquisition was performed on a 1.5 T wholebody MR system (Signa Echospeed EXCITE HDxt, GE Healthcare, Waukesha, WI, USA). A phased array cardiac receiver coil for signal reception was placed on the chest with the animal in right decubitus. Cardiac synchronization was performed by ECG. The true short-axis of the left ventricle was determined from long-axis scout images. Additional long-axis views including two-chamber and four-chamber views of the heart were acquired. A 2D multi echo gradient-echo images with 8 different echo times were acquired under suspended respiration in end-expiration according to the following parameters: repetition time, 12ms; echo time, 3.5-25.3 ms; flip angle, 45°; field of view, 280 mm; matrix, 256 x 128; bandwidth 62.5 kHz, slice thickness, 8 mm.

Computed Tomography

Post-mortem ex-vivo CT examinations were performed on a 128-slice dual-source CT (Somatom Definition Flash, Siemens Healthcare, Erlangen, Germany) with the following scan parameters: tube voltage 120 kVp, 200 mAs/rot, automatic exposure control with tube current time modulation was switched off (CareDose4D, Siemens Healthcare, Forchheim, Germany); slice collimation, 0.6 mm; slice acquisition, 2 x 128 x 0.6 mm by means of a *z*-flying focal spot; rotation time, 0.5 s; and pitch, 0.6. Images were reconstructed using a soft tissue convolution kernel (B30f) with a slice thickness of 1.0 mm and an increment of 0.6 mm.

Post-interventional Care & Follow Up

After transplantation, the heartbeat was monitored to confirm post-procedural wellbeing. The animals were left to recover and underwent a daily, clinical check-up with specific regards to arrhythmogenic, embolic or neurological events.

Termination and post mortem analysis

After the respective FU, the animals were sacrificed as previously described for post mortem analysis. To assess the presence and survival of human ATMSC based 3D-MTs, the heart was excised and the transplantation sites were carefully localized. Next, after cutting away the apical and basal region, the LV anterior wall (3D-MTs) and the LV lateral wall (ATMSCs single cell suspension transplantation site; control) were divided into two parts which were fixed in 4% formalin and then processed for PCR, histology and immunohistochemistry.

PCR Analysis

RNA was extracted from formalin fixed, paraffin embedded tissue sections using RecoverAll™ Total Nucleic Acid Isolation Kit (Ambion, Switzerland). The extraction was performed according to Manufacturer's instruction. The quantity and quality was measured with a nanodrop machine (Witec AG, Switzerland). The first-strand cDNA synthesis was generated with 1ug of total RNA and random-hexamer primer using ThermoScript RT-PCR system (Invitrogen, Switzerland). PCR was performed as described previously. The human specific 2-microglobulin sequence (upstream primer: 5'-GTGTCTGGGTTTCATCCATC-3', downstream primer: 5'–GGCAGGCATACTCATCTTTT–3') and the housekeeping gene actin (upstream primer: 5'–CGGGACCTGACTGACTAC–3', downstream primer: 5'–GAAGGAAGGCTGGAAGAG–3') were amplified with the following conditions: initialization

at 95°C for 10 min followed by 30 cycles of denaturation at 95°C for 30 s, annealing at 55°C for 45 s, elongation at 72°C for 45 s and final elongation at 72°C for 10 min. The PCR product was analyzed on a 2% agarose gel stained with GelRed nucleic acid stain (Chemie Brunschwig, Switzerland). Afterwards, DNA fragments of 163 bp for 2-microglobulin or 252 bp for actin were detected.

Histology and immunohistochemistry

Paraffin embedded tissue slides of the porcine myocardium were assessed and characterized in the following manner: First, Hematoxylin and eosin staining (Kantonsapotheke Zürich, Switzerland) was perfomed as described elsewhere. To assess the presence and the survival of human ATMSC based 3D-MTs in the porcine myocardium the tissue was analyzed for human-specific MHC-1 (Epitomics, USA).

Disclosures and Freedom of Investigation

The equipment and technology used in the study were purchased using academic funds. The authors had full control of the design of the study, methods used, analysis of data, and production of the manuscript.

Results

Characterization and MPIO Labeling of human ATMSCs

Cell surface markers of human ATMSCs were evaluated by Flow cytometry. Positive expression of CD29 (mean ± SD, 99.2%±0.7%), CD73 (99.2%±0.6%), CD90 (98.5%±0.7%), CD166 (53.1%±32.2%) and HLA-ABC (30.7%±30.4%) was observed, while negative levels were detected for CD14 (2.8%±2.1%) CD31 (0%), CD34 (0.1%±0.1%) and CD45 (0.2%±0.2%) (figure 3A). Using the assays described, human ATMSCs demonstrated their differentiation potential to the adipogenic, osteogenic and chondrogenic lineages (figure 3B-G). Successful in vitro labeling of human ATMSCs was confirmed via immunofluorescence clearly showing the intracellular the presence of MPIOs (figure 3H and I). This was then further confirmed on flow cytometry analysis displaying a cell labeling efficiency in excess of 70% (figure 3J). The comparison of the generation time between labeled und unlabeled cells showed a similar proliferation capacity (labeled cells 4.7 ± 0.71 days, unlabeled cells 5.4 ± 0.74 days) and the cells also appeared to be comparable with regards to metabolic activity (figure 3K and L).

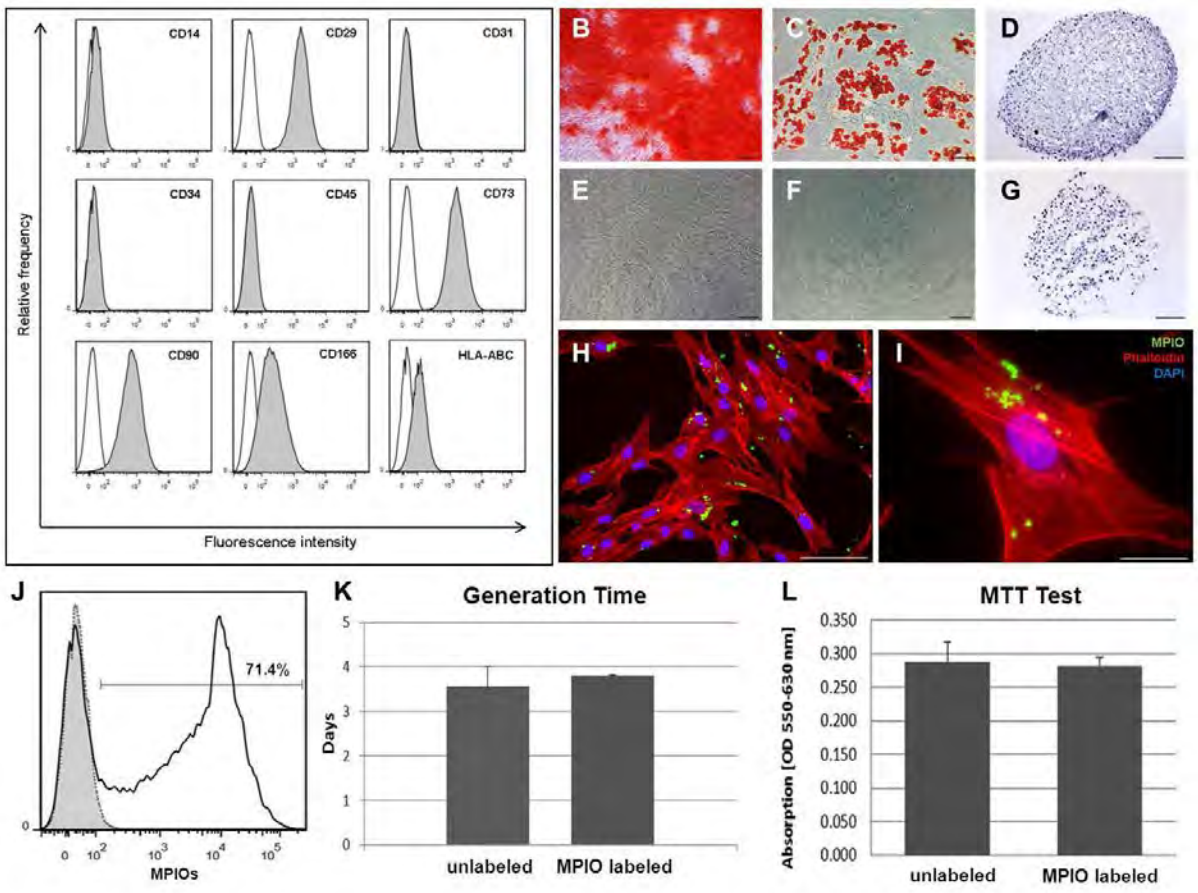

Figure 3: Characterization and Labeling with superparamagnetic microparticles (MPIOs; co-labeled with Dragon-green fluorochromes) of human adipose tissue derived mesenchymal stem cells (ATMSCs)

Human ATMSCs were evaluated by flow cytometry: Positive expression of CD29 (mean ± SD, 99.2%±0.7%), CD73 (99.2%±0.6%), CD90 (98.5%±0.7%), CD166 (53.1%±32.2%) and HLA-ABC (30.7%±30.4%) was observed, while negative levels were detected for CD14 (2.8%±2.1%) CD31 (0%), CD34 (0.1%±0.1%) and CD45 (0.2%±0.2%) **(A)**. Human ATMSCs demonstrated their differentiation potential to the adipogenic *(Oil Red O Staining, Scale Bar: 100um;* **B)**, osteogenic *(Alizarin Red S Staining, Scale Bar: 100um;* **C)** and chondrogenic lineages *(Toluidine Blue Staining, Scale Bar: 100um;* **D).** *Respective negative controls are shown below* **(E-G)**. Successful in vitro labeling of human ATMSCs was confirmed via immunofluorescence microscopy clearly indicating the intracellular the presence of MPIOs **(H and I;** *Scale Bars: 100um and 30um*). This was then further confirmed on flow cytometry analysis displaying a cell labeling efficiency in excess of 70% **(J)**. The comparison of the generation time between labeled und unlabeled cells showed a similar proliferation capacity and the cells also appeared to be comparable with regards to metabolic activity **(K and L)**.

Generation and characterization of human ATMSC based 3D-MTs

Generation of human ATMSC based 3D-MTs using a modified hanging drop procedure

Human ATMSCs (figure 4A) were labelled with MPIOs (figure 4B) and tested for the proliferative capacity (figure 4C) before 3D-MTs were successfully generated within 72 hours starting the 3D formation process within 24-48 hours after beginning the hanging drop culture. After 72 hours, the cells within the 3D-MT displayed a homogenous distribution pattern and appeared to be integrated and viable (figure 4D and E). The 3D-MTs were round-shaped with a homogenous uniformity and a predictable size according to the number of cells used for the 3D-MT generation (figure 4D and E).

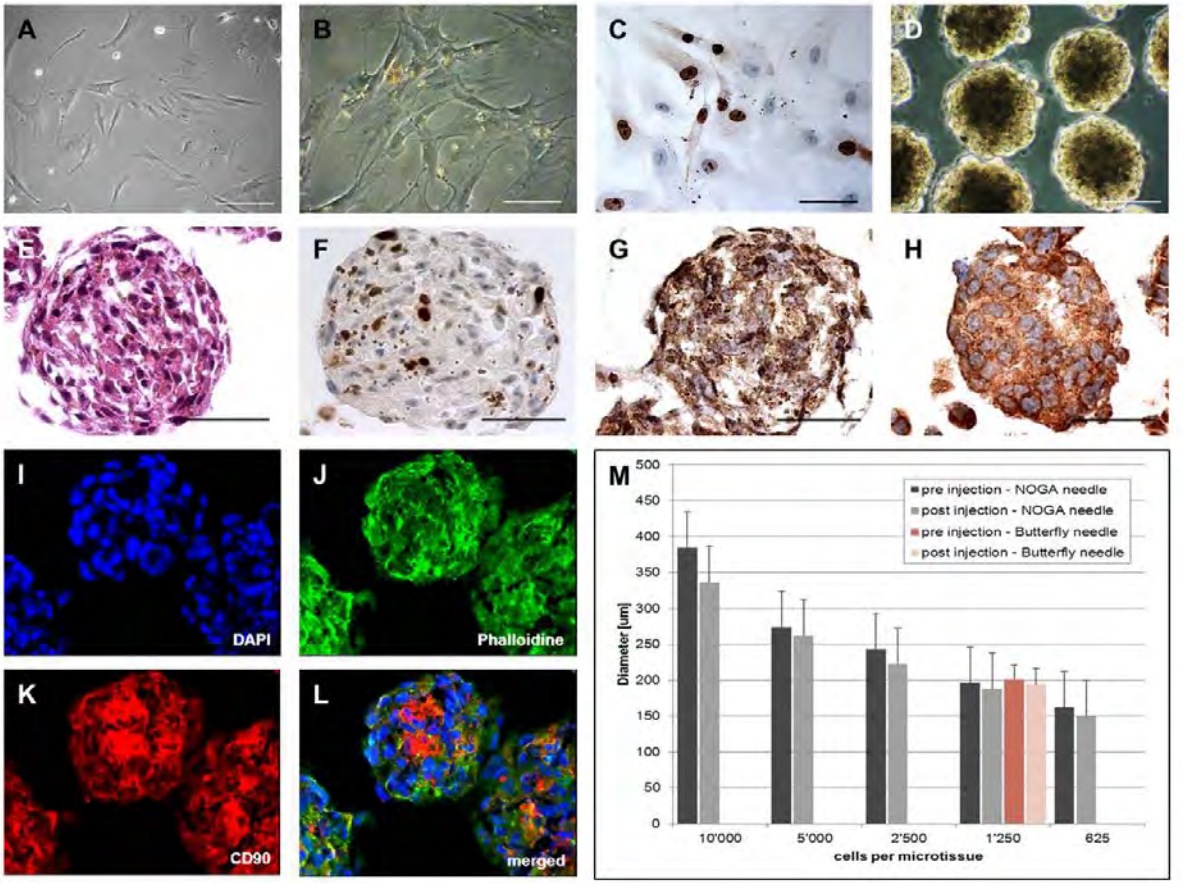

Figure 4: Generation and Characterization of human ATMSCs based three dimensional microtissues (3D-MTs)

Human ATMSCs **(A)** were labelled with MPIOs **(B)** and tested for the proliferative capacity **(C)** before 3D-MTs were generated within 72 hours The cells within the 3D-MT displayed a homogenous distribution pattern and appeared to be well integrated and viable **(D and E).** The 3D-MTs were round-shaped with a homogenous uniformity and a predictable size according to the number of cells used for the 3D-MT generation **(D and E).** Positive staining for Ki67 was indicative for a continuing proliferation potential of human ATMSCs after cellular self-assembly into 3D-MTs **(F).** The formation of extracellular matrix (ECM) within the 3D-MTs was reflected via positive staining for Collagen IV and Laminin after hanging drop culture **(G and H).** The ATMSC based 3D-MTs maintained the typical expression pattern comprising classical surface markers such as CD90 **(I-L).** While 3D-MTs generated from 10.000 cells displayed a mean size of 383.91 um ± 45.98 um, 3D-MTs of 1.250 cells had a mean size of 195.60 um ± 23.35 um and 3D-MTs fabricated from 625 cells showed a mean size of 161.79 um ± 22.99 um **(M).**

Characterization of 3D-MTs

Positive staining for Ki67 was indicative for a continuing proliferation potential of human ATMSCs after cellular self-assembly into 3D-MTs (figure 4F). Next, the formation and generation of extracellular matrix (ECM) within the 3D-MTs to an organized, 3D micro environment could be demonstrated via positive staining for Collagen IV and Laminin starting instantly within the first 24 hours (data not shown) after hanging drop culture (figure 4G and H). Importantly, the ATMSC based 3D-MTs maintained the typical expression pattern comprising classical surface markers such as CD90 (figure 4I-L).

Size assessment of 3D-MTs for catheter based applications

While 3D-MTs generated from 10.000 cells displayed a mean size of 383.91 um ± 45.98 um, 3D-MTs of 1.250 cells had a mean size of 195.60 um ± 23.35 um and 3D-MTs fabricated from 625 cells showed a mean size of 161.79 um ± 22.99 um (figure 4M). The in vitro NOGA needle (OD: 410um) assessment of the optimal 3D-MT size for the NOGA catheter based application identified a 3D-MT generated from 1.250 cells as the optimal format (figure 4M, figure 5). Larger 3D-MTs (10.000 cells, 5.000 cells and 2.500 cells) required a higher pressure to pass through the NOGA needle and importantly, their stability and shape were significantly influenced presenting with a deformation from the classical rounded shape into an oval appearance (figure 5). In contrast, 3D-MTs generated from 1.250 easily passed through the NOGA needle and appeared to be resistant and stable with regards to uniformity, stability and shape (figure 5) suggesting the optimal size format for a NOGA catheter based in vivo transplantation.

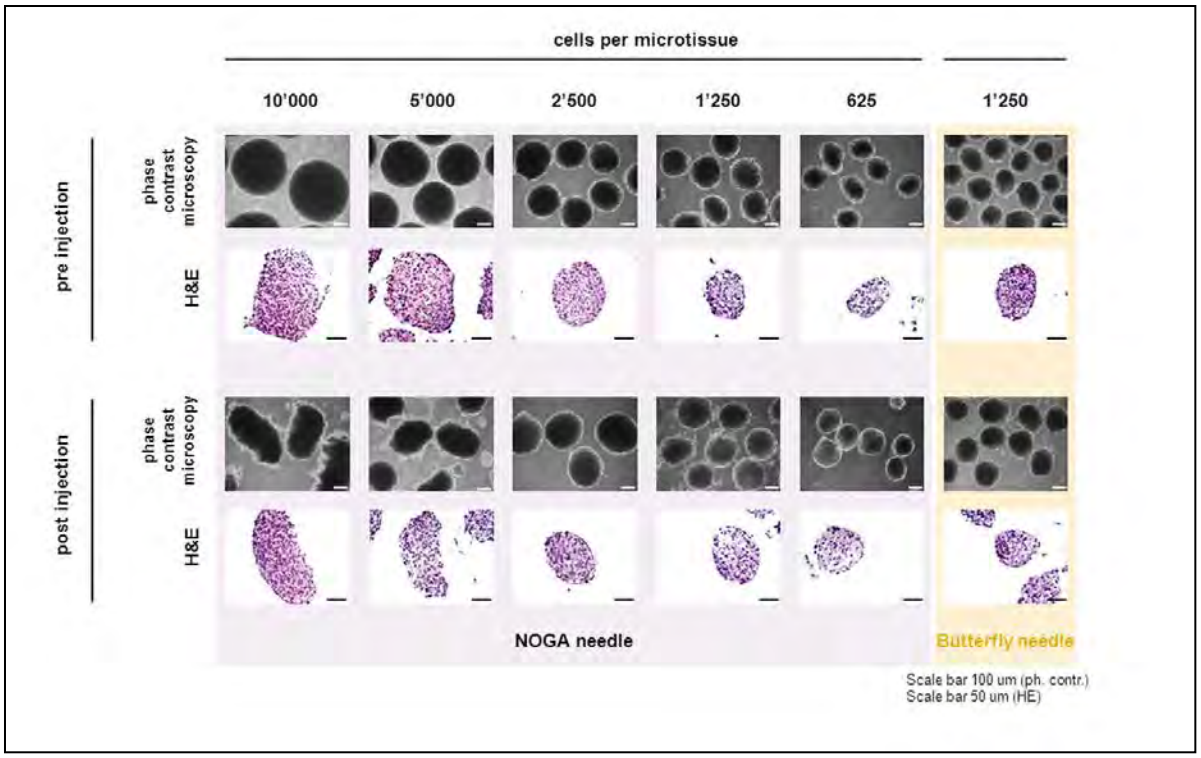

Figure 5: Size assessment and in-vitro needle testing for catheter based application of human ATMSC based 3D-MTs

The in vitro NOGA needle (OD: 410um) assessment of the optimal 3D-MT size for the NOGA catheter based application identified a 3D-MT generated from 1.250 cells as the optimal format *(see also table 1).* Larger 3D-MTs (10.000 cells, 5.000 cells and 2.500 cells) required a higher pressure to pass through the NOGA needle and importantly, their stability and shape were significantly influenced presenting with a deformation from the classical rounded shape into an oval appearance *(see also table 1)*. In contrast, 3D-MTs generated from 1.250 easily passed through the NOGA needle and appeared to be resistant and stable with regards to uniformity, stability and shape *(see also table 1)* suggesting the optimal size format for a NOGA catheter based in vivo transplantation.

Intramyocardial transplantation of 3D-MTs into the porcine myocardium

Intramyocardial transplantation of human ATMSCs based 3D-MTs could be successfully performed in eight animals either using a surgical approach (thoracotomy; n=2) or a catheter-based, NOGA mapping guided application (n=6) (figure 6A-I). One animal (without MI) died during the NOGA mapping procedure due to sudden cardiac arrest. In all other animals (n=8), the respective procedure could be safely performed, no intra-operative complications such as arrhythmogenic, embolic or neurological events occurred and the mean duration of the procedure was 95±8 minutes (thoracotomy; n=2) and 100±12 minutes (NOGA guided procedure; n=6) respectively. Postoperatively, the animals had a swift recovery and during FU, no major cardiac or neurological complications were observed.

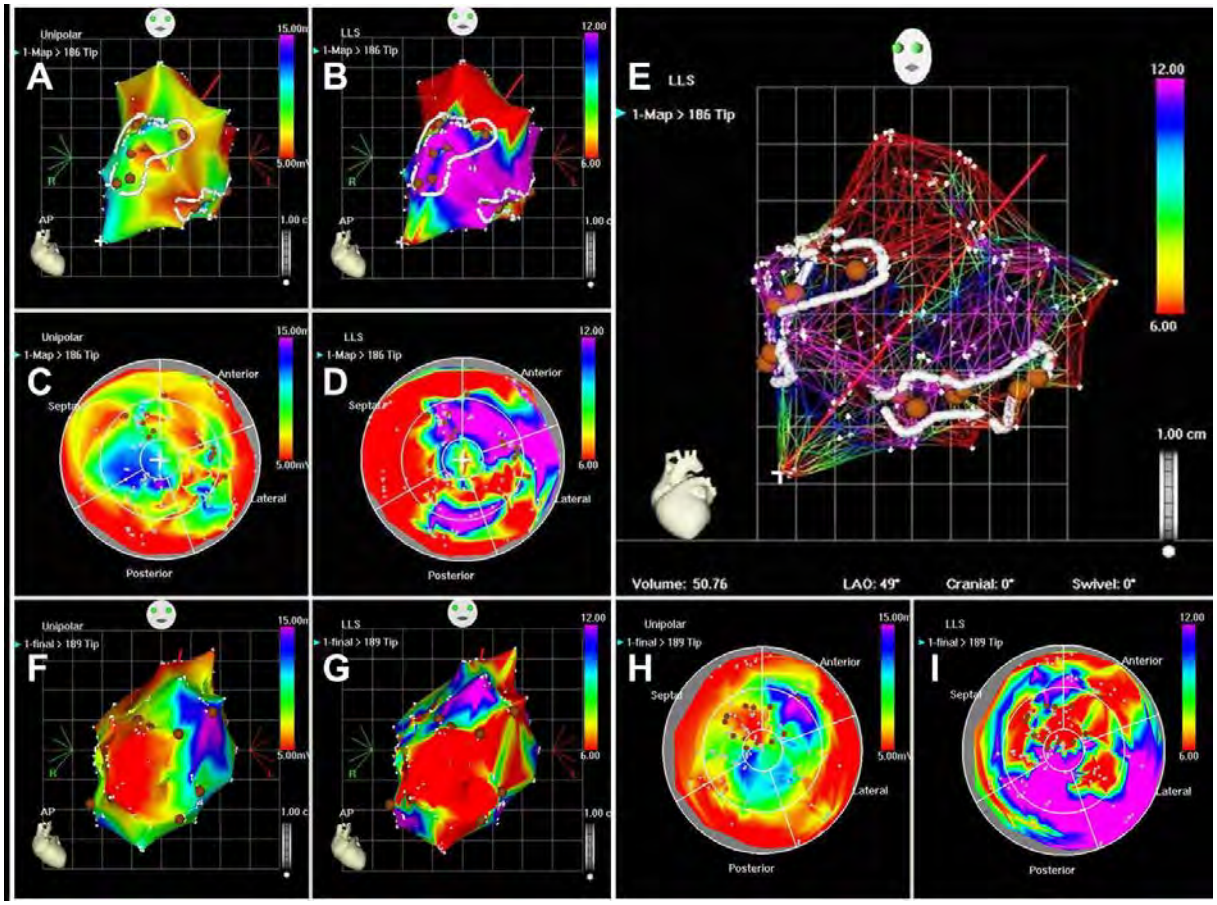

Figure 6: Transcatheter based, NOGA mapping guided intramyocardial transplantation of human ATMSC based 3D-MTs into the porcine myocardium

Exemplary study of NOGA mapping guided, intramyocardial transplantation of human ATMSC based 3D-MTs into the left anterior wall (anterior LV wall: marked area / red dots) of a healthy porcine heart (guided by unipolar voltage (**A,** *AP view and* **C,** *bull eye view*) and lineal local shortening (LLS) (**B,** *AP view;* **D,** *bull eye view and* **E,** *mesh view*). Respective human 2D ATMSCs single cell suspensions (control) were injected into the lateral wall of the ventricle (lateral LV wall: marked area / red dots). In animals with chronic myocardial infarction (CMI), 3D-MTs were intramyocardially injected into the CMI border zone (red dots) which was carefully determined via NOGA mapping guidance prior to transplantation **(F-I)**. The definition of the CMI border zone was based on unipolar voltage values (in mV) being low in the scar area of CMI (color coded in red), moderate in the border zone (color coded in yellow) and normal in the healthy myocardium (color coded in purple) (**F,** *AP view and* **H,** *bull eye view*). In parallel, the impact of CMI on the ventricular function (shown as lineal local shortening (LLS)) was color coded accordingly (**G,** *AP view and* **I,** *bull eye view*).

In vivo tracking of 3D-MTs using serial MRI

Utilizing MRI and targeting the intra-cellular MPIOs, human ATMSCs based 3D-MTs could be successfully detected after intramyocardial transplantation in the LV anterior wall (non-infarcted animals; n=6) (figure 7A-G and 8A-G) and in the MI border zone of the LV anterior wall (n=2) (figure 8H-N and 9A-C) for up to 5 weeks in vivo. In all animals, clusters of 3D-MTs were clearly visible in the porcine myocardium as areas of strong focal signal loss corresponding to the injection sites postoperatively and then serially until the end of FU. While the 3D-MTs that were transplanted via a thoracotomy (n=2) were detected intramyocardially originating from the epicardium

(supplementary figure 2), the ones transplanted using the NOGA catheter (n=6) could be found intramyocardially originating from the endocardium (figure 7A-G and 8A-N). In parallel, the transplanted ATMSCs single cell suspensions (control) could be identified within the LV lateral wall postoperatively and after FU (figure 7A-G and 8A-G).

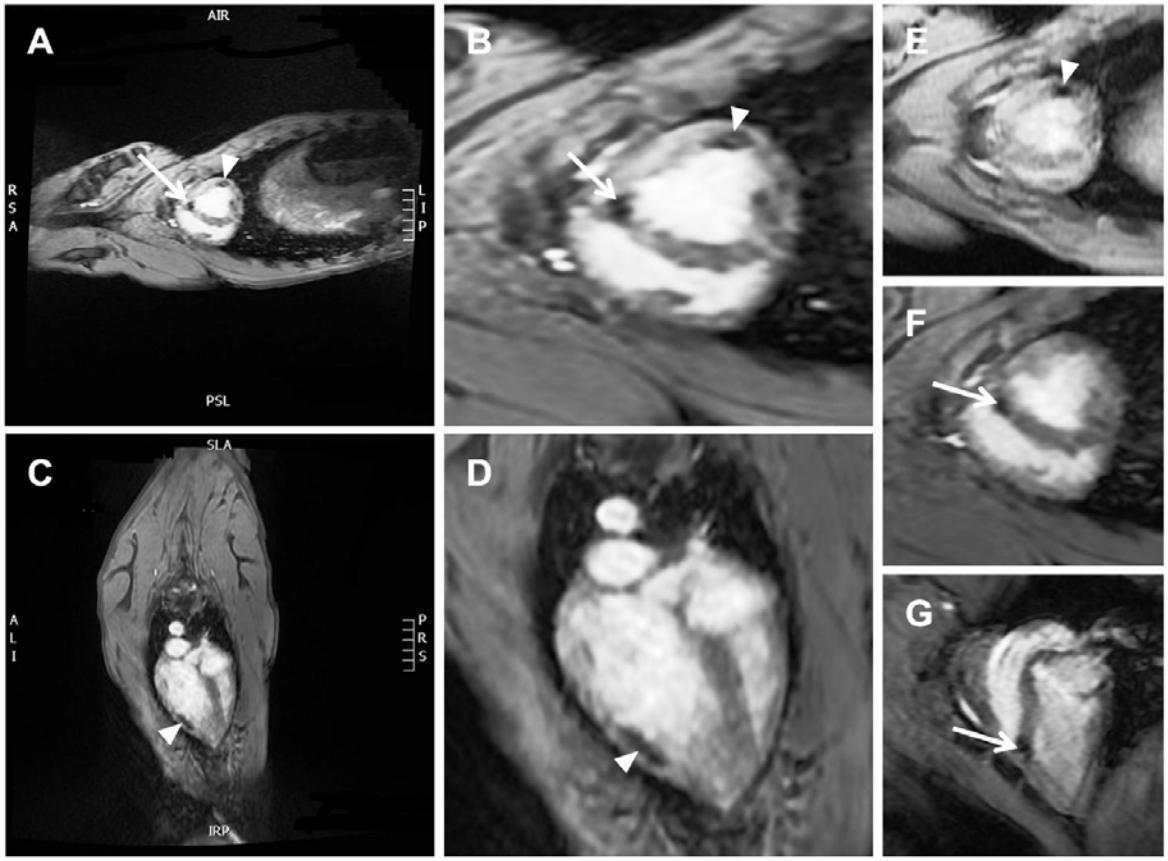

Figure 7: Postoperative MRI based in-vivo tracking of 3D-MTs following 3D NOGA mapping guided, catheter-based intramyocardial transplantation

Direct postoperative MRI based in-vivo evaluation detected the 3D-MTs in the anterior septal LV wall *(white arrows,* **A, B** and **E,** *short axis,* **G,** *two chamber view)* and 2D single cell suspensions (control) in the LV lateral wall (*white arrow heads,* **A, B** and **E,** *short axis,* **C** and **D,** *four chamber view*) corresponding to the injection sites that were defined via 3D electromechanical NOGA mapping prior to transplantation *(please see figure 6 A-E).*

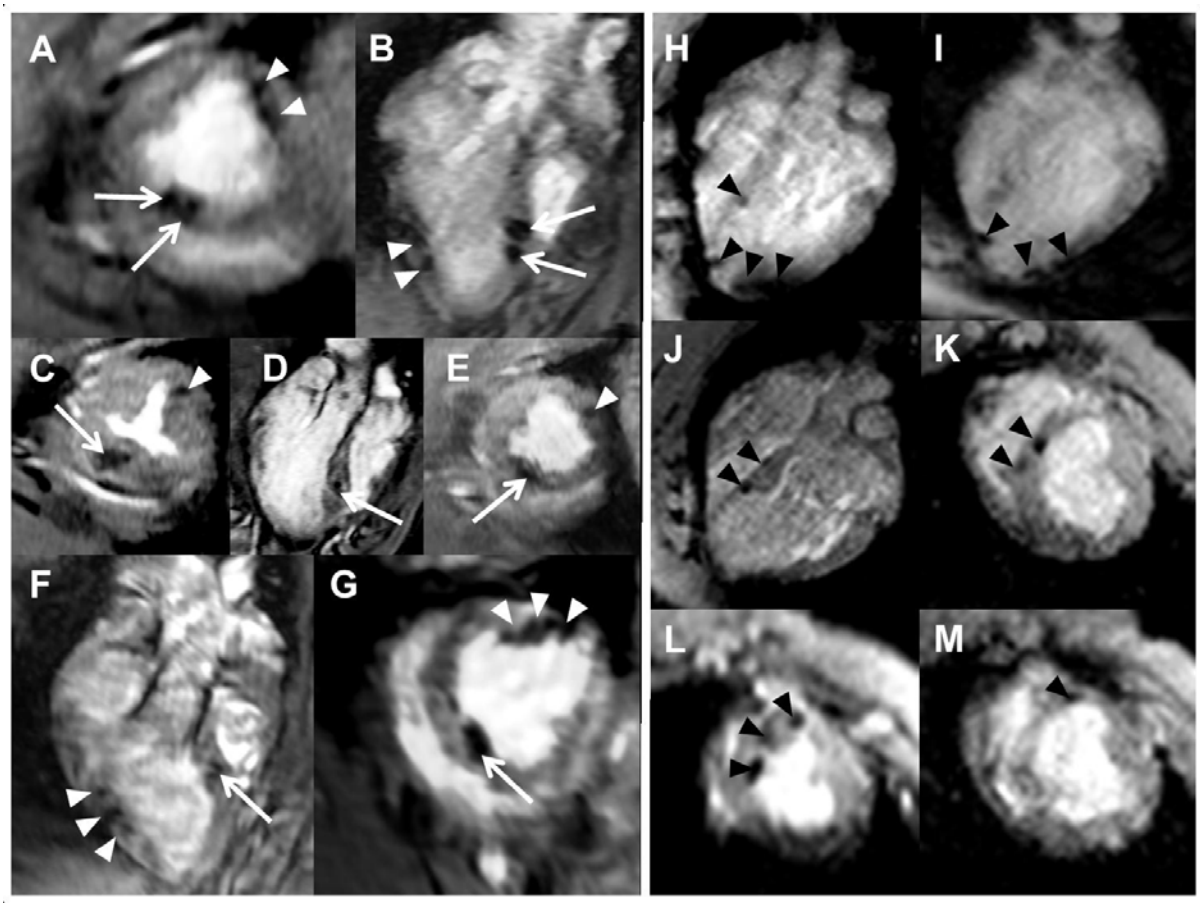

Figure 8: MRI guided in-vivo monitoring of 3D-MTs for up to five weeks after 3D NOGA mapping guided, catheter-based intramyocardial transplantation into the healthy and infarcted porcine heart

MRI based in-vivo monitoring detected the 3D-MTs in the anterior septal LV wall of an healthy porcine heart immediately after transplantation *(white arrows,* **A,** *short axis* and **B***, two chamber view)*, after two weeks *(white arrow,* **C,** *short axis),* four weeks *(white arrows,* **D,** *short axis* and **E***, two chamber view)* and before harvest at five weeks *(white arrows,* **F,** *two chamber view* and **G***, short axis)* corresponding to the injection sites that were defined via 3D electromechanical NOGA mapping prior to transplantation *(please see figure 6 A-E).* In line with that, 2D single cell suspensions (control) could be identified in the LV lateral wall (*white arrow heads,* **A-C** and **D-G)** for the entire study period respectively. In animals with chronic myocardial infarction (CMI) in the anterior septal left ventricular wall, 3D-MTs were injected in a circular fashion into the CMI border zone and could be detected immediately post transplantation *(black arrow heads,* **H** and **I,** *two chamber view)* after one week *(black arrow heads,* **J,** *two chamber view* and **K***, short axis view)* and after five weeks *(black arrow heads,* **L** and **M***, short axis view)* corresponding to the 3D electromechanical NOGA mapping guided transplantation sites.

Post-mortem computed tomography, PCR analysis and immunohistochemistry

After harvest intra-myocardial retention of 3D-MTs was further confirmed on post-mortem computed tomography analysis detecting the 3D-MTs in the anterior septal LV wall of the porcine myocardium (figure 9D-G). In line with that, intramyocardial retention and integration of 3D-MTs was further verified on PCR analysis utilizing human-specific β-2 microglobulin (a component of the class I antigen complex) (figure 9H). Negative controls from non-injected porcine hearts as well as

human ATMSCs used as a positive control clearly confirmed the specificity of human-specific β-2 microglobulin detected within the porcine myocardium after human ATMSC based 3D-MT transplantation (figure 9H). In addition, on immunohistochemistry, intramyocardial integration and engraftment of human ATMSC based 3D-MTs was further confirmed via positive staining for human-specific MHC-1 as well as the detection of the intracellular MPIOs (figure 9I and J).

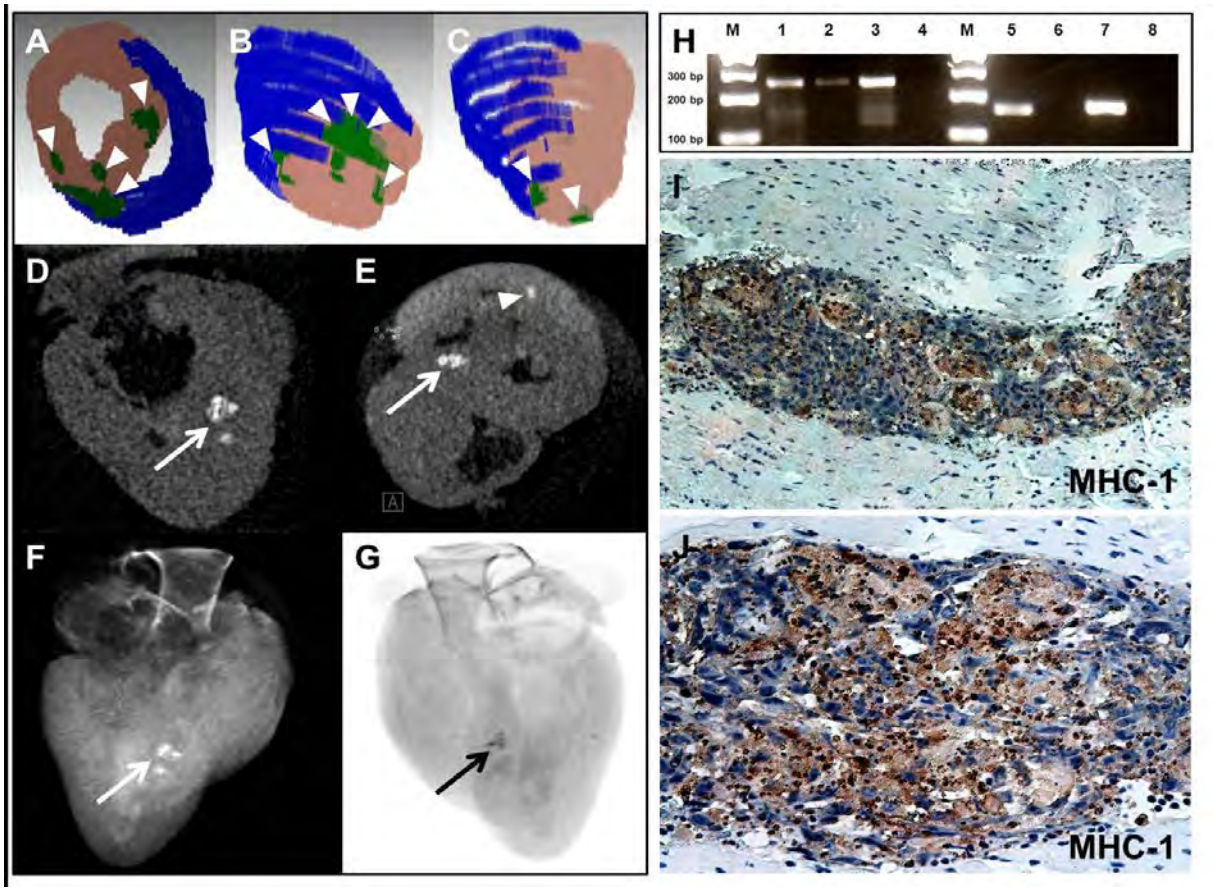

Figure 9: MRI 3D reconstruction analysis and post-mortem multimodal tracking of 3D-MTs in the porcine myocardium using computed tomography, PCR analysis and immunohistochemistry
In an infarcted animal, three-dimensional MRI reconstruction analysis confirmed the intramyocardial presence of 3D-MTs in the border zone of myocardial infarction **(A-C,** *white arrow heads*). Post-mortem computed tomography analysis demonstrated intramyocardial retention of 3D-MTs in the anterior septal LV wall **(D-G,** *white arrows*) and 2D single suspensions (control) in the lateral LV wall of a non-infarcted porcine heart **(E,** *white arrow heads*). In line with that, intramyocardial presence of 3D-MTs was further verified on PCR analysis utilizing human-specific β-2 microglobulin (a component of the class I antigen complex) **(H).** Negative controls from non-injected porcine hearts as well as human ATMSCs used as a positive control clearly confirmed the specificity of human-specific β-2 microglobulin *(Amplification of b-Actin (lanes 1-4, fragment size 252 bp) and β-2 microglobulin (lanes 5-8, fragment size 163 bp) by RT-PCR and analyzed on a 2% agarose gel. RNA was extracted from an animal treated with 3D-MTs (lanes 1, 5), native pig heart (lanes 2, 6) and human ATMSCs (lane 3, 7). H2O control (lanes 4, 8) and DNA basepair size marker (lane M))*. On immunohistochemistry, intramyocardial integration and engraftment of human ATMSC based 3D-MTs was further confirmed via positive staining for human-specific MHC-1 as well as the detection of the intracellular MPIOs **(I and J).**

Morphologically the 3D-MTs could be easily identified within the porcine myocardium (figure 10A-C and 11A-F). They could be found as clusters, appeared to be engrafted and could be found in their typical shape. Importantly, they maintained their stability and seemed to be well integrated within surrounding myocardium (figure 10A-C and 11A-F). In line with that, the human ATMSCs within the 3D-MTs appeared to be viable and the intracellular MPIOs could be easily identified (figure 11F). Human ATMSCs that have been transplanted as 2D single cell suspensions (controls) were also found within the porcine myocardium either appearing randomly distributed (figure 10D and 11G), in the shape of a typical injection channel (figure 11H), as clusters (figure 10E and F; 11I) or as single cells (figure 10G-I).

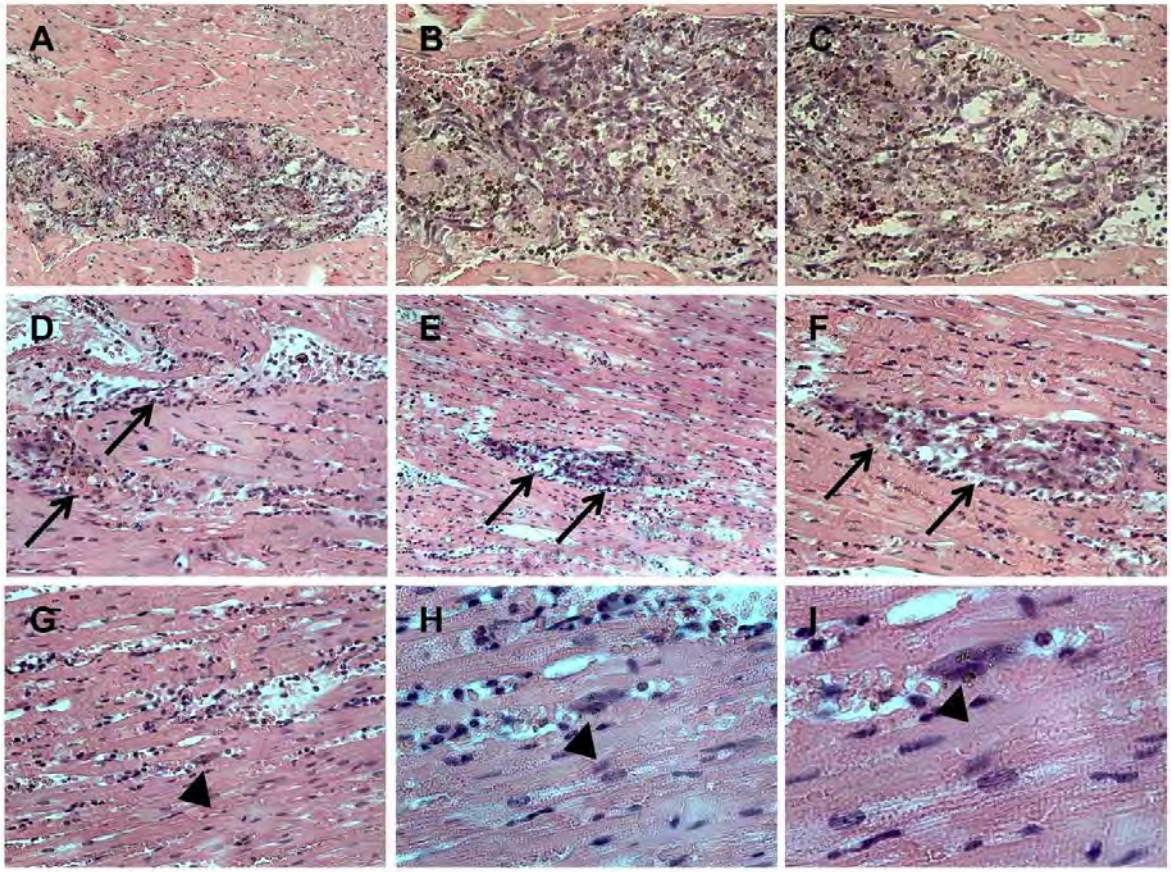

Figure 10: Histological evaluation of 3D-MTs after direct intramyocardial transplantation via an anterior left sided thoracotomy

Following direct intramyocardial delivery, 3D-MTs could be easily identified within the porcine myocardium. They appeared to be well integrated and had maintained their stability within surrounding myocardium **(A,** *magnification x10*, **B** and **C,** *magnification x20*). The human ATMSCs within the 3D-MTs appeared to be viable and the intracellular MPIOs could be easily identified **(B** and **C,** *magnification x20*). Human ATMSCs that have been transplanted as 2D single cell suspensions (controls) were also found within the porcine myocardium either appearing randomly distributed **(D,** *magnification x10; black arrows*), as clusters **(E,** *magnification x10* and **F,** *magnification x20; black arrows*) or as single cells **(G,** *magnification x20*, **H,** *magnification x40* and **I,** *magnification x63; black arrow heads*).

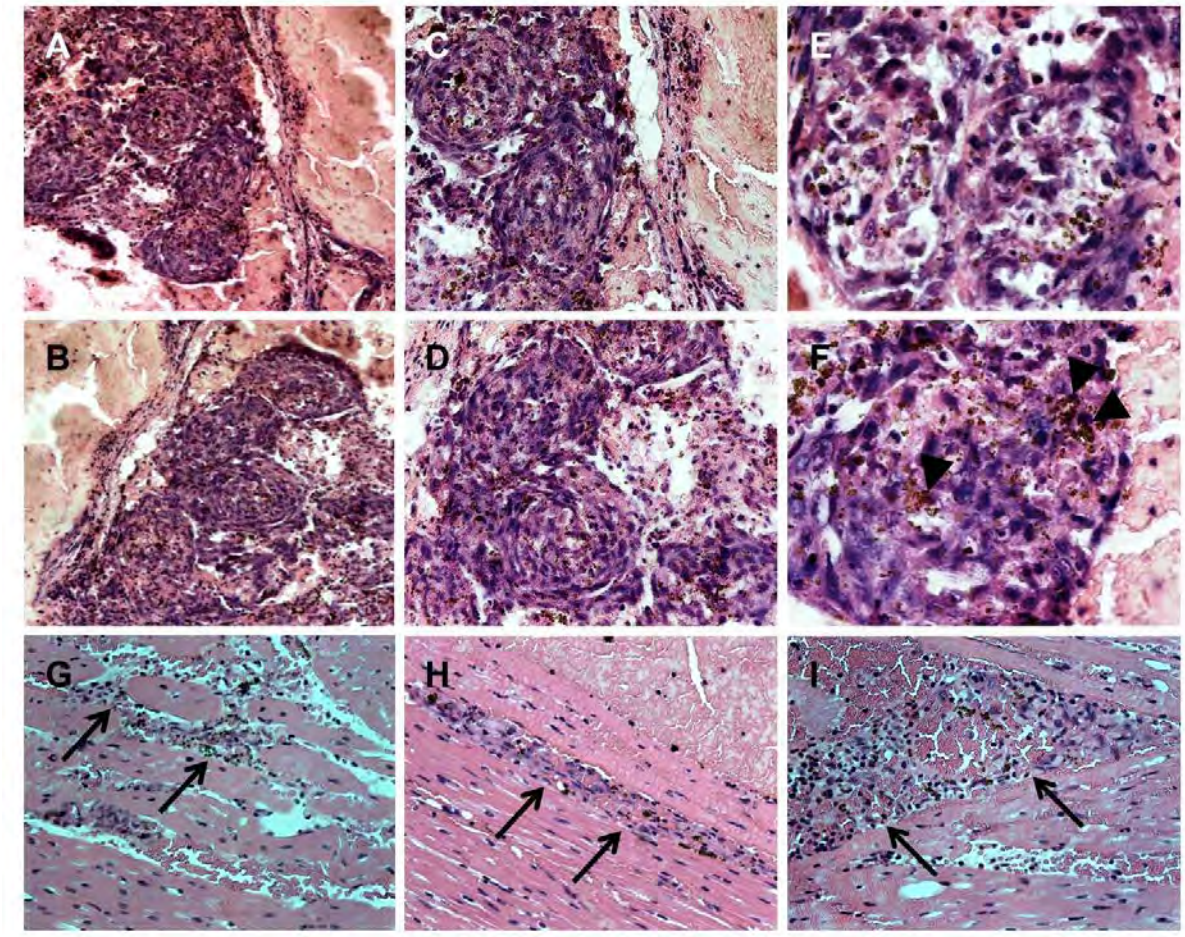

Figure 11: Histological assessment of 3D-MTs after NOGA mapping guided, intramyocardial transplantation into the porcine myocardium

After NOGA mapping guided, intramyocardial transplantation 3D-MTs were detected within the porcine myocardium **(A and B,** *magnification x10*, **C and D,** *magnification x20*, **E and F,** *magnification x40*). They could be identified in clusters and had efficiently integrated within the porcine myocardium. The appeared round-shaped and had maintained their stability **(A-F).** The human ATMSCs within the 3D-MTs were in physiological shape, viable and the intracellular MPIOs could be easily detected **(F,** *magnification x40; black arrow heads*). Human ATMSCs that have been transplanted as 2D single cell suspensions (controls) were also found within the porcine myocardium either appearing randomly distributed **(G,** *magnification x20, black arrows*), in the shape of a typical injection channel **(H,** *magnification x20, black arrows*) or as clusters **(I,** *magnification x20, black arrows*).

Discussion

Stem cell based therapies have been repeatedly suggested as a promising strategy to treat the failing heart after myocardial infarction (MI) or other cardiomyopathies with the major aim to not only restore heart function, but also to prevent or minimize the negative effects often seen from post-MI remodeling. Based on experimental and preclinical studies, numerous clinical pilot trials initiated [4-7, 67, 183] have been initiated and focusing on the clinical feasibility, safety and efficacy. However, while in particular the extensive preclinical studies utilizing different types of stem cells have shown promising results [51], the outcomes of first clinical pilot studies have only

demonstrated marginal effects with regards to the clinically relevant improvement of heart function after stem cell transplantation. The reasons for this limited and ineffective translation into the clinical setting are multi-faceted and are primarily related to key questions concerning the ideal cell type, the optimal delivery approach (intracoronary versus intramyocardial) and the definition of an effective application format (single cell suspensions versus in-vitro engineered, three dimensional cell-based constructs) [41-43, 219, 220].

In the present study we introduce a concept of a catheter-based, 3D NOGA mapping guided intramyocardial transplantation of in-vitro engineered stem cell based 3D microtissues (3D-MTs) using a preclinical animal model. The results of this study demonstrate the principal feasibility that ATMSCs based 3D-MTs can be successfully engineered in vitro within 72 hours and can be then safely transplanted into the healthy and infarcted porcine myocardium using a catheter-based 3D NOGA mapping guided approach.

To enhance the intramyocardial retention, survival and engraftment of transplanted stem cells, an advanced therapy concept [215] comprising an optimal cell application format as well as an efficient delivery mode is mandatory and represents a key feature for the efficient translation into the clinical routine. In this regard and in contrast to currently applied single cell suspension strategies that are known for their high cellular washout and low survival after intra-coronary and intramyocardial transplantation [218], the concept of cellular self-assembly into 3D microtissues prior to transplantation may overcome the limitations of the currently used protocols. Previous studies have demonstrated that 3D MTs can be successfully generated from different cell sources [40-45, 219-221]. Based on the continuous production of extracellular matrix, 3D MTs form a 3D micro environment that stimulates the production of pro-angiogenic factors to increasing their therapeutic potential in the diseased myocardium [41-45, 219-221]. In addition, and when using mesenchymal stem cells to generate 3D MTs, it was recently demonstrated that MSC based 3D MTs can increase their therapeutic efficacy by enhancing their anti-inflammatory properties. Human bone-marrow derived MSCs cultured in hanging drops can be activated to secrete significant quantities of potent anti-inflammatory proteins that may be beneficial for various therapy concepts [220].

In general, mesenchymal stem cells (MSCs) primarily derived from the bone marrow have been repeatedly suggested as a clinical benchmark cell for myocardial stem cell therapies and have been extensively applied in preclinical animal models [209, 210, 212, 213, 227] as well as in clinical pilot trials [7, 29, 183]. They are considered safe, easily available in clinically relevant numbers and it is commonly accepted that their therapeutic effect is primarily based on multiple paracrine effects that comprise suppression of the immune response, inhibition of fibrosis and apoptosis, activation of angiogenesis or the stimulation of endogenous precursor cells [29]. Moreover, recent reports indicate that MSCs may undergo a guided cardiopoiesis into a cardiac committed stage [30]. In this study, we used adipose tissue as a rich source for MSCs being well comparable to those derived from the bone marrow [214]. Importantly, due to their availability and the less invasive access via a simple liposuction, adipose tissue derived MSCs represent an attractive cell source for future therapy concepts [31] and can be considered as an efficient alternative to their counter parts derived from the bone marrow.

To track the transplanted 3D-MTs, advanced imaging strategies as well as efficient in vitro tools are necessary for the monitoring of their in vivo fate, and importantly to justify potential beneficial

effects on the myocardium [46, 47, 203, 226]. While numerous imaging strategies are currently under investigation including magnetic resonance imaging (MRI) using super-paramagnetic agents, computed tomography (CT), PET- or SPECT-imaging using radio-nuclides and reporter-genes as well as hybrid strategies [47, 226], the majority of the recent preclinical studies utilized MRI for the in vivo tracking of transplanted stem cells as it appears to be an efficient imaging tool comprising both, myocardial performance and efficacy evaluation as well as sufficient in vivo cell-tracking [46, 228]. In contrast, the usage of super-paramagnetic agents has been repeatedly criticised for the fact that the imaging signal is not directly linked to the cell itself and the inability to discriminate between vital, labeled cells and particle-loaded cell-debris or macrophages that have actively phagocytised the particles after cell-death [47, 203]. Thus, in order to detect the transplanted human ATMSC derived 3D-MTs within the porcine myocardium, in this study we applied a multimodal, MPIO based tracking approach comprising serial in vivo MRI as well as post mortem in vitro analysis comprising CT imaging, PCR analysis, histology and immunohistochemistry (IHC). Utilizing this multimodal approach, our results illustrate that 3D-MTs could be successfully detected and tracked within porcine heart for up to five weeks after transplantation. There are several limitations in our study that need to be addressed and could potentially improve subsequent studies: First, since this was a pilot study to establish the concept of 3D MT in vitro generation in combination with a catheter based, NOGA mapping guided intramyocardial transplantation, the overall number of the study animals was relatively low. Based on the feasibility and safety data provided from this report, future studies will focus on the improvement of myocardial performance after 3D-MTs transplantation in the setting of myocardial infarction with specific regards to the head-to-head comparison to single cell suspensions. Secondly, although the cardiovascular differentiation potential of human adipose tissue derived mesenchymal stem cell based 3D MTs would be of particular interest, this was beyond the scope of this study. Finally, further refinement on the MRI based 3D-MT tracking analysis will be necessary to facilitate the estimation of the intramyocardial amount of the transplanted 3D MTs direct postoperatively and during follow-up.

In this study we demonstrate the principal feasibility and safety of intramyocardial transplantation of in vitro generated adipose tissue derived mesenchymal stem cell based 3D microtissues. Combining the potential benefits of 3D cellular self-assembly and transcatheter based, intramyocardial transplantation, this hybrid concept comprising a promising cell application format as well as an efficient delivery mode may represent a translational therapy strategy and may have a significant impact with regards to enhanced cellular retention, survival and integration. Utilizing multimodal cell-tracking strategies including advanced imaging and in vitro analysis tools facilitates an efficient in vivo monitoring and post mortem analysis of transplanted 3D-MTs.

Acknowledgements
We thank Dr. Hanspeter Fischer from Bioscience Webster for technical assistance with the NOGA system.

Statictical Analysis
Quantitative data are presented as mean ± standard deviation (SPSS 17.0, IBM, Somers, NY, USA).

Chapter 5

Injectable Living Marrow Stromal Cell-based Autologous Tissue Engineered Heart Valves – *First Experiences with a One-Step Intervention in Primates*

The contents of this chapter are part of **Emmert MY**, Weber B, Scherman J, Gruenenfelder J, Verbeek R, Bracher M, Black M, Kortsmit J, Franz T, Schoenauer R, Baumgartner L, Brokopp C, Agarkova I, Wolint P, Zund G, Falk Zilla P, Hoerstrup SP. *Injectable Living Marrow Stromal Cell-based Autologous Tissue Engineered Heart Valves – First Experiences with a One-Step Intervention in Primates*. Eur Heart J. 2011 Nov;32(22):2830-40. doi: 10.1093/eurheartj/ehr059. Epub 2011 Mar 17.

Abstract

Aims: A living heart valve with regeneration capacity based on autologous cells and minimally invasive implantation technology would represent a substantial improvement upon contemporary heart valve prostheses. This study investigates the feasibility of injectable, marrow stromal cell-based, autologous, living tissue engineered heart valves (TEHV) generated and implanted in a one-step intervention in non-human primates.

Methods and results: Trileaflet heart valves were fabricated from non-woven biodegradable synthetic composite scaffolds and integrated into self-expanding nitinol stents. During the same intervention autologous bone marrow-derived mononuclear cells were harvested, seeded onto the scaffold matrix, and implanted transapically as pulmonary valve replacements into non-human primates (n=6). The transapical implantations were successful in all animals and the overall procedure time from cell harvest to TEHV implantation was 118±17 min. In vivo functionality assessed by echocardiography revealed preserved valvular structures and adequate functionality up to 4 weeks post implantation. Substantial cellular remodeling and in-growth into the scaffold materials resulted in layered, endothelialized tissues as visualized by histology and immunohistochemistry. Biomechanical analysis showed non-linear stress-strain curves of the leaflets, indicating replacement of the initial biodegradable matrix by living tissue.

Conclusion: Here we provide a novel concept demonstrating that heart valve tissue engineering based on a minimally invasive technique for both cell harvest and valve delivery as a one-step intervention is feasible in non-human primates. This innovative approach may overcome the limitations of contemporary surgical and interventional bioprosthetic heart valve prostheses.

Introduction

Valvular heart disease represents a major cause of morbidity and mortality worldwide [71]. Besides conventional treatment modalities based on surgical valve repair or replacement, the recent clinical implementation of minimally invasive implantation techniques is expected to have a major impact on the management of patients with valvular heart disease [229]. Various percutaneous catheter-based as well as transapical surgical implantation approaches have been developed and successfully used in both experimental and clinical settings, representing a promising alternative to conventional heart valve surgery [86, 230, 231]. However, despite these auspicious therapeutic advances, currently available valvular substitutes for minimally invasive replacement procedures are bio-prosthetic and as such inherently prone to calcification and progressive dysfunctional degeneration suggesting their primary clinical application in elderly patients [87].

Living autologous heart valve substitutes with regeneration and growth potential could overcome the limitations of today's valvular prostheses and enable the application of minimally invasive treatment modalities to a broader patient population, including young patients [232]. We recently demonstrated the principal feasibility of merging the two innovative heart valve replacement technologies of heart valve tissue engineering (HVTE) and minimally invasive delivery in an ovine model [111]. A clinically relevant HVTE concept ideally comprises minimally invasive techniques for both cell harvest and valve delivery. Therefore, several potential cell sources and protocols have been assessed [108, 113, 116, 121, 122]; however, most of them requiring an extensive and complex ex vivo cell and tissue culture phase. *Shin´oka* et al. described a method of creating tissue-engineered vascular grafts (TEVG) by using bone marrow-derived mononuclear cells (BMCs) without cell expansion culture. Constructed from biodegradable polyester tubes seeded with autologous cells, these grafts demonstrated functionality and appeared to transform into living vascular grafts [97, 133, 233-235]. Initial clinical pilot studies evaluating BMC-seeded vascular grafts as venous conduits for congenital heart surgery revealed adequate safety profiles and functionality up to 8 years [236-239].

The present study investigates for the first time the implantation of autologous BMC-based tissue engineered heart valves (TEHV) by minimally invasive implantation technologies in a primate model; thereby approximating the human situation as much as possible in a pre-clinical large animal model. The presented autologous approach provides a minimally invasive, one-step heart valve replacement procedure from cell harvest to in vitro engineering and transapical delivery of living tissue engineered heart valves.

Methods

Trileaflet heart valve scaffolds (n=6) were fabricated from non-woven polyglycolic-acid meshes (PGA; thickness 1.0 mm; specific gravity 70 mg/cm^3; Cellon, Luxembourg), coated with 1.75% poly-4-hydroxybutyrate (P4HB; MW: 1x106; TEPHA Inc., USA) by dipping into a tetrahydrofuran solution (THF; Fluka, Germany). After solvent evaporation, physical bonding of adjacent fibers and continuous coating was achieved. P4HB is a biologically derived rapidly degradable biopolymer, which besides being strong and pliable, is thermoplastic (61°C), and can be molded into three-dimensional shapes. From the PGA/P4HB composite scaffold material, the heart valve scaffolds were fabricated by using a metallic valve-shaped molding system. Thereafter, the scaffolds were integrated into radially self-expandable nitinol stents (length = 29.5±0.6 mm; OD = 20.2±1.6 mm when fully expanded at 37ºC; pfm AG, Germany) by attaching the scaffold matrix to the inner

surface of the nitinol stent wires using single interrupted sutures (5-0 Polypropylene, Ethicon, USA). After vacuum drying for 24 hours, the scaffolds were sterilized overnight by using ethylene oxide (EtO) gas sterilization. The EtO was allowed to evaporate for 3 days and the scaffolds were incubated in MCDB 131 Medium (Sigma Chemical Co., St. Louis, USA) for 10 (n=2), 14 (n=2) or 24 (n=2) hours to facilitate cell attachment by deposition of proteins. All media were supplemented with 0.05% Pen/Strep (P 0781; Sigma Chemical Co., USA) and 0.2 % Fungizone (Sigma Chemical Co., USA), adjusted to a pH of 7.4, buffered with $NaHCO_3$ (Sigma Chemical Co., USA) and sterilely filtered.

Isolation of primate BMCs

66.5±14.4 mL of bone marrow was aspirated from the sternum of adult Chacma Baboons into a heparinized syringe (50-100U/mL) using a 12 Gauge threpine needle. BMCs were obtained by centrifuging the samples on a histopaque density gradient (Sigma Chemical Co., USA) for 30 minutes at 1500 rpm. The viability of the isolated buffy coat was determined by flow cytometry and trypan blue staining after erythrocyte elimination and quantification with a hemocytometer.

Thereafter, cellular viability, granularity and size were assessed using flow cytometry analysis (BD Inc., LSR II4C, USA) with FSC (Forward Scatter) and SSC (Side Scatter) axes.

Seeding of the BMCs onto the stented heart valve scaffolds ($8\pm3x10^6$ cells/cm^2) was performed using fibrin (Sigma Chemical Co., USA) as a cell carrier [240] and the construct was left in the laminar flow for 30 – 60 sec. The concentration of Fibrinogen (10 AP mg/mL) / Thrombin (10IU/mL) was in accordance with the standard concentrations used in cardiovascular tissue engineering [240]. Next, the constructs were placed into vented 50 mL tubes for 10 minutes to allow the fibrin-thrombin solution to clot adequately. Thereafter, the seeded construct was loaded into the delivery device by decreasing the outer diameter from 20 mm to 8 mm and transferred to the theatre.

All animals received human care and the study was approved by the institutional review boards (Department of Surgery Research Committee: Approval Ref. 2009/096, Animal Research Ethics Committee; Approval Ref. 009/035, Faculty of Health Sciences, University of Cape Town) and in compliance with the Guide for the Care and Use of Laboratory Animals, published by the National Institutes of Health (NIH publication No. 85-23). The transport of explanted tissue for histological analysis was in accordance with the *Convention on International Trade in Endangered Species* (CITES) regulations for transport of protected species (CITES Export Permission No. 091992; Import Permission No.3710/09). Unseeded controls were not included for ethical reasons given the results of previous experiments in the sheep model. When using the same tissue engineering technology, unseeded (only fibrin-coated) scaffolds implanted in the orthotopic pulmonary position demonstrated severe structural failure already after 4 weeks (Suppl. Fig. 1).

Phenotyping of BMCs

Small samples of isolated BMCs of each animal were used for hematoxylin-eosin (H&E) staining and immunocytochemical analysis of the acquired cell populations. The cells were fixed with methanol or paraformaldehyde (PFA 4%) and immunofluorescence staining was performed using the following primary antibodies: CD45 (R&D Systems; Clone 2D1), CD34 (Immunotools; Clone 4H11), CD146 (R&D Systems; Clone 128018), CD90 (Biolegend; Clone 5E10), CD166 (5E10; Clone 3A6), CD44 (Immunotools, Clone NKI-P2), DAPI (Sigma Aldrich Co., USA), α-smooth muscle actin (α-SMA, clone 1A4; Sigma, USA), Desmin (clone M0760; Dako), Vimentin (clone V9; Dako) and Phalloidin Alexa 633 (Molecular Probes, Invitrogen Corp., USA). Matched isotype antibodies (Clone MOPC-21; IgG1, Biolegend; Clone 203; IgG1, Immunotools) served as controls. Primary antibodies were detected

with Cyanine-2 or Cyanine-3 coupled goat anti-mouse antibodies (Jackson ImmnunoResearch, UK). Human BMCs (cyto-spinned at 800 rpm/5 min; PFA 4% fixation), human MSCs, and primate MSCs (chamber slides; PFA 4% fixation) were stained accordingly. Baboon BMCs were transported to Europe using OptiCell® Chambers (Thermo Scientific, USA) and expanded in MCDB 131 Medium (Sigma Chemical Co., USA) buffered with HEPES (Sigma Chemical Co., USA; pH 7.41).

CFSE Cell Labeling and Tracking

In order to evaluate the in vivo fate of isolated primate BMCs (n=2) seeded cells were tracked for 4 weeks in vivo using the CellTrace™ CFSE Cell Proliferation Kit (C34554, Invitrogen Corp., USA). For this purpose the pellet of the isolated buffy coat BMCs was incubated for 10 minutes with a 25µM solution of carboxyfluorescein diacetate succinimidyl ester (CFSE) dissolved in DMSO (D2650, Sigma Chemical Co., USA) according to the manufacturer´s instructions prior to seeding onto the scaffold. After 4 weeks the constructs were analyzed using confocal microscopy (DMIRBE; Leica confocal system TCS/SP5 NT; Leica Microsystems GmbH Wetzlar, Germany). Image processing was performed using the Imaris® software (Bitplane AG, Zurich, Switzerland) and Adobe Photoshop 6.0 (Adobe Systems, USA). For in vitro evaluation of the seeding procedure human BMCs (n=4) were isolated, labeled with CFSE and seeded onto patches (n=4; 1x1cm) using fibrin as a cell carrier [117]. Un-labeled human mesenchymal stem cells (PT-2501; LONZA, Switzerland) seeded onto PGA patches served as negative control samples for determination of unspecific cellular autofluorescence (n=2).

Anesthetic protocol

All procedures were performed under general anesthesia. The animals were premedicated with Ketamine hydrochloride (10mg/kg). Anaesthesia induction was performed with Sodium Thiopental (2.5%) and maintained with Isoflurane (2-3% to effect) throughout the procedures. All animals were intubated orally with a single-lumen endotracheal tube. Routine intraoperative positive pressure ventilation was performed. Hemodynamic monitoring consisted of surface electrocardiography, pulse oximetry, invasive arterial blood pressure (right femoral artery) and central venous pressure (long line inserted via left Basilic vein). The animals were sacrificed using a bolus systemic injection of potassium chloride and exsanguination whilst under general anesthesia, after 12 hours (n=1) and 4 weeks (n=5).

TEHV implantation and in vivo functionality

For evaluation of in vivo functionality TEHV were minimally invasively delivered into the pulmonary valve position using a mini-sternotomy and antegrade transapical approach. The valves were crimped and loaded onto a custom-made inducing system (OD=8mm) consisting of a rigid tube and pusher. The right ventricle was punctured using needle through purse-string sutures. Next, the inducer system was inserted and the TEHV was delivered into the pulmonary artery under guidance of fluoroscopy (BV, Pulsera, Philips, Medical Systems, The Netherlands) and transesophageal echocardiography (2D-TEE, Philips, Medical Systems, The Netherlands). The radial expansion of the nitinol stent forced the native pulmonary valve leaflets against the pulmonary artery wall and kept them fixed. One construct was deployed in a supravalvular position not excluding the native valvular leaflets. The appropriate position and functionality of the implanted valve was confirmed by angiography. In addition, the in vivo functionality was monitored using transesophageal, transthoracic and/or epicardial echocardiography during the procedure, immediately after

implantation, weekly up to 4 weeks, and prior to sacrifice of the animal (Suppl. Methods E). The pulmonary artery pressure was measured in order to exclude stent-associated stenosis of the pulmonary outflow tract. Anticoagulation (Aspirin and Warfarin) was maintained for 4 weeks. The animals were sacrificed (potassium euthanization and exsanguination) after 12 hours (n=1) and 4 weeks (n=5) and the TEHV were explanted.

Qualitative explant tissue analysis

Explanted heart valve constructs (n=6) were evaluated macroscopically. Their tissue composition was analyzed qualitatively using immuno-/histology and compared to native heart valve leaflets also explanted from the study animals. The tissue sections were studied using Azan staining, von Kossa staining, H&E staining, Masson-Trichrome staining, and eVG staining. In addition, immunohistochemistry was performed using the Ventana Benchmark automated staining system (Ventana Medical Systems, USA) and antibodies for α-smooth muscle actin (α-SMA, clone 1A4; Sigma Co., USA), Desmin (clone M0760; Dako), CD 68 (clone M0876; Dako), CD34 (clone MCA5476, Serotec Ltd.), CD31 (clone M0823; Dako), eNOS (clone 610298; Transduction Laboratories, Inc.), and von Willebrand factor (vWf; clone A0082, Dako). Primary antibodies were detected with the Ventana *iVIEW* Diaminobenzidine (DAB) detection kit, yielding a brown reaction product. For single epitopes immunofluorescence staining was also performed. Primary antibodies comprised α-SMA (AB5694; Abcam Inc., USA), CD68 (M0814; DAKO), as well as CD31 (M0823, DAKO), and were detected using Alexa 488 (Invitrogen, USA) conjugated goat anti-rabbit or Cyanine-3-conjugated goat anti-mouse secondary antibodies (Jackson Immunoresearch, USA).

Scanning Electron Microscopy

Representative tissue samples of TEHV of tissue engineered and native explants (n=7) were fixed using 2% glutaralaldehyde. After preparation, samples were sputter-coated with platin and investigated with a Zeiss Supra 50 VP Microscope (Carl Zeiss Imaging, Germany). Unseeded PGA coated with P4HB, native primate as well as native human heart valve leaflets served as controls.

Quantitative Explant Tissue Analysis

Explanted TEHV leaflets (4 week explants, orthotopical position) were lyophilized and analyzed by biochemical assays for total DNA content as an indicator for cell number, hydroxyproline content as an indicator for collagen, as well as GAG content. For measuring the DNA amount, the Hoechst dye method [241] was used with a standard curve prepared from calf thymus DNA (Sigma Chemical Co., USA) in addition to the samples. The GAG content was determined using a modified version of the protocol described by *Farndale* et al. [242] and a standard curve prepared from chondroitin sulphate from shark cartilage (Sigma Chemical Co., USA) in addition to the samples. Hydroxyproline was determined with a modified version of the protocol provided by *Huszar* et al. [243] and a standard curve, prepared in addition to the samples.

Biomechanical characterization

The mechanical properties of the leaflets as well as the valve conduits were determined in radial direction by uniaxial tensile testings. The length, width and thickness of the tissue samples were measured before testing, using a caliper. The thickness of the strips was determined retrospectively from histological micrographs as data obtained by caliper measurement were unreliable. A correction factor of 1.046 was used to account for linear shrinkage associated with the loss of tissue

volume due to tissue processing [Schned et al., Am J Surg Pathol 1996;20:1501-6]. Stress-strain curves were obtained by performing uniaxial tensile tests (Instron 5544-RX; 500N load cell, Norwood, USA; load cell of 500N) with a constant strain rate of 1.0 (or 100%) per minute. The ultimate tensile stress (UTS), as a measure of strength, was determined from the curves. The modulus of elasticity (Young's modulus) was obtained from the slope of the linear section of the stress-strain curve as an indicator for tissue stiffness.

Isolation and Differentiation of Baboon MSCs

MSCs were obtained from bone marrow aspirate according to the method of *Pittenger* et al. [198] and were transported from Cape Town, South Africa to Zurich, Switzerland using OptiCell® chambers. The MCDB medium was composed as described above and HEPES buffer (transport) or $NaHCO_3$ buffer (culture) was used. The differentiation potential of adherent cells was determined by inducing adipocytic and osteogenic differentiation. Hence, cells were cultured in chamber slides and exposed to Dulbecco's modified eagle's medium (Sigma Chemical Co., USA; 2 mM L-glutamine, 50 U/mL penicillin, 50 µg/mL streptomycin and 10% FBS) containing ascorbic acid-2-phosphate (50µM) and dexamethasone (10 nM) for osteoblast-like cell differentiation. Adipocyte-like differentiation was induced using a DMEM-medium containing 3-isobutyl-1-methylxanthine (IBMX; 0.5 mM; Sigma-Aldrich, St. Louis, USA), dexamethasone (1 µM), indomethacin (120µM) and insulin (10 µg/ml). After three days the medium was changed to the above-described medium, but without IBMX. The control cells were cultured in α-MEM only. After 21 days, osteoblast-like cell differentiation was indicated by mineralized nodules detected with phase-contrast microscopy and/or by osteoid-like collagen formations visualized with Verhoeff's Van Gieson stain. Adipocyte-like cell differentiation was examined using oil red O staining (ROS), with the samples being fixed as described above and rinsed with 60% isopropanol before being stained with oil red O (Sigma Chemical Co., USA). After a 10 min staining period the samples were rinsed with distilled water and visualized under the microscope (Carl Zeiss Imaging, Germany).

Results

Viable BMCs harvested from the sternum: A cocktail of stem cells and leucocytes

The isolation of BMCs rendered 175±82x10^6 cells per animal for scaffold seeding. Cellular viability was in excess of 95% as verified by whole blood flow cytometry (Fig. 1a) and trypan blue exclusion staining (Fig. 1b). Isolated primate mononuclear cells (Fig. 1c) stained positively for common leukocytic antigens including CD45, CD44 and CD15 (Suppl. Fig. 2a-c). According to the flow cytometric analysis the marrow mononuclear cells comprised distinct leukocytic cell populations including granulocytes (20.8%), monocytes (7.6%), and lymphocytes (67.6%). The amount of dead cells, indicated by a population of low FSC-height and increased SSC-height in the scatter plot was less than 5% (Fig. 1a).

Primate bone marrow aspirate comprised CD34+ hematopoietic stem cells as well as mesenchymal stem cells (MSCs) staining positively for CD44, CD90, CD146 and CD166, but negatively for CD45 and CD34, representing a common staining pattern for MSCs (Fig. 1g-h; Suppl. Fig. 2d). The differentiation potential of isolated primate MSCs was assessed exemplarily using pre-adipocytic and osteoblastic differentiation assays (Suppl. Fig. 2e-f). After isolation, BMCs were labeled (Fig. 1d-

f) and successfully seeded onto PGA/P4HB heart valve scaffolds (Fig. 2a-d) and the TEHV could be inserted into the sheath system for transapical delivery.

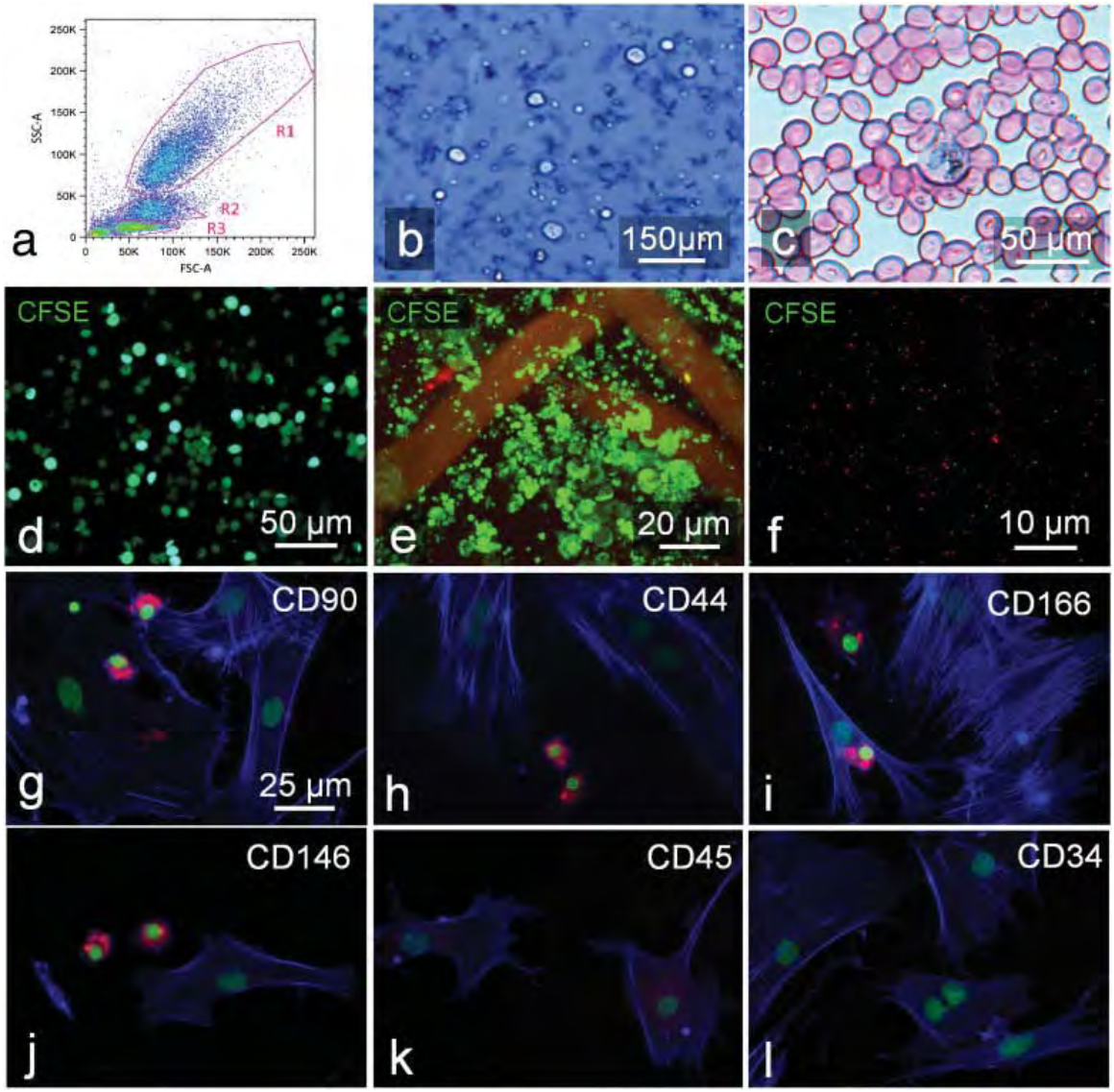

Figure 1 Isolation of BMCs. Flow cytometry scatter (a) plot of nucleated cells with microfluidic erythrocyte lysis labeled by population with as forward (FSC) vs. side (SSC) scatters. The fraction of dead cells, indicated by low FSC/high SSC values, is less than 5%. This is confirmed by trypan blue exclusion staining (TBS; b). Mononuclear cells (c; H&E staining) were labeled with CFSE (d) and seeded onto the PGA matrix (e). After 4 weeks no fluorescent cells could be detected in the explants tissue (f). A fraction of adherent BMCs stained positively for CD44, CD90, CD146, CD166, and negatively for CD45 and CD34 indicating a mesenchymal stem cell character (g-l). Specific staining is shown in red, DAPI (nuclei in green) and Phalloidin (f-actin in blue) were used as control stainings.

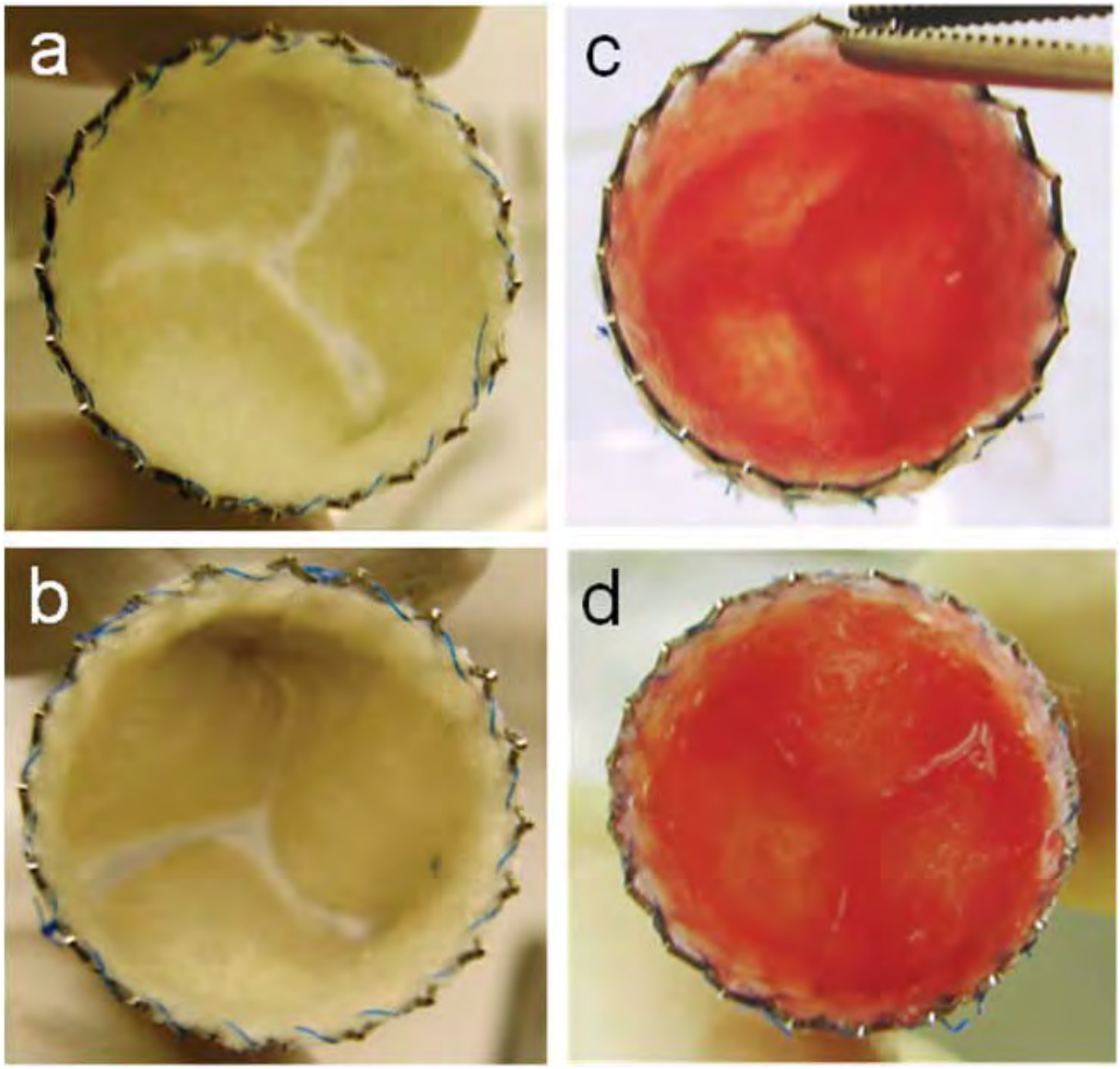

Figure 2 Bone Marrow-derived TEHV. After isolation of BMCs, stented PGA scaffold matrices (a,b) were seeded with cells using fibrin as a cell carrier (c,d).

Minimally invasive delivery: The transapical implantation of TEHV

The transapical implantations were successful in all animals. Of all six animals five valves were deployed in the orthotopic valvular position (Fig.3 a-c,e), whereas one valve was positioned supravalvularly thereby not excluding the native valvular leaflets. In one of the orthotopically implanted animals perioperative coronary perfusion complications not related to the TEHV functionality resulted in termination 12 hr after implantation. Positioning of the TEHV was verified intraoperatively using TEE and fluoroscopy (Fig. 4c,d; Suppl. Trailer 1). Neither migration of the TEHV nor paravalvular leakage has been observed. Proper opening and closing behavior was demonstrated by TEE measurements (Fig. 4e-h; See Suppl. Trailer 2,3). The mean crimping time of the TEHV (Fig. 3d A-C), from insertion into the application system until surgical deployment, was 17±8 minutes (Fig. 3d-e). The mean duration of the entire procedure, from bone marrow harvest until valve delivery, was 118±17 minutes.

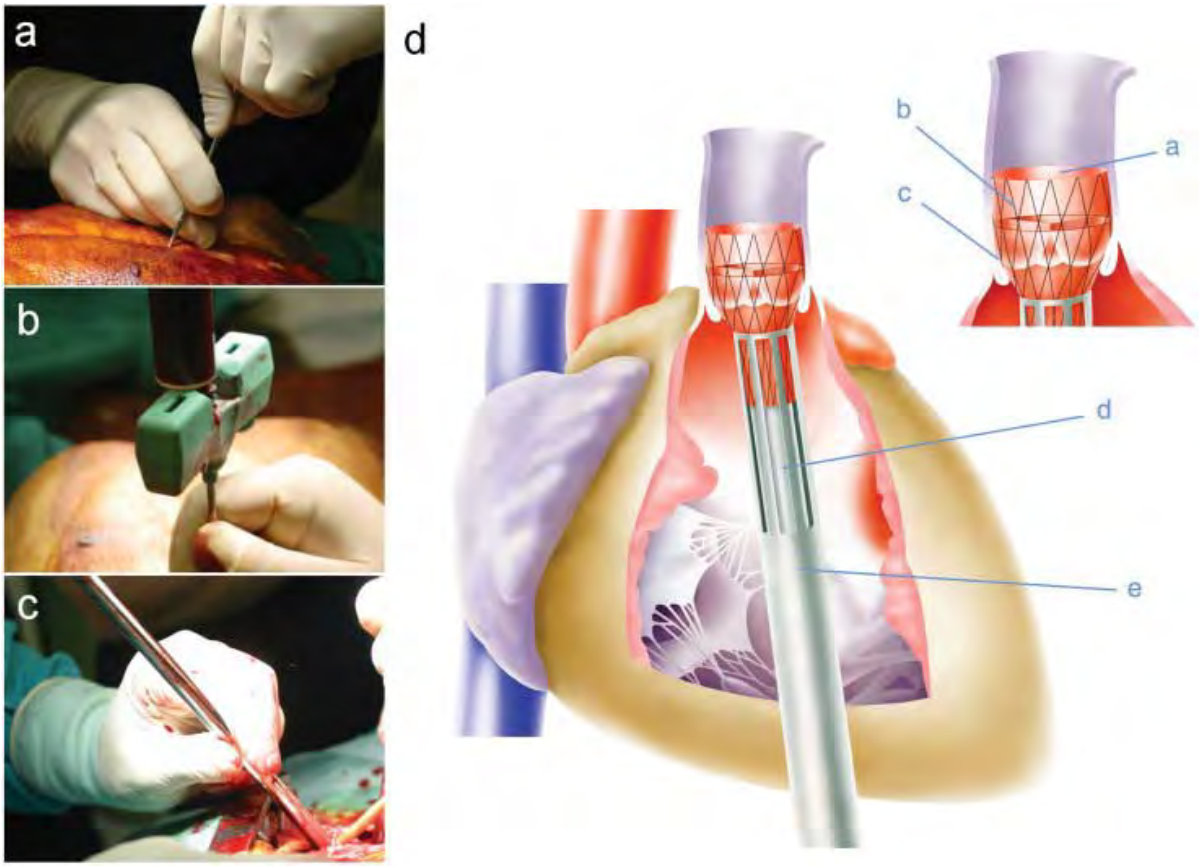

Figure 3 Minimally Invasive TEHV Implantation. After sternal bone marrow puncture (a) and aspiration of fluid (b), the TEHV was loaded into the delivery device (c), inserted into the right ventricle (d) and deployed in the pulmonary position (e) under sonographic and fluoroscopic guidance. The crimped TEHV (A), integrated into the nitinol stent (B), is carefully deployed into the pulmonary position (C) by slowly advancing the inner pusher (D) into the sheath system (E).

In vivo performance of TEHV

Valve functionality with leaflet mobility and sufficient opening and closing behavior was observed after implantation. No paravalvular leakage was detected during the follow-up period. Weekly TTE/TEE follow-up revealed a slight but not significant increase in transvalvular peak pressure (TVG; Table 1) starting around 25±7 mmHg (TEE) perioperatively, up to 30±7 mmHg after 3 weeks (TTE). At explantation (4 weeks), TVG gradient was clearly reduced to 16.1±1.9 mmHg (TEE). Moderate regurgitation was detected in three animals, which remained unchanged over the whole period of implantation time until harvest. Proper opening and closing behavior could be demonstrated by TTE/TEE measurements (Fig. 4d-g; Suppl. Trailer 2,3).

Table 1

Value	1 week	2 weeks	3 weeks	4 weeks
TVG*	26.9±7.5	28.6±5.1	30.4±7.8	16.1±1.9
INR†	1.2±2.5	1.5±3.5	1.25±0.13	*Ex*¶
Regurgitation‡	2.0±0.7	2.0±0.7	2.5±1.5	2.5±0.9

*TVG = Transvalvular Peak Pressure Gradient; †INR = International Normalized Ratio;
‡ Regurgitation – Grading: 0/1/2/3/4 – None/trivial/mild/moderate/severe; ¶*Explantation*

Explant macroscopy of TEHV

Explantation of the early TEHV (12h) revealed an intact leaflet structure dominated by a fibrin coated PGA scaffold matrix with lack of evidence for thrombus formation. Harvest of the remaining TEHV 4 weeks after delivery showed constructs that were well integrated into the adjacent tissue by tissue covering the stent margin and encircling stent strut endings (Fig. 4a). The valvular leaflets of the four orthotopically positioned constructs presented as pliable, well defined cusps (Fig. 4b). Although the leaflets appeared to be shortened in radial diameter, sufficient coaptation was demonstrated throughout the entire experimental period. Interestingly, in the hemodynamically non-fully loaded TEHV deployed in the supravalvular position the leaflet structure was almost entirely missing. Instead two small parietal nodes could be identified, most likely representing remnants of the original scaffold pockets (Fig. 4c).

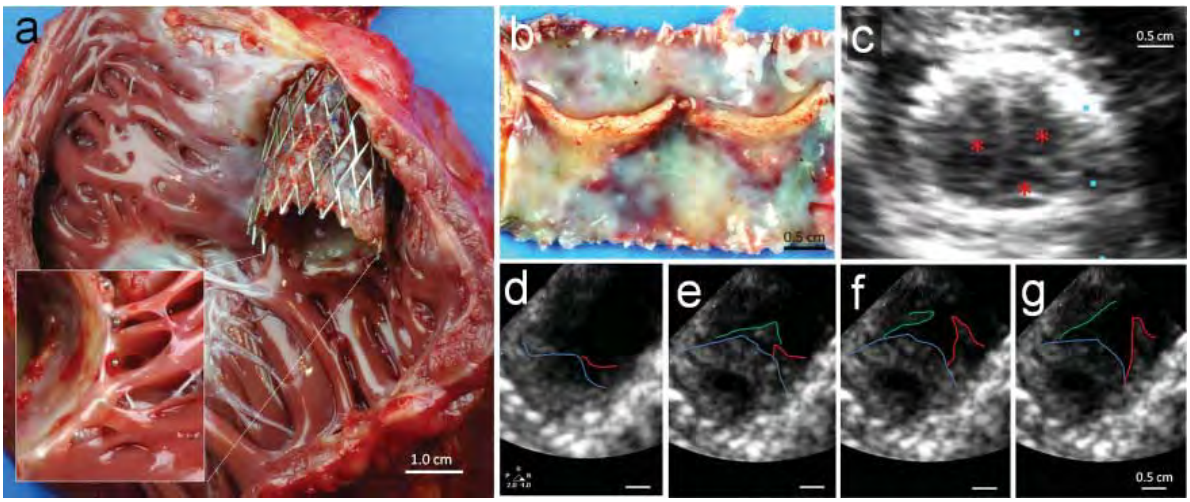

Figure 4 Explant Analysis of TEHV. After 4 weeks in vivo the stented constructs were well integrated into the adjacent tissue (a). Orthotopical TEHV (b) presented with a cusp-like leaflet structure, with shorter leaflets than native controls. In a final TEE-assessment the leaflet coaptation (c; * indicates leaflets) as well as opening movements of all three leaflets could be visualized (d-g).

Scanning electron microscopy

The surface of the early explants (12h) was mainly characterized by previously seeded mononuclear cells embedded into a fibrin matrix densely covering the entire scaffold (Fig. 5a,b). Analysis of the 4 week explants revealed that three of the orthotopically implanted leaflets showed already a mature structure, characterized by a well-defined endothelial lining on the conduit wall as well as partially

on the valvular leaflets (Fig. 5e,f). In several spots these endothelial coverages were confluent and not distinguishable from native primate (Fig. 5c) or human (Fig. 5d) valvular endothelium. The other orthotopic explant presented with a more premature surface remodeling, characterized by areas with extensive fibrin formation as well as leukocyte and thrombocyte attachment. Interestingly, in this explant all stages of surface remodeling could be detected, from beginning provisional thrombocyte-mediated surface coverage (Fig. 5g-i) to areas of almost confluent endothelial covering. The non-orthotopically positioned construct also revealed a well established endothelial coverage with the remaining leaflet structure firmly integrated into the conduit wall.

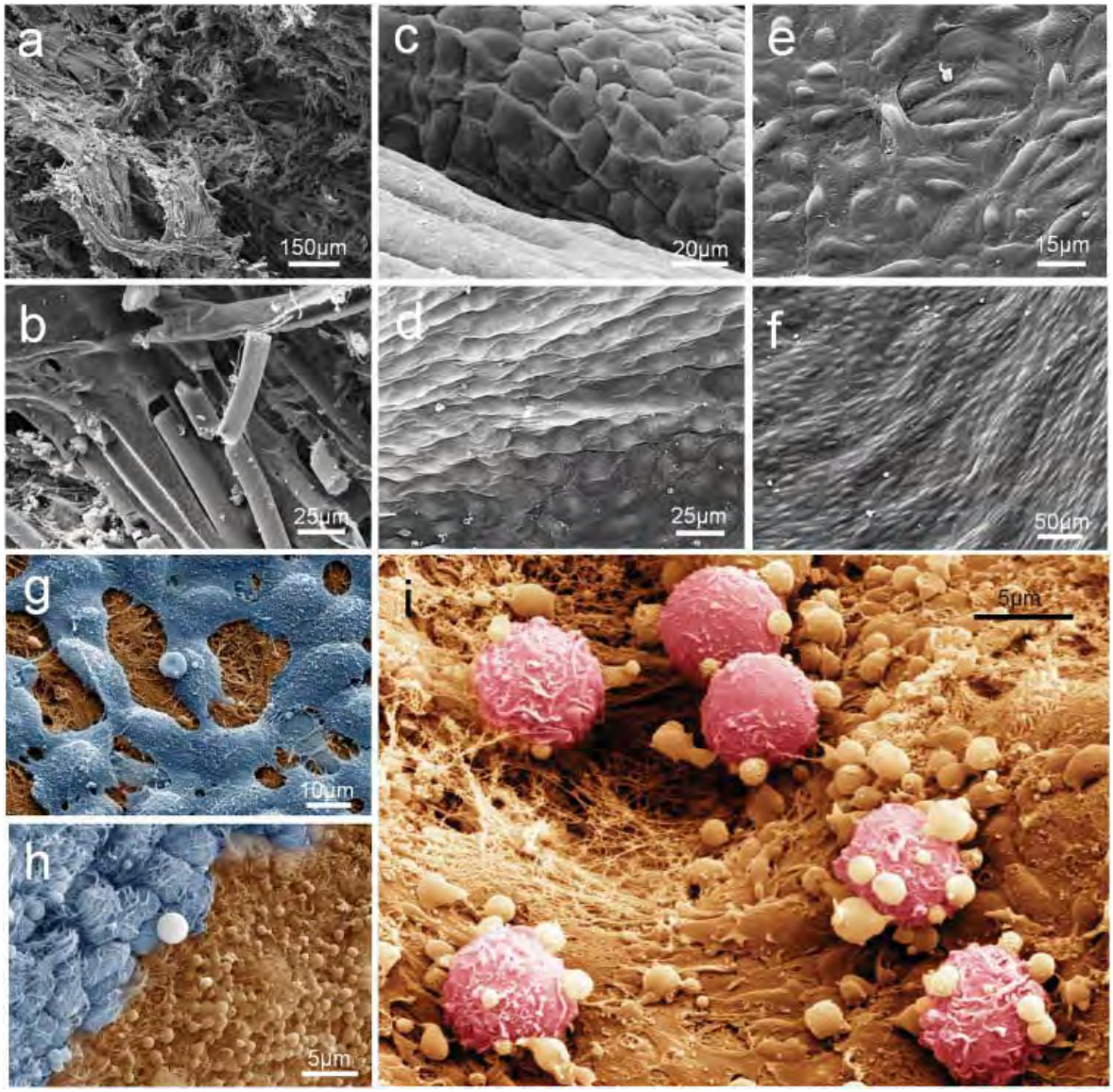

Figure 5 Scanning Electron Microscopy. SEM of the PGA-P4HB scaffold (a,b), primate (c) and human (d) control leaflets. In most areas the surface of the 4 week explants showed confluent (e,f) or initial (g) endothelial coverage. In some areas the surface remodeling was still evident involving thrombocyte attachment (h) and leukocyte attraction (i).

Histology and immunohistochemistry

H&E staining (Fig. 6a-d) of the explants demonstrated layered tissue morphology, characterized by a central core of non-degraded PGA matrix surrounded by dense tissue formation on the luminal as well as on the vascular side. Masson's Trichrome and eVG staining confirmed the presence of collagen predominantly in the outer layers of the conduit wall and the leaflet (Fig. 6e-l). As confirmed by SEM, the surface of the conduit was covered by a confluent endothelial layer in large areas of the constructs. Cells of the constructs' surface layer expressed CD31 (Fig. 6m-p) and vWF, resembling the staining pattern of native valve endothelial cells (Fig. 6m). Moreover, α-SMA expression could be detected in interstitial cells of the newly formed surface layers of the conduit (Fig. 6s) and partially of the leaflet (Fig. 6t). In contrast to previous studies [8], the leaflets' hinge region was free of α-SMA and/or Desmin positivity (Suppl. Fig. 3c-d). The early (12hr) as well as the late (4 weeks) explants stained positively for CD68 (Suppl. Fig. 3 g-i), indicating a distinct monocytic infiltration and continuous remodeling. Cell tracking analysis using CFSE-dye and confocal microcopy (Fig. 1d-e) revealed no signal within the explanted tissue (Fig. 1f), indicating that most of the seeded BMCs were not present after 4 weeks in vivo.

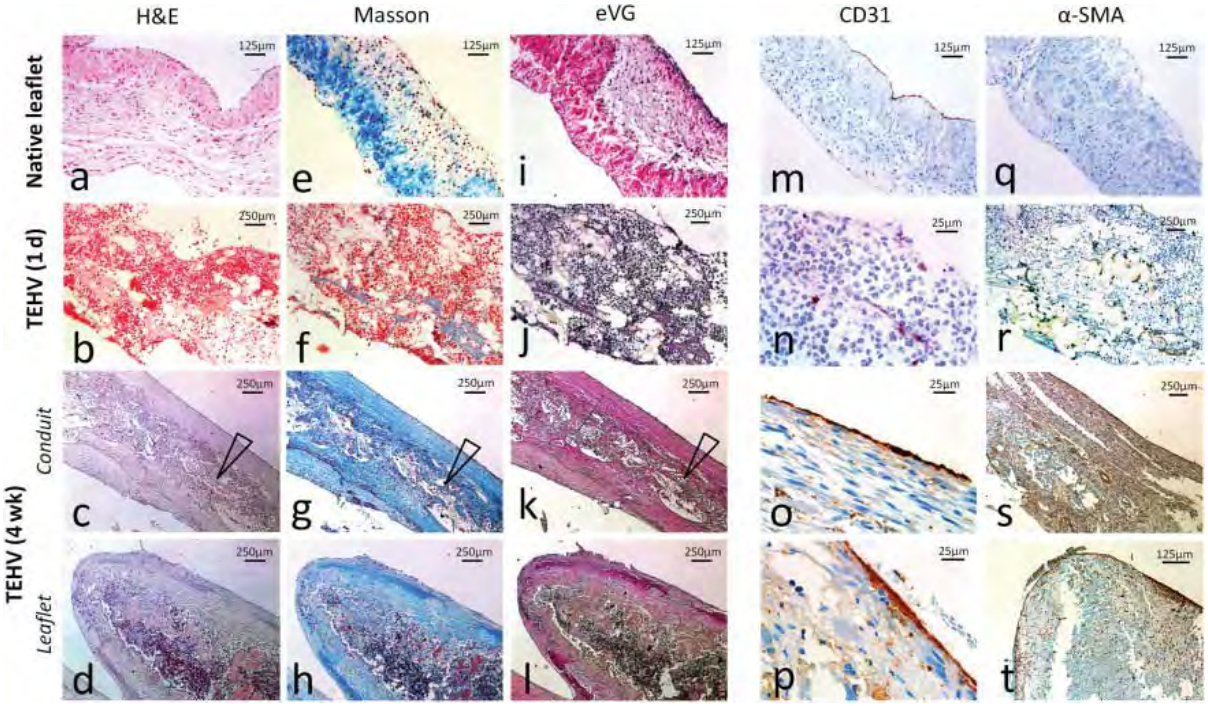

Figure 6 Histology of the explanted TEHV. Explanted tissues showed layered tissue architecture visualized by H&E staining (c,d). In Masson's Trichrome staining and eVG staining collagen fibers were predominantly found in the outer tissue layer of the conduit and leaflets (g-h, k-l). Cells of the conduit (o) and leaflet (p) surface layer expressed CD31. α-SMA expression could be detected in the outer layers of the conduit (s) and the leaflet (t), but was missing in the proximal leaflet region. Arrows indicate reminiscent scaffold material.

Biomechanical and ECM analysis: The remodeling of viable tissue

Mechanical evaluation was performed separately for the valvular leaflets and the wall region. Analysis of the 4 week explants revealed that the tissue strength (UTS 0.19±0.12 MPa) as well as the stiffness (YM 1.0±0.54 MPa) of the conduit wall was higher than that of the valvular leaflet itself (UTS 0.08±0.05 MPa; YM 0.19±0.08 MPa). The stress-strain curves of both the heart valve leaflet and

the conduit wall revealed non-linear behavior until rupture. The Young's moduli obtained in the low strain (0.0-10.0%) as well as the high strain (> 10.0%) showed to be significantly different (all P's <0.05), which is characteristic for properties of biological tissue (Suppl. Fig. 4), indicating the in vivo replacement of the biodegradable matrix by living tissue (Fig. 7a).

Quantitative extracellular matrix (ECM) analysis of the TEHV explants showed that the GAG as well as the DNA content of the constructs' leaflets was higher than compared to native tissue (GAG 140.28±36.17%; DNA 168.10±87.07%), indicating a high cellular infiltration as well as ECM remodeling. Consistent with previous studies [8], the collagen content in the leaflets and the conduit wall was substantially lower in the newly formed tissues than compared to native controls (HYP 59.24±16.87%; Fig. 7b).

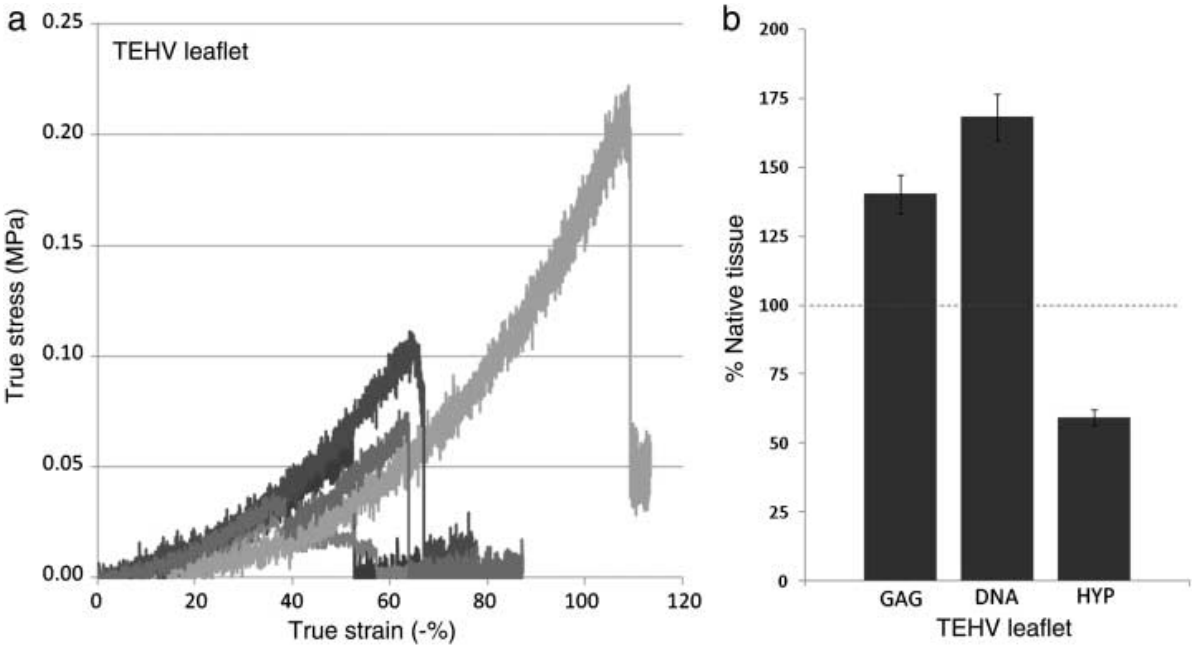

Figure 7 Qualitative Tissue Analysis. Mechanical properties of explanted tissue engineered leaflets after 4 weeks in vivo are displayed as stress–strain curves [MPa/%] characteristic for biological tissue (a). Extracellular matrix analysis of the explants for glycosaminogylcans (GAG) and DNA shows enhanced values compared to native tissues. Hydroxyproline (HYP) normalized to tissue weight is decreased compared to native controls (b).

Discussion

Minimally invasive heart valve replacement techniques have recently emerged as a promising technology in interventional cardiovascular therapeutics [87, 88, 229, 244, 245]. Despite the potential of this novel technology, currently used replacement materials for transcatheter or transapical valves are bioprosthetic and therefore highly prone to calcification as well as structural degeneration [87, 88, 91, 229, 244, 246]. Living TEHV, based on rapidly biodegrading scaffolds and autologous cells could overcome these limitations with characteristics such as repair, remodeling and growth. We recently demonstrated the principal feasibility of merging tissue engineering and minimally invasive heart valve replacement technologies [111]. Ideally, a clinically relevant HVTE concept must involve low invasive techniques for both cell harvest and valve delivery. Consequently, several non-invasive potential cell sources comprising stem cells have been assessed with regard to the clinical realization of the concept. However, most of these concepts require extensive,

logistically complex, and time-consuming in vitro tissue engineering processes that limit their clinical feasibility.

The present study demonstrates for the first time the feasibility of merging heart valve tissue engineering based on a low invasive stem cell source, with a minimally invasive, injectable implantation technology combined in a single intervention. Stem cell sources previously used for HVTE, including MSCs, fetal stem cells and blood-derived progenitors [108, 111, 113, 116, 121], necessitate cell harvest in a particular intervention, followed by protracted and complex in vitro cell expansion and implantation of fabricated TEHV in a second procedure [111]. To the contrary, autologous BMCs can be isolated in sufficient numbers from sternum bone marrow aspirates, thereby enabling immediate re-implantation as autologous TEHV. Therefore, the presented one-step approach suggests a highly clinically relevant concept and may represent a significant step towards the routine utilization of TEHVs.

The principle of using BMCs for cardiovascular tissue engineering was described by *Shin'oka* et al. [233] and has been assessed in pre-clinical [97, 234, 247] as well as initial clinical investigations [236-239]. It was hypothesized that multipotent bone marrow–derived stem cells proliferate, differentiate, and constitute new tissues [237]. In a recent study, *Roh* et al. [133] elucidated the potential underlying molecular mechanism of autologous BMC-induced tissue formation. In contrast to previous assumptions, no evidence for (trans-) differentiation of bone marrow-derived stem cells into mature vascular cells has been found. Interestingly, seeded BMCs were not detectable in the tissue engineered constructs one week after implantation. In fact, it was shown that BMC-seeded biodegradable scaffolds transform into functional blood vessels via an inflammation-mediated process of vascular remodeling. While the role of BMCs in this remodeling process remains largely conjectural, a growing body of evidence suggests their role within inflammation-mediated processes.

This paracrine role of seeded BMCs as a constituent of an inflammatory vascular remodeling process is consistent with multiple studies reporting that (trans-)differentiation of bone marrow-derived stem cells in vivo is deemed rare [63-65, 116, 248, 249]. The present study concurs with this mechanism, as the initially labeled BMCs were not detectable within the explants 4 weeks after implantation. Also, a distinct remodeling process was evident, characterized by a monocytic infiltration of the leaflets as well as the conduit wall. Besides this critical role of seeded BMCs for in vivo remodeling and tissue formation [133, 237], the precise contribution of the detectable multipotent BMC stem cell fractions is of great interest to understand the underlying regenerative mechanism [250-253].

Experimentally, it would have been elegant to include an unseeded control group in his study. However, previous experiments in the sheep model using the same tissue engineering technology and unseeded (only fibrin-coated) scaffolds implanted in the orthotopic pulmonary position demonstrated severe structural failure after 4 weeks (Suppl. Fig. 1). Given the fact that remodeling phenomena in the ovine model are expected to be substantially more intense than in the human/primate cardiovascular system [254], the implantation of unseeded controls into primates appeared ethically not justifiable.

A very interesting observation of the current study was the influence of hemodynamic loading on remodeling, tissue formation and maturation in vivo. This is a known phenomenon from embryology and has been used for in vitro tissue engineering experiments utilizing biomimetic flow and pressure conditions to achieve optimal tissue maturation in so-called bioreactors [109, 117, 118, 255]. In the present investigation the role of mechanical loading on functional remodeling was uniquely

demonstrated by the supra-valvular positioned TEHV not excluding the native valvular leaflets. In contrast to the orthotopic implants, the non-loaded supravalvular TEHV lacked any leaflet structure after 4 weeks, indicating missing tissue formation as well as BMC-mediated leaflet remodeling.
Macroscopically the orthotopic constructs presented with cusp-like leaflet structures and did not appear thickened compared to previous reports based on the sheep model [111, 256]. Although principal valvular functionality was demonstrated, mild to moderate regurgitation was observed by echocardiography in 3 of 5 valves in the presence of leaflet co-aptation. This may be explained by the rather prototypic design of the TEHV in this proof of concept study. Furthermore, a minimal structural shortening of the TEHV cusps was detectable which will be addressed in future TEHV scaffold designs e.g. by oversizing of the coaptation areas of the starter matrices. Further enhancement of cellular attraction and, thus, tissue formation particularly in the distal leaflet region may provide solutions [257]. Finally, following this feasibility study introducing injectable TEHV generated and minimally invasively implanted in a single intervention, extended long-term studies are mandatory in order to further elucidate the fate of such living autologous cell based engineered heart valves as well as the underlying tissue remodeling mechanisms observed in vivo. Particularly, the precise role of seeded stem cells with respect to their function in chemo-attraction and tissue formation has to be systematically assessed. However, addressing these questions was beyond the scope of this pilot-study and will be investigated in future experiments.

Conclusions

These first results of combining minimally invasive valve replacement procedures with heart valve tissue engineering in a single intervention in a preclinical primate model are promising and demonstrate the feasibility of using BMCs for the fabrication of TEHV. Moreover, utilizing the body's natural abilities to regenerate TEHV in vivo, may greatly simplify, and improve the clinical feasibility of the autologous cell-based TEHV approach. Such autologous and living heart valves with repair and regeneration capacities may represent the next generation of transcatheter and transapical heart valves overcoming the time limitations of the currently used bioprosthetic valves suggesting their future clinical application also beyond elderly patients.

Acknowledgements

The authors thank Deon Bezuidenhout, Ronnett Seldon, Elizabeth VanderMerwe, Ursula Steckholzer, Pia Fuchs, Klaus Marquardt and Silvia Behnke for their technical support, as well as all the members of the Animal Unit, Faculty of Health Sciences, University of Cape Town for their excellent contribution.

Statistical Analysis

All quantitative data are presented as mean +/- standard deviation (SPSS 17.0, IBM, Somers, NY, USA).

Chapter 6

Stem Cell Based Transcatheter Aortic Valve Implantation: *First Experiences in a preclinical model*

The contents of this chapter are part of **Emmert MY,** Weber B, Behr L, Frauenfelder T, Brokopp CE, Grunenfelder J, Falk V, Hoerstrup SP. *Transapical Aortic Implantation of Autologous Marrow Stromal Cell-based Tissue Engineered Heart Valves – First Experiences in the Systemic Circulation*. JACC Cardiovasc Interv. 2011 Jul;4(7):822-3. doi: 10.1016/j.jcin.2011.02.020.

and

Emmert MY, Weber B, Wolint P, Behr L, Sammut S, Frauenfelder T, Frese L, Scherman J, Brokopp C, Templin C, Grünenfelder J, Zund G, Falk V, Hoerstrup SP. *Stem Cell Based Transcatheter Aortic Valve Implantation: First Experiences in a preclinical model.* JACC Cardiovasc Interv. 2012 Aug;5(8):874-83. doi: 10.1016/j.jcin.2012.04.010.

Acute technical feasibility pre-study

In order to broaden the future clinical application of trans-catheter tissue engineered heart valves and based on the novel approach introduced in chapter 5, the one-step interventional, marrow stromal cell based concept was challenged in the high-pressure system of the systemic circulation. To assess technical and acute feasibility and to circumvent potential complications that are associated with the complex anatomy of the aortic root, in an initial in vivo experiment the fabricated TEHVs using the above mentioned concept were transapically delivered into the descending aorta (distal to the brachiocephalic-trunk) and brachiocephalic-trunk of a sheep. To achieve a sufficient loading, native valve incompetence was created by applying the *Hufnagel* procedure prior to implantation.

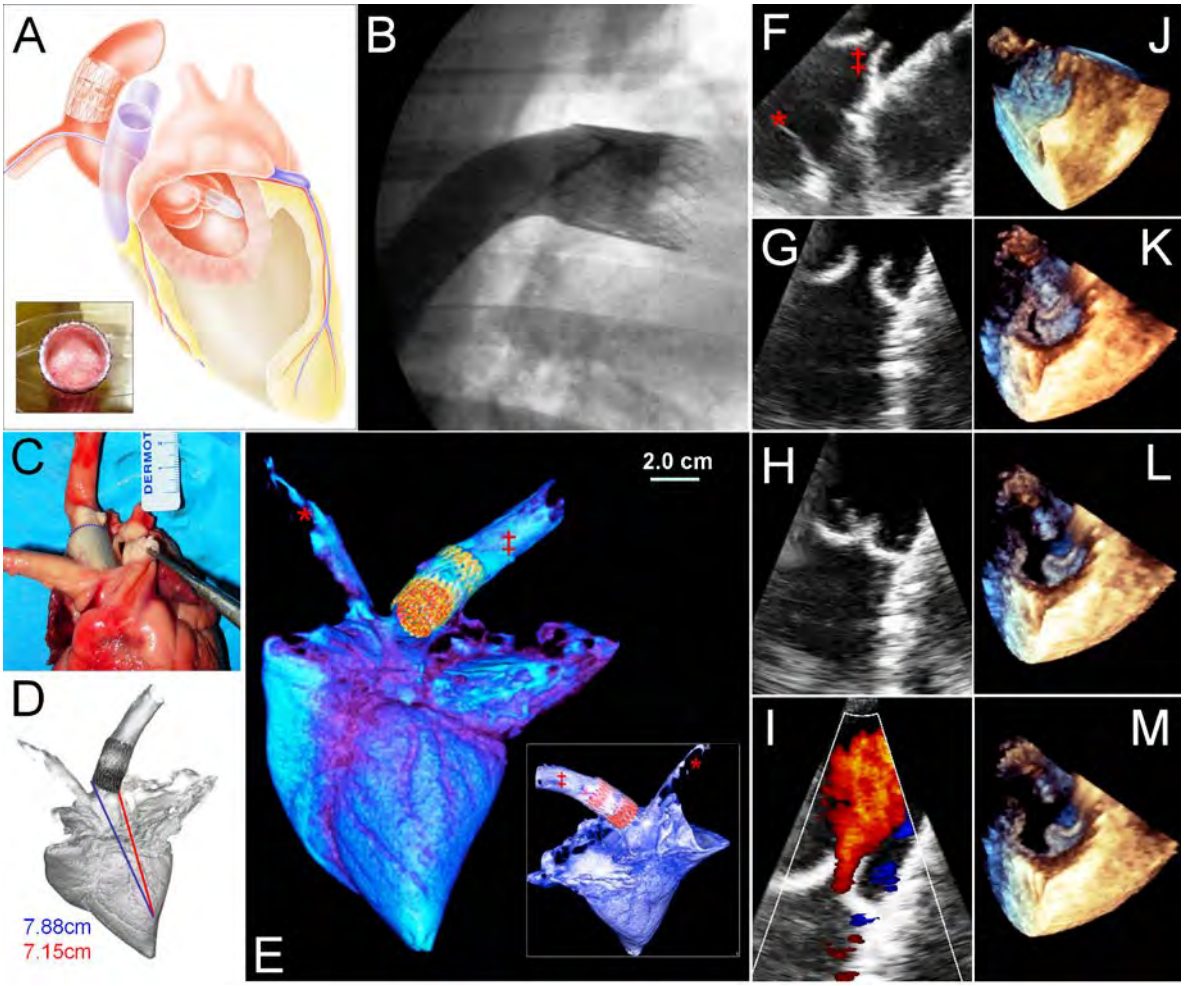

Figure 1: Transapical implantation of marrow stromal cell based TEHV into the systemic circulation

Within one procedure tissue-engineered, living heart valves (TEHV) fabricated from biodegradable scaffolds seeded with autologous bone-marrow derived mononuclear cells (Fig.1a/inset), were integrated into self-expanding nitinol stents (20mmx30mm) and transapically delivered into the descending aorta (distal to the brachiocephalic trunk) and brachiocephalic trunk of sheep (Fig.1a). Native valve incompetence was created by applying the Hufnagel procedure prior to implantation (Fig.1a). After successful deployment (Fig.1b-c), valve-function and optimal positioning were confirmed using fluoroscopy (Fig.1b), computed-tomography (CT) (Fig.1d-e/inset) and echocardiography (Fig.1f-m). Trans-esophageal echocardiography (TEE) in the 2D (g and h), 2D Color (i) and 3D Mode (j-m) displayed the TEHV in the descending aorta (‡) above the native valve (*). In particular, the TEE analysis showed well defined leaflets showing sufficient coaptation. The crimping-

time of the TEHVs was 15±2 minutes. The overall duration of the procedure from the preparation of cells to the successful delivery was two hours. Post-mortem analysis displayed fully intact TEHVs and in particular well defined leaflets showing coaptation. There were no signs of leaflet-rupture, microstructure damage or thrombus formation detectable.

The results of this acute study demonstrated the principal feasibility of the minimal-invasive, transapical implantation of TEHV into the systemic circulation with an adequate valvular functionality comprising of sufficient leaflet mobility and co-aptation fully accepting the systemic pressure loading. Post mortem analysis displayed fully intact TEHVs and in particular well defined leaflets, while there were no signs of pressure damage, leaflet rupture or thrombus formation detectable.

Based on these promising results the orthotopic application of this one-step intervention concept was challenged. After the detailed adaption of the TEHV and stent design to the anatomic conditions of an orthotopic aortic valve, the subsequent trial was initiated to assess the feasibility to implant marrow stromal cell based tissue engineered heart valves into the orthotopic aortic position utilizing an advanced transcatheter delivery system.

Abstract

Objectives: We investigate the combination of transcatheter aortic-valve implantation (TAVI) and a novel concept of stem cell-based, tissue-engineered heart-valves (TEHV) comprising minimally-invasive techniques for both, cell-harvest and valve-delivery.

Background: TAVI represents an emerging technology for the treatment of aortic-valve disease. The utilized bioprostheses are inherently prone to calcific-degeneration and recent evidence suggests even accelerated degeneration resulting from structural-damage due to the crimping-procedures. Autologous, living heart-valve prosthesis with regeneration and repair capacities would overcome such limitations.

Methods: Within a one-step intervention, tri-leaflet TEHV, generated from biodegradable synthetic-scaffolds, were integrated into self-expanding nitinol-stents, seeded with autologous bone-marrow mononuclear cells, crimped and transapically delivered into adult sheep (n=12). Planned follow-up (FU) was 4hours (group A/n=4), 48hours (group B/=5) or 1 and 2weeks (group C/n=3). TEHV-functionality was assessed by fluoroscopy, echocardiography and computed-tomography. Post-mortem analysis was performed using histology, extracellular-matrix analysis and electron-microscopy.

Results: Transapical implantation of TEHV was successful in all animals (n=12). FU was complete in all animals of group A, 3/5 of group B and 2/3 of group C (1week n=1; 2weeks; n=1). Fluoroscopy and echocardiography displayed TEHV-functionality demonstrating adequate leaflet-mobility and co-aptation. TEHV showed intact leaflet-structures with well-defined cusps without signs of thrombus-formation or structural-damage. Histology and ECM displayed a high cellularity indicative for an early cellular-remodelling and in-growth after 2weeks.

Conclusion: We demonstrate the principal feasibility of a transcatheter, stem cell-based TEHV implantation into the aortic-valve position within a one-step intervention. Its long term functionality proven, a stem cell-based TEHV approach may represent a next generation heart-valve concept.

Introduction

The therapy options for patients with valvular heart disease (VHD) are currently undergoing rapid changes and in addition to conventional, surgical valve replacement representing the standard of care since several decades, transcatheter aortic valve techniques have entered the clinical-routine representing an efficient alternative for the treatment of elderly high-risk patients [84, 86, 258, 259]. Given sufficient long-term safety, it can be predicted that these minimally-invasive techniques may have a major impact on the treatment strategy of patients with VHD.

However, despite this rapid technical progress, the currently available prostheses for transcatheter-approaches are bio-prosthetic associated with the known disadvantages comprising progressive calcification and degeneration. Furthermore, recent evidence suggests even accelerated degeneration resulting from structural-damage due to the crimping-procedures [260, 261].

A living heart-valve prosthesis created by tissue-engineering technologies with regeneration and repair capacities would overcome such limitations [232]. A clinically relevant heart-valve tissue-engineering concept (HVTE) would ideally comprise minimally-invasive techniques for both, cell-harvest and valve-implantation. We have demonstrated the technical feasibility of combining the concept of HVTE and trans-apical delivery into the pulmonary-position of adult sheep [111]. Thereafter, in a recent *proof-of-concept* study we introduced a novel and clinically highly relevant concept of in-vivo implantation of autologous bone-marrow mononuclear cell (BMMC)-derived tissue-engineered heart-valves (TEHV) in a primate model.[28]. Based on previously described techniques that are currently entering the clinical-arena following recent FDA approval [262] to generate tissue-engineered vascular-grafts (TEVG) by using BMMCs without any phase of in-vitro culturing or expansion [97, 133, 238, 239, 263], we successfully generated and implanted autologous BMMC-derived TEHV in a one-step intervention comprising cell-harvest, in-vitro engineering and transapical-delivery [28]. However, except an acute, technical feasibility study using a modified *Hufnagel* procedure [264] to implant TEHV into the descending aorta in an ovine model [26], chronic studies of successful TEHV-implantations have only been reported for the low-pressure system in the pulmonary-position [28, 111, 116].

The aim of this study was to assess the principal feasibility of implanting stem cell-based, tissue-engineered heart-valves (TEHV) into the aortic-valve position using a transcatheter, one-step interventional approach. Beside the technical feasibility of the deployment of a TEHV in the aortic-position, the major endpoints of this study were the assessment of the valve-functionality and initial tissue-remodelling phenomena of TEHV in the aortic-position.

Materials & Methods

Experimentation approval

All animals received humane care in compliance with the "Principles of Laboratory Animal-Care" as well as with the ''Guide for the care and use of laboratory animals" published by the National Institutes of Health (publication no. 85-23/revised 1985). All procedures were approved by the Institutional Ethics Committee [Approval-No 11-15/2011].

Study Design

The study aim was to assess the principal feasibility of implanting stem cell-based, tissue-engineered heart-valves (TEHV) into the orthotopic, aortic-valve position using a transcatheter, one-step

interventional approach (figure 1, supplementary figure 1). The study animals (adult sheep/n=12) were divided into three groups: group A (follow up: 4 hours; n=4), group B (follow-up: 48hours; n=5) and group C (follow-up: 1 and 2 weeks; n=3) (figure 2).

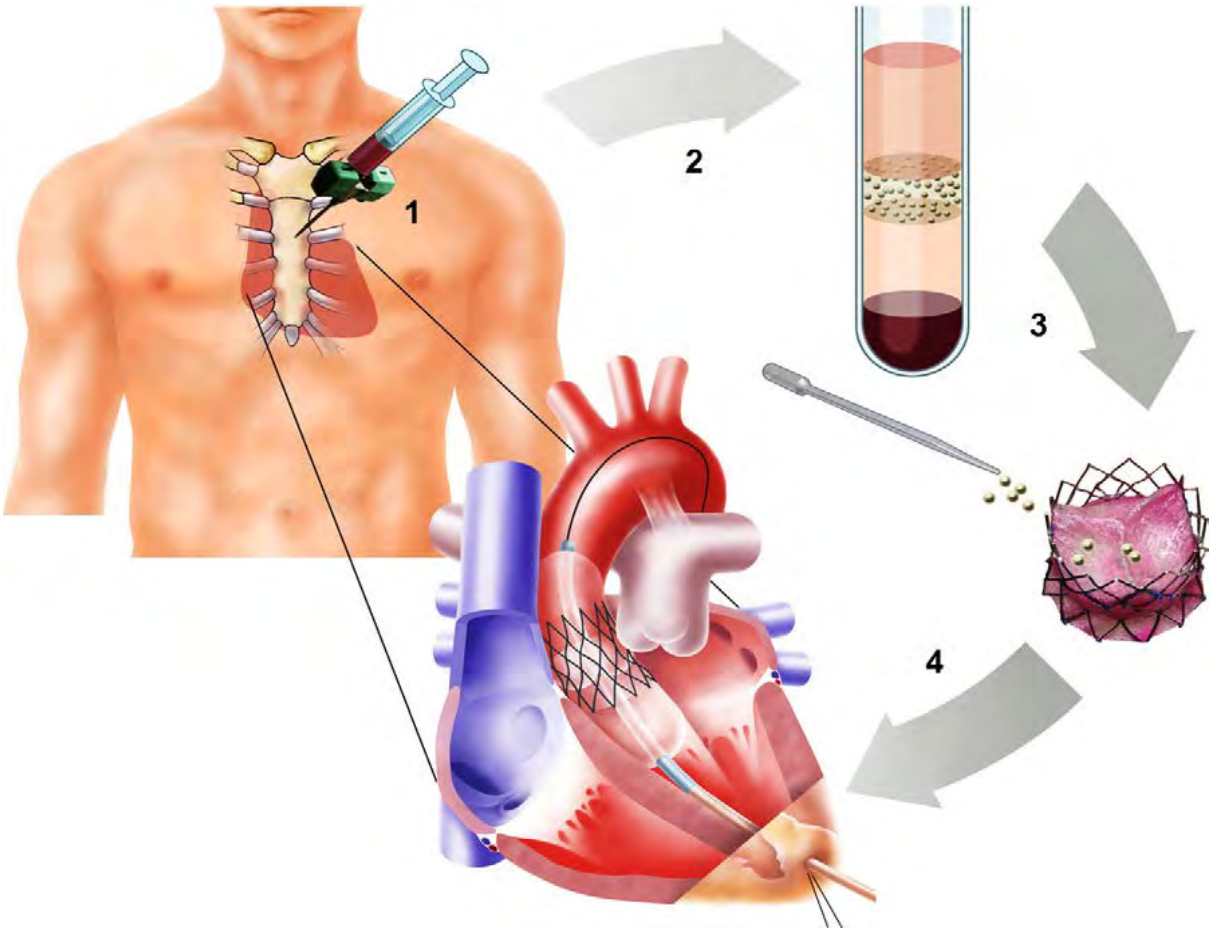

Figure 1: Stem cell-based, tissue-engineered heart-valve (TEHV) implantation into the aortic-valve position via a transcatheter, one-step interventional approach

Bone-marrow is aspirated from the sternum into a heparinized syringe **(step 1)** and bone-marrow mononuclear cells (BMMCs) are obtained by centrifuging the samples on a histopaque density-gradient **(step 2).** The BMMCs are seeded onto the stented heart-valve scaffolds using fibrin as a cell-carrier **(step 3).** Thereafter the TEHV is loaded into the delivery device by crimping the outer diameter down to 8mm and transapically delivered **(step 4).** The mean duration of the entire procedure, starting from cell-harvest until TEHV-implantation takes approximately 2hours.

In the first set of experiments, the animals of group A (n=4) were used in an acute fashion (follow-up: 4hours) to establish the technical-feasibility of transapical TEHV implantation into the orthotopic, aortic-position with a specific focus on technical aspects such as device-insertion, stepwise delivery and optimal positioning considering the anatomical condition of the aortic-annulus, the aortic-root and the coronaries. In order to assess TEHV stability and functionality as well as early tissue-reaction and remodeling in the systemic-pressure system, the other animals were planned to be either followed up for 48hours (group B; n=5) or for 1 and 2 weeks (group C; n=3) (figure 2).

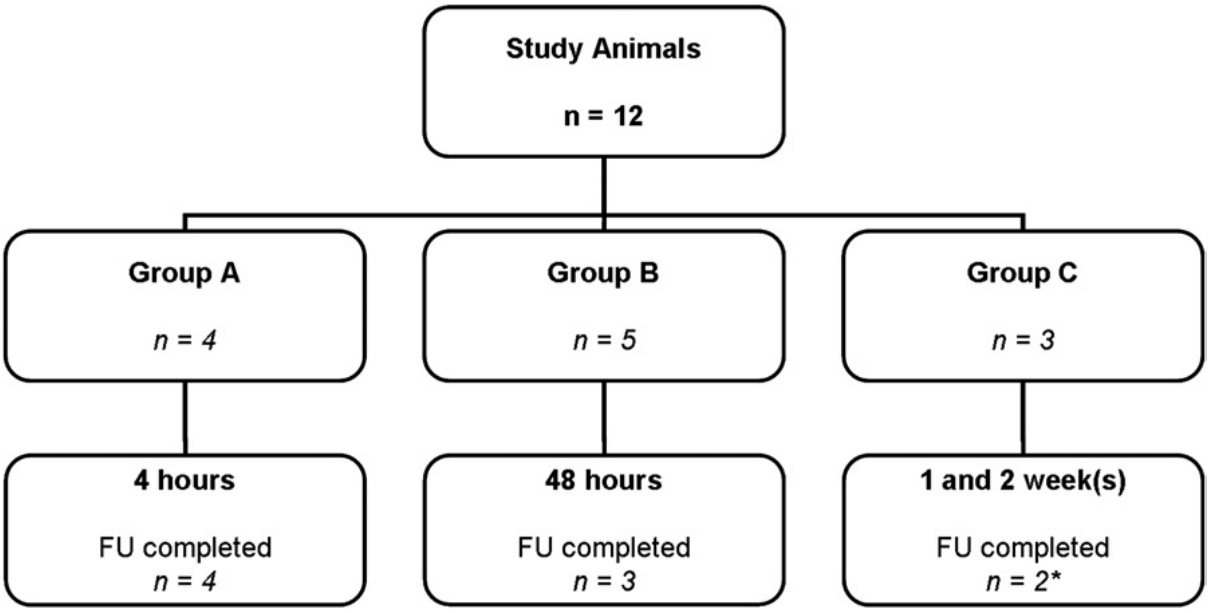

Figure 2: Study Design: Animal Distribution and Follow Up (FU).

Scaffold Fabrication

Trileaflet heart-valve scaffolds were fabricated as previously described [26, 28]. In brief, trileaflet heart valve scaffolds were fabricated as previously described [26, 28]. In brief, they were produced from non-woven polyglycolic-acid meshes (PGA; Cellon, Luxembourg), coated with 1.75% poly-4-hydroxybutyrate (P4HB; TEPHA Inc., USA). Thereafter, the scaffolds were integrated into radially self-expandable nitinol stents attaching the scaffold matrix to the inner surface of the nitinol stent wires (supplementary figure 1A). After vacuum drying for 24 hours, the scaffolds were sterilized overnight by using ethylene oxide (EtO) gas sterilization.

Isolation, Characterization and Differentiation of ovine Bone-Marrow Mononuclear Cells (BMMCs)

Isolation of ovine Bone Marrow Mononuclear Cells (ovine BMMCs)

61±2.5 mL of bone marrow was aspirated from the sternum of adult sheep into a heparinized syringe (50-100U/mL) using a 12 Gauge threpine needle (supplementary figure 1B and C). BMMCs were obtained by centrifuging the samples on a histopaque density gradient (Sigma Chemical Co., USA) for 30 minutes at 1500 rpm. The viability of the isolated buffy coat was determined by flow cytometry as well as by staining the cells with tryptan blue after erythrocyte elimination and quantifying with a hemocytometer [26, 28].

Characterization of ovine BMMCs and Bone Marrow derived mesenchymal Stem Cells (ovine MSCs) using Fluorescence Activated Cell Sorting (FACS) analysis and immunohistochemistry

Ovine BMMCs and MSCs at passage 1 were characterized for the following markers: mouse anti-human CD166 (BioLegend, USA), CD44 (Santa Cruz Biotechnology, USA), mouse anti-sheep CD31 (Fitzgerald, USA), CD34 (kindly provided by Chris Porada, USA), Stro4 and CD29 (kindly provided by Sharon Paton, Australia). The appropriate isotype controls were used for comparison. The cells were labeled with the primary antibodies described at 4°C and washed with FACS buffer consisting of 2% FCS (Biowest, France), 0.5 M EDTA and 0.05% sodium azide (Sigma Aldrich, Switzerland) in phosphate buffered saline (Invitrogen, Switzerland). DyLight488-conjugated goat anti-mouse IgG (Jackson ImmunoResearch Europe, UK) was used as secondary antibody and incubated at 4°C. Finally, the stained cells were fixed in PBS containing 1% paraformaldehyde (Sigma Aldrich,

Switzerland) and measured with a BD FACSCalibur (Becton Dickinson, USA). Data were analyzed using FlowJo software (Tree Star, USA) (supplementary figure 2).

Immunofluorescence staining of ovine MSCs

Briefly, for immunofluorescence staining, cells were plated into 2-well chamber slides (BD Biosciences, Switzerland) and after 72 hours fixed with 4% formalin (Kantonsapotheke Zürich, Switzerland) at room temperature for one hour. Prior to labelling, cells were permeabilized with PBS (Invitrogen, Switzerland) containing 0.2% Triton X-100 (Sigma Aldrich, Switzerland) for 7 minutes at room temperature and afterwards incubated with mouse anti-human CD166 (BioLegend, USA), mouse anti-human CD44 (Santa Cruz Biotechnology, USA), mouse anti-ovine Stro4 or mouse anti-ovine CD29 (kindly provided by Sharon Paton, Australia) in PBS containing 1 mg/ml bovine serum albumin (Sigma Aldrich, Switzerland) for one hour at room temperature. The secondary staining step was done with a goat anti-mouse IgG-DyLight488 (Jackson ImmunoResearch Europe, UK) antibody together with DAPI and Alexa Fluor 546 phalloidin (Invitrogen, Switzerland) for one hour at room temperature and analyzed by fluorescent microscopy (Leica CTR6000, Leica Microsystems AG, Switzerland). Between steps, slides were washed three times with PBS (supplementary figure 2).

Functionality and Differentiation Potential of ovine MSCs

Isolated and cultured oMSCs at passage 2 were analyzed for their differentiation capacity to the adipogenic, osteogenic and chondrogenic lineages as previously described [198]. Briefly, adipogenic differentiation was induced by culturing cells in induction medium containing DMEM low glucose (Invitrogen, Switzerland), 10% FCS (Biowest, France), 1 mM Dexamethasone, 10 mg/ml Insulin, 120 mM Indomethacin, 0.5 mM 3-Isobutyl-1-methylxantine (IBMX, Sigma Aldrich, Switzerland) and 1% Penicillin and Streptomycin (Invitrogen, Switzerland). After 3 days, medium was changed to maintenance medium consisting of induction medium with the deletion of IBMX. After 3 weeks, cells were fixed with 4% formalin (Kantonsapotheke Zürich, Switzerland) and accumulation of lipid vacuoles was stained with 3% Oil Red-O (Sigma Aldrich, Switzerland). Osteogenesis was induced in the presence of DMEM low glucose (Invitrogen, Switzerland), 10% FCS (Biowest, France), 10 mM b-Glycerophosphate, 50 mM L-Ascorbic acid 2-phosphate, 10 nM Dexamethasone (Sigma Aldrich, Switzerland) and 1% Penicillin and Streptomycin (Invitrogen, Switzerland). Cultures were fixed after 5 weeks with 4% formalin and mineralized deposits were detected using 2% Alizarin red (Sigma Aldrich, Switzerland). Cultures were observed under an inverted microscope (Axiovert 40 CFL, Zeiss, Germany). For the chondrogenic differentiation, cell aggregate was placed in induction medium consisting of DMEM high glucose (Invitrogen, Switzerland), 1% FCS (Biowest, France), 0.5 mg/ml Insulin, 50 mM L-Ascorbic acid 2-phosphate (Sigma Aldrich, Switzerland), 10 ng/ml Transforming growth factor-beta1 (PeproTech, UK) and 1% Penicillin and Streptomycin (Invitrogen, Switzerland) for 3 weeks. The pellet was fixed with 4% formalin, embedded in paraffin and proteoglycan synthesis was identified by 0.1% Toluidine blue (Sigma Aldrich, Switzerland) staining. The slides were analyzed by microscopy (Leica CTR6000, Leica Microsystems AG, Switzerland) (supplementary figure 2).

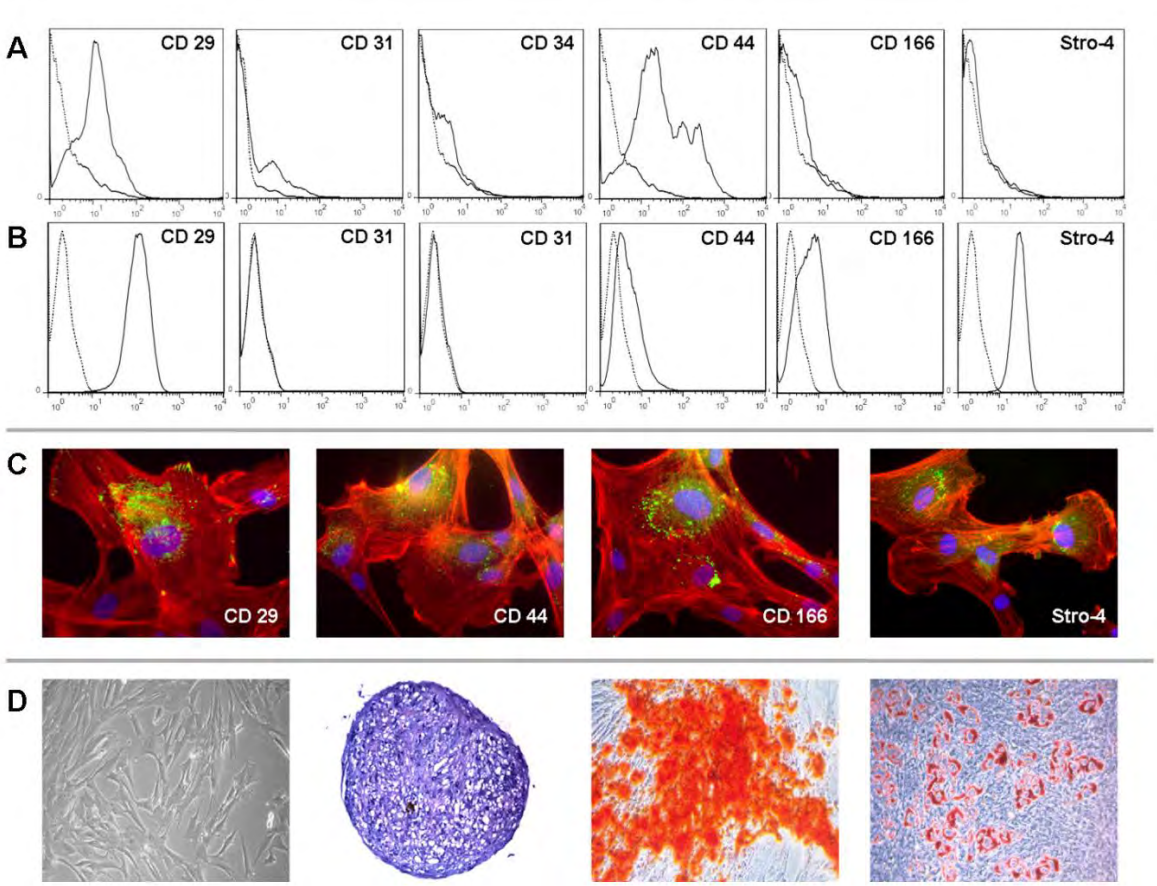

Supplementary Figure 2: Characterization and Differentiation of ovine bone-marrow derived mononuclear cells and mesenchymal stem cells

Ovine BMMCs were evaluated by flow cytometric analysis. Surface-marker expression of CD29 and CD44 was detected. Less than 4% of the cells were positive for CD31, CD34 and CD166 and no expression of Stro-4 was observed **(panel A).** Ovine MSCs were positive for CD29, CD44, CD166 and Stro-4. In contrast, low expression of the hematopoietic lineage markers CD31 and CD34 was observed **(panel B).** The results of the ovine MSC phenotype were confirmed using immunofluorescence (**panel C).** Ovine MSCs displayed a characteristic spindle-shaped fibroblastic morphology. Their differentiation potential was demonstrated by inducing cells to specific lineages: adipogenic, osteogenic and chondrogenic **(panel D).**

Seeding of ovine BMMCs

Fibrin was used as a cell carrier to seed BMMCs onto the stented heart valve scaffolds (1.73 ± 0.47 x 10^6 cells/cm^2 valve leaflets) (Sigma Chemical Co., USA). Thereafter, the TEHV were placed into vented 50 mL tubes for 10 minutes to allow the fibrin-thrombin solution to clot adequately (supplementary figure 1D). Next, the TEHV was washed in heparinized blood of the recipient animal and was loaded into the delivery device by crimping the outer diameter from 25 mm down to 8 mm**.**

Preoperative Assessment, Planning and Sizing

Prior to implantation all sheep underwent trans-thoracic echocardiography (TTE) in order to adapt the ideal stent-size to each animal. Before starting the implantation-procedure the following

parameters were measured by intra-operative angiography to re-confirm the ideal stent-size: diameters of the Aortic-Annulus (AA), Sinus-Portion (SP), the Sinus-Tubular Junction (STJ) and the Brachiocephalic-Trunc (BCT) as well as the distance to the BCT and the height of the SP *(table 1)*. Animals with an annulus between 22-23mm received a 25mm stented TEHV (n=8), while animals with an annulus of 24-25mm received a 27mm stented TEHV (n=4).

Table 1. Pre-Operative Data and Angiographic Measurements

Body weight, kg	53.3 ± 8.1
Diameter AA on pre-op TTE, mm	22.1 ± 0.7
Diameter AA, mm	22.7 ± 1.0
Diameter BCT, mm	15.2 ± 1.4
Distance to BCT, mm	45.1 ± 2.7
Diameter SP, mm	28.3 ± 2.0
Diameter STJ, mm	24.5 ± 1.4
Height of SP, mm	13.3 ± 2.0

Values are mean ± SD.
AA = aortic annulus; BCT = brachiocephalic trunc; pre-op = pre-operative; SP = sinus portion; STJ = sinus-tubular junction; TTE = transthoracic echocardiography.

Transcatheter Implantation of stem cell-based TEHV into the aortic-valve position

TEHV were transapically delivered into the aortic-valve position via a mini-sternotomy (figure 1). The valves were crimped and loaded onto a custom-made, guide-wired inducing system (OD=8mm). The apex of the left-ventricle was punctured after 5/0 Prolene pledged, purse-string sutures were placed. TEHV were delivered into the aortic-valve position under fluoroscopic-control (OECW 9900 Elite GE, Fairfield/USA). After the stepwise opening and positioning of the distal part of the stent in the aortic-root under fluoroscopic-control, the proximal part of the stent was instantly delivered. The appropriate placement and functionality of the implanted valve was confirmed by contrast-angiography, before the device was carefully removed and the purse-string sutures were tightened.

Assessment of stent positioning and TEHV-functionality

Stent positioning was controlled using angiography and computed-tomography (CT, Siemens, Munich/Germany). In-vivo functionality was evaluated using intra-operative, epicardial 2D- and 3D-echocardiography ((Philips Healthcare iE33W xMATRIX Ultrasound/Netherlands). Trans-thoracic echocardiography (TTE) was serially performed until to the sacrifice of the animal. Three-dimensional CT reconstruction and volume rendering were performed using the OsiriX Image Processing Software (OsiriX Mac OSX; Version 3.8.1).

Postoperative Care & Follow-Up

Anticoagulation was done with Aspirine 100mg/day and a clinical checkup was performed on a daily basis until sacrifice. The animals were sacrificed applying potassium euthanization and exsanguination. Thereafter the hearts were harvested and the TEHV were excised for in-vitro analysis.

Histology & Scanning Electron Microscopy

Tissue samples of the explanted TEHV were analyzed qualitatively via immunohistochemistry / histology using Hematoxylin & Eosin staining and Masson-Trichrome staining. Representative tissue samples of TEHV were analyzed using Scanning Electron Microscopy (supplementary figure 4) and were fixed using 2% glutaralaldehyde. After preparation, samples were sputter-coated with platin and investigated with a Zeiss Supra 50 VP Microscope (Carl Zeiss Imaging, Germany).

Quantitative Explant Tissue Analysis

Explanted TEHV were lyophilized and analyzed by biochemical assays for total DNA and GAG content. For measuring the DNA amount, the Hoechst dye method was used [241]. The GAG content was determined using a modified version of the protocol described by *Farndale* et al. [242] and a standard curve prepared from chondroitin sulphate from shark cartilage (Sigma Chemical Co., St. Louis, USA) (supplementary figure 5).

Results

Cell Isolation, Characterization and Preparation of TEHV

Ovine BMMCs were evaluated by flow cytometric analysis. Surface-marker expression of CD29 (mean±SD, 59.0%±7.0%) and CD44 (61.0%±16.7%) was detected. Less than 4% of the cells were positive for CD31 (3.7%±1.7%), CD34 (3.7%±1.0%) and CD166 (3.5%±4.4%) and no expression of Stro-4 was observed (supplementary figure 2/panel A). Ovine MSCs were positive for CD29 (92.3%±2.1%), CD44 (24.3%±11.9%), CD166 (73.0%±14.2%) and Stro-4 (93.7%±14.2%). In contrast, low expression of the hematopoietic lineage markers CD31 (1.3%±0.9%) and CD34 (2.1%±1.8%) was observed (supplementary figure 2/panel B). The results of the ovine MSCs phenotype were confirmed using immunofluorescence (supplementary figure 2/panel C). Ovine MSCs displayed a characteristic spindle-shaped fibroblastic morphology (figure 2/panel D). Their differentiation potential was demonstrated by inducing cells to specific lineages: adipogenic, osteogenic and chondrogenic (supplementary figure 2/panel D).

Trans-catheter aortic-valve implantation of stem cell-based TEHV

Delivery, positioning and intra-operative complications

Transcatheter aortic-valve implantation of stem cell-based TEHV could be performed successfully in all animals (n=12) (figure 3, supplementary trailer 1). The aortic-root was visualized (figure 3A), before the loaded delivery-device was inserted and positioned (figure 3B). Under instant fluoroscopic-control, the TEHV was stepwise delivered beginning with the deployment of the distal part (figure 3C-D) followed by the proximal part (figure 3E). Immediately after full deployment, coronary-perfusion (figure 3F) and valve-functionality was confirmed in the fluoroscopy (figure 3G). The animals remained hemodynamically stable during the entire procedure. Device removal was uneventful and no major complications such as bleeding or cardiac-arrhythmia occurred. As on fluoroscopy (figure 3A-G, supplementary trailer 1) and as confirmed on computed tomography (supplementary figure 3A-G), TEHV could be successfully placed into the aortic-valve position, thereby fully excluding the native leaflets while not compromising the coronary-perfusion (figure 3D-G, supplementary trailer 1). In one animal of group B the TEHV appeared to be placed too proximal into the left-ventricular outflow-tract (LVOT). Consecutively, after a few hours it further migrated into the left-ventricle and the animal was sacrificed due to beginning acute left heart-failure. Another animal of group B had to be terminated after successful delivery due to severe valvular leaflet dysfunction displaying severe central-regurgitation immediately after implantation.

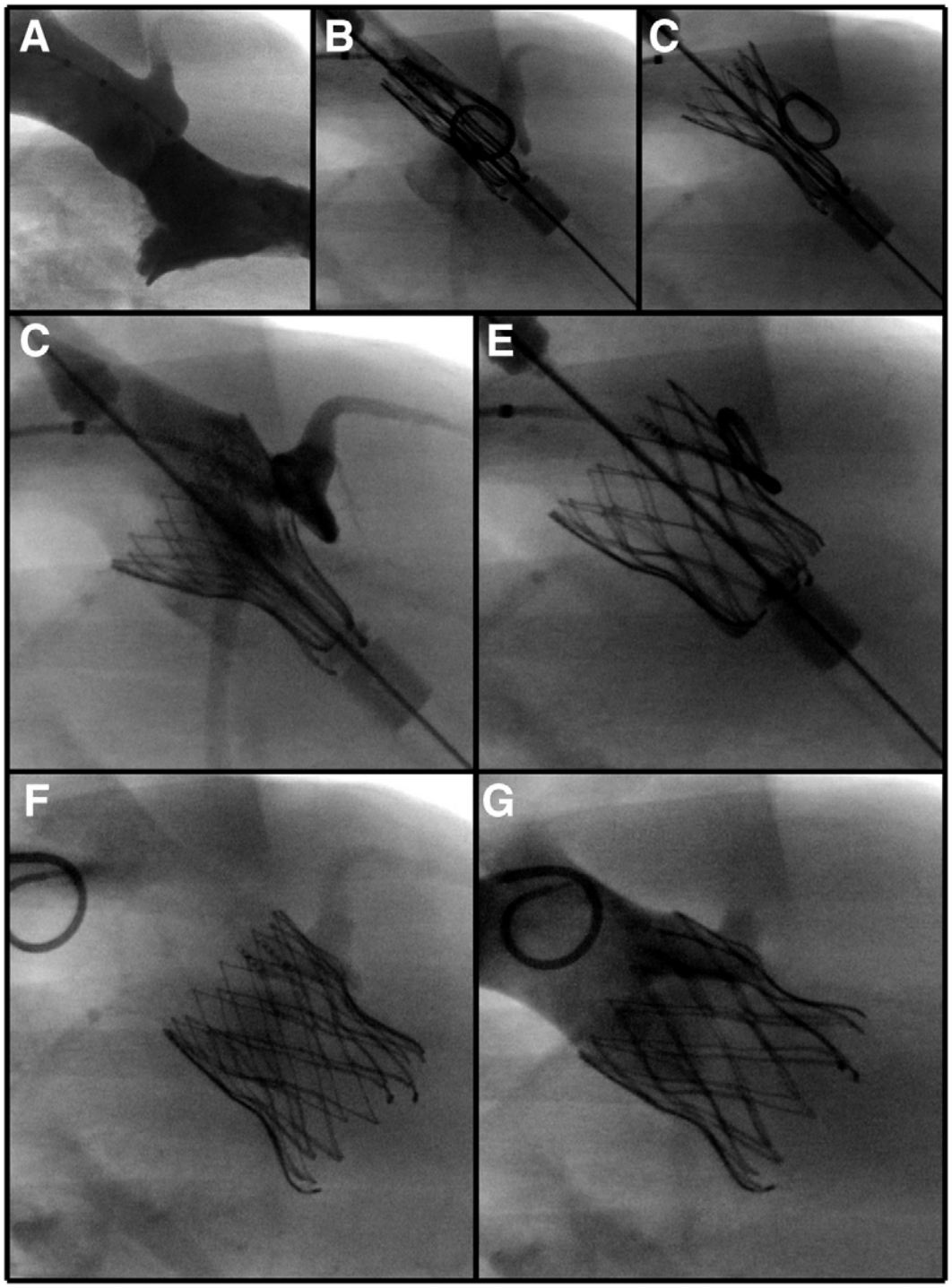

Figure 3: Fluoroscopy-guided transapical delivery of stem cell-based tissue-engineered heart-valves (TEHV) into the aortic-valve position

The aortic-root was visualized **(A),** before the loaded delivery-device was inserted and positioned **(B).** Under instant fluoroscopic-control, the TEHV was stepwise delivered beginning with the deployment of the distal part **(C and D)** followed by the proximal part **(E).** Immediately after full deployment, coronary-perfusion **(F)** and valve-functionality **(G)** was confirmed. The animals remained hemodynamically stable during the entire procedure and the TEHVs could be successfully placed into the aortic-valve position, thereby fully excluding the native leaflets while not compromising the coronary-perfusion.

The mean duration from cell-harvest until TEHV-loading was 64±8 minutes and the mean crimping time until trans-apical delivery, was 12±6 minutes. The mean duration of the entire procedure, starting from cell-harvest until TEHV implantation, was 109±14 minutes (table 2).

Table 2. Intraoperative Data and Echocardiography Measurements After Implantation

Duration from cell harvest to TEHV loading, min	64 ± 8
Crimping time until TEHV delivery, min	12 ± 6
Duration of the entire 1-step procedure, min	109 ± 14
TVG mean, mm Hg	8.4 ± 2.0
TVG peak, mm Hg	16.9 ± 5.8
EOA, cm^2	1.4 ± 0.1
Central aortic regurgitation	None
Paravalvular leakage*	2.1 ± 1.7
Regurgitation of mitral valve*	None†
Leaflet motion	Normal
Cardiac output, l/min	5.7 ± 1.2

Values are mean ± SD. *Regurgitation/paravalvular leakage grading: 0 = none; 1 = trivial; 2 = mild; 3 = moderate; 4 = severe. †Except 1 animal displaying mitral regurgitation grade 2.
EOA = effective orifice area; TEHV = tissue-engineered heart valve; TVG = transvalvular gradient.

Performance of TEHV and acute echocardiography findings

Acute TEHV functionality and mobility was controlled via fluoroscopy (figure 3G) and epicardial echocardiography (EE). Except the two terminated animals, in all other study animals (n=10) a sufficient opening and closing pattern of the TEHV was observed and the loading-pressure of the systemic-circulation was well tolerated (figure 4A and B, supplementary trailer 2A). TEHV functionality was confirmed in the 2D-color mode and the 3D-mode demonstrating good leaflet mobility and co-aptation (figure 4C-G, supplementary trailer 2B-C). The mean trans-valvular gradient was 8.4±2.0mmHg and the mean effective orifice-area (EOA) was 1.4±0.1cm² (table 2). Only one animal displayed a mild mitral-regurgitation and none of the animals showed central aortic-regurgitation. In contrast, in 40% of the animals, an at least mild paravalvular-leakage was present (table 2) which was rather related to the stent-shape and design, but not to the TEHV itself.

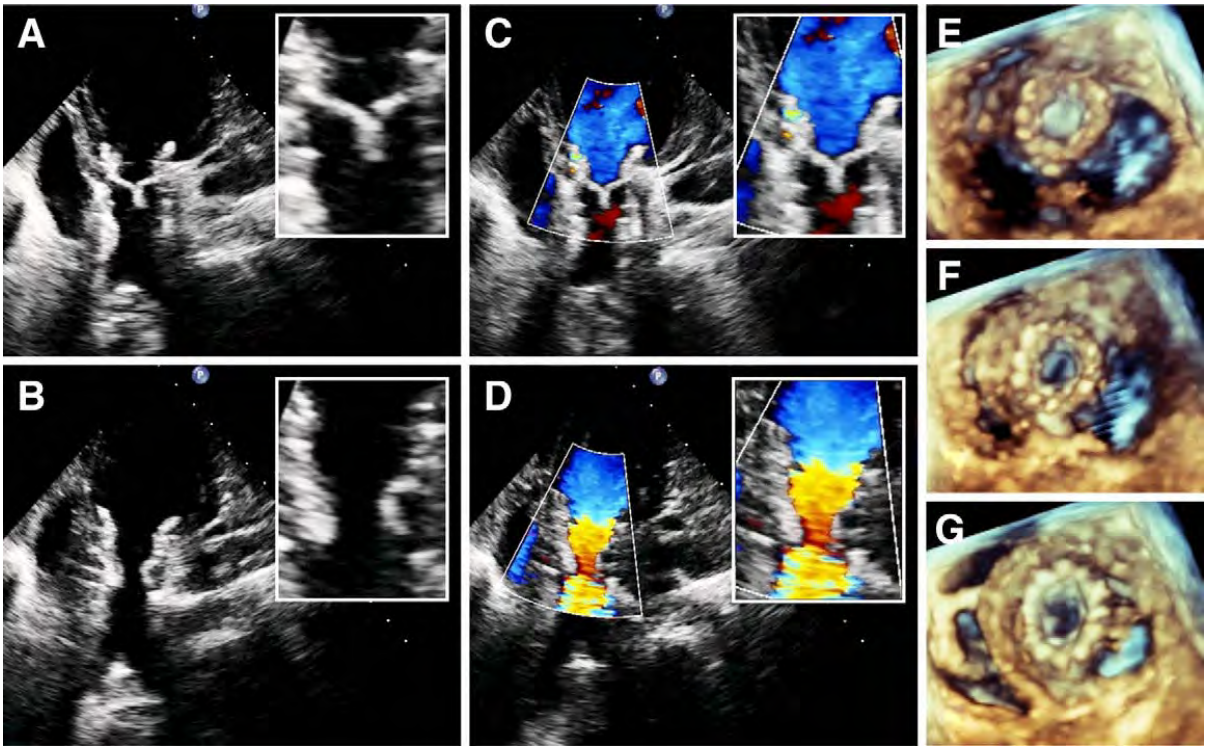

Figure 4: Performance of TEHV and echocardiography findings

TEHV-functionality and mobility was controlled via epicardial and trans-esophageal echocardiography (EE/TEE). TEHV tolerated the loading pressure of the systemic circulation adequately and demonstrated a sufficient co-aptation (A, B and insets). TEHV functionality and absence of regurgitation was confirmed in the 2D-color mode (C, D and insets) and in the 3D-mode demonstrating adequate leaflet-mobility (F, G and insets).

Early postoperative period, complications and follow-up

Except the two terminated animals, all other animals of group B (3/5) and group C (3/3) tolerated the procedure very well without any hemodynamic compromise and could be waken up immediately. Despite of an uneventful TEHV-delivery and an excellent TEHV functionality without any signs of regurgitation or paravalvular-leakage, one animal of group C died due to acute stent-dislocation. All other study animals were monitored regularly and received regular doses of aspirine until the planned harvest. The two remaining animals of group C (planned to be followed-up for 1 and 2 weeks) displayed a sufficient TEHV in-vivo functionality on trans-thoracic and trans-esophageal echocardiography (TTE/TEE) at 1week with a mean transvalvular gradient of 8.0±1.7mmHg and a mean EOA of 1.5±0.1cm². Therefore, it was decided to harvest one animal at 1 week and to keep the last remaining animal for an additional week to gain further insight into the early remodeling process. The remaining animal was clinically followed-up on a daily basis and the pre-final TTE-control on day10 before the planned harvest displayed sufficient TEHV-performance. While preparing for the final-assessment and harvest, the animal suddenly decompensated hours before the planned sacrifice at day14 due to a sudden stent-dislocation.

Explant Macroscopy

Except the animal which had to be terminated due to sudden valve-dysfunction, all other TEHV (n=11) displayed intact leaflet-structures with well-defined cusps and sufficient co-aptation, without signs of thrombus-formation, thickening, shrinking or structural-damage (figure 5A, inset and B). The TEHV harvested at 1 and 2weeks after implantation displayed to be well integrated into the surrounding tissue by complete tissue covering of the stent-frame (figure 5C). The TEHV explanted at 2weeks showed tissue-formation and co-aptation in two fully intact leaflets. The third leaflet (non-coronary) displayed a thin fissure which we assume was however most likely related to the harmful explantation procedure as the stent was completely entrapped in the mitral-valve and adequate tri-leaflet TEHV-functionality was confirmed on TTE 3days before.

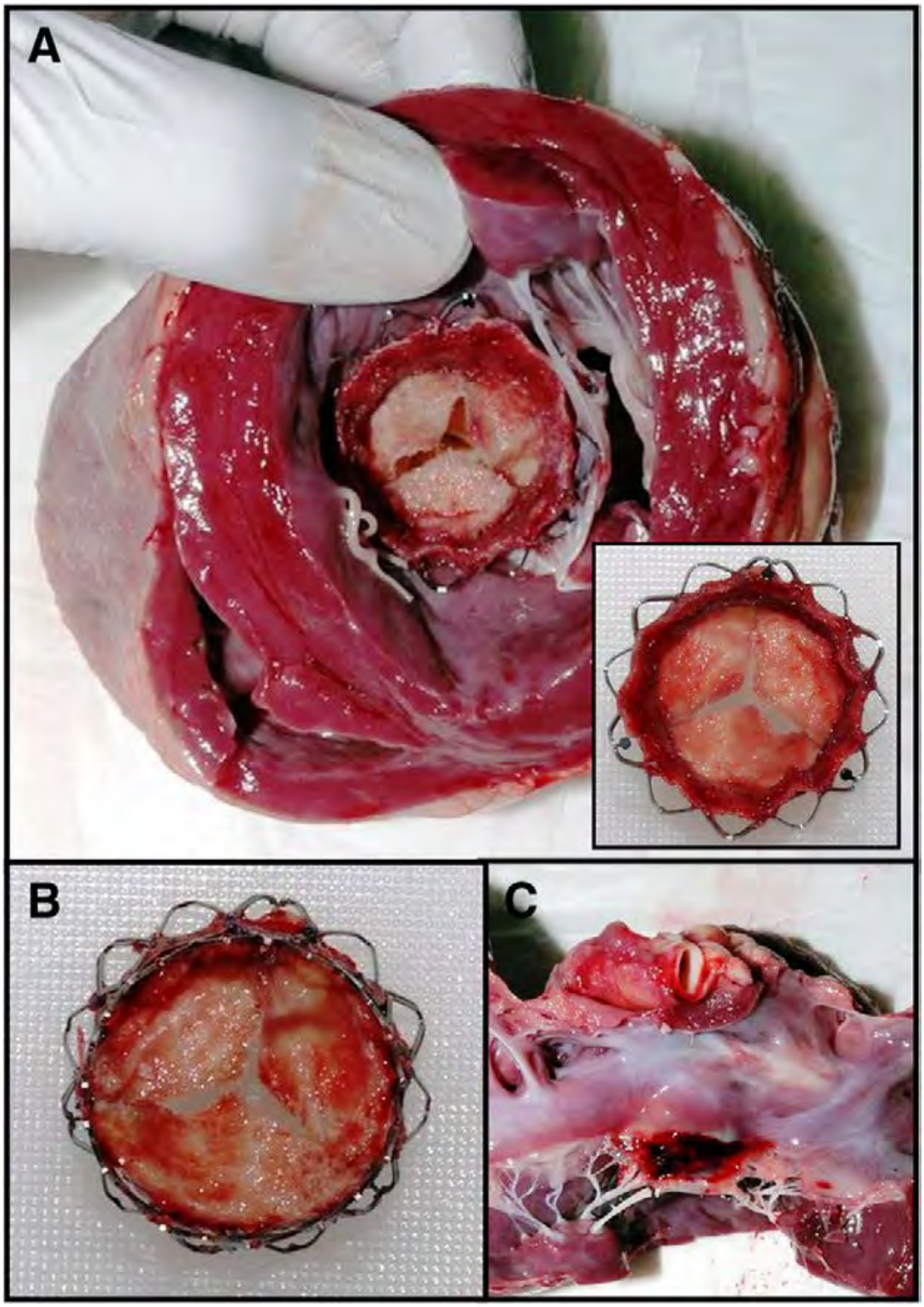

Figure 5: Explant Macroscopy of TEHV

Explanted TEHVs displayed intact leaflet structures with well defined cusps and sufficient co-aptation, without signs of thrombus-formation, thickening, shrinking or structural-damage from the lower view **(A and inset)** and the upper view **(B).** The TEHV harvested at 1 and 2 weeks after implantation displayed to be well integrated into the surrounding tissue by complete tissue covering of the stent-frame **(C).**

Explant Microscopy

After explantation, harvested tissues were analysed using scanning electron microscopy, histology, and extracellular-matrix analysis (ECM). In SEM, acute TEHV explants revealed a surface with fibrin-reaction characterized by thrombocyte-aggregation as well as leucocyte-attachment (supplementary figure 4). This was also confirmed in histology, where acute explants showed clear cellular-infiltrates and fibrin-formation in H&E staining (figure 6A-D). Interestingly, this cellularity only slightly increased in the tissues of the 24hour explants, while all later explant stages -including the 1week and the 2week explant tissues– showed a clearly increased cellularity (figure 6E-L). This observation was also supported by the ECM, which showed increasing DNA and GAG values in the TEHV with increasing time in-vivo (supplementary figure 5A and B).

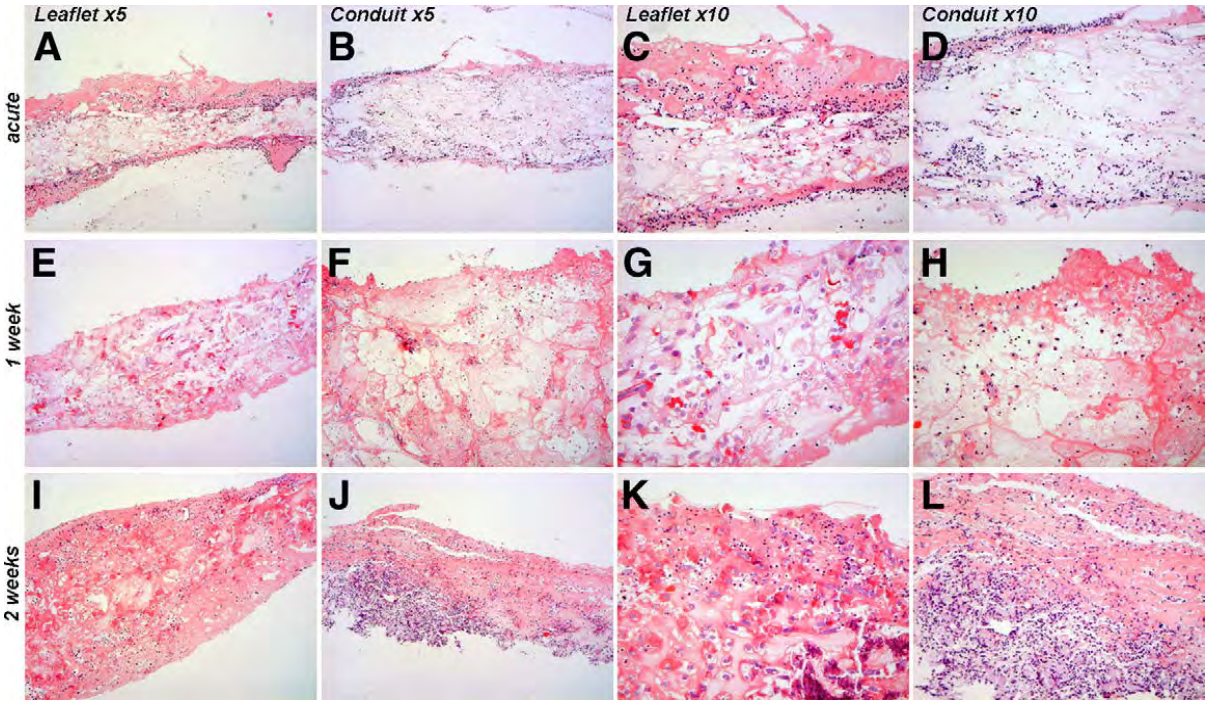

Figure 6: Histological Analysis of TEHV explants

On histology, acute explants showed clear cellular infiltrates and fibrin-formation in H&E staining **(A-D; *magnification x5 and x10).*** Interestingly, this cellularity only slightly increased in the tissues of the 24 hour explants (images not shown), while all later explants stages at 1 week and two weeks showed a clearly increased cellularity **(E-L; *magnification x5 and x10*).**

Discussion

Transcatheter aortic-valve implantation (TAVI) that has been recently implemented into the clinical routine as an attractive alternative for conventional aortic-valve replacement is expected to have a major impact on the management of VHD [84, 86, 258, 259]. Although these techniques are currently primarily applied to the elderly, high-risk patients [258, 259], the extension of indication also for younger patient is awaited for the near future. However, despite the tremendous potential of transcatheter techniques, the currently used valvular prostheses for these approaches are bio-prosthetic and all major disadvantages apply including progressive calcification and functional degeneration [28, 90, 91].

The concept of tissue engineered heart valves (TEHV) has been repeatedly suggested as a potential solution to overcome the limitations of currently used bioprostheses [91, 246]. The use of living, autologous cell-based valvular constructs with the capacity of growth and regeneration may be significantly beneficial for both, the congenital setting as well as the adult setting. Numerous tissue-engineering concepts as well as cell-sources are currently under evaluation for their clinical relevance and we have recently demonstrated the principal feasibility of combining the concept of heart valve tissue engineering (HVTE) and trans-catheter approaches in a preclinical large animal-model [111]. However, so far, most of these concepts require extensive technical, logistical and financial efforts limiting their broad implementation into the clinical-arena. Therefore, more simplicity is mandatory for an efficient translation into the clinical-arena. A clinically relevant HVTE concept comprises minimally-invasive techniques for both, cell-harvest and valve-delivery.

We have recently introduced a new concept of combining autologous, TEHV and transcatheter approaches in a one-step procedure [26, 28]. Based on various previous animal studies and clinical pilot-trials [238, 239, 263] to generate BMMC-derived tissue-engineered vascular-grafts (TEVG), in recent *proof-of-concept studies*, we were able to show the successful implantation of autologous BMMC-derived TEHV in a one-step intervention into the pulmonary-position in a primate model [28] as well as in the descending-aorta using a modified *Hufnagel-Procedure* in an technical, acute ovine model [26].

In this study and for the first time, we demonstrate the feasibility of this one-step procedure comprising minimally-invasive cell-harvest and transapical delivery for the aortic-valve position successfully replacing aortic-valves in an ovine model. By help of an improved catheter-system allowing for orthotopic, aortic-valve implantation, we were able to further develop and adapt this novel, clinically, highly-relevant one-step procedure for the high-pressure circulation. Our data indicate that BMMC-based TEHV can be successfully implanted into the aortic-position exhibiting competent valve-functionality and leaflet co-aptation sufficiently withstanding the systemic-pressure load, while any signs of valvular-rupture, tear or structural-damage were absent.

Importantly, this study elucidates that the TEHV fully accepted the systemic-pressure responding with a high degree of early cellularization indicative for an active and extensive tissue-formation and remodeling-process. As previously described, sufficient hemodynamic loading appears to play a key role in tissue-remodeling and formation and is a well established mechanism [117]. The histological findings of this study are supported by the interesting observation in our recent study that elucidated the crucial impact of sufficient hemodynamic loading on functional tissue-remodeling in a non-human primate model. In contrast to orthotopically delivered TEHV fully excluding the native leaflets, TEHV that were implanted into the supra-valvular position -not excluding the native leaflets and thereby being fully unloaded- lacked any leaflet-structure, being indicative for complete absence of tissue-formation as well as BMMC-mediated remodeling processes [28].

The underlying molecular mechanisms of autologous BMMC-based tissue-remodeling appear to be complex and have not been completely understood so far. Recent studies suggest a multi-factorial, BMMC-mediated chemo-attractive process [28, 90, 133, 265, 266]. This extensive, paracrine process appears to involve numerous cells including monocytes as well as mediator cytokines controlling the different steps of remodeling and tissue-formation [28, 90, 133, 265, 266]. In the setting of TEVG, Roh et al recently demonstrated that seeded BMMCs release significant amounts of monocyte chemo-attractant protein- 1 (MCP-1) and leading to an increased early monocyte recruitment.

Importantly, they also showed that the seeded BMMCs were no longer detectable within a few days after implantation suggesting that the scaffolds were initially repopulated by mouse monocytes by a MCP-1 mediated process [133]. In line with that, the recent study of Hibino confirmed the early absence of seeded BMMCs declining to below 1% after two weeks indicating that the bone-marrow does not represent the significant source of EC or SMC that comprise the newly formed vessel. In contrast, the adjacent vessel wall appeared to be the primary source of these cells forming the major part of the neo-tissue. The authors concluded that tissue-engineered constructs functions by mobilizing the body's innate healing capabilities to "regenerate" neo-tissue from pre-existing committed tissue-cells [265]. The mechanism of a BMMC-mediated chemo-attractive process appears to be confirmed in the present study indicating an early and extensive remodeling process primarily characterized by an early monocytic-infiltration that may even be accelerated due to the systemic pressure-loading. Another interesting observation in this study was the fact, that macroscopically the TEHV did not display any sign of thickening or shrinking when compared to the previous reports in sheep [111, 116] or primates [28] that presented with functional, but shortened leaflets limiting an optimal co-aptation area. A potential reason may be reflected in the fact, that this study was the first trial performed in the high-pressure circulation while all other studies have been performed in the low-pressure pulmonary circulation [28, 111, 116]. Although highly speculative, the high-pressure environment may play a key role in this regard and may prevent the TEHV from shrinking and thickening. Consecutive studies will be mandatory to further elucidate the important key-issue of shrinking and to determine the role of pressure in this regard.

Based on this proof-of-concept study demonstrating the principal feasibility of trans-catheter aortic-valve replacement using BMMC-based valves in a one-step procedure, long-term studies are mandatory to further assess the fate and the underlying remodeling mechanisms of such TEHV. Secondly, the role of the seeded BMMCs and the associated multi-factorial, chemo-attractive remodeling process needs to be systematically evaluated to define quality-criteria of tissue-formation representing a key prerequisite for a safe translation into the clinical-setting. Finally, additional effort is needed to improve the stent-design to further minimize the principle problem of paravalvular-leakage and stent-dislocation that is associated with current transcatheter-approaches and as it was also encountered in the present study.

Conclusions

Considering the tremendous clinical potential of a BMMC-based tissue-engineering approach that has already received FDA approval for clinical application in the setting of tissue engineered vascular grafts and is expected to have an even vaster impact with regards to tissue-engineered heart-valves [262], our study provides the first evidence to facilitate this concept for the successful replacement of aortic-valves using a minimally-invasive trans-catheter approach. Its long-term durability proven, and taking into account the so called ``Ten commandments`` of the heart-valve pioneer Dr. D.E. Harken [267] defining an optimal heart-valve prosthesis and thereby characterizing a prosthesis with native valve attributes, such tissue-engineered heart-valves may represent the next generation of heart-valves potentially overcoming some of the limitations of currently used bioprosthetic valves.

Statistical Analysis

Quantitative data are presented as mean±standard-deviation (SPSS 17.0, IBM, Somers/USA).

Chapter 7

General discussion

7.1 Summary of main findings

The concept of regenerative medicine comprising of cell-based therapies, bio engineering technologies and hybrid solutions has been proposed as a potential future approach to address cardiovascular diseases including Coronary Artery Disease (CAD) and Valvular Heart Disease (VHD). However, despite the high potential that was shown in experimental studies, the translation into the clinical routine has either been limited or has been too fast and premature leaving many key aspects unaddressed. The major goal of this thesis was the systematic development of translational, marrow stromal cell-based bio engineering concepts addressing myocardial regeneration in the setting of myocardial infarction (part A) as well as VHD (part B) with a particular focus on minimally invasive, transcatheter-based implantation approaches.

In the setting of myocardial regeneration (part A), at first the intrinsic regenerative potential of the heart was assessed in chapter 2. In this study, it could be demonstrated that $BRCP^+$ cells can be detected within the human heart. They were more abundant than their c-kit^+ counterparts and in the non-ischemic heart they were preferentially located in the atria while following ischemia, their numbers were increased significantly and, most interestingly, the highest change was found in the left ventricle. $BCRP^+$ cells could also be isolated from the human heart adopting certain markers of immature cardiomyocytes *in vitro*, however without the ability of full differentiation into beating cells. It could be shown that there were no c-kit^+/$BCRP^+$ co-expressing stem/progenitor cell populations suggesting that these two markers are expressed by two distinct cell populations in the human heart. Although the data of this analysis provide a detailed insight at cardiac progenitor cells after acute ischemia, the results also indicate that the absolute numbers of cells acquiring a myocardial phenotype are rather low and further effort is required to upscale such cells into clinically relevant numbers.

Thereafter, in chapter 3, it was demonstrated that bone marrow and adipose tissue derived mesenchymal stem cells can be efficiently isolated via minimally invasive procedures as well as cultured and expanded using clinically relevant protocols. Next, a defined quality control protocol for these cells comprising their adherence to plastic, a specific surface marker profile and their ability to differentiate into all three lineages was defined before they were tested in a uniquely developed intrauterine, fetal, preimmune ovine myocardial infarction model. After the successful intrauterine induction of acute myocardial infarction, the cells were intramyocardially delivered and tracked using a multimodal imaging approach comprising MRI, Micro CT as well as in vitro analysis tools such as Flow-Cytometry, PCR and immunohistochemistry. The principal feasibility of intra-myocardial stem-cell delivery after intra-uterine induction of myocardial infarction in the preimmune ovine fetus could be proven suggesting this as a novel platform to assess human cell-fate in a relevant large animal model without the necessity of immunosuppressive therapy.

Using the previously established protocols for the standardized isolation and expansion of adipose tissue derived MSCs, in chapter 4, these cells were up-scaled to clinically relevant numbers before they were processed for the generation of three dimensional microtissues (3D-MTs) in order to improve the integration and survival of transplanted stem cells in the myocardium. After the principal feasibility of ATMSCs based 3D-MT generation was demonstrated, they were transplanted into the healthy and infarcted porcine myocardium using a catheter-based, 3D electromechanical mapping guided approach. Beside the proof-of-principle to combine the in vitro generation of

ATMSCs based 3D-MTs with an intramyocardial, transcathter based transplantation technique, the previously used MRI based tracking concept could be successfully applied and translated into this preclinical model allowing for the in vivo monitoring of transplanted single cells / microtissues for up to five weeks post implantation.

To address Valvular Heart Disease (VHD), in part B, marrow stromal derived cells were used to develop a unique autologous, cell-based engineered heart valve concept comprising of minimally-invasive techniques for both, cell harvest and valve implantation. In chapter 5, the feasibility of generating marrow stromal cell-based, autologous, living tissue engineered heart valves (TEHVs) and the transapical implantation in a one-step intervention in non-human primates was investigated. The results of these experiments demonstrated the principal feasibility of transcatheter, marrow stromal cell based TEHV-implantation into the pulmonary position within the same intervention. While avoiding any need of an in vitro bio-reactor phase, autologous bone marrow-derived mononuclear cells were isolated, seeded on biodegradable scaffolds and integrated into self-expanding nitinol stents, before they were transapically implanted (Chapter 5).

Based on this novel approach and in order to broaden the future clinical application of trans-catheter tissue engineered heart valves, this concept was also successfully applied to the high-pressure system of the systemic circulation (chapter 6). In an initial experiment to assess technical feasibility, the fabricated TEHV using the above mentioned concept were transapically delivered into the descending aorta (distal to the brachiocephalic-trunk) and brachiocephalic-trunk of a sheep. To achieve a sufficient loading, native valve incompetence was created by applying the *Hufnagel* procedure prior to implantation. Post mortem analysis displayed fully intact TEHVs and in particular well defined leaflets showing co-aptation, while there were no signs of pressure damage, leaflet rupture or thrombus formation detectable. Based on these promising results the orthotopic application of this one-step intervention concept was challenged. After further development of the TEHV and stent design according to the anatomic conditions of an orthotopic aortic valve, in a follow-up trial, marrow stromal cell based TEHV were for the first time implanted into the orthotopic position of the high pressure system using an advanced transcatheter delivery system. The implantations were successful and sufficient valve functionality was confirmed using fluoroscopy and trans-esophageal echocardiography. While displaying an efficient opening and closing behaviour with a sufficient co-aptation and a low pressure gradient, there were no signs of coronary occlusion or mal perfusion.

In summery, the results in this thesis represent a promising portfolio of translational concepts for cardiovascular regenerative medicine addressing Coronary Artery Disease (CAD) and Valvular Heart Disease (VHD). They demonstrate 1) that the intrinsic regenerative potential of the heart is low and alternative cell sources are needed 2) that the preimmune fetal sheep represents a unique platform for the in vivo evaluation of human mesenchymal stem cells without the necessity of immunosuppressive therapy in the setting of myocardial infarction 3) that in vitro generated, mesenchymal stem cell based 3D microtissues can be intramyocardially transplanted using a guided, catheter based approach 4) that mesenchymal stem cells can be successfully labeled with MPIOs and tracked within the heart following intramyocardial transplantation 5) that mesenchymal stem cells / marrow stromal derived cells represent a clinically relevant cell source in the setting of myocardial regeneration and heart valve tissue engineering 6) that marrow stromal cell based tissue engineered heart valves (TEHVs) can be generated and transapically implanted into the pulmonary

position within a single intervention 7) that the implantation of marrow stromal cell based tissue engineered heart valves (TEHVs) into the aortic position is principally feasible, but has to be further verified on the long term.

7.2 Discussion and study considerations

Before providing directions for future research, the results, key aspects of the thesis, limitations, and considerations of the present thesis will be discussed below.

7.2.1 Part A Cardiac Cell Therapy

The heart`s intrinsic regenerative potential

In chapter 2, it was elucidated that $BRCP^+/CD31^-$ cells are detected more frequently in the human myocardium when compared to their $c\text{-}kit^+$ counterparts. In the non-ischemic heart they were preferentially located in the atria. Following ischemia, their numbers were increased significantly with highest change in the left ventricle. The number of these $BCRP^+$ cells expressing the cardiac marker titin was also highest in the left ventricle. The localization of $BCRP^+$ cells in non-ischemic atria is in line with previous reports on the special role of the atria for $c\text{-}kit^+$ cells, described as protected niches located in anatomical areas exposed to low levels of wall stress [169], with higher numbers of cardiac progenitor cells produced from right atrial tissue than obtained from other parts of the heart [170]. $BCRP^+$ cells could be isolated from the human heart and adopted certain markers of immature cardiomyocytes *in vitro,* but without full differentiation into beating cells. Additionally, it could be shown that there were no $c\text{-}kit^+/BCRP^+$ co-expressing stem/progenitor cell populations suggesting that these two markers are expressed by two distinct cell populations in the human heart as was already proposed by Anversa et al. for various species [174, 175, 268]. Additionally, the presence of $c\text{-}kit^+$ CRPC could be confirmed in the adult myocardium [158, 173], with higher frequencies (up to fivefold) in ischemic ventricles and much lower numbers in the non-ischemic myocardium. In contrast to several previous reports [16, 157, 158, 166, 167, 174-176], the numbers of $c\text{-}kit^+$ cells found in our study in adult patients were significantly lower, with about 0.004% in the non-ischemic samples and 0.001% in the ischemic samples. Our data are in line with independent reports on frequencies of $c\text{-}kit^+$ cells of about 0.002% in the adult human heart [177]. In general, a comparison of progenitor cell frequencies observed in the human heart is difficult so far. Earlier reports used a variety of units, e.g. $c\text{-}kit^+$ cells per 100 mm^2 [157, 158], c-kit+ cells per cm^3 (x 10^3) [166, 167] (reviewed in [174, 175], there: cells per mm^3) or $c\text{-}kit^+$ cells as percentage of the entire cell population [16]. The latter publication described a frequency of $c\text{-}kit^+$ cells of 1.1 % ± 1.0 % after enzymatic dissociation of about 60 mg myocardial tissue (n=6). Highest numbers of $c\text{-}kit^+$ cells with 8.9% ± 0.4 % were reported for the right atrium of neonatal children < 30d of age [176]. In summary, the data presented in this thesis might provide a valuable snapshot and a further insight at cardiac progenitor cells after acute ischemia. However, the data also indicates that the absolute numbers of cells acquiring a myocardial phenotype are rather low and although phase 1 trials utilizing such cells have already been initiated [5, 67] further effort is needed to upscale such cells into clinically relevant numbers and, more importantly the overall impact on cardiac regeneration has to be investigated in the future.

Mesenchymal Stem Cells as a clinically relevant cell source for myocardial repair

While various stem cell sources are currently under evaluation for their ability to promote cardiac repair [14, 63, 146, 152, 153, 165, 207, 208], mesenchymal stem cells (MSCs) either derived from the bone marrow or the adipose tissue are considered a clinical benchmark cell for cardiac repair [26-28]. In chapter 3 and 4, it was demonstrated that bone marrow and adipose tissue derived mesenchymal stem cells can be efficiently isolated via minimally invasive procedures as well as cultured and expanded using clinically relevant protocols. When compared to other cell types such as cardiac resident progenitor cells (chapter 2) these cells could easily be up-scaled to clinically relevant numbers (chapter 4). The exact definition of a functional mesenchymal stem cell has been repeatedly controversially described in literature. Therefore, in all of the presented studies (chapter 3 and 4) we have defined and established a quality control protocol for these cells comprising their adherence to plastic, a specific surface marker profile (CD90, CD105, CD166, etc.) and their ability to differentiate into all three lineages (adipogenic, chondrogenic and osteogenic differentiation) prior to further processing for cell therapy applications.

Bone-marrow derived MSCs have been repeatedly been used in preclinical animal models [209-213] as well as in clinical pilot trials [7, 29, 183]. Besides their suggested beneficial effects via established, multiple paracrine effects [29] recent reports indicate that bone-marrow MSCs can also be programmed into a cardiac committed stage further increasing their clinical relevance and potential [30]. In parallel to the traditional bone marrow derived MSCs, the data presented in chapter 3 and 4 indicate that the adipose tissue represents an alternative source of MSCs that are comparable to those derived from the bone marrow [214]. Their isolation requires fewer invasive access and in particular, their abundant availability makes them an attractive and clinically highly relevant stem cell source for future therapy concepts [31] that were already introduced into clinical pilot trials (i.e. The APOLLO trial / NCT00442806).

The preimmune fetal sheep as a novel model to study human in vivo cell fate after myocardial infarction

The availability of suitable animal models to assess human stem-cell fate and bio-distribution in-vivo is known to be rather limited. Most available large animal models require immunosuppressive therapy when utilizing human cells [51] compromising the clinical relevance. In order to evaluate human stem-cell fate including bio-distribution, engraftment and survival in the absence of any xenogenic immune response a surrogate animal model is mandatory. Therefore, the pre-immune fetal sheep, being preimmune until the 75 day of gestation, has been repeatedly suggested as a valuable tool, but has so far primarily been used in the field of experimental haematology to assess in-vivo cell-fate and bio-distribution after ultrasound-guided, intra-peritoneal stem cell delivery [53, 194-197, 202]. Based on these data, in chapter 3 we introduced the novel concept of direct, intrauterine intramyocardial stem-cell transplantation after myocardial infarction into the preimmune ovine fetus offering a novel platform to assess human cell-fate in a relevant large animal-model without the necessity of immunosuppressive therapy. Our results showed that after intramyocardial transplantation, the human cells were detected within the ventricular-wall corresponding to the injection-sites. The cells were found to be distributed within the intra-peritoneal cavity involving the liver and kidneys, but not within the heart after intra-peritoneal injection. Our novel fetal intramyocardial transplantation model appears to be more appropriate in

the setting of cardiovascular stem cell therapy concepts and offers a significant improvement with regards to myocardial cell retention and integration. Since the overall aim of this proof-of-concept study was to establish a novel model of intra-uterine induction of MI and direct intra-myocardial stem cell transplantation in a technically challenging and very delicate fetal environment, the number of animals was low and the follow-up time was relatively short requiring further studies with an increased number of animals and a longer follow-up. Besides the infarction histology, a functional assessment (i.e. with echo) of the fetal heart after myocardial infarction would be desirable and has to be pursued in subsequent studies in order to assess the regenerative potential on the myocardium for specific cell types.

Three dimensional microtissues as an alternative format for advanced cell therapy concepts

In chapter 4, we introduced a novel concept of a catheter-based, 3D NOGA mapping guided intramyocardial transplantation of in-vitro engineered adipose tissue derived mesenchymal stem cell (ATMSC) based 3D microtissues (3D-MTs). The results of this study showed the principal feasibility that ATMSCs based 3D-MTs can be engineered successfully in vitro within 72 hours and can then be safely transplanted into the healthy and infarcted porcine myocardium using a catheter-based 3D NOGA mapping guided technique. An optimal application format along with an efficient delivery technique is necessary to improve intramyocardial retention, survival and engraftment of transplanted stem cells, thus enhancing the therapeutic effect of current therapy concepts [215]. In contrast to currently applied single cell suspension strategies that are well known to be associated with high washout phenomena and low survival rates [218], the idea of cellular self-assembly into 3D microtissues prior to transplantation may represent an interesting alternative to overcome these limitations. Previous studies have for one demonstrated that 3D MTs can be successfully generated from different cell sources [40-45, 219-221] and secondly indicated their potential beneficial effects comprising continuous production of extracellular matrix, the production of pro-angiogenic factors as well as the secretion of anti-inflammatory proteins increasing their therapeutic potential in the diseased myocardium [41-45, 219-221]. In this study microtissues were produced utilizing ATMSCs which are established as a clinically relevant cell source. However, to assess the therapeutic potential of microtissues with regards to enhanced retention and functional improvement of the myocardium further studies are mandatory. So, to further increase the therapeutic potential of the microtissues the combination of cell types [209, 226] within the microtissue or even the addition of therapeutic drugs such as statins [269] may increase therapeutic effects and should be considered in subsequent studies.

Multimodal MRI based imaging concept as an effective approach to track stem cells / microtissues after intramyocardial transplantation

An effective, clinically relevant multimodal cell imaging concept was introduced comprising MRI, Micro CT and immunohistochemistry utilizing micron-sized, Dragon-green fluorochrome labelled iron-oxide particles (MPIO). The efficacy of this concept was initially demonstrated in the fetal sheep (chapter 3) and was then translated into a preclinical setting using the porcine model (chapter 4). The results of these studies indicated that these MPIOs that had been primarily used in the field of liver research [50, 200, 201] can be sufficiently used to track mesenchymal stem cells (as single cells

or as microtissues) within the ovine and porcine myocardium. The data from the porcine experiments (chapter 4) indicated that this imaging concept is applicable in the large animal and can be used as an effective in vivo monitoring tool.
In general, state of the art imaging modalities to track stem cells with regards to survival, engraftment and differentiation are mandatory to explain beneficial effects of cell-based therapy strategies [47, 203]. While numerous imaging concepts and hybrid approaches are currently investigation, the utilization super-paramagnetic agents (MPIOs) to track stem cells on MRI has been suggested a useful tool for the preclinical and clinical setting [47]. The advantage of MRI is that in provides both, a detailed functional analysis as well as MPIO enabled cell tracking.
To the contrary, the fact that the imaging signal is not directly linked to cell-viability has been reported as a shortcoming as this may result in the inability to discriminate between vital, labelled cells and particle-loaded cell-debris as well as hosting macrophages that may have actively phagocytised the particles after cell-death [203]. However, limitation can be successfully reduced when using state-of-the-art MPIOs that are co-labeled with fluorochrome dye. In our studies, we were able to confirm the MRI findings and to proof the presence of the transplanted cells / microtissues within the ovine and porcine myocardium by the utilization of specific antibodies either against human cells or the fluorochrome co-labeled MPIOs or both. This clearly indicates the efficacy of this approach suggesting the MRI to be a valuable imaging tool to comprise both, efficacy evaluation and the opportunity for cell-tracking.

7.2.2 Part B Heart Valve Tissue Engineering

The BMMC based in situ approach and underlying mechanisms

In this thesis, we used a marrow stromal cell derived approach to generate autologous, living TEHVs for the low and high pressure circulation (chapter 5 and 6). The underlying molecular mechanism of autologous BMMC-based tissue remodeling appears to be multifaceted, complex and remains to be elucidated. Recent studies have suggested a multi-factorial, BMMC-mediated chemo-attractive process [28, 90, 133, 265, 266] which seems to involve numerous endogenous cell types such as monocytes as well as specific mediator cytokines that control the different steps of remodeling and tissue-formation [28, 90, 133, 265, 266]. *Shin´oka* and colleagues were the first to use the BMMC based approach in the setting of tissue-engineered vascular grafts (TEVG). Next, Roh et al recently suggested that seeded BMMCs appear to release significant amounts of monocyte chemo-attractant protein- 1 (MCP-1) leading to an enhanced recruitment of monocytes. Another important result of this study was the rapid replacement of the seeded BMMCs within a few days after implantation suggesting that the scaffolds were instantly repopulated by murine monocytes driven by a MCP-1 mediated process [133]. Similar phenomena could be detected in our BMMC based TEHV that were implanted into primates (chapter 5). Strikingly, the initially labeled BMMCs could not be detected four weeks after implantation. A distinct remodeling process was observed, characterized by a monocytic infiltration of the leaflets as well as the conduit wall. Similarly, in the experiments performed in the aortic position (chapter 6) an early remodeling process that was primarily driven by an early monocytic-infiltration could be observed which might have even been accelerated due to the systemic pressure-loading. In all cases the initial cell seeding was done on a porous synthetic biodegradable starter matrix that was implanted shortly after cell seeding. The recent study of Hibino confirmed the early absence of seeded BMMCs which declined to below 1% after two weeks

indicating that the bone-marrow does not represent the significant source of EC or SMC that form the new vessel. In contrast, the adjacent vessel wall appeared to be the primary origin of these cells forming the major part of the neo-tissue. The authors concluded that tissue-engineered constructs function by mobilizing the body's innate healing capabilities to "regenerate" neo-tissue from pre-existing committed tissue-cells [270]. Although the understanding of the seeded BMMCs and the associated multi-factorial, chemo-attractive remodeling process needs further evaluation, the growing body of rapid cell replacement based on BMMC mediated paracrine pathways is of high interest and may open new options for future tissue engineering strategies.

The impact of systemic pressure loading on TEHVs

Our preliminary study (chapter 6) highlighted that TEHV did fully accept the systemic-pressure. In response, the detection of an early and rapid cellularization was indicative for an active and instant tissue formation and remodeling process based on the BMMC mediated approach. It has previously been described that hemodynamic loading appears to play a major role in tissue remodeling and formation [117]. The histological findings of this study are in line with the interesting observation in the baboon study (chapter 5) which highlighted the importance of sufficient loading on functional tissue remodeling. In contrast to the orthotopically delivered TEHVs (n=5) which completely excluded the native leaflets, the one TEHV which was implanted into the supra-valvular position did not fully exclude the native leaflets. Thus, not being fully loaded, this TEHV lacked any leaflet structure being indicative for the absence of tissue formation and remodeling processes [26]. The other, orthotopically implanted TEHVs macroscopically did not show any signs of retraction when compared to the baboon study (chapter 5) or previously reported data on sheep [111, 116] that were all associated with shortened leaflets limiting the co-aptation area. Leaflet shortening leading to valve incompetence and regurgitation is a known problem of autologous living TEHVs [28, 90, 111] which was described regardless of implantation mode (surgically versus transapical) [271] or the selection of starter matrices. Leaflet shortening has been observed when using PGA/P4HB [111] PGA-PLLA scaffolds in combination with bone marrow derived stem cells as well as when applying fibrin as starter matrix that was seeded with vascular derived cells [256]. Despite being highly speculative since this was a proof-of-concept study with only a short term follow up, it could be speculated that the high-pressure loading may play a key role and may prevent the TEHV from leaflet retraction. Consecutive studies will be necessary to assess this in more detail. A recent report suggested that leaflet retraction and shortening is cell-induced [272]. To overcome the problem of leaflet retraction from a technical point of view, a certain stent oversizing that is associated with an incomplete opening. This may lead to a maintained co-aptation area even after the process of retraction could be of interest.

Animal Models

In this thesis, the feasibility and functionality of marrow stromal cell derived TEHVs was investigated in baboons (chapter 5) and sheep (chapter 6) addressing the low and high pressure circulation. The primate model appears to represent an ideal preclinical model due to its high comparability to humans with regards to anatomy and (patho-) physiology. Therefore, as a final step prior to clinical translation of TEHVs the assessment of TEHVs in a human-like cardiovascular environment would be highly beneficial. For example, the in situ remodeling in primates (chapter 5) differed significantly from previous data reported for sheep with regards to leaflet thickening [111] further highlighting

the high potential of this animal model. In addition, several recent global expression studies of the heart and the lung have demonstrated gene expression levels to be almost identical in these organs for humans and non-human primates [273, 274]. However, its availability for large number investigations is limited and in particular ethical concernsfor this model may remain. The sheep in comparison is the most often used animal model to assess cardiovascular implants. Due to its high calcium metabolism the sheep is well established as an excellent predictor of the durability and performance of biological heart valves (``worst case model``) with regards to progressive degeneration and calcification [275]. However, as it applies for most animal models it remains unclear to what extent the results can be directly translated and extrapolated into the human setting. The sheep model failed to predict the fatal failure of non-seeded decellularized xenografts implanted into children [276] which was assumed to be primarily linked to the remnants of xenogenic cells and the more robust immune response of the treated children. To overcome this crucial problem, the use of autologous cells as presented in this thesis (chapter 5 and 6) or at least utilization of allogenic cells could be pursued in future therapy concepts.

The need for improved stent designs and delivery systems

The advantage of transapical implantation concepts is the minimally invasiveness when compared to traditional surgical approaches requiring median sternotomy. Although transapical technique is more invasive than the percutaneous approach via the femoral artery, the delivery device offers a larger crimping diameter which is a key issue when crimping TEHV as the leaflets are still a bit thicker than their native counterparts. We have recently demonstrated for the first time the technical feasibility of combining the concept of HVTE and trans-apical delivery into the pulmonary-position of adult sheep and baboons [28, 111]. However, as shown in this thesis, when addressing the orthotopic aortic position the known problem of paravalvular-leakage was encountered which was primarily related to the stent design and not the THEV itself. Although this is a known problem also from commercially available stented heart valves, importantly increasing evidence associates more-than-mild paravalvular leakage with increased mortality and recent clinical data indicate that postprocedural paravalvular aortic regurgitation ≥ 2+ mainly impact late outcomes between 30 days and 1 year. Therefore, precise evaluation of paravalvular leakage after TAVI is absolutely essential [277-279] and an additional effort should be made to improve the stent-design of currently available prostheses to further minimize this crucial problem.

Simplifying Logistics

A clinically relevant concept for heart valve tissue engineering comprises as minimally-invasive techniques as possible for both, cell isolation and valve implantation. Various tissue engineering approaches and cell sources are currently under evaluation for their clinical relevance. So far, most of these concepts necessitate extensive technical, logistical and financial efforts limiting their broad translation into the clinical routine. Thus, more simplicity is crucial. *Shin´oka* and colleagues were the first to describe the technique to generate tissue-engineered vascular grafts (TEVG) by the utilization of bone marrow-derived mononuclear cells (BMMCs) without any period cell culture or bio-reactor phase and by using biodegradable polyester based tubes that were seeded with autologous cells. Such TEVGs displayed in vivo functionality and appeared to transform into living vascular grafts [97, 133, 238, 239, 263]. Based on these techniques that are also currently entering the clinical-arena in the United States following recent FDA approval [262], this concept (chapter 5 and 6) was translated into the setting of heart valve tissue engineering to successfully generate and

transapically implant autologous BMMC-derived TEHVs in a one-step intervention into the pulmonary and aortic position of baboons and adult sheep. Considering the significant simplification with regards to technical, logistical and economic aspects such concepts may represent a promising next generation concept of high clinical relevance.

7.3 Next steps, challenges and future outlook

7.3.1 Part A Cardiac Cell Therapy

While numerous experimental and preclinical studies, utilizing a huge range of various stem cell types and progenitor cells, have shown promising data [51], the results of initiated clinical trials have only shown marginal effects and revealed only a limited effect with regards to the improvement of cardiac performance. Current meta-analyses summarize a mean of only 3% improvement of heart function. In fact, the optimal utilization and exploitation of the stem cells and their precise role in cardiovascular regeneration is not well understood. The rapid translation into clinical studies has left many questions unanswered, in particular with regards to the crucial aspect of the so called ``stem cell fate`` which is important for explaining a beneficial effect. The optimal cell type, the number of cells to be delivered, the optimal format (i.e. microtissues, hydrogels or synthetic carrier matrices), the most suitable route for cell delivery, and the optimal time point for cell delivery after myocardial infarction are still unknown and discussed controversially. The bio-distribution of the therapeutic cells after delivery and in particular the specific mechanism by which therapeutic cells contribute to functional improvement, including cell retention, engraftment and survival remain to be investigated. The development of surrogate animal models and advanced, non-invasive imaging techniques to monitor the effect of cell therapy are mandatory for the assessment of cell based-therapies and represent the key requisite for a safe translation into the clinical setting. A clear definition of endpoints is also necessary in the clinical setting in order to assess the true efficacy of a certain cell based concept. In the past the improvement of ejection fraction has always been suggested as a primary endpoint, more recent studies also propose the reduction of scar size, wall thickness as well as remodeling aspects as valuable markers to assess the efficacy of cell therapy.

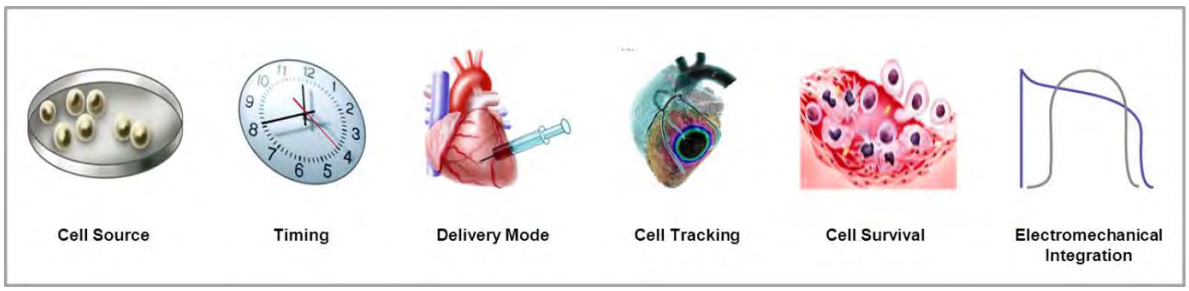

Figure 5: Future Goals in Cardiac Stem Cell Therapy

The future goals in translational cardiac stem cell research include the definition of the optimal cell source, the timing of application, the delivery format and route as well as efficient cell tracking strategies. Crucial aspects to be addressed in the future are cell survival and electromechanical integration into the hosting myocardium (Emmert and Templin, Praxis Bern 2013).

In addition, the optimal selection of cell type in accordance to the treated patient *(``which cell for which patient in which clinical setting?``)* may have an important aspect on the outcome. In this regard, recent data indicate the significant difference in cell quality and regenerative potential when comparing cells derived from patients with coronary heart disease or diabetes versus cells isolated from healthy donors [280-282]. Finally, the amount of cells that are applied has to be considered carefully as in the experimental setting significantly more cells per bodyweight were used than in clinical studies. When using 1 x 10^7 $CD34^+$ cells/25gr in a small animal model, a 80kg patient would require a dosage of at least 32 x 10^9 $CD34^+$ cells which equals an increase of factor ~3000 of currently used cell doses in the clinical setting [283, 284]. Despite the manifold of generated data, the most important questions in cardiac stem cell therapy are not answered yet. The long term success of cell therapy will only be achieved by better understanding the mechanisms driving the repair and regeneration within the heart. The disparate studies and clinical trials will not bring us any further as only a systematic evaluation of the early and late stem cell fate in the same experimental setting will help to define the optimal cell-based technology for enhanced cardiac regeneration.

In the future, current cell based therapy concepts need further optimization in terms of cell selection and efficacy. The concept of pre-differentiation / pre-programming as well as epigenetic modeling prior to transplantation could further enhance their therapeutic potential. Recent reports identified several microRNAs as potent regulators for stem cell differentiation [285-287] and could be of high interest for future concepts. The investigation of patient- and disease specific cell quality (i.e. aged patients, diabetic patients, patients with acute myocardial infarction, etc.) could also provide further insight into the functionality and the efficacy of stem cells and, importantly elucidate the mixed outcomes of the available clinical trials. Furthermore, the utilization of induced pluripotent cells (IPCs) [288, 289] with their ability to provide ``real`` myocardial regeneration by differentiation into cardiomyocytes could be an effective approach if the major drawbacks comprising of safety issues and the feasibility of up-scaling to sufficient numbers can be solved [290]. Further research is needed with regards to an improved homing to the myocardium after cell transplantation. Recent studies have indicated that the efficacy and homing of cardiac progenitor cells (CPCs) can be significantly enhanced if they are transplanted together with mesenchymal stem cells [291]. As presented in this thesis introducing the microtissue technology for intramyocardial transplantation, also the development and in vivo testing of alternative ``cell carriers`` such as scaffolds or gel-based applications will be necessary to further address the crucial aspect of cellular retention. The concept of direct reprogramming of fibroblasts into cardiomyocytes was recently reported [292, 293] and represents a promising approach to transform infarcted tissue into functional myocardium [294] Although the proof of principle of this concept was recently demonstrated in a murine animal model, [295] extensive further research will be necessary before such approaches can be translated into a preclinical, or even clinical setting.

7.3.2 Part B Heart Valve Tissue Engineering

More than 50 years ago, Dr. D.E. Harken, a pioneer in the field of heart valve surgery, was the first who successfully implanted a heart valve into the sub-coronary, aortic position in a patient suffering from severe aortic stenosis [296]. After this breakthrough in the field of heart valve diseases, the evolution of heart valve prostheses has undergone rapid changes and made significant advances over the past decades. While the initial valve prostheses were fabricated from mechanical components based on concept models derived from the aviation industry, the field has changed stepwise into the direction of biological prostheses. Simultaneously, even though the conventional surgical technique of heart valve replacement has served as a very safe and reliable method for many years, the valve replacement techniques have continuously changed into the direction of minimally invasive, transcatheter-based approaches.

After Dr. D.E. Harken was the first who successfully implanted a heart valve into the subcoronary, aortic position in a patient suffering from severe aortic stenosis in 1960, the evolution heart valve prostheses has undergone rapid changes and made significant advances over the past decades. The valve replacement techniques have also continuously changed into the direction of minimally invasive, transcatheter-based approaches. The concept of heart valve tissue engineering offering the potential of growth and remodeling, may represent an ideal, next generation therapy concept for trans-catheter heart valve replacements.

Despite these tremendous advances over the past fifty years with regards to the refinement of heart valve prostheses and the surgical technologies for implantation, major issues have remained unsolved. Although current available prostheses demonstrate excellent structural durability [70, 76-78], the currently available bio-prostheses for minimally invasive, transcatheter-based procedures are still inherently prone to progressive degeneration and calcification requiring redo surgery within 10-15 years after implantation and therefore suggesting their clinical indication primarily in the elderly, high-risk patients [87]. The lack of growth capacity as well as in vivo repair and remodeling properties remain key issues with particular regards to congenital applications.

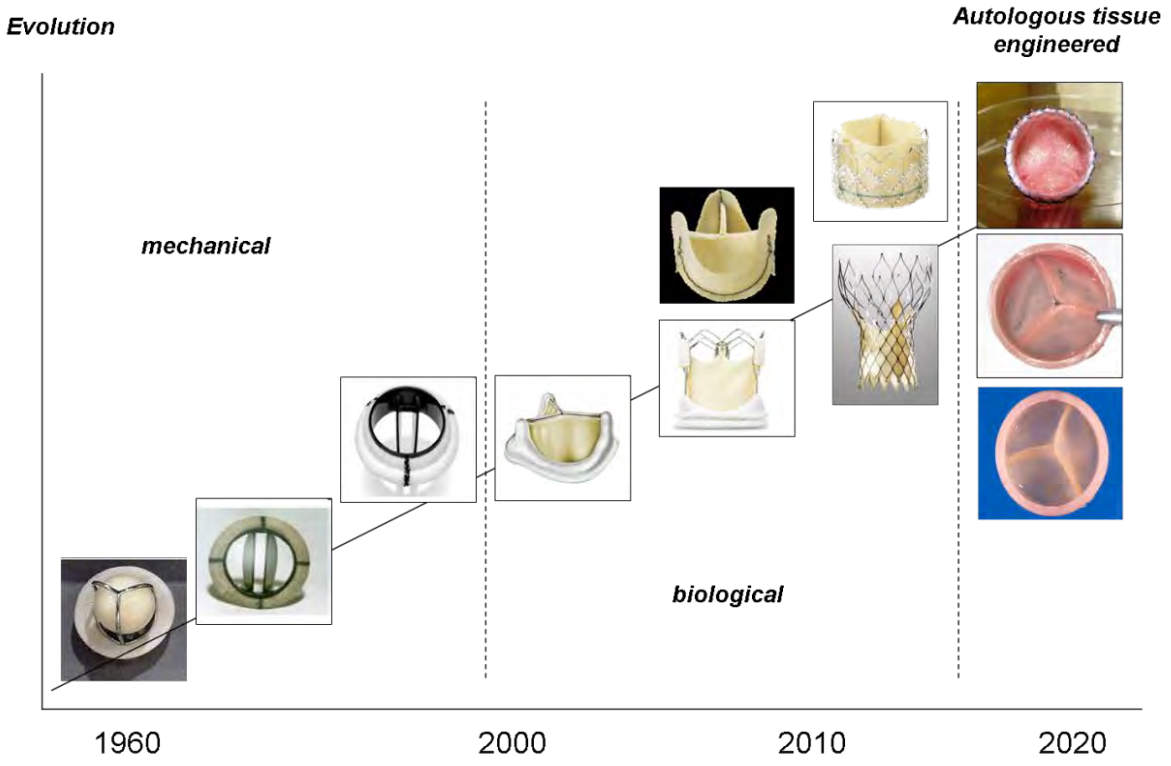

Figure 6: The Evolution of Heart Valve Prostheses

The evolution of heart valve prostheses started more than fifty years ago with the development of mechanical prostheses. This was followed by the development of biological heart valve prostheses which were then late combined with transcatheter, stent based technologies. The concept of living, autologous tissue engineered heart valves may represent a next generation heart valve technology with remodelling and growth capacities.

After Dr. D.E. Harken was the first who successfully implanted a heart valve into the subcoronary, aortic position in a patient suffering from severe aortic stenosis in 1960, the evolution heart valve prostheses has undergone rapid changes and made significant advances over the past decades. The valve replacement techniques have also continuously changed into the direction of minimally invasive, transcatheter-based approaches. The concept of heart valve tissue engineering offering the potential of growth and remodeling, may represent an ideal, next generation therapy concept for trans-catheter heart valve replacements.

Despite these tremendous advances over the past fifty years with regards to the refinement of heart valve prostheses and the surgical technologies for implantation, major issues have remained unsolved. Although current available prostheses demonstrate excellent structural durability [70, 76-78], the currently available bio-prostheses for minimally invasive, transcatheter-based procedures are still inherently prone to progressive degeneration and calcification requiring redo surgery within 10-15 years after implantation and therefore suggesting their clinical indication primarily in the elderly, high-risk patients [87]. The lack of growth capacity as well as in vivo repair and remodeling properties remain key issues with particular regards to congenital applications.

These limitations clearly indicate that the ideal approach needs to be developed [75]. Interestingly, it was also Dr. D.E. Harken, who already defined in the 1950s the essential characteristics of the

ideal valve prosthesis. In his so-called `Ten Commandments` [267], the pioneer Harken summarized the major aspects of the ideal heart valve construct, including durability, absence of thrombogenicity, resistance to infections, lack of antigenicity, and the potential of growth, thereby stating the key characteristics of natural, living heart valves [267].

To overcome these limitations, the concept of heart valve tissue engineering has been suggested as a promising approach and has created substantial hope as well as expectations. Despite of its huge potential to significantly improve the therapy of valvular heart disease and despite all enthusiasm, several key steps have to be accomplished before the standardized implementation of heart valve tissue engineering into the clinical arena will be possible.

Besides the principal demonstration of the long-term safety and efficacy of an implanted construct to prevent from catastrophic failure, pre-clinical guidelines defining how to characterize the safety, efficacy, and quality of a tissue engineered construct need to be established [94]. Future research directions (summarized in table 2) should focus on the fundamental understanding of underlying remodeling and repair mechanisms including a better knowledge of the biochemical and immunological characteristics of the cells and tissues undergoing in vitro growth. The disposition of implanted structures to typical biomaterial tissue interactions of medical devices, such as calcification, thrombosis and excessive inflammatory response have to be elucidated [90].

Novel concepts with regards to starter matrices such as the utilization of decellularized in-vitro grown TEHVs that are reseeded with autologous cells [297] prior to transapical implantation could be an interesting concept for the future as on the one hand it would avoid the established risks of immunogenic reaction and disease transmission, and on the other hand it would significantly simplify current concepts considering that such valves could be generated of the shelf [297]. Recent in vivo studies in the ovine model have demonstrated that this concept is feasible in the setting of transapical valve implantation for up to six months (Driessen-Mol et al., unpublished data).

Another key consideration is the important aspect that currently available valve prostheses reveal a certain, predictable behaviour with regards to durability and biocompatibility; while tissue engineered constructs, potentially relying on in vivo remodeling, may show substantial variability among different patients due to the heterogeneity of the physiological tissue remodeling potential. For this reason, the development of sufficient clinical guidelines defining the inclusion criteria for specific patient cohorts with regards to safety, efficacy and quality of the engineered constructs is mandatory [90]. Therefore, the identification of biomarkers as independent predictors as well as conventional or innovative imaging modalities may represent useful and important tools to assess the success, but also the failure of an implanted construct.

From the logistical point of view when considering initial clinical trials (pilot study), laboratory processes and logistics need to be adapted in accordance with the good manufacturing practice (GMP) guidelines providing a maximum degree of process control and bio-safety. In the context of a classical tissue engineering approach, an exemplary algorithm would comprise the following steps: (a) isolation of autologous cells from designated sources (i.e. by a bone marrow puncture or adipose tissue aspiration under local anesthesia), (b) differentiation and expansion of cells and engineering of a heart valve prostheses in vitro; and (c) following defined quality criteria (biological, histological, bio-safety), re-implantation of living autologous valve replacements into patients after a defined time period of a maximum of six to eight weeks [90].

Challenges	Research Directions
TEHV components and their interactions are complex, heterogeneous and dynamic	Define cell / scaffold / bioreactor combinations that optimize construct composition and properties (in vitro)
Correlation of in vitro generated TEHV structure and properties with in vivo outcomes has not been demonstrated	Determine and validate correlations between in vitro conditions, elements, structure, properties and in vivo function
Quality control of construct structure and function is likely to be difficult	Develop guidelines and assessment tools for the pre-implantation characterization of TEHV structure, function and quality
Animal models may not reliably predict human outcomes	Develop and validate animal models that will test key biological processes and correlate with human outcomes
TEHV structure is likely to be evolving in vivo and ongoing function may be less predictable than with conventional valve replacement technology	Develop guidelines, tools and metrics for the in vivo characterization of dynamic TEHV structure, function and quality
TEHV function will depend upon patient response to implantation and integration with the recipient's tissues more than with conventional valve replacement, and individual patient responses may be highly variable	Identify/validate biomarkers both predictive of and assess patient variability in implant success/failure and capable of non-invasive in vivo monitoring and potential control
Remodeling processes after implantation may release or change seeded cells and recruit host cells;	Develop tools to monitor the fate of transplanted and endogenous cells (location, function, viability, phenotype)
Patient-specific co-morbidities may have significant impact on in vivo remodelling processes	Adequate patient selection (inclusion and exclusion criteria) is mandatory to prevent from fatal failure
Regulatory processes and approaches are not yet well established	Create suitable regulatory approaches to engineered tissue valves that will ensure safety and efficacy

Table 2: Key steps and future research challenges for the clinical translation of Heart Valve Tissue Engineering *(adapted from Schoen, Review; Current Opinion in Biotechnology, 2011)*

Conclusion and clinical relevance

In this thesis a multifaceted portfolio of translational, clinically relevant multi-potent stromal cell based concepts is introduced for both, myocardial regeneration and Valvular Heart Disease.

In particular, the results in this thesis demonstrate the important key role and high clinical relevance of marrow stromal derived cells for cardiovascular regenerative medicine. Due to their abundant availability, simple isolation protocols, and importantly their clinical safety, these cells can be used for multiple purposes comprising myocardial cell therapy as well as heart valve tissue engineering.

In the setting of myocardial regeneration (part A) and with a particular focus on clinical relevance, this thesis introduces interesting concepts targeting the current challenges of myocardial cell therapy comprising of the development of advanced cell application formats (3D microtissues) that can be intramyocardially delivered, a novel animal model that allows for the in vivo evaluation of human stem cells without the necessity of immunosuppressive therapy in the setting of myocardial infarction, optimized imaging strategies for in vivo cell tracking by using fluorochrome labeled, micro-sized iron oxide particles (MPIOs) as well as transcatheter, electromechanical mapping guided transplantation technologies in order to improve and to further develop current therapy strategies.

With regards to Valvular Heart Disease (part B) the results of this thesis provide systematic evidence of the development of clinically relevant tissue engineered heart valve concepts by combining the use of marrow stromal cells, *state-of-the-art* tissue engineering protocols and minimally invasive, transcatheter based valve implantation techniques. In preclinical pilot studies it could be demonstrated that marrow stromal cell based tissue engineered heart valves (TEHVs) can be generated and transapically implanted into the pulmonary and aortic position within a one-step intervention. In particular, the avoidance of any expensive and logistically demanding in vitro or bio-reactor process may represent a significantly optimized and simplified approach towards clinical application. Its long-term feasibility proven this novel concept may represent the next generation of transcatheter heart valves overcoming the limitations of the currently used prostheses and may be rapidly translated into a clinical setting.

References

1. Olson EN. (2004) A decade of discoveries in cardiac biology. Nat Med 10: 467-474.
2. Strauer BE, Brehm M, Zeus T, Gattermann N, Hernandez A, et al. (2001) [Intracoronary, human autologous stem cell transplantation for myocardial regeneration following myocardial infarction]. Dtsch Med Wochenschr 126: 932-938.
3. Strauer BE, Steinhoff G. (2011) 10 years of intracoronary and intramyocardial bone marrow stem cell therapy of the heart: from the methodological origin to clinical practice. J Am Coll Cardiol 58: 1095-1104.
4. Assmus B, Honold J, Schachinger V, Britten MB, Fischer-Rasokat U, et al. (2006) Transcoronary transplantation of progenitor cells after myocardial infarction. N Engl J Med 355: 1222-1232.
5. Bolli R, Chugh AR, D'Amario D, Loughran JH, Stoddard MF, et al. (2011) Cardiac stem cells in patients with ischaemic cardiomyopathy (SCIPIO): initial results of a randomised phase 1 trial. Lancet 378: 1847-1857.
6. Schachinger V, Erbs S, Elsasser A, Haberbosch W, Hambrecht R, et al. (2006) Intracoronary bone marrow-derived progenitor cells in acute myocardial infarction. N Engl J Med 355: 1210-1221.
7. Williams AR, Trachtenberg B, Velazquez DL, McNiece I, Altman P, et al. (2011) Intramyocardial stem cell injection in patients with ischemic cardiomyopathy: functional recovery and reverse remodeling. Circ Res 108: 792-796.
8. Segers VF, Lee RT. (2008) Stem-cell therapy for cardiac disease. Nature 451: 937-942.
9. Wei F, Wang T, Liu J, Du Y, Ma A. (2011) The subpopulation of mesenchymal stem cells that differentiate toward cardiomyocytes is cardiac progenitor cells. Exp Cell Res
10. Menasche P. (2008) Skeletal myoblasts and cardiac repair. J Mol Cell Cardiol 45: 545-553.
11. Roell W, Lewalter T, Sasse P, Tallini YN, Choi BR, et al. (2007) Engraftment of connexin 43-expressing cells prevents post-infarct arrhythmia. Nature 450: 819-824.
12. Laflamme MA, Gold J, Xu C, Hassanipour M, Rosler E, et al. (2005) Formation of human myocardium in the rat heart from human embryonic stem cells. Am J Pathol 167: 663-671.
13. Cleland JGF, Coletta AP, Abdellah AT, Nasir M, Hobson N, et al. (2007) Clinical trials update from the American Heart Association 2006: OAT, SALT 1 and 2, MAGIC, ABCD, PABA-CHF, IMPROVE-CHF, and percutaneous mitral annuloplasty. European Journal of Heart Failure 9: 92-97.
14. Messina E, De Angelis L, Frati G, Morrone S, Chimenti S, et al. (2004) Isolation and expansion of adult cardiac stem cells from human and murine heart. Circ Res 95: 911-921.
15. Laugwitz KL, Moretti A, Lam J, Gruber P, Chen Y, et al. (2005) Postnatal isl1+ cardioblasts enter fully differentiated cardiomyocyte lineages. Nature 433: 647-653.
16. Bearzi C, Rota M, Hosoda T, Tillmanns J, Nascimbene A, et al. (2007) Human cardiac stem cells. Proc Natl Acad Sci U S A
17. Emmert MY, Emmert LS, Martens A, Ismail I, Schmidt-Richter I, et al. (2012) Higher frequencies of BCRP+ cardiac resident cells in ischaemic human myocardium. Eur Heart J
18. Flynn A, O'Brien T. (2011) Stem cell therapy for cardiac disease. Expert Opin Biol Ther 11: 177-187.
19. Laflamme MA, Chen KY, Naumova AV, Muskheli V, Fugate JA, et al. (2007) Cardiomyocytes derived from human embryonic stem cells in pro-survival factors enhance function of infarcted rat hearts. Nat Biotechnol 25: 1015-1024.
20. Yang Y, Min JY, Rana JS, Ke Q, Cai J, et al. (2002) VEGF enhances functional improvement of postinfarcted hearts by transplantation of ESC-differentiated cells. J Appl Physiol 93: 1140-1151.
21. Nakagawa M, Koyanagi M, Tanabe K, Takahashi K, Ichisaka T, et al. (2008) Generation of induced pluripotent stem cells without Myc from mouse and human fibroblasts. Nat Biotechnol 26: 101-106.
22. Park IH, Zhao R, West JA, Yabuuchi A, Huo H, et al. (2008) Reprogramming of human somatic cells to pluripotency with defined factors. Nature 451: 141-146.
23. Yamanaka S. (2008) Induction of pluripotent stem cells from mouse fibroblasts by four transcription factors. Cell Prolif 41 Suppl 1: 51-56.
24. Yu J, Vodyanik MA, Smuga-Otto K, Antosiewicz-Bourget J, Frane JL, et al. (2007) Induced pluripotent stem cell lines derived from human somatic cells. Science 318: 1917-1920.
25. Singla DK, Long X, Glass C, Singla RD, Yan B. (2011) Induced Pluripotent Stem (iPS) Cells Repair and Regenerate Infarcted Myocardium. Mol Pharm
26. Emmert MY, Weber B, Behr L, Frauenfelder T, Brokopp CE, et al. (2011) Transapical aortic implantation of autologous marrow stromal cell-based tissue-engineered heart valves: first experiences in the systemic circulation. JACC Cardiovasc Interv 4: 822-823.
27. Emmert MY, Weber B, Wolint P, Behr L, Sammut S, et al. (2012) Stem Cell Based Transcatheter Aortic Valve Implantation: First Experiences in a preclinical model. JACC Cardiovasc Interv
28. Weber B, Scherman J, Emmert MY, Gruenenfelder J, Verbeek R, et al. (2011) Injectable living marrow stromal cell-based autologous tissue engineered heart valves: first experiences with a one-step intervention in primates. Eur Heart J
29. Williams AR, Hare JM. (2011) Mesenchymal stem cells: biology, pathophysiology, translational findings, and therapeutic implications for cardiac disease. Circ Res 109: 923-940.

30. Behfar A, Yamada S, Crespo-Diaz R, Nesbitt JJ, Rowe LA, et al. (2010) Guided cardiopoiesis enhances therapeutic benefit of bone marrow human mesenchymal stem cells in chronic myocardial infarction. J Am Coll Cardiol 56: 721-734.
31. Valina C, Pinkernell K, Song YH, Bai X, Sadat S, et al. (2007) Intracoronary administration of autologous adipose tissue-derived stem cells improves left ventricular function, perfusion, and remodelling after acute myocardial infarction. Eur Heart J 28: 2667-2677.
32. Barbash IM, Chouraqui P, Baron J, Feinberg MS, Etzion S, et al. (2003) Systemic delivery of bone marrow-derived mesenchymal stem cells to the infarcted myocardium: feasibility, cell migration, and body distribution. Circulation 108: 863-868.
33. Strauer BE, Brehm M, Zeus T, Kostering M, Hernandez A, et al. (2002) Repair of infarcted myocardium by autologous intracoronary mononuclear bone marrow cell transplantation in humans. Circulation 106: 1913-1918.
34. Sherman W, Martens TP, Viles-Gonzalez JF, Siminiak T. (2006) Catheter-based delivery of cells to the heart. Nat Clin Pract Cardiovasc Med 3 Suppl 1: S57-64.
35. Gyongyosi M, Dib N. Diagnostic and prognostic value of 3D NOGA mapping in ischemic heart disease. Nat Rev Cardiol 8: 393-404.
36. Perin EC, Lopez J. (2006) Methods of stem cell delivery in cardiac diseases. Nat Clin Pract Cardiovasc Med 3 Suppl 1: S110-113.
37. Thompson CA, Nasseri BA, Makower J, Houser S, McGarry M, et al. (2003) Percutaneous transvenous cellular cardiomyoplasty. A novel nonsurgical approach for myocardial cell transplantation. J Am Coll Cardiol 41: 1964-1971.
38. Price MJ, Chou CC, Frantzen M, Miyamoto T, Kar S, et al. (2006) Intravenous mesenchymal stem cell therapy early after reperfused acute myocardial infarction improves left ventricular function and alters electrophysiologic properties. Int J Cardiol 111: 231-239.
39. Makela J, Anttila V, Ylitalo K, Takalo R, Lehtonen S, et al. (2009) Acute homing of bone marrow-derived mononuclear cells in intramyocardial vs. intracoronary transplantation. Scand Cardiovasc J 43: 366-373.
40. Kelm JM, Diaz Sanchez-Bustamante C, Ehler E, Hoerstrup SP, Djonov V, et al. (2005) VEGF profiling and angiogenesis in human microtissues. J Biotechnol 118: 213-229.
41. Kelm JM, Djonov V, Hoerstrup SP, Guenter CI, Ittner LM, et al. (2006) Tissue-transplant fusion and vascularization of myocardial microtissues and macrotissues implanted into chicken embryos and rats. Tissue Eng 12: 2541-2553.
42. Kelm JM, Djonov V, Ittner LM, Fluri D, Born W, et al. (2006) Design of custom-shaped vascularized tissues using microtissue spheroids as minimal building units. Tissue Eng 12: 2151-2160.
43. Kelm JM, Fussenegger M. (2004) Microscale tissue engineering using gravity-enforced cell assembly. Trends Biotechnol 22: 195-202.
44. Kelm JM, Lorber V, Snedeker JG, Schmidt D, Broggini-Tenzer A, et al. (2010) A novel concept for scaffold-free vessel tissue engineering: self-assembly of microtissue building blocks. J Biotechnol 148: 46-55.
45. Garzoni LR, Rossi MI, de Barros AP, Guarani V, Keramidas M, et al. (2009) Dissecting coronary angiogenesis: 3D co-culture of cardiomyocytes with endothelial or mesenchymal cells. Exp Cell Res 315: 3406-3418.
46. Fu Y, Azene N, Xu Y, Kraitchman DL. (2011) Tracking stem cells for cardiovascular applications in vivo: focus on imaging techniques. Imaging Med 3: 473-486.
47. Beeres SL, Bengel FM, Bartunek J, Atsma DE, Hill JM, et al. (2007) Role of imaging in cardiac stem cell therapy. J Am Coll Cardiol 49: 1137-1148.
48. Shapiro EM, Skrtic S, Koretsky AP. (2005) Sizing it up: cellular MRI using micron-sized iron oxide particles. Magn Reson Med 53: 329-338.
49. Shapiro EM, Skrtic S, Sharer K, Hill JM, Dunbar CE, et al. (2004) MRI detection of single particles for cellular imaging. Proc Natl Acad Sci U S A 101: 10901-10906.
50. Raschzok N, Morgul MH, Pinkernelle J, Vondran FW, Billecke N, et al. (2008) Imaging of primary human hepatocytes performed with micron-sized iron oxide particles and clinical magnetic resonance tomography. J Cell Mol Med 12: 1384-1394.
51. van der Spoel TI, Jansen of Lorkeers SJ, Agostoni P, van Belle E, Gyongyosi M, et al. (2011) Human relevance of pre-clinical studies in stem cell therapy: systematic review and meta-analysis of large animal models of ischaemic heart disease. Cardiovasc Res 91: 649-658.
52. Flake AW, Harrison MR, Adzick NS, Zanjani ED. (1986) Transplantation of fetal hematopoietic stem cells in utero: the creation of hematopoietic chimeras. Science 233: 776-778.
53. Liechty KW, MacKenzie TC, Shaaban AF, Radu A, Moseley AM, et al. (2000) Human mesenchymal stem cells engraft and demonstrate site-specific differentiation after in utero transplantation in sheep. Nat Med 6: 1282-1286.
54. Assmus B, Schachinger V, Teupe C, Britten M, Lehmann R, et al. (2002) Transplantation of Progenitor Cells and Regeneration Enhancement in Acute Myocardial Infarction (TOPCARE-AMI). Circulation 106: 3009-3017.
55. Wollert KC, Meyer GP, Lotz J, Ringes-Lichtenberg S, Lippolt P, et al. (2004) Intracoronary autologous bone-marrow cell transfer after myocardial infarction: the BOOST randomised controlled clinical trial. Lancet 364: 141-148.

56. Meyer GP, Wollert KC, Lotz J, Steffens J, Lippolt P, et al. (2006) Intracoronary bone marrow cell transfer after myocardial infarction: eighteen months' follow-up data from the randomized, controlled BOOST (BOne marrOw transfer to enhance ST-elevation infarct regeneration) trial. Circulation 113: 1287-1294.
57. Zimmet H, Porapakkham P, Sata Y, Haas SJ, Itescu S, et al. (2012) Short- and long-term outcomes of intracoronary and endogenously mobilized bone marrow stem cells in the treatment of ST-segment elevation myocardial infarction: a meta-analysis of randomized control trials. Eur J Heart Fail 14: 91-105.
58. Strauer BE, Yousef M, Schannwell CM. (2010) The acute and long-term effects of intracoronary Stem cell Transplantation in 191 patients with chronic heARt failure: the STAR-heart study. Eur J Heart Fail 12: 721-729.
59. Meyer GP, Wollert KC, Lotz J, Pirr J, Rager U, et al. (2009) Intracoronary bone marrow cell transfer after myocardial infarction: 5-year follow-up from the randomized-controlled BOOST trial. Eur Heart J 30: 2978-2984.
60. Martin-Rendon E, Brunskill SJ, Hyde CJ, Stanworth SJ, Mathur A, et al. (2008) Autologous bone marrow stem cells to treat acute myocardial infarction: a systematic review. Eur Heart J 29: 1807-1818.
61. Hagege AA, Marolleau JP, Vilquin JT, Alheritiere A, Peyrard S, et al. (2006) Skeletal myoblast transplantation in ischemic heart failure: long-term follow-up of the first phase I cohort of patients. Circulation 114: I108-113.
62. Reinecke H, Poppa V, Murry CE. (2002) Skeletal muscle stem cells do not transdifferentiate into cardiomyocytes after cardiac grafting. J Mol Cell Cardiol 34: 241-249.
63. Balsam LB, Wagers AJ, Christensen JL, Kofidis T, Weissman IL, et al. (2004) Haematopoietic stem cells adopt mature haematopoietic fates in ischaemic myocardium. Nature 428: 668-673.
64. Murry CE, Soonpaa MH, Reinecke H, Nakajima H, Nakajima HO, et al. (2004) Haematopoietic stem cells do not transdifferentiate into cardiac myocytes in myocardial infarcts. Nature 428: 664-668.
65. Nygren JM, Jovinge S, Breitbach M, Sawen P, Roll W, et al. (2004) Bone marrow-derived hematopoietic cells generate cardiomyocytes at a low frequency through cell fusion, but not transdifferentiation. Nat Med 10: 494-501.
66. Trachtenberg B, Velazquez DL, Williams AR, McNiece I, Fishman J, et al. (2011) Rationale and design of the Transendocardial Injection of Autologous Human Cells (bone marrow or mesenchymal) in Chronic Ischemic Left Ventricular Dysfunction and Heart Failure Secondary to Myocardial Infarction (TAC-HFT) trial: A randomized, double-blind, placebo-controlled study of safety and efficacy. Am Heart J 161: 487-493.
67. Makkar RR, Smith RR, Cheng K, Malliaras K, Thomson LE, et al. (2012) Intracoronary cardiosphere-derived cells for heart regeneration after myocardial infarction (CADUCEUS): a prospective, randomised phase 1 trial. Lancet 379: 895-904.
68. Lunde K, Solheim S, Aakhus S, Arnesen H, Abdelnoor M, et al. (2006) Intracoronary injection of mononuclear bone marrow cells in acute myocardial infarction. N Engl J Med 355: 1199-1209.
69. Hofmann M, Wollert KC, Meyer GP, Menke A, Arseniev L, et al. (2005) Monitoring of bone marrow cell homing into the infarcted human myocardium. Circulation 111: 2198-2202.
70. Otto CM. (2000) Timing of aortic valve surgery. Heart 84: 211-218.
71. Supino PG, Borer JS, Preibisz J, Bornstein A. (2006) The epidemiology of valvular heart disease: a growing public health problem. Heart Fail Clin 2: 379-393.
72. Supino PG, Borer JS, Yin A, Dillingham E, McClymont W. (2004) The epidemiology of valvular heart diseases: the problem is growing. Adv Cardiol 41: 9-15.
73. Nkomo VT, Gardin JM, Skelton TN, Gottdiener JS, Scott CG, et al. (2006) Burden of valvular heart diseases: a population-based study. Lancet 368: 1005-1011.
74. Pibarot P, Dumesnil JG. (2009) Prosthetic heart valves: selection of the optimal prosthesis and long-term management. Circulation 119: 1034-1048.
75. Yacoub MH, Takkenberg JJ. (2005) Will heart valve tissue engineering change the world? Nat Clin Pract Cardiovasc Med 2: 60-61.
76. Bonow RO, Carabello BA, Chatterjee K, de Leon AC, Jr., Faxon DP, et al. (2008) 2008 focused update incorporated into the ACC/AHA 2006 guidelines for the management of patients with valvular heart disease: a report of the American College of Cardiology/American Heart Association Task Force on Practice Guidelines (Writing Committee to revise the 1998 guidelines for the management of patients with valvular heart disease). Endorsed by the Society of Cardiovascular Anesthesiologists, Society for Cardiovascular Angiography and Interventions, and Society of Thoracic Surgeons. J Am Coll Cardiol 52: e1-142.
77. Bonow RO, Carabello BA, Chatterjee K, de Leon AC, Jr., Faxon DP, et al. (2006) ACC/AHA 2006 guidelines for the management of patients with valvular heart disease: a report of the American College of Cardiology/American Heart Association Task Force on Practice Guidelines (writing Committee to Revise the 1998 guidelines for the management of patients with valvular heart disease) developed in collaboration with the Society of Cardiovascular Anesthesiologists endorsed by the Society for Cardiovascular Angiography and Interventions and the Society of Thoracic Surgeons. J Am Coll Cardiol 48: e1-148.
78. Kvidal P, Bergstrom R, Horte LG, Stahle E. (2000) Observed and relative survival after aortic valve replacement. J Am Coll Cardiol 35: 747-756.
79. Dasi LP, Simon HA, Sucosky P, Yoganathan AP. (2009) Fluid mechanics of artificial heart valves. Clin Exp Pharmacol Physiol 36: 225-237.
80. Zilla P, Brink J, Human P, Bezuidenhout D. (2008) Prosthetic heart valves: catering for the few. Biomaterials 29: 385-406.

81. Kraehenbuehl TP, Zammaretti P, Van der Vlies AJ, Schoenmakers RG, Lutolf MP, et al. (2008) Three-dimensional extracellular matrix-directed cardioprogenitor differentiation: systematic modulation of a synthetic cell-responsive PEG-hydrogel. Biomaterials 29: 2757-2766.
82. Senthilnathan V, Treasure T, Grunkemeier G, Starr A. (1999) Heart valves: which is the best choice? Cardiovasc Surg 7: 393-397.
83. Falk V, Schwammenthal EE, Kempfert J, Linke A, Schuler G, et al. (2009) New anatomically oriented transapical aortic valve implantation. Ann Thorac Surg 87: 925-926.
84. Falk V, Walther T, Schwammenthal E, Strauch J, Aicher D, et al. (2011) Transapical aortic valve implantation with a self-expanding anatomically oriented valve. Eur Heart J 32: 878-887.
85. Walther T, Dewey T, Borger MA, Kempfert J, Linke A, et al. (2009) Transapical aortic valve implantation: step by step. Ann Thorac Surg 87: 276-283.
86. Walther T, Mollmann H, van Linden A, Kempfert J. (2011) Transcatheter aortic valve implantation transapical: step by step. Semin Thorac Cardiovasc Surg 23: 55-61.
87. Walther T, Simon P, Dewey T, Wimmer-Greinecker G, Falk V, et al. (2007) Transapical minimally invasive aortic valve implantation: multicenter experience. Circulation 116: I240-245.
88. Cribier A, Eltchaninoff H, Bash A, Borenstein N, Tron C, et al. (2002) Percutaneous transcatheter implantation of an aortic valve prosthesis for calcific aortic stenosis: first human case description. Circulation 106: 3006-3008.
89. Vahanian A, Alfieri O, Al-Attar N, Antunes M, Bax J, et al. (2008) Transcatheter valve implantation for patients with aortic stenosis: a position statement from the European Association of Cardio-Thoracic Surgery (EACTS) and the European Society of Cardiology (ESC), in collaboration with the European Association of Percutaneous Cardiovascular Interventions (EAPCI). Eur Heart J 29: 1463-1470.
90. Weber B, Emmert MY, Schoenauer R, Brokopp C, Baumgartner L, et al. (2011) Tissue engineering on matrix: future of autologous tissue replacement. Semin Immunopathol 33: 307-315.
91. Schoen FJ. (2008) Evolving concepts of cardiac valve dynamics: the continuum of development, functional structure, pathobiology, and tissue engineering. Circulation 118: 1864-1880.
92. Langer R, Vacanti JP. (1993) Tissue engineering. Science 260: 920-926.
93. Mendelson K, Schoen FJ. (2006) Heart valve tissue engineering: concepts, approaches, progress, and challenges. Ann Biomed Eng 34: 1799-1819.
94. Schoen FJ. (2011) Heart valve tissue engineering: quo vadis? Curr Opin Biotechnol
95. Yamanami M, Yahata Y, Uechi M, Fujiwara M, Ishibashi-Ueda H, et al. (2010) Development of a completely autologous valved conduit with the sinus of Valsalva using in-body tissue architecture technology: a pilot study in pulmonary valve replacement in a beagle model. Circulation 122: S100-106.
96. Mol A, Smits AI, Bouten CV, Baaijens FP. (2009) Tissue engineering of heart valves: advances and current challenges. Expert Rev Med Devices 6: 259-275.
97. Brennan MP, Dardik A, Hibino N, Roh JD, Nelson GN, et al. (2008) Tissue-engineered vascular grafts demonstrate evidence of growth and development when implanted in a juvenile animal model. Ann Surg 248: 370-377.
98. Breuer CK, Mettler BA, Anthony T, Sales VL, Schoen FJ, et al. (2004) Application of tissue-engineering principles toward the development of a semilunar heart valve substitute. Tissue Eng 10: 1725-1736.
99. Brody S, Pandit A. (2007) Approaches to heart valve tissue engineering scaffold design. J Biomed Mater Res B Appl Biomater 83: 16-43.
100. Affonso da Costa FD, Dohmen PM, Lopes SV, Lacerda G, Pohl F, et al. (2004) Comparison of cryopreserved homografts and decellularized porcine heterografts implanted in sheep. Artif Organs 28: 366-370.
101. Allen BS, El-Zein C, Cuneo B, Cava JP, Barth MJ, et al. (2002) Pericardial tissue valves and Gore-Tex conduits as an alternative for right ventricular outflow tract replacement in children. Ann Thorac Surg 74: 771-777.
102. Bielefeld MR, Bishop DA, Campbell DN, Mitchell MB, Grover FL, et al. (2001) Reoperative homograft right ventricular outflow tract reconstruction. Ann Thorac Surg 71: 482-487; discussion 487-488.
103. Carr-White GS, Glennan S, Edwards S, Ferdinand FD, Desouza AC, et al. (1999) Pulmonary autograft versus aortic homograft for rereplacement of the aortic valve: results from a subset of a prospective randomized trial. Circulation 100: II103-106.
104. Neidert MR, Tranquillo RT. (2006) Tissue-engineered valves with commissural alignment. Tissue Eng 12: 891-903.
105. Williams C, Johnson SL, Robinson PS, Tranquillo RT. (2006) Cell sourcing and culture conditions for fibrin-based valve constructs. Tissue Eng 12: 1489-1502.
106. Robinson PS, Johnson SL, Evans MC, Barocas VH, Tranquillo RT. (2008) Functional tissue-engineered valves from cell-remodeled fibrin with commissural alignment of cell-produced collagen. Tissue Eng Part A 14: 83-95.
107. Syedain ZH, Weinberg JS, Tranquillo RT. (2008) Cyclic distension of fibrin-based tissue constructs: evidence of adaptation during growth of engineered connective tissue. Proc Natl Acad Sci U S A 105: 6537-6542.
108. Hoerstrup SP, Kadner A, Melnitchouk S, Trojan A, Eid K, et al. (2002) Tissue engineering of functional trileaflet heart valves from human marrow stromal cells. Circulation 106: I143-150.
109. Hoerstrup SP, Sodian R, Daebritz S, Wang J, Bacha EA, et al. (2000) Functional living trileaflet heart valves grown in vitro. Circulation 102: III44-49.
110. Mol A, Rutten MC, Driessen NJ, Bouten CV, Zund G, et al. (2006) Autologous human tissue-engineered heart valves: prospects for systemic application. Circulation 114: I152-158.

111. Schmidt D, Dijkman PE, Driessen-Mol A, Stenger R, Mariani C, et al. (2010) Minimally-invasive implantation of living tissue engineered heart valves: a comprehensive approach from autologous vascular cells to stem cells. J Am Coll Cardiol 56: 510-520.
112. Schmidt D, Achermann J, Odermatt B, Breymann C, Mol A, et al. (2007) Prenatally fabricated autologous human living heart valves based on amniotic fluid derived progenitor cells as single cell source. Circulation 116: I64-70.
113. Schmidt D, Mol A, Breymann C, Achermann J, Odermatt B, et al. (2006) Living autologous heart valves engineered from human prenatally harvested progenitors. Circulation 114: I125-131.
114. Shinoka T, Ma PX, Shum-Tim D, Breuer CK, Cusick RA, et al. (1996) Tissue-engineered heart valves. Autologous valve leaflet replacement study in a lamb model. Circulation 94: II164-168.
115. Shinoka T, Shum-Tim D, Ma PX, Tanel RE, Langer R, et al. (1997) Tissue-engineered heart valve leaflets: does cell origin affect outcome? Circulation 96: II-102-107.
116. Sutherland FW, Perry TE, Yu Y, Sherwood MC, Rabkin E, et al. (2005) From stem cells to viable autologous semilunar heart valve. Circulation 111: 2783-2791.
117. Hoerstrup SP, Sodian R, Sperling JS, Vacanti JP, Mayer JE, Jr. (2000) New pulsatile bioreactor for in vitro formation of tissue engineered heart valves. Tissue Eng 6: 75-79.
118. Hoerstrup SP, Zund G, Schnell AM, Kolb SA, Visjager JF, et al. (2000) Optimized growth conditions for tissue engineering of human cardiovascular structures. Int J Artif Organs 23: 817-823.
119. Kadner A, Zund G, Maurus C, Breymann C, Yakarisik S, et al. (2004) Human umbilical cord cells for cardiovascular tissue engineering: a comparative study. Eur J Cardiothorac Surg 25: 635-641.
120. Rabkin E, Hoerstrup SP, Aikawa M, Mayer JE, Jr., Schoen FJ. (2002) Evolution of cell phenotype and extracellular matrix in tissue-engineered heart valves during in-vitro maturation and in-vivo remodeling. J Heart Valve Dis 11: 308-314; discussion 314.
121. Schmidt D, Hoerstrup SP. (2007) Tissue engineered heart valves based on human cells. Swiss Med Wkly 137 Suppl 155: 80S-85S.
122. Schmidt D, Stock UA, Hoerstrup SP. (2007) Tissue engineering of heart valves using decellularized xenogeneic or polymeric starter matrices. Philos Trans R Soc Lond B Biol Sci 362: 1505-1512.
123. Schmidt D, Mol A, Odermatt B, Neuenschwander S, Breymann C, et al. (2006) Engineering of biologically active living heart valve leaflets using human umbilical cord-derived progenitor cells. Tissue Eng 12: 3223-3232.
124. Schmidt D, Mol A, Neuenschwander S, Breymann C, Gossi M, et al. (2005) Living patches engineered from human umbilical cord derived fibroblasts and endothelial progenitor cells. Eur J Cardiothorac Surg 27: 795-800.
125. Weber B, Emmert MY, Hoerstrup SP. (2012) Stem cells for heart valve regeneration. Swiss Med Wkly 142: w13622.
126. Hoerstrup SP, Zund G, Schoeberlein A, Ye Q, Vogt PR, et al. (1998) Fluorescence activated cell sorting: a reliable method in tissue engineering of a bioprosthetic heart valve. Ann Thorac Surg 66: 1653-1657.
127. Sodian R, Hoerstrup SP, Sperling JS, Daebritz S, Martin DP, et al. (2000) Early in vivo experience with tissue-engineered trileaflet heart valves. Circulation 102: III22-29.
128. Schnell AM, Hoerstrup SP, Zund G, Kolb S, Sodian R, et al. (2001) Optimal cell source for cardiovascular tissue engineering: venous vs. aortic human myofibroblasts. Thorac Cardiovasc Surg 49: 221-225.
129. Zund G, Hoerstrup SP, Schoeberlein A, Lachat M, Uhlschmid G, et al. (1998) Tissue engineering: a new approach in cardiovascular surgery: Seeding of human fibroblasts followed by human endothelial cells on resorbable mesh. Eur J Cardiothorac Surg 13: 160-164.
130. Kadner A, Hoerstrup SP, Zund G, Eid K, Maurus C, et al. (2002) A new source for cardiovascular tissue engineering: human bone marrow stromal cells. Eur J Cardiothorac Surg 21: 1055-1060.
131. Latif N, Sarathchandra P, Thomas PS, Antoniw J, Batten P, et al. (2007) Characterization of structural and signaling molecules by human valve interstitial cells and comparison to human mesenchymal stem cells. J Heart Valve Dis 16: 56-66.
132. Iop L, Renier V, Naso F, Piccoli M, Bonetti A, et al. (2009) The influence of heart valve leaflet matrix characteristics on the interaction between human mesenchymal stem cells and decellularized scaffolds. Biomaterials 30: 4104-4116.
133. Roh JD, Sawh-Martinez R, Brennan MP, Jay SM, Devine L, et al. (2010) Tissue-engineered vascular grafts transform into mature blood vessels via an inflammation-mediated process of vascular remodeling. Proc Natl Acad Sci U S A 107: 4669-4674.
134. Kim S, von Recum H. (2008) Endothelial stem cells and precursors for tissue engineering: cell source, differentiation, selection, and application. Tissue Eng Part B Rev 14: 133-147.
135. Kim S, von Recum HA. (2009) Endothelial progenitor populations in differentiating embryonic stem cells I: Identification and differentiation kinetics. Tissue Eng Part A 15: 3709-3718.
136. Hoerstrup SP, Kadner A, Breymann C, Maurus CF, Guenter CI, et al. (2002) Living, autologous pulmonary artery conduits tissue engineered from human umbilical cord cells. Ann Thorac Surg 74: 46-52; discussion 52.
137. Kadner A, Hoerstrup SP, Tracy J, Breymann C, Maurus CF, et al. (2002) Human umbilical cord cells: a new cell source for cardiovascular tissue engineering. Ann Thorac Surg 74: S1422-1428.
138. Pansky A, Roitzheim B, Tobiasch E. (2007) Differentiation potential of adult human mesenchymal stem cells. Clin Lab 53: 81-84.
139. Tuan RS, Boland G, Tuli R. (2003) Adult mesenchymal stem cells and cell-based tissue engineering. Arthritis Res Ther 5: 32-45.

140. Cao Y, Sun Z, Liao L, Meng Y, Han Q, et al. (2005) Human adipose tissue-derived stem cells differentiate into endothelial cells in vitro and improve postnatal neovascularization in vivo. Biochem Biophys Res Commun 332: 370-379.
141. Cao Y, Meng Y, Sun Z, Liao LM, Han Q, et al. (2005) [Potential of human adipose tissue derived adult stem cells differentiate into endothelial cells]. Zhongguo Yi Xue Ke Xue Yuan Xue Bao 27: 678-682.
142. DiMuzio P, Tulenko T. (2007) Tissue engineering applications to vascular bypass graft development: the use of adipose-derived stem cells. J Vasc Surg 45 Suppl A: A99-103.
143. Parolini O, Soncini M, Evangelista M, Schmidt D. (2009) Amniotic membrane and amniotic fluid-derived cells: potential tools for regenerative medicine? Regen Med 4: 275-291.
144. Nadal-Ginard B, Mahdavi V. (1989) Molecular basis of cardiac performance. Plasticity of the myocardium generated through protein isoform switches. J Clin Invest 84: 1693-1700.
145. Soonpaa MH, Field LJ. (1998) Survey of studies examining mammalian cardiomyocyte DNA synthesis. Circ Res 83: 15-26.
146. Asahara T, Kawamoto A. (2004) Endothelial progenitor cells for postnatal vasculogenesis. Am J Physiol Cell Physiol 287: C572-579.
147. Makino S, Fukuda K, Miyoshi S, Konishi F, Kodama H, et al. (1999) Cardiomyocytes can be generated from marrow stromal cells in vitro. J Clin Invest 103: 697-705.
148. Zhou S, Schuetz JD, Bunting KD, Colapietro AM, Sampath J, et al. (2001) The ABC transporter Bcrp1/ABCG2 is expressed in a wide variety of stem cells and is a molecular determinant of the side-population phenotype. Nat Med 7: 1028-1034.
149. Scharenberg CW, Harkey MA, Torok-Storb B. (2002) The ABCG2 transporter is an efficient Hoechst 33342 efflux pump and is preferentially expressed by immature human hematopoietic progenitors. Blood 99: 507-512.
150. Menasche P. (2002) Myoblast transplantation for the treatment of heart failure. Minerva Cardioangiol 50: 565-568.
151. Kehat I, Kenyagin-Karsenti D, Snir M, Segev H, Amit M, et al. (2001) Human embryonic stem cells can differentiate into myocytes with structural and functional properties of cardiomyocytes. J Clin Invest 108: 407-414.
152. Haase A, Olmer R, Schwanke K, Wunderlich S, Merkert S, et al. (2009) Generation of induced pluripotent stem cells from human cord blood. Cell Stem Cell 5: 434-441.
153. Mauritz C, Schwanke K, Reppel M, Neef S, Katsirntaki K, et al. (2008) Generation of functional murine cardiac myocytes from induced pluripotent stem cells. Circulation 118: 507-517.
154. Oh H, Bradfute SB, Gallardo TD, Nakamura T, Gaussin V, et al. (2003) Cardiac progenitor cells from adult myocardium: homing, differentiation, and fusion after infarction. Proc Natl Acad Sci U S A 100: 12313-12318.
155. Urbanek K, Quaini F, Tasca G, Torella D, Castaldo C, et al. (2003) Intense myocyte formation from cardiac stem cells in human cardiac hypertrophy. Proc Natl Acad Sci U S A 100: 10440-10445.
156. Beltrami AP, Urbanek K, Kajstura J, Yan SM, Finato N, et al. (2001) Evidence that human cardiac myocytes divide after myocardial infarction. N Engl J Med 344: 1750-1757.
157. Quaini F, Urbanek K, Beltrami AP, Finato N, Beltrami CA, et al. (2002) Chimerism of the transplanted heart. N Engl J Med 346: 5-15.
158. Beltrami AP, Barlucchi L, Torella D, Baker M, Limana F, et al. (2003) Adult cardiac stem cells are multipotent and support myocardial regeneration. Cell 114: 763-776.
159. van Vliet P, Roccio M, Smits AM, van Oorschot AA, Metz CH, et al. (2008) Progenitor cells isolated from the human heart: a potential cell source for regenerative therapy. Neth Heart J 16: 163-169.
160. Weissman IL, Anderson DJ, Gage F. (2001) Stem and progenitor cells: origins, phenotypes, lineage commitments, and transdifferentiations. Annu Rev Cell Dev Biol 17: 387-403.
161. Martin CM, Meeson AP, Robertson SM, Hawke TJ, Richardson JA, et al. (2004) Persistent expression of the ATP-binding cassette transporter, Abcg2, identifies cardiac SP cells in the developing and adult heart. Dev Biol 265: 262-275.
162. Pfister O, Oikonomopoulos A, Sereti KI, Sohn RL, Cullen D, et al. (2008) Role of the ATP-binding cassette transporter Abcg2 in the phenotype and function of cardiac side population cells. Circ Res 103: 825-835.
163. Meissner K, Heydrich B, Jedlitschky G, Meyer Zu Schwabedissen H, Mosyagin I, et al. (2006) The ATP-binding cassette transporter ABCG2 (BCRP), a marker for side population stem cells, is expressed in human heart. J Histochem Cytochem 54: 215-221.
164. Pfister O, Oikonomopoulos A, Sereti KI, Liao R. Isolation of resident cardiac progenitor cells by Hoechst 33342 staining. Methods Mol Biol 660: 53-63.
165. Oyama T, Nagai T, Wada H, Naito AT, Matsuura K, et al. (2007) Cardiac side population cells have a potential to migrate and differentiate into cardiomyocytes in vitro and in vivo. J Cell Biol 176: 329-341.
166. Urbanek K, Rota M, Cascapera S, Bearzi C, Nascimbene A, et al. (2005) Cardiac stem cells possess growth factor-receptor systems that after activation regenerate the infarcted myocardium, improving ventricular function and long-term survival. Circ Res 97: 663-673.
167. Urbanek K, Torella D, Sheikh F, De Angelis A, Nurzynska D, et al. (2005) Myocardial regeneration by activation of multipotent cardiac stem cells in ischemic heart failure. Proc Natl Acad Sci U S A 102: 8692-8697.
168. Pfister O, Mouquet F, Jain M, Summer R, Helmes M, et al. (2005) CD31- but Not CD31+ cardiac side population cells exhibit functional cardiomyogenic differentiation. Circ Res 97: 52-61.

169. Sussman MA, Anversa P. (2004) Myocardial aging and senescence: where have the stem cells gone? Annu Rev Physiol 66: 29-48.
170. Itzhaki-Alfia A, Leor J, Raanani E, Sternik L, Spiegelstein D, et al. (2009) Patient characteristics and cell source determine the number of isolated human cardiac progenitor cells. Circulation 120: 2559-2566.
171. Ott HC, Matthiesen TS, Brechtken J, Grindle S, Goh SK, et al. (2007) The adult human heart as a source for stem cells: repair strategies with embryonic-like progenitor cells. Nat Clin Pract Cardiovasc Med 4 Suppl 1: S27-39.
172. Yamahara K, Fukushima S, Coppen SR, Felkin LE, Varela-Carver A, et al. (2008) Heterogeneic nature of adult cardiac side population cells. Biochem Biophys Res Commun 371: 615-620.
173. Rosenblatt-Velin N, Lepore MG, Cartoni C, Beermann F, Pedrazzini T. (2005) FGF-2 controls the differentiation of resident cardiac precursors into functional cardiomyocytes. J Clin Invest 115: 1724-1733.
174. Anversa P, Kajstura J, Leri A, Bolli R. (2006) Life and death of cardiac stem cells: a paradigm shift in cardiac biology. Circulation 113: 1451-1463.
175. Anversa P, Leri A, Kajstura J. (2006) Cardiac regeneration. J Am Coll Cardiol 47: 1769-1776.
176. Mishra R, Vijayan K, Colletti EJ, Harrington DA, Matthiesen TS, et al. Characterization and functionality of cardiac progenitor cells in congenital heart patients. Circulation 123: 364-373.
177. Sato H, Shiraishi I, Takamatsu T, Hamaoka K. (2007) Detection of TUNEL-positive cardiomyocytes and c-kit-positive progenitor cells in children with congenital heart disease. J Mol Cell Cardiol 43: 254-261.
178. Linke A, Muller P, Nurzynska D, Casarsa C, Torella D, et al. (2005) Stem cells in the dog heart are self-renewing, clonogenic, and multipotent and regenerate infarcted myocardium, improving cardiac function. Proc Natl Acad Sci U S A 102: 8966-8971.
179. Mezey E. (2011) The therapeutic potential of bone marrow-derived stromal cells. J Cell Biochem 112: 2683-2687.
180. Rhee D, Sanger JM, Sanger JW. (1994) The premyofibril: evidence for its role in myofibrillogenesis. Cell Motil Cytoskeleton 28: 1-24.
181. Schwanke K, Wunderlich S, Reppel M, Winkler ME, Matzkies M, et al. (2006) Generation and characterization of functional cardiomyocytes from rhesus monkey embryonic stem cells. Stem Cells 24: 1423-1432.
182. Koninckx R, Hensen K, Daniels A, Moreels M, Lambrichts I, et al. (2009) Human bone marrow stem cells co-cultured with neonatal rat cardiomyocytes display limited cardiomyogenic plasticity. Cytotherapy 11: 778-792.
183. Hare JM, Traverse JH, Henry TD, Dib N, Strumpf RK, et al. (2009) A randomized, double-blind, placebo-controlled, dose-escalation study of intravenous adult human mesenchymal stem cells (prochymal) after acute myocardial infarction. J Am Coll Cardiol 54: 2277-2286.
184. Porada CD, Park P, Almeida-Porada G, Zanjani ED. (2004) The sheep model of in utero gene therapy. Fetal Diagn Ther 19: 23-30.
185. Porada GA, Porada C, Zanjani ED. (2004) The fetal sheep: a unique model system for assessing the full differentiative potential of human stem cells. Yonsei Med J 45 Suppl: 7-14.
186. Airey JA, Almeida-Porada G, Colletti EJ, Porada CD, Chamberlain J, et al. (2004) Human mesenchymal stem cells form Purkinje fibers in fetal sheep heart. Circulation 109: 1401-1407.
187. Almeida-Porada G, Porada C, Gupta N, Torabi A, Thain D, et al. (2007) The human-sheep chimeras as a model for human stem cell mobilization and evaluation of hematopoietic grafts' potential. Exp Hematol 35: 1594-1600.
188. Almeida-Porada G, Porada C, Zanjani ED. (2004) Plasticity of human stem cells in the fetal sheep model of human stem cell transplantation. Int J Hematol 79: 1-6.
189. Almeida-Porada G, Porada CD, Tran N, Zanjani ED. (2000) Cotransplantation of human stromal cell progenitors into preimmune fetal sheep results in early appearance of human donor cells in circulation and boosts cell levels in bone marrow at later time points after transplantation. Blood 95: 3620-3627.
190. Zanjani ED, Almeida-Porada G, Flake AW. (1996) The human/sheep xenograft model: a large animal model of human hematopoiesis. Int J Hematol 63: 179-192.
191. Flake AW, Zanjani ED. (1993) In utero transplantation of hematopoietic stem cells. Crit Rev Oncol Hematol 15: 35-48.
192. Zanjani ED, Flake AW, Rice H, Hedrick M, Tavassoli M. (1994) Long-term repopulating ability of xenogeneic transplanted human fetal liver hematopoietic stem cells in sheep. J Clin Invest 93: 1051-1055.
193. Zanjani ED, Silva MR, Flake AW. (1994) Retention and multilineage expression of human hematopoietic stem cells in human-sheep chimeras. Blood Cells 20: 331-338; discussion 338-340.
194. Schoeberlein A, Holzgreve W, Dudler L, Hahn S, Surbek DV. (2004) In utero transplantation of autologous and allogeneic fetal liver stem cells in ovine fetuses. Am J Obstet Gynecol 191: 1030-1036.
195. Schoeberlein A, Holzgreve W, Dudler L, Hahn S, Surbek DV. (2005) Tissue-specific engraftment after in utero transplantation of allogeneic mesenchymal stem cells into sheep fetuses. Am J Obstet Gynecol 192: 1044-1052.
196. Surbek DV, Young A, Danzer E, Schoeberlein A, Dudler L, et al. (2002) Ultrasound-guided stem cell sampling from the early ovine fetus for prenatal ex vivo gene therapy. Am J Obstet Gynecol 187: 960-963.
197. Shaw SW, Bollini S, Nader KA, Gastadello A, Mehta V, et al. (2011) Autologous transplantation of amniotic fluid-derived mesenchymal stem cells into sheep fetuses. Cell Transplant 20: 1015-1031.
198. Pittenger MF, Mackay AM, Beck SC, Jaiswal RK, Douglas R, et al. (1999) Multilineage potential of adult human mesenchymal stem cells. Science 284: 143-147.
199. De Ugarte DA, Alfonso Z, Zuk PA, Elbarbary A, Zhu M, et al. (2003) Differential expression of stem cell mobilization-associated molecules on multi-lineage cells from adipose tissue and bone marrow. Immunol Lett 89: 267-270.

200. Raschzok N, Billecke N, Kammer NN, Morgul MH, Adonopoulou MK, et al. (2009) Quantification of cell labeling with micron-sized iron oxide particles using continuum source atomic absorption spectrometry. Tissue Eng Part C Methods 15: 681-686.
201. Raschzok N, Muecke DA, Adonopoulou MK, Billecke N, Werner W, et al. (2011) In vitro evaluation of magnetic resonance imaging contrast agents for labeling human liver cells: implications for clinical translation. Mol Imaging Biol 13: 613-622.
202. Young AJ, Holzgreve W, Dudler L, Schoeberlein A, Surbek DV. (2003) Engraftment of human cord blood-derived stem cells in preimmune ovine fetuses after ultrasound-guided in utero transplantation. Am J Obstet Gynecol 189: 698-701.
203. Ruggiero A, Thorek DL, Guenoun J, Krestin GP, Bernsen MR. (2012) Cell tracking in cardiac repair: what to image and how to image. Eur Radiol 22: 189-204.
204. Hill JM, Dick AJ, Raman VK, Thompson RB, Yu ZX, et al. (2003) Serial cardiac magnetic resonance imaging of injected mesenchymal stem cells. Circulation 108: 1009-1014.
205. Kraitchman DL, Heldman AW, Atalar E, Amado LC, Martin BJ, et al. (2003) In vivo magnetic resonance imaging of mesenchymal stem cells in myocardial infarction. Circulation 107: 2290-2293.
206. Kraitchman DL, Tatsumi M, Gilson WD, Ishimori T, Kedziorek D, et al. (2005) Dynamic imaging of allogeneic mesenchymal stem cells trafficking to myocardial infarction. Circulation 112: 1451-1461.
207. Kehat I, Khimovich L, Caspi O, Gepstein A, Shofti R, et al. (2004) Electromechanical integration of cardiomyocytes derived from human embryonic stem cells. Nat Biotechnol 22: 1282-1289.
208. Menasche P. (2002) Myoblast transplantation: feasibility, safety and efficacy. Ann Med 34: 314-315.
209. Hatzistergos KE, Quevedo H, Oskouei BN, Hu Q, Feigenbaum GS, et al. (2010) Bone marrow mesenchymal stem cells stimulate cardiac stem cell proliferation and differentiation. Circ Res 107: 913-922.
210. Quevedo HC, Hatzistergos KE, Oskouei BN, Feigenbaum GS, Rodriguez JE, et al. (2009) Allogeneic mesenchymal stem cells restore cardiac function in chronic ischemic cardiomyopathy via trilineage differentiating capacity. Proc Natl Acad Sci U S A 106: 14022-14027.
211. Schuleri KH, Boyle AJ, Centola M, Amado LC, Evers R, et al. (2008) The adult Gottingen minipig as a model for chronic heart failure after myocardial infarction: focus on cardiovascular imaging and regenerative therapies. Comp Med 58: 568-579.
212. Schuleri KH, Amado LC, Boyle AJ, Centola M, Saliaris AP, et al. (2008) Early improvement in cardiac tissue perfusion due to mesenchymal stem cells. Am J Physiol Heart Circ Physiol 294: H2002-2011.
213. Schuleri KH, Feigenbaum GS, Centola M, Weiss ES, Zimmet JM, et al. (2009) Autologous mesenchymal stem cells produce reverse remodelling in chronic ischaemic cardiomyopathy. Eur Heart J 30: 2722-2732.
214. Lee RH, Kim B, Choi I, Kim H, Choi HS, et al. (2004) Characterization and expression analysis of mesenchymal stem cells from human bone marrow and adipose tissue. Cell Physiol Biochem 14: 311-324.
215. Christman KL, Vardanian AJ, Fang Q, Sievers RE, Fok HH, et al. (2004) Injectable Fibrin Scaffold Improves Cell Transplant Survival, Reduces Infarct Expansion, and Induces Neovasculature Formation in Ischemic Myocardium. Journal of the American College of Cardiology 44: 654-660.
216. Huwer H, Winning J, Vollmar B, Welter C, Lohbach C, et al. (2003) Long-term cell survival and hemodynamic improvements after neonatal cardiomyocyte and satellite cell transplantation into healed myocardial cryoinfarcted lesions in rats. Cell Transplant 12: 757-767.
217. Kang WJ, Kang HJ, Kim HS, Chung JK, Lee MC, et al. (2006) Tissue distribution of 18F-FDG-labeled peripheral hematopoietic stem cells after intracoronary administration in patients with myocardial infarction. J Nucl Med 47: 1295-1301.
218. van der Bogt KE, Schrepfer S, Yu J, Sheikh AY, Hoyt G, et al. (2009) Comparison of transplantation of adipose tissue- and bone marrow-derived mesenchymal stem cells in the infarcted heart. Transplantation 87: 642-652.
219. Frith JE, Thomson B, Genever PG. (2010) Dynamic three-dimensional culture methods enhance mesenchymal stem cell properties and increase therapeutic potential. Tissue Eng Part C Methods 16: 735-749.
220. Wang W, Itaka K, Ohba S, Nishiyama N, Chung UI, et al. (2009) 3D spheroid culture system on micropatterned substrates for improved differentiation efficiency of multipotent mesenchymal stem cells. Biomaterials 30: 2705-2715.
221. Testa U, Pannitteri G, Condorelli GL. (2008) Vascular endothelial growth factors in cardiovascular medicine. J Cardiovasc Med (Hagerstown) 9: 1190-1221.
222. Bartosh TJ, Ylostalo JH, Mohammadipoor A, Bazhanov N, Coble K, et al. (2010) Aggregation of human mesenchymal stromal cells (MSCs) into 3D spheroids enhances their antiinflammatory properties. Proc Natl Acad Sci U S A 107: 13724-13729.
223. Zhu Y, Liu T, Song K, Fan X, Ma X, et al. (2008) Adipose-derived stem cell: a better stem cell than BMSC. Cell Biochem Funct 26: 664-675.
224. Bieback K, Hecker A, Kocaomer A, Lannert H, Schallmoser K, et al. (2009) Human alternatives to fetal bovine serum for the expansion of mesenchymal stromal cells from bone marrow. Stem Cells 27: 2331-2341.
225. Kelm JM, Timmins NE, Brown CJ, Fussenegger M, Nielsen LK. (2003) Method for generation of homogeneous multicellular tumor spheroids applicable to a wide variety of cell types. Biotechnol Bioeng 83: 173-180.
226. Templin C, Zweigerdt R, Schwanke K, Olmer R, Ghadri JR, et al. (2012) Transplantation and tracking of human-induced pluripotent stem cells in a pig model of myocardial infarction: assessment of cell survival, engraftment,

and distribution by hybrid single photon emission computed tomography/computed tomography of sodium iodide symporter transgene expression. Circulation 126: 430-439.
227. Schuleri KH, Boyle AJ, Hare JM. (2007) Mesenchymal stem cells for cardiac regenerative therapy. Handb Exp Pharmacol 195-218.
228. Kraitchman DL, Kedziorek DA, Bulte JW. (2011) MR imaging of transplanted stem cells in myocardial infarction. Methods Mol Biol 680: 141-152.
229. Lurz P, Gaudin R, Taylor AM, Bonhoeffer P. (2009) Percutaneous pulmonary valve implantation. Semin Thorac Cardiovasc Surg Pediatr Card Surg Annu 112-117.
230. Asoh K, Walsh M, Hickey E, Nagiub M, Chaturvedi R, et al. Percutaneous pulmonary valve implantation within bioprosthetic valves. Eur Heart J 31: 1404-1409.
231. Momenah TS, El Oakley R, Al Najashi K, Khoshhal S, Al Qethamy H, et al. (2009) Extended application of percutaneous pulmonary valve implantation. J Am Coll Cardiol 53: 1859-1863.
232. Fernandes SM, Khairy P, Sanders SP, Colan SD. (2007) Bicuspid aortic valve morphology and interventions in the young. J Am Coll Cardiol 49: 2211-2214.
233. Hibino N, Shin'oka T, Matsumura G, Ikada Y, Kurosawa H. (2005) The tissue-engineered vascular graft using bone marrow without culture. J Thorac Cardiovasc Surg 129: 1064-1070.
234. Matsumura G, Ishihara Y, Miyagawa-Tomita S, Ikada Y, Matsuda S, et al. (2006) Evaluation of tissue-engineered vascular autografts. Tissue Eng 12: 3075-3083.
235. Mirensky TL, Nelson GN, Brennan MP, Roh JD, Hibino N, et al. (2009) Tissue-engineered arterial grafts: long-term results after implantation in a small animal model. J Pediatr Surg 44: 1127-1132; discussion 1132-1123.
236. Isomatsu Y, Shin'oka T, Matsumura G, Hibino N, Konuma T, et al. (2003) Extracardiac total cavopulmonary connection using a tissue-engineered graft. J Thorac Cardiovasc Surg 126: 1958-1962.
237. Matsumura G, Miyagawa-Tomita S, Shin'oka T, Ikada Y, Kurosawa H. (2003) First evidence that bone marrow cells contribute to the construction of tissue-engineered vascular autografts in vivo. Circulation 108: 1729-1734.
238. Shin'oka T, Imai Y, Ikada Y. (2001) Transplantation of a tissue-engineered pulmonary artery. N Engl J Med 344: 532-533.
239. Shin'oka T, Matsumura G, Hibino N, Naito Y, Watanabe M, et al. (2005) Midterm clinical result of tissue-engineered vascular autografts seeded with autologous bone marrow cells. J Thorac Cardiovasc Surg 129: 1330-1338.
240. Mol A, van Lieshout MI, Dam-de Veen CG, Neuenschwander S, Hoerstrup SP, et al. (2005) Fibrin as a cell carrier in cardiovascular tissue engineering applications. Biomaterials 26: 3113-3121.
241. Cesarone CF, Bolognesi C, Santi L. (1979) Improved microfluorometric DNA determination in biological material using 33258 Hoechst. Anal Biochem 100: 188-197.
242. Farndale RW, Buttle DJ, Barrett AJ. (1986) Improved quantitation and discrimination of sulphated glycosaminoglycans by use of dimethylmethylene blue. Biochim Biophys Acta 883: 173-177.
243. Huszar G, Maiocco J, Naftolin F. (1980) Monitoring of collagen and collagen fragments in chromatography of protein mixtures. Anal Biochem 105: 424-429.
244. Bonhoeffer P, Boudjemline Y, Qureshi SA, Le Bidois J, Iserin L, et al. (2002) Percutaneous insertion of the pulmonary valve. J Am Coll Cardiol 39: 1664-1669.
245. Cribier A, Eltchaninoff H, Tron C, Bauer F, Agatiello C, et al. (2004) Early experience with percutaneous transcatheter implantation of heart valve prosthesis for the treatment of end-stage inoperable patients with calcific aortic stenosis. J Am Coll Cardiol 43: 698-703.
246. Coats L, Bonhoeffer P. (2007) New percutaneous treatments for valve disease. Heart 93: 639-644.
247. Mirensky TL, Hibino N, Sawh-Martinez RF, Yi T, Villalona G, et al. (2010) Tissue-engineered vascular grafts: does cell seeding matter? J Pediatr Surg 45: 1299-1305.
248. Terada N, Hamazaki T, Oka M, Hoki M, Mastalerz DM, et al. (2002) Bone marrow cells adopt the phenotype of other cells by spontaneous cell fusion. Nature 416: 542-545.
249. Wagers AJ, Sherwood RI, Christensen JL, Weissman IL. (2002) Little evidence for developmental plasticity of adult hematopoietic stem cells. Science 297: 2256-2259.
250. Gnecchi M, Zhang Z, Ni A, Dzau VJ. (2008) Paracrine mechanisms in adult stem cell signaling and therapy. Circ Res 103: 1204-1219.
251. Kinnaird T, Stabile E, Burnett MS, Shou M, Lee CW, et al. (2004) Local delivery of marrow-derived stromal cells augments collateral perfusion through paracrine mechanisms. Circulation 109: 1543-1549.
252. O'Neill TJt, Wamhoff BR, Owens GK, Skalak TC. (2005) Mobilization of bone marrow-derived cells enhances the angiogenic response to hypoxia without transdifferentiation into endothelial cells. Circ Res 97: 1027-1035.
253. Uemura R, Xu M, Ahmad N, Ashraf M. (2006) Bone marrow stem cells prevent left ventricular remodeling of ischemic heart through paracrine signaling. Circ Res 98: 1414-1421.
254. Schoen FJ, Levy RJ. (2005) Calcification of tissue heart valve substitutes: progress toward understanding and prevention. Ann Thorac Surg 79: 1072-1080.
255. Mol A, Driessen NJ, Rutten MC, Hoerstrup SP, Bouten CV, et al. (2005) Tissue engineering of human heart valve leaflets: a novel bioreactor for a strain-based conditioning approach. Ann Biomed Eng 33: 1778-1788.
256. Flanagan TC, Sachweh JS, Frese J, Schnoring H, Gronloh N, et al. (2009) In vivo remodeling and structural characterization of fibrin-based tissue-engineered heart valves in the adult sheep model. Tissue Eng Part A 15: 2965-2976.

257. Lutolf MP, Gilbert PM, Blau HM. (2009) Designing materials to direct stem-cell fate. Nature 462: 433-441.
258. Leon MB, Smith CR, Mack M, Miller DC, Moses JW, et al. (2010) Transcatheter aortic-valve implantation for aortic stenosis in patients who cannot undergo surgery. N Engl J Med 363: 1597-1607.
259. Smith CR, Leon MB, Mack MJ, Miller DC, Moses JW, et al. (2011) Transcatheter versus surgical aortic-valve replacement in high-risk patients. N Engl J Med 364: 2187-2198.
260. Kiefer P, Gruenwald F, Kempfert J, Aupperle H, Seeburger J, et al. (2011) Crimping may affect the durability of transcatheter valves: an experimental analysis. Ann Thorac Surg 92: 155-160.
261. Zegdi R, Bruneval P, Blanchard D, Fabiani JN. (2011) Evidence of leaflet injury during percutaneous aortic valve deployment. Eur J Cardiothorac Surg 40: 257-259.
262. Dolgin E. (2011) Taking tissue engineering to heart. Nat Med 17: 1032-1035.
263. Hibino N, McGillicuddy E, Matsumura G, Ichihara Y, Naito Y, et al. (2010) Late-term results of tissue-engineered vascular grafts in humans. J Thorac Cardiovasc Surg 139: 431-436, 436 e431-432.
264. Cale AR, Sang CT, Campanella C, Cameron EW. (1993) Hufnagel revisited: a descending thoracic aortic valve to treat prosthetic valve insufficiency. Ann Thorac Surg 55: 1218-1221.
265. Hibino N, Villalona G, Pietris N, Duncan DR, Schoffner A, et al. (2011) Tissue-engineered vascular grafts form neovessels that arise from regeneration of the adjacent blood vessel. FASEB J 25: 2731-2739.
266. Hibino N, Yi T, Duncan DR, Rathore A, Dean E, et al. A critical role for macrophages in neovessel formation and the development of stenosis in tissue-engineered vascular grafts. Faseb J 25: 4253-4263.
267. Harken DE. (1989) Heart valves: ten commandments and still counting. Ann Thorac Surg 48: S18-19.
268. Wiehe JM, Zimmermann O, Greiner J, Homann JM, Wiesneth M, et al. (2005) Labeling of adult stem cells for in vivo-application in the human heart. Histol Histopathol 20: 901-906.
269. Yang YJ, Qian HY, Huang J, Geng YJ, Gao RL, et al. (2008) Atorvastatin treatment improves survival and effects of implanted mesenchymal stem cells in post-infarct swine hearts. Eur Heart J 29: 1578-1590.
270. Harrington JK, Chahboune H, Criscione JM, Li AY, Hibino N, et al. (2011) Determining the fate of seeded cells in venous tissue-engineered vascular grafts using serial MRI. FASEB J
271. Dijkman PE, Driessen-Mol A, de Heer LM, Kluin J, van Herwerden LA, et al. Trans-apical versus surgical implantation of autologous ovine tissue-engineered heart valves. J Heart Valve Dis 21: 670-678.
272. van Vlimmeren MA, Driessen-Mol A, Oomens CW, Baaijens FP. An in vitro model system to quantify stress generation, compaction, and retraction in engineered heart valve tissue. Tissue Eng Part C Methods 17: 983-991.
273. Caceres M, Lachuer J, Zapala MA, Redmond JC, Kudo L, et al. (2003) Elevated gene expression levels distinguish human from non-human primate brains. Proc Natl Acad Sci U S A 100: 13030-13035.
274. Roth GS, Mattison JA, Ottinger MA, Chachich ME, Lane MA, et al. (2004) Aging in rhesus monkeys: relevance to human health interventions. Science 305: 1423-1426.
275. Hopkins RA, Jones AL, Wolfinbarger L, Moore MA, Bert AA, et al. (2009) Decellularization reduces calcification while improving both durability and 1-year functional results of pulmonary homograft valves in juvenile sheep. J Thorac Cardiovasc Surg 137: 907-913, 913e901-904.
276. Simon P, Kasimir MT, Seebacher G, Weigel G, Ullrich R, et al. (2003) Early failure of the tissue engineered porcine heart valve SYNERGRAFT in pediatric patients. Eur J Cardiothorac Surg 23: 1002-1006; discussion 1006.
277. Tamburino C, Capodanno D, Ramondo A, Petronio AS, Ettori F, et al. (2011) Incidence and predictors of early and late mortality after transcatheter aortic valve implantation in 663 patients with severe aortic stenosis. Circulation 123: 299-308.
278. Vasa-Nicotera M, Sinning JM, Chin D, Lim TK, Spyt T, et al. (2012) Impact of paravalvular leakage on outcome in patients after transcatheter aortic valve implantation. JACC Cardiovasc Interv 5: 858-865.
279. Yang L, Bryder D, Adolfsson J, Nygren J, Mansson R, et al. (2005) Identification of Lin(-)Sca1(+)kit(+)CD34(+)Flt3-short-term hematopoietic stem cells capable of rapidly reconstituting and rescuing myeloablated transplant recipients. Blood 105: 2717-2723.
280. Liguori A, Fiorito C, Balestrieri ML, Crimi E, Bruzzese G, et al. (2008) Functional impairment of hematopoietic progenitor cells in patients with coronary heart disease. Eur J Haematol 80: 258-264.
281. Bozdag-Turan I, Turan RG, Ludovicy S, Akin I, Kische S, et al. (2012) Intra coronary freshly isolated bone marrow cells transplantation improve cardiac function in patients with ischemic heart disease. BMC Res Notes 5: 195.
282. Bozdag-Turan I, Turan RG, Turan CH, Ludovicy S, Akin I, et al. (2011) Relation between the frequency of CD34(+) bone marrow derived circulating progenitor cells and the number of diseased coronary arteries in patients with myocardial ischemia and diabetes. Cardiovasc Diabetol 10: 107.
283. Templin C, Krankel N, Luscher TF, Landmesser U. (2011) Stem cells in cardiovascular regeneration: from preservation of endogenous repair to future cardiovascular therapies. Curr Pharm Des 17: 3280-3294.
284. Templin C, Luscher TF, Landmesser U. (2011) Cell-based cardiovascular repair and regeneration in acute myocardial infarction and chronic ischemic cardiomyopathy-current status and future developments. Int J Dev Biol 55: 407-417.
285. van Rooij E, Marshall WS, Olson EN. (2008) Toward microRNA-based therapeutics for heart disease: the sense in antisense. Circ Res 103: 919-928.
286. Suarez Y, Fernandez-Hernando C, Pober JS, Sessa WC. (2007) Dicer dependent microRNAs regulate gene expression and functions in human endothelial cells. Circ Res 100: 1164-1173.
287. Suarez Y, Sessa WC. (2009) MicroRNAs as novel regulators of angiogenesis. Circ Res 104: 442-454.

288. Takahashi K, Yamanaka S. (2006) Induction of pluripotent stem cells from mouse embryonic and adult fibroblast cultures by defined factors. Cell 126: 663-676.
289. Takahashi K, Tanabe K, Ohnuki M, Narita M, Ichisaka T, et al. (2007) Induction of pluripotent stem cells from adult human fibroblasts by defined factors. Cell 131: 861-872.
290. Okita K, Hong H, Takahashi K, Yamanaka S. (2010) Generation of mouse-induced pluripotent stem cells with plasmid vectors. Nat Protoc 5: 418-428.
291. Loffredo FS, Steinhauser ML, Gannon J, Lee RT. Bone marrow-derived cell therapy stimulates endogenous cardiomyocyte progenitors and promotes cardiac repair. Cell Stem Cell 8: 389-398.
292. Ieda M, Fu JD, Delgado-Olguin P, Vedantham V, Hayashi Y, et al. (2010) Direct reprogramming of fibroblasts into functional cardiomyocytes by defined factors. Cell 142: 375-386.
293. Efe JA, Hilcove S, Kim J, Zhou H, Ouyang K, et al. (2011) Conversion of mouse fibroblasts into cardiomyocytes using a direct reprogramming strategy. Nat Cell Biol 13: 215-222.
294. Laflamme MA, Murry CE. (2011) Heart regeneration. Nature 473: 326-335.
295. Qian L, Huang Y, Spencer CI, Foley A, Vedantham V, et al. (2012) In vivo reprogramming of murine cardiac fibroblasts into induced cardiomyocytes. Nature 485: 593-598.
296. Gott VL, Alejo DE, Cameron DE. (2003) Mechanical heart valves: 50 years of evolution. Ann Thorac Surg 76: S2230-2239.
297. Dijkman PE, Driessen-Mol A, Frese L, Hoerstrup SP, Baaijens FP. (2012) Decellularized homologous tissue-engineered heart valves as off-the-shelf alternatives to xeno- and homografts. Biomaterials 33: 4545-4554.

Acknowledgements

It is my great pleasure to express my gratitude to everyone who supported me while completing this thesis. Firstly, I would like to thank my 1st promoter Prof. Simon P. Hoerstrup for giving me the opportunity to write this thesis, for his supervision and guidance, and in particular for his exceptional and systematic support to pursue my academic career in the field of regenerative cardiovascular therapies. I would also like to thank my 2nd promoter Prof. Frank Baaijens who provided guidance and advice for this thesis whenever needed. I am also deeply thankful to Prof. Volkmar Falk who made it possible for me to focus on this research project while giving me the opportunity to obtain clinical training in cardiac surgery. Warmest thanks to my co-promoter Anita Driessen-Mol for her fantastic help to promote me accomplishing this thesis. Furthermore, I would like to thank my colleague Mrs. Petra Wolint for her outstanding support and technical assistance to complete the subprojects presented in this thesis. Moreover, I greatly appreciate the support from all current and former members of the Swiss Center of Regenerative Medicine as well as Biomedical Tissue Engineering group of Technical University Eindhoven. Finally, I particularly like to thank my family and my partner Careen for their continuous and highly valued support for my academic and medical career from the early beginning.

Curriculum Vitae

Maximilian Emmert was born on August 28th in Hannover, Germany. He finished his secondary education (“Abitur”) at the high school of Sarstedt, Germany, before he started studying medicine at the universities of Frankfurt, Hamburg, and Hannover, Germany. Thereafter he obtained practical training (“Praktisches Jahr”) in London, United Kingdom, Sydney, Australia, Zurich, Switzerland and Singapore. In December 2007, Maximilian Emmert received his diploma in Human Medicine (“Approbation”) from the Hannover Medical School in 2007 after which he obtained a clinical position in the Clinic for Cardiovascular Surgery at the University Hospital Zurich, Switzerland in 2008. In September 2009 he received a scholarship (Special Program University Medicine (SPUM)) from the Swiss National Science Foundation (SNSF) and joined the Laboratory for Tissue Engineering and Cell Transplantation (Swiss Centre for Regenerative Medicine) of Prof. S.P. Hoerstrup at the University and University Hospital Zurich where he worked in parallel to his clinical activities. In his research he primarily focused on translational cardiovascular medicine including cardiac cell therapy and heart valve tissue engineering concepts which was also in close collaboration with Prof. F.P.T. Baaijens at the Department of Biomedical Engineering at Eindhoven University of Technology, The Netherlands. In November 2010 he finished his clinical thesis (Dr. med.) at the University of Zurich, which was then followed by the completion of his habilitation thesis (Privatdozent Dr. med., Herzchirurgie) in March 2012.